Spatial dynamics of nearshore marine habitats from low altitude remote sensing for conservation and planning

Subhash Chand

A thesis submitted to

Auckland University of Technology

In fulfilment of the requirements for the degree of

Doctor of Philosophy (Ph.D.)

2022

School of Science

Faculty of Health and Environmental Sciences

Abstract

Biogenic habitats such as wild oyster reefs and seagrass meadows support biodiversity and essential ecological services. However, these biogenic habitats are susceptible to change from anthropogenic and environmental impacts. Hence, they are the subjects of significant conservation and planning research. Mapping and monitoring the spatial dynamics of the nearshore marine environment is challenging due to its dynamic nature, where many processes operate simultaneously over varying temporal and spatial scales within tidal variations. To address this challenge, this study aimed to develop the scientific understanding and novel applications of proximal low altitude remote sensing of nearshore marine environments using visible (VIS) and near-infrared (VIS+NIR) sensors from 50m altitude. The research examined the application of remotely piloted aircraft system (RPAS) technology in two nearshore marine environments, a rocky intertidal reef (Meola reef) and a mudflat (Cox's Bay) in Waitemata Harbour, North Island of New Zealand.

Over time remotely sensed products derived from airborne and spaceborne platforms were highly influential in mitigating this challenge, but limitations with these technologies persist. Aerial mapping and monitoring wild oyster reefs and seagrass meadows require high spectral and spatial resolution imagery to be successfully delineated and classified. Hence, the advent of proximal low altitude remote sensing technology such as lightweight RPAS has been a step-change in mapping and monitoring research. RPAS technology is accessible and can reliably collect high-resolution aerial datasets in various locations at user-defined periods with repeated surveys and high accuracy.

In this research, the comparison between RPAS aerial data collection and standard field observations highlighted that the aerial perspective provided by the RPAS allowed for a more precise spatial assessment of wild oyster reefs and seagrass meadows. In particular, the application of RPAS at 50m provided a ground sampling distance of 1.3cm/pixel (VIS sensor) and 3.5cm/pixel (VIS+NIR sensor), which improved the detection and classification of wild oyster reefs and seagrass meadows.

Most studies on wild oyster reefs used RPAS within the VIS electromagnetic spectrum along temperate intertidal rocky reefs. Therefore, there was an opportunity to demonstrate the potential of an RPAS with a VIS+NIR sensor and structure from motion photogrammetry technique to identify and characterise wild oyster reefs in a temperate intertidal estuary (Chapter 3). The findings showed that additional spectral bands (RedEdge and NIR) enhanced feature detection and increased the potential to delineate oyster reefs within a heterogeneous marine ecosystem in this study. A rule-based classification technique was used to detect and classify oyster reefs based on their spectral characteristics following segmentation and achieved an overall accuracy of

83.9% and a Kappa coefficient of 69.8%. The findings from this study also established that RPAS as a survey tool is optimum to target marine tidal and metrological conditions and could be ideal for monitoring and locating the distribution of predatory borer snails from low altitudes.

Researchers in New Zealand have established that seagrass meadows, a valuable resource, are under pressure from human activities and climate change and are at risk of declining. Although progress has been made locally to understand the marine environment, there are still gaps in temporal data consistency, limiting the full potential to understand drivers of change. Therefore, there was a research opportunity to bridge these gaps by developing new scale-appropriate techniques for rapid assessment and monitoring changes in the seagrass ecosystems (Chapter 4). This study demonstrated the potential of an RPAS with a VIS+NIR sensor for low altitude mapping and high-resolution spatial assessment of intertidal seagrass meadow and modified a spectral index. The results from object-based image analysis (OBIA) and the maximum likelihood classification technique achieved an overall accuracy of 95% and a Kappa coefficient of 81%. The findings from this study showed that researchers could gain valuable insights to observe local changes and identify drivers of change. Results have established that RPAS with a VIS+NIR sensor could consistently fill the multi-temporal data gap with repeated surveys. Marine managers can use the methodology from this study to quickly identify the drivers of change and prevent this crucial resource from reaching its tipping point.

Furthermore, researchers found that the RPAS VIS sensor limited the spectral and textural separability between oyster reefs and sediment. Researchers also established that broad spectral resolution from many multispectral satellite sensors restricted the detection of wild oyster reefs. Hence there was a research opportunity to explore VIS and VIS+NIR sensors for spatial assessments, monitoring, and mapping of wild oyster reefs from proximal low altitude remote sensing (Chapter 5). The results from this study showed that wild oyster reefs in the VIS+NIR imagery achieved an overall classification accuracy of 85% compared to 70% from the VIS imagery. The findings showed that spectral resolution was more critical than the spatial resolution that correctly detected and classified oyster reefs in this study. The findings also established that the remote sensing technique used for ecology and conservation offers scale-appropriate spatial assessment, monitoring, and mapping of benthic habitats in challenging and inaccessible temperate marine environments.

Moreover, seagrass decline also affects associated species and their vital linkage with the adjacent habitats, igniting a broader degradation with long-lasting impacts on other habitats and biodiversity dependent on seagrass within an ecosystem. Researchers have established that the possibility of identifying subtle fine-scale seasonal change goes undetected and undocumented. While different RPAS mapping and monitoring techniques have been applied for seagrass

research, there is a gap in simultaneously testing VIS and VIS+NIR domains to detect fine-scale seasonal seagrass change in a dynamic nearshore marine environment. This gap gave rise to a research opportunity that tested the performance of VIS and VIS+NIR sensors to detect fine-scale time-series seagrass seasonal change in a dynamic nearshore marine environment using spectral indices and supervised machine learning classification technique (Chapter 6). No attempts were made to identify and quantify the abundance and distribution of marine macrofauna benthic activity from proximal low altitude remotely sensed drone imagery. Hence, this research also tested whether macrofauna benthic activity abundance and distribution amongst seagrass meadows can be determined from proximal low altitude remotely sensed drone aerial imagery. The VIS imagery and support vector machine (SVM) classification results produced an average overall class accuracy of 93% and an average Kappa coefficient of 0.90, and VIS+NIR sensors had an average overall class accuracy of 95% and an average Kappa coefficient of 0.93. These accuracies established that the spectral indices were fundamental in this study to identify and classify seagrass density. The other important finding revealed that seagrass-associated macrofauna benthic activity showed increased or decreased abundance and distribution with seasonal seagrass variability from drone high spatial resolution orthomosaic. These findings are essential for seagrass conservation because managers can quickly detect fine-scale seasonal changes and take mitigation actions before the decline of this keystone species affects the entire ecosystem. Also, proximal low-altitude, remotely sensed time-series seasonal data provided valuable contributions for documenting spatial ecological seasonal change in this dynamic marine environment.

Collectively, this research improved the understanding of proximal low altitude remote sensing in a dynamic nearshore marine environment and its competency to supplement *in-situ* and other remotely sensed datasets for conservation and planning. In addition, this research identified the limitations and strengths of its application for monitoring, mapping, and understanding the spatial dynamics of the nearshore marine environments.

Table of Contents

List of Figures

List of Tables

Attestation of Authorship

I hereby declare that this submission is my work and that, to the best of my knowledge and belief, it contains no material previously published or written by another person (except where explicitly defined in the acknowledgments), nor material which, to the substantial extent has been submitted for the award of any other degree or diploma of a university or other institute of higher learning.

Subhash Chand

28 January 2022

Candidate Contributions to Co-authored papers

Peer-Reviewed Chapters	Contributions
Chapter 3 (Published) Chand, S., Bollard, B. and Gillman, L. (2020). Low-cost remotely piloted aircraft system (RPAS) with multispectral sensor for mapping and classification of intertidal biogenic oyster reefs. 4(4), 148–154. https://doi.org/10.15406/aaoaj.2020.04.00116	Chand 90% Bollard 5% Gillman 5%
Chapter 4 (Published) Chand, S., and Bollard, B. (2021). Low altitude spatial assessment and monitoring of intertidal seagrass meadows beyond the visible spectrum using a remotely piloted aircraft system. Estuarine, Coastal and Shelf Science, 255(February), 107299. https://doi.org/10.1016/j.ecss.2021.107299	Chand 90% Bollard 10%
Chapter 5 (Published) Chand, S., and Bollard, B. (2021). Multispectral low altitude remote sensing of wild oyster reefs. Global Ecology and Conservation, 30(August), e01810. https://doi.org/10.1016/j.gecco.2021.e01810	Chand 90% Bollard 10%
Chapter 6 (Published) Chand, S., Bollard, B. (2022). Detecting the Spatial Variability of Seagrass Meadows and Their Consequences on Associated Macrofauna Benthic Activity Using Novel Drone Technology. Remote Sens. 2022, 14, 160. https://doi.org/10.3390/rs14010160	Chand 90% Bollard 10%

Subhash Chand	Prof. Barbara Bollard	Prof. Len Gillman
28/01/2022	28/01/2022	28/01/2022

Acknowledgments

This Ph.D. journey has been arduous, but it has made me much stronger to persevere through any impediments. This research project would not have been accomplished without the involvement and assistance of these people and institutional support. I appreciate the guidance of my supervisors, Prof. Barbara Bollard, for her absolute commitment in assisting me to achieve this milestone, and Dr. Nick Shears, for their continued support through various stages of this Ph.D. journey. Not forgetting Prof. Mark Orams, my mentor supervisor; thank you, Sir, for your valuable time for regular meetings on progress and continual support throughout this research. Also, cheers to Prof. Len Gillman, Ashray Doshi from Auckland University of Technology (AUT) drone lab for providing the drones and equipment for this project, and Evan Brown for taking us out for high tide aerial surveys. Thanks to the staff of AUT, School of Science, for providing administrative support and research funding throughout my Ph.D. journey. A sincere thanks to the AUT scholarship office for funding my Doctoral Scholarship. Thank you all for your confidence in me and the support provided over the years for completing this Ph.D. research project.

Moreover, I wish to acknowledge the anonymous reviewers' valuable comments, which improved all the manuscripts, now embedded as subsequent chapters of this thesis.

Not forgetting my parents and my sister, who are with me in spirit and would have been proud of me for reaching this stage of my life.

My most tremendous gratitude is reserved for my compass, my wife Kavita Prasad, for her unconditional support both morally and financially. You have been incredibly patient and compassionate toward me throughout this journey, and a special award should be given to you for bringing me back to sanity. I am forever grateful to you for giving up your career and following me to New Zealand (Aotearoa), The Land of the Long White Clouds, and I count myself very privileged to have such a lovely partner and friend. Kavita, you are a wonderful human being, and this Doctoral research was only achievable with you always on my side.

Chapter 1 Introduction

Cover image. An aerial image shows grazed seagrass meadows at Cox's Bay and the concentration of houses along the coastline adjacent to the Meola reef. The RPAS imagery was captured during the winter of 2019 during field works.

1.1 Changing coastal ecosystems and biodiversity

The nearshore marine environment is a dynamic interface between the land and the sea. Hence, it represents one of the most challenging frontiers between human civilization and marine conservation and planning. Globally, 50% of coastal countries have approximately 80% of their population living within 100km of the coastlines (Dunn et al., 2018). Demand for space and increased populations along coastlines have high local impacts on nearshore ecosystems from coastline modifications, sewage discharge, agricultural run-off, increased sedimentation, and habitat destruction (Maavara et al., 2017; MacDiarmid et al., 2013). In addition, a flux in normal climatic conditions, such as an increase in acidification and marine heatwaves, poses severe risks to ecosystem functioning and their morphology (Gattuso et al., 2015). Combined, human and climate change impacts have direct cascading, long-lasting effects on biological diversity, ecosystem health, and ecological dynamics, eventually leading to large-scale marine habitat declines and the collapse of the broader ecosystem (Anderson et al., 2019). Consequently, these impacts lead to adverse changes from which recovery would be difficult for many species, and alterations could allow invasive species to thrive and rapidly evolve (Hughes et al., 2017).

New Zealand's temperate nearshore marine environment encompasses diverse biogenic habitats such as seagrass meadows (*Zostera muelleri*), wild oyster reefs: Rock Oyster (*Saccostera commercialis*), Bluff oyster (Ostrea edulis), and Pacific oysters (*Crassostrea gigas*), kelp forests:

Bladder kelp (*Macrocystis pyrifera*), Common kelp (*Ecklonia radiata*), Bull kelp or rimurapa (*Durvillaea species*) and Asian kelp (*Undaria pinnatifida*), salt marshes: needle grass (*Austrostipa stipoides*), saltmarsh ribbonwood (*Plagianthius divaricatus*), mangroves: (*Avicennia marina*), and intertidal rocky reefs (Anderson et al., 2019). Biogenic habitats are habitats formed by plants such as seagrass meadows and animals, such as coral, mussels, and wild oysters (Costanza et al., 2014; Krumhansl et al., 2016). These nearshore marine environments are among the most dynamic and rapidly evolving systems (Reshitnyk et al., 2014; Schwantes et al., 2018). Although their spatial extent in the global ocean is only 7.6%, nearshore biogenic habitats provide up to 30% of the global primary production and supply approximately 50% of organic carbon to the deep ocean (Bauer et al., 2013; Chmura et al., 2016). These biogenic habitats provide many ecosystem services that keep New Zealand's marine environments healthy and are essential for supporting biodiversity and primary productivity (Castellanos-Galindo et al., 2019; Marcello et al., 2015; Tait et al., 2019). Collectively, biogenic habitats are hotspots for marine biodiversity and provide invaluable ecosystem services such as (1) nursery, and feeding grounds for marine biota, (2) are the most prolific carbon fixers, (3) provide sediment cohesion and stabilization for coastal protection, (4) water quality improvement through filtering sediments and (5) marine ecosystems provide a rich habitat for biodiversity (Krumhansl et al., 2016; Nagelkerken et al., 2015; Weerman et al., 2010). However, anthropogenic and climate change combined effects have unprecedented impacts on these habitats, including short and long-term cascading effects on the whole ecosystem (Anderson et al., 2019). These impacts could occur at fine spatial scales and are challenging to map and monitor but essential for resource management, administration, conservation, and planning. Hence, to understand and mitigate impacts in coastal ecosystems, a versatile monitoring effort and contemporary monitoring techniques to detect fine-scale changes over time must adapt and evolve with this essential but dynamic environment.

1.2 Challenges of monitoring the dynamic marine environment

Understanding impacts in dynamic marine environments requires monitoring that can detect short-term changes and changes arising from intra-annual and inter-annual variation from cyclones and hurricanes, and other extreme weather events. Moreover, it is essential to establish baselines regarding the function of the natural environment and the ecosystem structure, identify and quantify response to changes and determine increased anthropogenic and climate-related pressures. Understanding the natural environmental processes can characterise the effects of anthropogenic and climate-related pressures more accurately. If well designed and planned, marine environment monitoring can be a cost-effective technique to care for natural resources and, at the same time, be scientifically rigorous to motivate policymakers to deliver effective management for conservation and planning (Narayan et al., 2016). Although recently, vast progress has been made towards coastal monitoring, the ability to collect scale-appropriate

datasets at user-define times to resolve processes of interest is still hampered by many challenges (Johnston, 2019). For example, *in-situ* surveys and data collection are resource-intensive (due to the cost of maintenance and upkeep of equipment), logistically challenging, and survey times are dependent on tidal variations (Brewin et al., 2015). Coastal environments can be very hard on equipment with salt water, sand, mudflats, and variable wind conditions, making it challenging for researchers. Hence, remote sensing technologies from airborne, space-borne, and low-altitude remotely piloted aircraft systems (RPAS) systems have profoundly changed the practice of mapping, monitoring, and understanding the spatial dynamics of nearshore marine environments (Chand and Bollard, 2021; Klemas, 2016).

1.3 Remote sensing for ecology and conservation

The marine environment's spatial variability, dynamic nature, and the processes that operate at fine scales require comparable high spatial and temporal resolution data. Therefore, multi-spatial and multi-temporal mapping and monitoring techniques are fundamental to identifying and quantifying climatic and anthropogenic impacts on nearshore marine environments. These techniques will help identify community shifts and track subsequent declines and restoration initiatives. Remote sensing technologies have provided reasonable solutions for long-term monitoring programmes, enabled the study of extensive marine environments to assess spatial patterns, and simultaneously offered frequent observations of temporal changes (Duffy et al., 2018; Hedley et al., 2016; Johnston, 2019).

Remote sensing from crewed aircraft and low constellation space-borne satellites has had many technological advances, has become a core component of spatial ecology, and provides data for various applications (D'Urban et al., 2020; Johnston, 2019). For example, responding to a request from the conservation community, The National Aeronautics and Space Administration (NASA) in the year 2001 provided free Landsat imagery for 1990 and 2000 (Mullerova et al., 2017). Since that time, much higher resolution satellite imagery has been freely available. An unprecedented number of datasets have become available from low-cost, low orbiting satellites, e.g., CubeSats, which harness consumer technology instead of bespoke technologies (Pimm et al., 2015). However, mapping and monitoring benthic marine habitats is challenging with space-borne and crewed aircraft imagery (1) due to complexities of heterogeneous benthic habitats, (2) limitations of sensors due to spectral attenuation, when detailed information is required for smaller spatial extents within a small time-frame (3) insufficient spectral, spatial and temporal resolutions, (4) high spatial resolution resulting to high-cost from commercial providers, (5) cloud cover at the time of acquisition and humidity (6) still many satellite sensors are sensitive to atmospheric effects and weather leading to image-degrading (Hedley et al., 2012; Wicaksono and Lazuardi, 2018).

Low-altitude aerial imagery captured by remotely piloted aircraft systems (RPAS) is bridging the gap between space-borne earth observation satellites, crewed aerial, and *in-situ* surveys (Chand and Bollard, 2021; Duffy et al., 2019). Used for many applications, RPAS has provided a step-change in marine spatial ecology (Anderson and Gaston, 2013; Castellanos-Galindo et al., 2019). For example, RPAS flown at lower altitudes allows researchers to capture and process marine imagery directly captured under optimum weather and oceanographic conditions with centimetre to millimetre spatial resolutions (Duffy et al., 2018; Manfreda et al., 2018; Tait et al., 2019; Ventura et al., 2018). This flexibility permits researchers to survey more frequently to detect subtle fine-scale changes before habitats reach their tipping points (Manfreda et al., 2018).

1.4 Rationale and significance of the study

New Zealand's marine environment is essential for economic activity and employment. In 2017, the marine environment had contributed $7 billion to the economy and provided over 30,000 jobs (MfE, 2019). However, cumulative human activities and climate change pressures have impacted New Zealand's marine ecosystem and biodiversity. These pressures from human activities included (1) sediment overload, (2) reclamation of coastlines for developments, (3) forestry, (4) chemical discharge, (5) plastics, and (6) agriculture (MfE, 2019). Pressures from climate change included (1) an increase in sea-surface temperature affecting the reproduction of fisheries, e.g., Snapper (*Pagrus auratus*) and Hoki (*Macruronus novaezelandiae*), (2) increased invasive species, (3) rising sea levels affecting low-lying coastal communities (MfE, 2019). These pressures interact in complex ways to degrade habitats and ecosystems, and impacts accumulate over decades (Marcello et al., 2015). The degradation of habitats in shallow waters restricts and hinders other processes in the ocean and compromises the Indigenous people's (Māori) values and New Zealand's recreational enjoyment of coastlines and beaches (MfE, 2019). One crucial issue in protecting the marine environment is the lack of quality data to quantify the state of nearshore marine habitats at a national level (MfE, 2019). Therefore, to fill this gap, this study acquired high spatial and spectral resolution RPAS aerial imagery to supplement data collection in the nearshore marine environment. This study also identified and quantified fine-scale changes to seagrass meadows and wild oyster reefs as nature-based solutions to protect the marine environment from further degradation.

1.5 Why focus on seagrass meadows?

One of the most important reasons for studying seagrass meadows (*Zostera muelleri*) is that they continue to be productive as other habitats, such as coral reefs, decline rapidly (Matheson and Manley-Harris, 2018). Several researchers have established that seagrass meadows are better suited to deal with extreme temperatures, rising sea levels, and ocean acidification (Arias-Oritz et al., 2018; Koch et al., 2013). This suitability is because seagrass meadows have not yet reached

their thermal extreme, and highly unlikely that increasing seawater acidity will impact their productivity (Unsworth et al., 2018).

Also, seagrass meadows act as bio-indicators to monitor ecosystem health (Lamb et al., 2017). For example, to monitor ecosystem degradation, there is a reduction in seagrass blade density before a complete loss (Barbier et al., 2011). Furthermore, in temperate estuaries, increased abundance in seagrass meadows improves water quality and enhances ecosystem health naturally (Bertelli and Unsworth, 2014). Despite their contribution to ecosystem health, the status of seagrass meadows in New Zealand has been identified as a habitat under pressure and categorised as "At Risk-Declining" mainly from agricultural run-off, smothering by sediment overload, coastal developments, seagrass roots damaged by mooring, and boat anchors (Matheson et al., 2017).

Moreover, seagrass meadows were once widespread throughout New Zealand in the subtidal and intertidal zones (Morrison et al., 2014). However, their abundance has declined in many New Zealand localities since the 1920s (Turner and Schwarz, 2006). This decline could be more significant than the estimate suggested, as there is insufficient historical spatio-temporal information to confirm these declines (Anderson et al., 2019; Turner and Schwarz, 2006). The challenge of mapping and monitoring seagrass bed decline is difficult for marine managers as the paucity of information cannot distinguish natural changes from the impacts of anthropogenic activities (Bertelli et al., 2018).

1.6 Why focus on wild oyster reefs?

In New Zealand, native Rock oysters (*Saccostrea glomerata*) were essential to the Māori communities around Kaipara Harbour (Kelly, 2009). Rock oysters were present in abundance in the Kaipara, Manukau, Whangaroa, and Whangaruru Harbours, which led to commercial harvesting (50-100 tonnes)—concerned about the depleting stocks of wild oysters, The New Zealand government passed the first fisheries law (the Oyster Fisheries Act 1866) (Morrison et al., 2014). As the native rock oyster stocks depleted, local authorities sustained the depleting oyster stocks by establishing artificial oyster beds but were unsuccessful (Kelly, 2009). In the Kaipara Harbour, Kelly, 2009 estimated the distribution and abundance of oysters from a helicopter video and established that the invasive Pacific oysters (*Crassostrea gigas*) have mostly replaced the native Rock oysters **(Figure 1)**. There are no national accounts of wild oyster reefs distribution of any magnitude in New Zealand (Morrison et al., 2014). Apart from Meola reef and Kaipara Harbour, which have been identified as having wild oyster reefs distributed at a large scale (Morrison et al., 2014).

The abundance and distribution of wild oysters (mainly Pacific and Rock oysters) at the Meola reef are susceptible to impacts from human activities. The Meola intertidal reef is close to New

Zealand's largest city, Auckland, and the Port of Auckland. This spatial location makes the Meola intertidal reef a perfect host for non-native species to settle, distribute, and continually vulnerable to anthropogenic impacts (Foley and Shears, 2019). For example, the arrival of invasive Pacific oysters was a significant and most apparent human impact on the Meola reef (Shears, 2010). In addition, collectively, anthropogenic activities occurring extensively around the Waitemata Harbour, and climatic variations modify this ecosystem regularly. For example, in 2012, an increase in predatory oyster borer snails (*Haustrum scobina*) and increased sediments correspond to a marked decline in the abundance of oysters using traditional *in-situ* sampling techniques (Foley and Shears, 2019).

Wild oyster reefs also support other habitats. For example, adjacent to the Meola reef is an extensive seagrass mudflat; researchers have established a connection between the two habitats that has allowed the population of macrofauna communities to increase over the years (Lundquist et al., 2018). Oyster reefs also support surrounding habitats by filtering nutrients and maintaining a diverse range of biota.

The lack of research on naturally established wild oyster reefs is due to the primary focus of oysters being the aquaculture industry in New Zealand (Morrison et al., 2014). For example, Bio-marine Ltd. runs seven oyster farms in Kaipara Harbour, an open ocean farm that produces 24 million oysters yearly (Kelly, 2009). This calls to the attention that in New Zealand, no studies have focused on the distribution and abundance of wild oyster reefs from RPAS high-resolution imagery to the best of my knowledge.

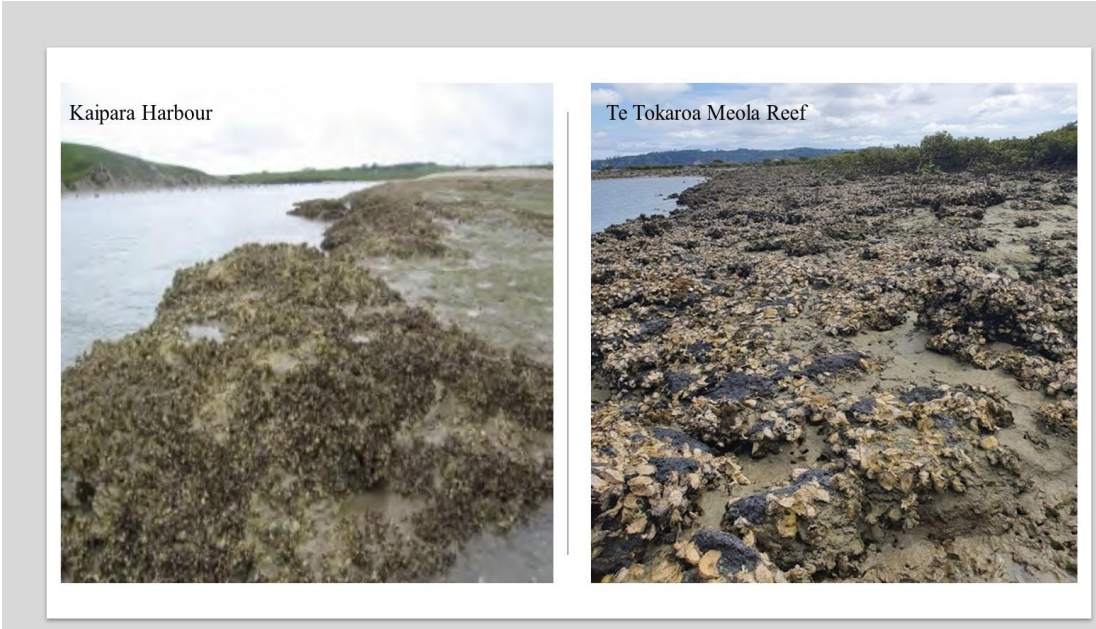

Figure 1. The abundance and distribution of wild oysters in the Kaipara Harbour and the Meola reef. Image source for Kaipara Harbour, Morrison et al., 2014. The image for the Meola reef was courtesy of Kavita Prasad.

1.7 The land-sea interface explored in this thesis

As described in section 1.1, the marine intertidal zone holds a vast diversity of ecosystems, generally grouped by their spatial position within the land-sea interface. In this thesis, two critical intertidal coastal environments were empirically researched; wild oyster reefs at Meola intertidal rocky reef (Chapters 3 and 5) and seagrass meadows at Cox's Bay (Chapters 4 and 6) (**Figure 2**).

Absolute location details of the study site for oyster reef research are presented in Chapters 3 and 5 and for seagrass in Chapters 4 and 6. These environments presented unique challenges and research opportunities for aerial image capture and processing with proximal low altitude RPAS. These intertidal zones researched are composed of different substrate types and vegetation, including complexities (rugged structure) and environmental conditions (tidal variations). Accessibility is highly variable across the two ecosystems, with the Meola reef accessible on foot seagrass mudflat only exposed during low tides. The following section introduces the thesis aim. Objectives to reach the aim and explain the structure of the thesis.

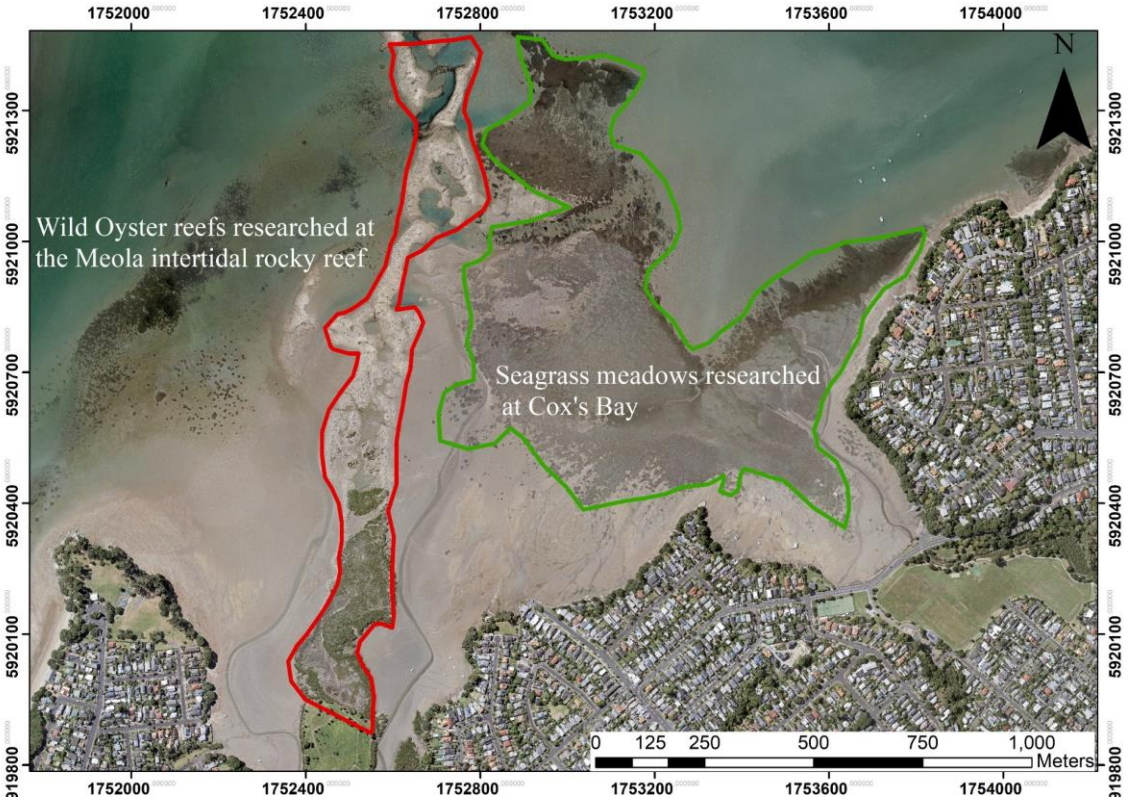

Figure 2. Showing the land-sea interface explored in this thesis. Wild oyster reefs were researched at Meela intertidal rocky reef (red outlined), and seagrass meadows were researched at Cox's Bay (green outlined). Imagery sourced from Land Information New Zealand (LINZ, 2019).

1.8 Thesis aim and objectives

1.8.1 General-purpose

This study intended to increase the reliability of monitoring the spatial dynamics of marine environments through the rapid collection of aerial datasets to determine fine-scale changes in the

nearshore marine habitats along the study area. The empirical techniques from this study are aimed to supplement *in-situ* and other remote sensing techniques for mapping, monitoring, and spatial assessments of nearshore benthic habitats.

1.8.2 Research aim and objectives

This thesis aims to use novel remotely piloted aircraft systems with multispectral sensors to enhance spatial and temporal data collection in the temperate nearshore estuarine in Auckland, New Zealand. Therefore, to address this aim, this study had the following objectives:

a) To demonstrate the potential of a low-cost RPAS coupled with a miniaturized multispectral sensor (MicaSense® RedEdge™) and use structure from motion photogrammetry to deliver very high-resolution maps useable for identification and characterization of biogenic oyster reefs.
b) To demonstrate the suitability of RPAS imagery and the accuracy of Object-based image analysis (OBIA) combined with rule-based classification for detecting and delineating oyster reefs from a heterogeneous intertidal rocky reef ecosystem.
c) To assess the potential of an RPAS with a multispectral sensor for low altitude mapping and high-resolution spatial assessment of intertidal seagrass meadows.
d) To develop a spectral index and demonstrate its potential to distinguish seagrass meadows from other land cover features.
e) To investigate the potential of VIS and VIS+NIR low altitude aerial imagery for distinguishing wild oyster reefs in a heterogeneous intertidal rocky reef ecosystem.
f) To assess spectral signatures collected from RPAS and *in-situ* handheld Spectro-radiometer.
g) To evaluate the accuracy of an object-based image analysis technique (OBIA) and a Support Vector Machine (SVM) to classify high-resolution multispectral RPAS imagery.
h) To test the performance of VIS and VIS+NIR sensors to detect fine-scale seasonal time-series seagrass changes in a dynamic nearshore marine environment using spectral indices and a supervised machine learning classification technique.
i) To determine if the abundance and distribution of macrofauna benthic activity among seagrass meadows can be determined from proximal low altitude remotely sensed drone aerial imagery?

1.8.3 Thesis structure

This thesis is organized into seven chapters **(Figure 3)**. Comprising four research chapters (Chapters 3 to 6) that have been written in publication format and represent manuscripts that have been published (refer to Candidate Contributions to Co-authored papers, Pg. 13). This format has resulted in unavoidable and repetitive text, particularly in the introduction, methods, and discussion sections. However, all effort has been made to limit duplication where possible.

Chapter 1, the current chapter, introduced the thesis and outlined the research aim and objectives. Chapter 2, the research context, is established through a literature review to identify the importance and susceptibility of biogenic habitats to human activities and climate-related changes, their contributions to estuaries, and their status. In addition, Chapter 2 reviewed traditional and low altitude remote sensing methods, challenges, and solutions.

Chapter 3 demonstrated the potential of an RPAS with a miniaturized multispectral (MicaSense® RedEdge™) sensor to capture low-altitude aerial imagery and the application of photogrammetry technique to produce a high spatial resolution orthomosaic (Objective a). In addition, in this chapter, object-based image analysis (OBIA) and rule-based classification techniques were applied to detect and delineate wild oyster reefs in a heterogeneous intertidal rocky reef ecosystem (Objective b).

Chapter 4 demonstrated the potential of an RPAS with a multispectral sensor for low altitude aerial survey of intertidal seagrass meadows (objective c). In addition, in this chapter, a spectral index was modified to establish its potential to accurately distinguish seagrass meadows from other land cover features (objective d). Moreover, an OBIA technique with a maximum likelihood supervised classification technique was used to accurately detect and distinguish seagrass meadows in the study area.

Chapter 5 investigated the potential of VIS and VIS+NIR sensors for low altitude aerial surveys of wild oyster reefs (objective e). This chapter also evaluated the spectral signatures from the RPAS orthomosaic and *in-situ* Spectro-radiometer (objective f). Moreover, in this chapter, an OBIA technique and a Support Vector Machine learning technique were evaluated to classify wild oyster reefs accurately in the study area (objective g). This chapter contributed to the primary aim by developing empirical methods for the spatial assessment of wild oyster reefs and filling the gap in sampling capabilities over the large spatial extent.

Chapter 6 tests the performance of VIS and VIS+NIR sensors for low altitude aerial survey of intertidal seagrass meadows capable of detecting fine-scale seasonal changes using spectral indices and a machine learning technique (objective h). In addition, this chapter evaluated the abundance of distribution of macrofauna benthic activity from remotely sensed imagery (objective i). This chapter contributes to the primary aim by developing a practical technique to detect fine-scale seasonal changes in seagrass meadows and quantify the abundance of macrofauna benthic activity from remotely sensed imagery.

Chapter 7 provides general remarks, an empirical discussion, and potential research questions from seagrass and wild oyster reef research. Furthermore, this chapter discusses the importance of citizen scientists for data sharing during uncertain times, such as during a COVID-19

pandemic. In addition, this chapter identifies the drivers of change impacting biogenic habitats. Chapter 7 also establishes the connection between this study to management, presents the research's limitations, and provides recommendations to protect these critical habitats.

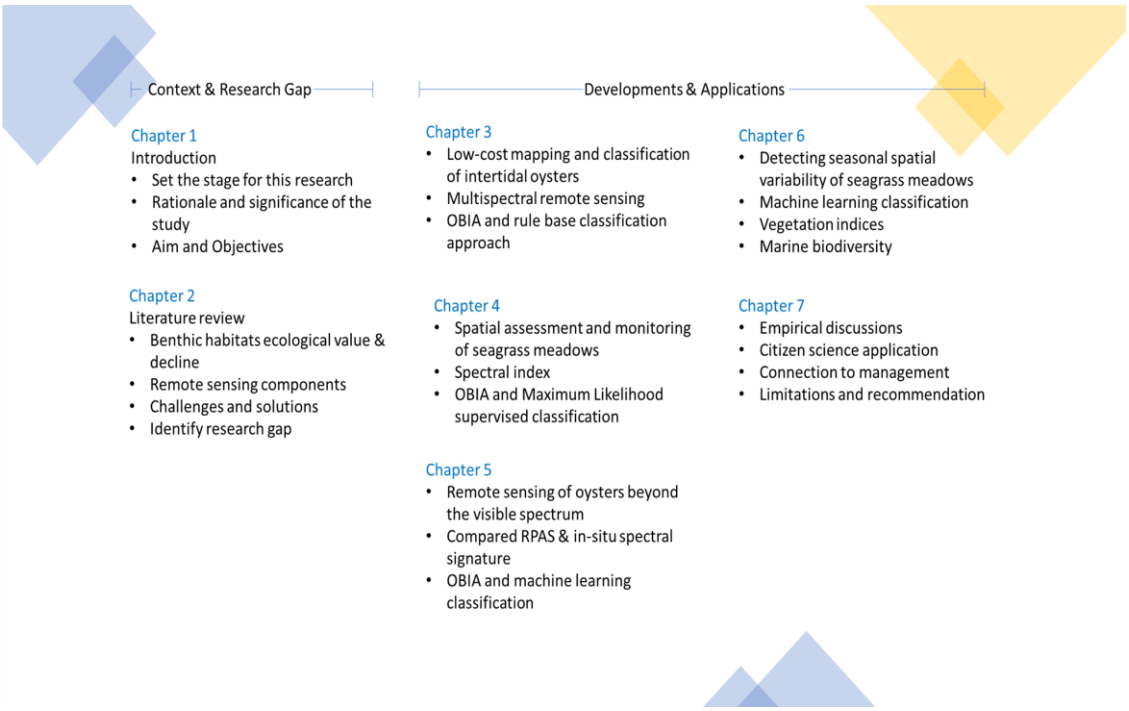

Figure 3. Summary of thesis structure from initiation to completion.

Chapter 2 Literature Review

Cover image. An RPAS aerial imagery shows a seagrass bed section in Cox's Bay, Waitemata Harbour, Auckland, New Zealand.

This chapter, the literature review, is organised into five sections. The first section introduced biogenic habitats and their susceptibility to environmental and anthropogenic impacts in New Zealand's nearshore marine environments. It is important to note that benthic habitats cover a diverse range of vegetative and animal-derived habitats; hence, this research focused on two primary benthic habitats: (1) seagrass meadows and (2) wild oyster reefs. Furthermore, the second section focused on the ecological function, value, and decline of seagrass and wild oyster reefs in New Zealand's marine environment. The third section reviewed past remote sensing and traditional seagrass meadows and wild oyster reef research methods. The fourth section expanded on RPAS remote sensing for marine ecology and conservation. Finally, the fifth section reviewed remote sensing application challenges and solutions for successful RPAS applications in nearshore marine environments.

2.1 Background- susceptibility of biogenic habitats to natural and anthropogenic impacts

Estuarine and intertidal ecosystems are biogenically structured landscapes that contain some of the most productive and ecologically important biogenic habitats (Gray et al., 2019). Biogenic habitats are habitats formed by vegetation, e.g., seagrass meadows, mangroves, saltmarsh, and animals, e.g., shellfish such as coral, mussels, and wild oyster reefs (Costanza et al., 2014; Kumans et al., 2016). Biogenic habitats form three-dimensional structures to function as spawning and nursery grounds for fisheries, provide shelter and protection from predators, and are critical to the marine food chain (Thorngren et al., 2017). Concurrently, they filter out organic and inorganic particles while stabilizing sediments to prevent coastal erosion and sequester carbon (Beck et al., 2011).

Although these benthic habitats are ecologically important, they are also susceptible to environmental and anthropogenic impacts (Bertelli et al., 2018). For example, their susceptibility has increased due to sediment overload and excessive nutrient deposits from runoff and pollution, overfishing, and shellfish dredging (Beck et al., 2009; Kellogg et al., 2014; Matheson and Wadhwa, 2012). Researchers in New Zealand have established that land use such as agriculture has significantly impacted coastal systems, species population, and their size from increased sedimentation (Morrison et al., 2014). For example, evidence of runoff from sediment overload impacts is directly related to reducing snapper (*Pagrus auratus*) abundance and size once commonly found in local estuaries (Bertelli and Unsworth, 2014). Another example was the Poor Knights Marine Reserve, which showed the constant long-term decline in tube sponges (*Calyx imperialis*), packhorse lobsters (*Sagmariasus verreauxi*), black corals (*Lillipathes lilliei*), and large predatory fish due to sediment overload from agricultural runoffs into the ocean (Taylor et al., 2011). Another example of environmental and anthropogenic impact was observed at the Meola rocky intertidal reef in Waitemata Harbour, which transformed this ecosystem with introduced invasive oyster species that replaced native oysters (Foley and Shears, 2019; Shears, 2010) **(Figure 4)**.

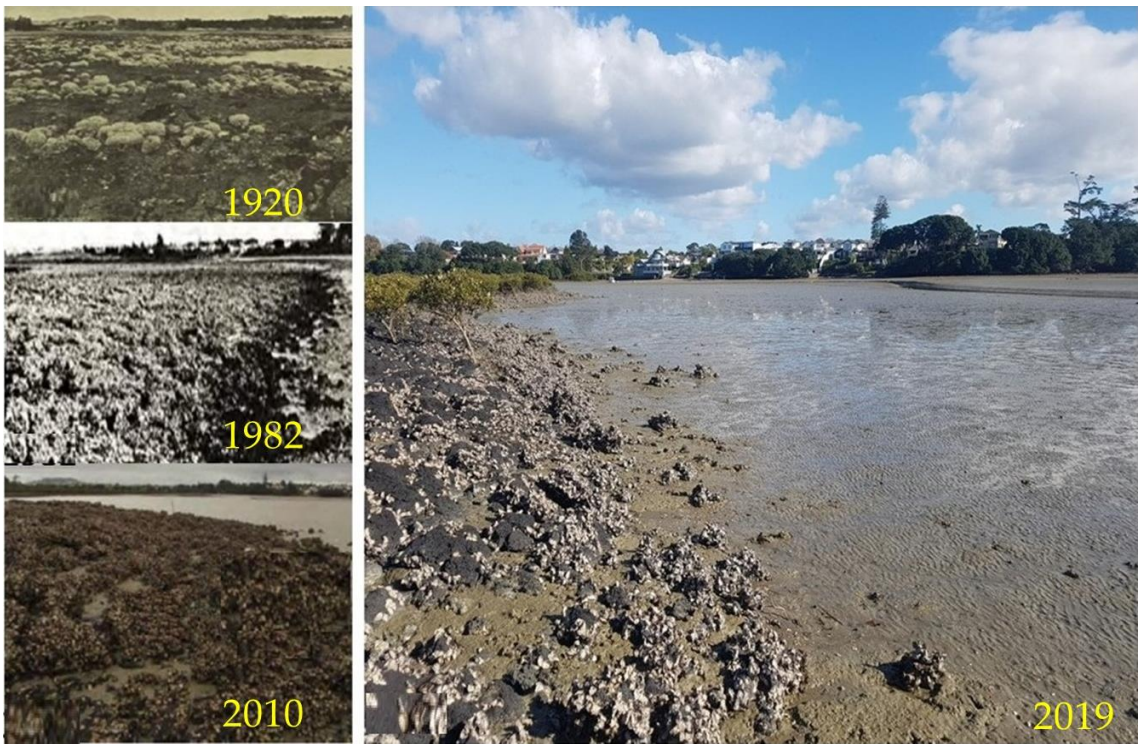

Figure 4. An example of a changing marine ecosystem is at the Meola rocky reef in New Zealand. In 1920 this reef was covered with tubeworms with little sediment. In 1982, invasive Pacific wild oysters were first discovered with small sediment deposits. In 2010, Shears (2010) found large portions of this reef covered with sediment deposits among the wild oyster reefs. In 2019, a decline in live oyster populations was consistent with consolidated sediments trapped among the oyster reefs, resulted in more mangrove regeneration. Images 1920, 1982, and 2010 are sourced from Shears (2010): image 2019, courtesy of Kavita Prasad.

Marine ecosystems are also impacted by weather events from the El Nino Southern Oscillation (ENSO) (unpredictable periodic variation in sea surface temperatures and wind conditions affecting the climate over an area), such as marine heatwaves and precipitation anomalies that alter the ecosystem structure and disrupt normal ecological functions (Strydom et al., 2020). The impact of ENSO on ecosystems results in (1) disease outbreaks, (2) species range shifts, and (3) massive die-offs (Hughes et al., 2017; Nowicki et al., 2017; Oliver et al., 2017). For example, the marine heatwave due to the El Nino event between November 2017 to February 2018 near the Chatham Islands resulted in the warmest summer on record in New Zealand (Pinkerton et al., 2019). Warmer sea-surface temperatures affected phytoplankton growth and survival rates and interrupted the ocean's primary productivity (MfE, 2019). Also, in the South Island of New Zealand, marine heatwaves have decreased the species ranges, for example, the loss of Bull Kelp (*Durvillaea species*) in Kaikoura, Christchurch, and Lyttelton (Thomsen et al., 2019). Many environmental and anthropogenic impacts that affect marine ecosystems occur at a much finer scale and can be challenging to detect in dynamic marine environments. These fine-scale changes can be abrupt and frequent, resulting in a complete habitat loss where recovery may be difficult (Frolicher et al., 2018).

Increasing sea-surface temperatures and sea-level rise are environmental threats that impact and alter marine environments. For example, New Zealand's mean sea level has risen by an average of 1.81(±0.05) mm/yr. (MfE, 2019). The main concern with sea-level rise is an increased risk of coastal erosion and increased wave exposure, impacting seaweeds, intertidal seagrass, biodiversity on exposed rocky reefs, and shellfish such as oysters and mussels (Clements and Chopin, 2017).

Another threat to marine biodiversity is increased ocean acidity (Thomsen et al., 2019). Ocean acidity occurs when chemical reactions produce hydrogen ions that acidify the seawater and reduce their pH when carbon dioxide is absorbed from the atmosphere (Clements and Chopin, 2017). According to climate predictions, New Zealand's pH levels in the ocean will drop by 0.3 to 0.04 pH units (MfE, 2019; Stats NZ, 2016). This increase in acidification and temperature will affect biogenic habitats such as oysters and mussels by limiting their carbonate shells growth and larvae distribution leading to a high mortality rate (Clements and Chopin, 2017; Geange et al., 2019).

Impacts from human activities such as development, international shipping and tourism, agriculture, and forestry are significant threats to New Zealand's marine environment (Anderson and Gaston, 2013; MfE, 2019). For example, some significant pollutants from developments are plastic waste and synthetic materials carried by heavy rain and wind, ending up in New Zealand's rivers and oceans (MfE, 2019). Another example is increased pollutants from pharmaceutical chemicals, which mainly threaten nearshore species such as shellfish (oysters and mussels), affecting their survival rates by altering their feeding patterns and reproductive rates (Gaw et al., 2014; Sussarellu et al., 2016). A higher chemical concentration can also soften the outer protective shells and expose the animal to environmental impacts and predators (Dudley et al., 2017).

Additionally, increased vessel arrivals for international trade and tourism threaten New Zealand's native marine species (Seebens et al., 2016). The issue with vessels entering local Harbours is that they could carry invasive species attached to their hull and enter local waters without being detected until their numbers increase (Seebens et al., 2016). These invasive species spread quickly due to their environmental tolerance and fast growth rates, resulting in out-competing native species (Foley and Shears, 2019). For example, the brown seaweed (*Undaria pinnatafida*) continues to spread even after actively removing them (Thomsen et al., 2019). Another example is the Indo-Pacific Sea squirt (*Puyra doppelgangera*), which has displaced the native, green-lipped mussel (MfE, 2019). The Indo-Pacific Sea squirt was discovered in 2015 in Whangarei Harbour and had rapidly spread to Waitemata Harbour by 2016 and spread to the adjacent areas by 2017 (MfE, 2019).

Combined effects from anthropogenic and environmental acts in complex ways to impact intertidal ecosystems, where threats accumulate over decades (Marcello et al., 2015). Consequently, this threat eradicates important keystone species, where recovery might be impossible (Anderson et al., 2019). Therefore, to protect and continuously monitor the status of the ecosystem and critical biogenic habitats, an agile technique is needed to detect the spatial dynamics of nearshore marine environments.

2.2 Ecological function, value, and decline of biogenic benthic habitats

Biogenic habitats form hotspots for biodiversity to support other marine organisms (MacDiarmid et al., 2013). This section will discuss a general overview of seagrass meadows and wild oyster reefs, their ecological function, services, and value. Also, why these habitats are under stress and declining in New Zealand.

2.2.1 Overview of New Zealand seagrass

Seagrass meadows are distributed globally, with approximately 60 species worldwide and 12 genera (Dos-Santos and Matheson, 2017). These meadows share similar leaf architecture, composition, and ecosystem functions in coastal zones ranging from the tropics to temperate regions (Turner and Schwarz, 2006). In addition, these meadows can range from discrete to large continuous patches of homogeneous meadows, ranging from single species to ten species globally (Green and Short, 2003). New Zealand has only one seagrass species, *Zostera muelleri* (Turner and Schwarz, 2006). The spatial scale of seagrass beds in New Zealand at different localities varies in shoots ranging from centimetres to meters **(Figure 5)** to form continuous and discrete patches in diverse landscapes. These seagrass patches exhibit temporal and spatial variations, reflecting recruitment dynamics and dispersal aptitudes (Morrison et al., 2014).

Seagrass meadows commonly occur in sheltered intertidal bays established on mud, sand, and bedrock (Green and Short, 2003). However, they can also be found in subtidal zones of depth up to 7m from the coastline in Ruapuke Island and Foveaux Strait (Morrison et al., 2014).

Figure 5. The spatial variation of seagrass meadows at two localities in New Zealand's North Island. (a) Seagrass at Snell's beach, ~68km North of Auckland from Meola Reef. (b) Seagrass shoot at Meola Reef. Image courtesy of Kavita Prasad

Seagrass meadows maintain their genetic composition from seedling recruitment and propagation (Matheson et al., 2017). Recruitment occurs by rafting shoots and growth from underground roots with a connected network of rhizomes (Kettles and Bell, 2016). Another critical element of dispersal is floating reproductive shoots with roots intact that could indicate rapid natural colonization **(Figure 6)**. However, for growth and distribution, seagrass requires high sunlight levels for photosynthesis, i.e., 25% incident radiation or direct sunlight compared to other angiosperms (Dennison et al., 1993). Hence, seagrass growth rates could be physically variable in different areas.

Therefore, monitoring programmes would need to consider many environmental factors, including (1) dispersal and natural growth rates, (2) rates of change, (3) source of nutrients, (4) sedimentation, (5) water quality, (6) disturbance, and (7) existing and competing vegetation (Dos-Santos and Matheson, 2017). These environmental factors are essential variables that primarily impact the trajectory of seagrass meadows growth and decline, and they should be considered during research. Seagrass meadows are very reactive to environmental changes, such as increased turbidity, and are considered '*sentinels*' for changes to their environment (MacDiarmid et al., 2013).

Figure 6. Floating seagrass meadows with roots intact for rapid natural recolonization in the Waitemata Harbour. Image courtesy of Kavita Prasad

2.2.2 Seagrass ecological function, services, and value

Globally seagrass meadows provide important ecological functions in the coastal ecosystem (Bertelli and Unsworth, 2014). For example, seagrass meadows primary production rate, plankton, and macro epiphytes (such as mangroves and saltmarshes) exceed many cultivated terrestrial ecosystems (Lamb et al., 2017). Their most valued ecological function is regulating carbon through carbon sequestration (Orth et al., 2006). Seagrass produces and exports organic carbon and recycles bacterial pathogens from waste discharge (Barbier et al., 2011; Lamb et al., 2017). These functions are essential for humans, the environment, and maintaining a healthy ecosystem.

Seagrass meadows are locally recognised for providing various ecological services and goods. In New Zealand, ecosystem services provided by seagrass included (1) increased primary productivity to grazing food webs and detrital food webs (Turner and Schwarz, 2006), (2) nutrient recycling, trapping of nutrients, and supply oxygen (Matheson and Wadhwa, 2012), (3) attenuate water flow to stabilize bottom sediments, (4) acted as a crucial feeding and foraging habitat for commercially and recreationally crucial juvenile snapper (*Pagrus auratus*) (Garner et al., 2015), (5) are recognised to increase biodiversity (Lundquist et al., 2018) and (6) provided refuge from predators and maintains food availability for fish and macrofaunal communities (Grech et al., 2012). Researchers from the National Institute of Water and Atmospheric Research (NIWA) sampled fisheries in intertidal and subtidal seagrass assemblages (Morrison et al., 2014). They

found that the subtidal seagrass meadows from Northern New Zealand were crucial juvenile trevally and snapper nurseries.

The fish nursery value of seagrass meadows depends on the coast and landscape setting, tidal position, depth, and latitude (Unsworth et al., 2018). In addition, the economic value of seagrass is affected by seagrass spatial extent, patchiness, seagrass blade density, height, and seagrass health (Matheson and Wadhwa, 2012). Moreover, a recent study confirmed that seagrass density and abundance also affect species diversity (Lundquist et al., 2018). For example, in the Manukau Harbour, Auckland, Northern New Zealand, researchers found greater species diversity and abundance in seagrass meadows in Manukau Harbour, Auckland, New Zealand, compared to surrounding non-vegetated areas (Matheson et al., 2017).

2.2.3 The decline of seagrass in New Zealand

Seagrass meadows in New Zealand are primarily an intertidal habitat, close to coastlines, making them most vulnerable to human-driven stressors and threats (Anderson et al., 2019). Significant coastal infrastructure developments and demand for housing near coastlines in New Zealand are primary contributors to seagrass declines (MfE, 2019). For example, coastal developments in Whangarei Harbour, New Zealand, resulted in heavy vehicles dumping soil for land reclamation along the coastline where seagrass meadows existed (Matheson et al., 2011). Excess sedimentation runoff from developments limits light penetration for seagrass photosynthesis and prompts epiphytes overgrowth from higher nutrient levels (Turner and Schwarz, 2006). Sediment overload is a serious issue because the blades stuck to the deposit start to decay and die off **(Figure 7)**. Another concern is nutrient deposits from streams and stormwater inflows, moving contaminants such as greywater discharge (rich in phosphorus) (Matheson and Schwarz, 2007).

Natural causes of seagrass decline are attributed to grazing by Black Swans in Tauranga Harbour and the Waitemata Harbour during moulting season (Chand and Bollard, 2021; Matheson et al., 2011). In addition, increased ocean temperatures, wasting disease (browning of seagrass leaf blade caused by a fungal infection of the internal tissues) caused by the marine slime mould, *Labyrinthula zosterae* (Matheson et al., 2009). *Labyrinthula zosterae* was detected in New Zealand during the 1960s and has contributed to an extensive decline and "browning-off" of seagrass in the wider Waitemata Harbour (Kettles and Bell, 2016). Anthropogenic contributors to seagrass decline in local Harbours are excessive nutrients from boat effluents, anchorage on seagrass beds, and septic tank leachate discharge (Morrison et al., 2014). A summary of seagrass meadow declines across New Zealand is presented in **(Table 1).**

Some of the severe consequences of seagrass decline in New Zealand's marine ecosystems are (1) reduced biodiversity, (2) poor water quality, and (3) increased turbidity from sedimentation (Anderson et al., 2019). The result of seagrass decline has a cascading effect on the whole

ecosystem. These effects included: (1) reduced production of fisheries, (2) reduction in the ability to filter water, (3) reductions in carbon sequestration, and (4) an increase in harmful algal blooms (Cullen-Unsworth et al., 2014). Changes may be subtle and masked by dynamic coastal and ecological processes (Cullen-Unsworth et al., 2016). Consequently, undetectable changes in seagrass meadows would lead to population fragmentation and a negative effect on metapopulation (Matheson et al., 2011). Undetectable changes could result in a decreased patch size and increased patch loss rate.

The spatial extent of seagrass meadows in New Zealand had been estimated at 44km^2 (Morrison et al., 2014). However, this accuracy is questionable as systematic spatial mapping data is unavailable (Anderson et al., 2019; Spalding et al., 2003). Also, historical losses of seagrass in New Zealand have been poorly documented, and many have gone unrecorded (Morrison et al., 2014).

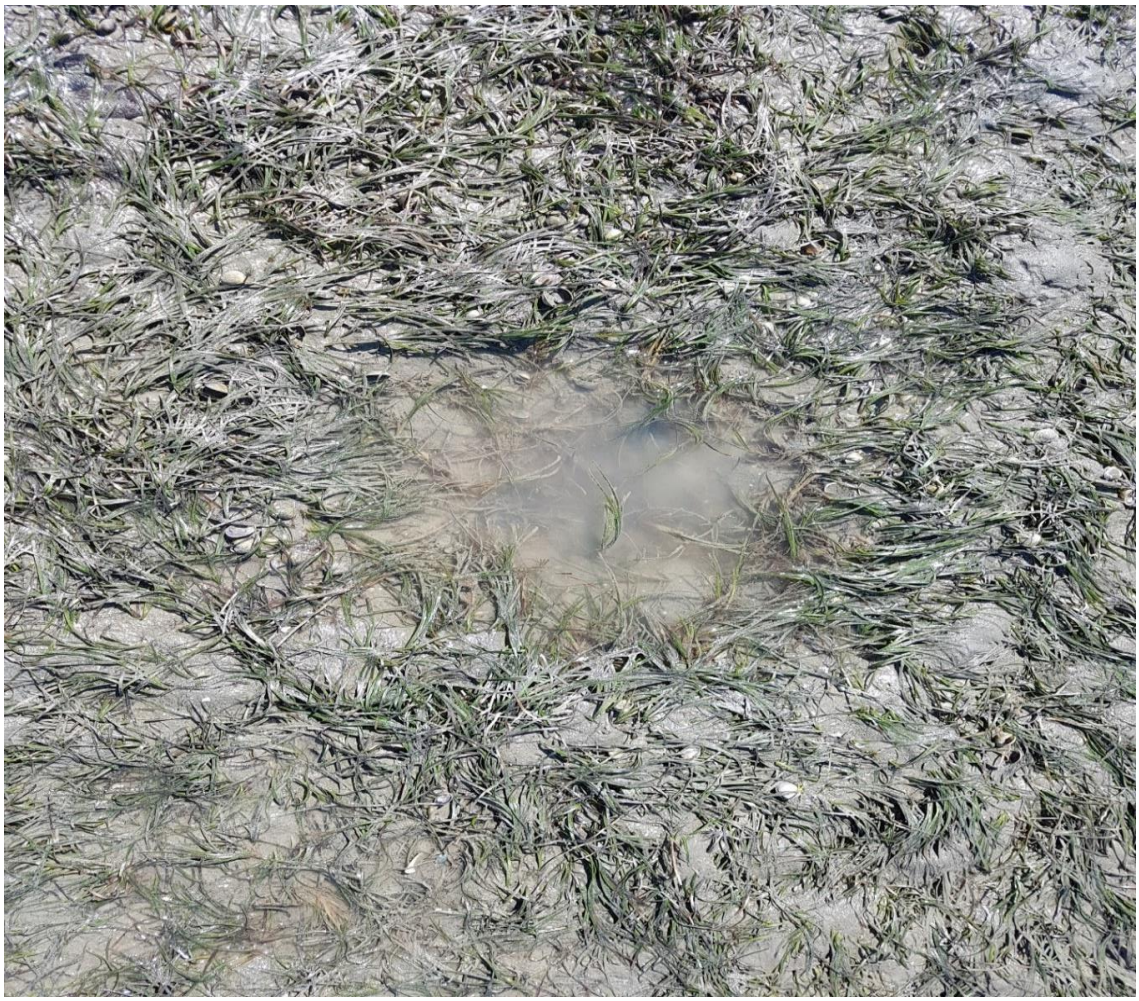

Figure 7. Image showing sediment overload leading to smothering of seagrass meadows during low tide at Cox's Bay adjacent to the Meola Reef. Image courtesy of Kavita Prasad.

Table 1. Summary of seagrass declines across New Zealand's Harbour

Geographic location	Period	Spatial decline	Cause	References
The North Island of New Zealand				
Whangarei Harbour	The 1960s	12-14km^2	Five million tonnes of sediment dumped for port extension	Morrison et al., 2007
Mainland Bay (Rawhiti, Kaimarama, Hauai, Kaingahoa)	1961-2005	Declined from 320000m^2 to <10000m^2	Nutrient enrichment and sedimentation run-offs and boat effluent	Matheson et al., 2017
Waitemata Harbour	1930	Extensive loss	Reclamation and port works	Morrison et al., 2009
	1940-2015	Increased from 7.29 to 43.51 ha	Unknown	Lundquist et al., 2018
Tauranga Harbour	1959 to 1995	34%	Sedimentation run-off	Anderson et al., 2019
Kaipara Harbour	Mid to late 2000	Decreased	Unknown	Anderson et al., 2019
Manukau Harbour	Mid to late 2010	Some recovery	Unknown	Anderson et al., 2019
The South Island of New Zealand				
Avon Heathcote Harbour	Unknown	Complete loss	Unknown	Inglis, 2003

2.3 General Overview of wild oyster reefs in New Zealand

New Zealand has two native species of oysters that are linked with establishing biogenic reefs, (1) the Flat (Bluff) oysters (*Ostrea chilensis*) and (2) the Rock oysters (*Saccostrea glomerata*), including the non-native Pacific oysters (*Crassostrea gigas*) (Foley and Shears, 2019; Morrison et al., 2014). The Pacific wild oysters were introduced during the 1960s in New Zealand from Japan (Foley and Shears, 2019). Pacific oysters were first documented in Northern Auckland, New Zealand, in 1970 (Shears, 2010). In Auckland, on the Te Tokaroa Meola intertidal rocky reef, Pacific oysters were recorded as the dominant species (Ford and Pawley, 2008). However, more assessment is required to confirm the abundance of native Rock oysters on this rocky reef (Foley and Shears, 2019).

The location and distribution of oyster reefs vary across regions and sub-regions in temperate New Zealand estuaries (Foley and Shears, 2019). The Pacific oysters have dominated northern estuaries in New Zealand and displaced Rock oysters in many locations (Morrison et al., 2014). Pacific wild oysters and Rock wild oysters have a North Island distribution, and the Flat oysters

have established themselves all around New Zealand (Morrison et al., 2014). In the Southern region of New Zealand, from Nelson to Marlborough, Pacific oysters have formed biogenic reef beds (Morrison et al., 2014). It is worth noting that the Pacific oyster is a significant contributor to the aquaculture industry in New Zealand (Morrison et al., 2014).

2.3.1 Wild oyster reefs ecological function, services, and value

Oyster reefs function as ecosystem engineers in temperate nearshore marine environments (Thorngren et al., 2017). They provide essential ecological services to support marine biodiversity, including (1) water filtration, (2) creating 3D style structures to store and trap food for associated biodiversity, e.g., invertebrates, juvenile fish, and (3) nesting grounds for seabirds (Beck et al., 2011; Thorngren et al., 2017). Blank oyster shells stabilize and defend the coastlines from surging waves (Butchart et al., 2010). Live oysters filter and recycle suspended solids from the water column to help prevent harmful algal blooms directly and simultaneously help maintain water clarity for seagrass growth (Newell, 2004). Other important ecological services provided by wild oysters include removing excess nutrients, such as nitrogen, from polluted coastal waters from agricultural runoff and sewage (Newell et al., 2005). Other vital functions of wild oyster reefs include enriching coastal fisheries biodiversity, directly linked to social and recreational activities such as game fishing and tourism (Ridge et al., 2020).

The value of wild oyster reefs can be associated with their functions primarily through growth and improved recruitment (Byers et al., 2015). Their value is directly related to the production rate and revenue generated from fisheries sale. For example, full credit is given to a species whose expected production rate is enhanced, while fractional credit is given to those species whose production rate is modestly improved (Peterson et al., 2003). The estimated value of wild oyster reefs was calculated by the rate of fisheries recruitment and expected production rates per unit area in a re-established oyster reef (Peterson et al., 2003). Using this technique, a $10m^2$ space of the re-established wild oyster reefs yielded an additional 2.6 kg of large mobile crustaceans and fisheries annually (Morrison et al., 2014). In New Zealand, wild oysters by customary local fishers of the Awarua Runanga are a natural resource that is highly prized (Anderson et al., 2019). The actual value and contributions of Pacific and Rock wild oyster reefs to local fisheries in New Zealand remain unknown (Morrison et al., 2014).

2.3.2 Declining of wild oysters in New Zealand

Globally wild oyster populations have declined over the last 130 years, with a total global loss estimated at 85% (Beck et al., 2011). In New Zealand, the Foveaux Strait region experienced a 90-99% historical loss of Rock oysters, and the Bluff oysters were categorized as in "Poor condition" (Morrison et al., 2014). Mainland New Zealand had a 50-89% wild oyster population decline and was classified as "Fair condition" (Morrison et al., 2014). In the Foveaux Strait region,

large-scale mortality of Bluff oysters has been attributed to the microcell parasite *Bonamia exitiosa* (Michael, 2007).

On the Meola reef **(Figure 2)**, the population of Rock oysters has declined in Auckland, New Zealand, due to (1) invasive Pacific oysters, (2) an escalation in oyster borer snail (*Haustrum scobina*) population, (3) increased sedimentation, and (4) heavy metal concentration (Aguirre et al., 2016; Foley and Shears, 2019). Over-harvesting is another cause of wild oysters decline, leading to a fragmented metapopulation without recovery (Beck et al., 2011). Other contributors to wild oyster decline are attributed to (1) dredging, (2) trawling, (3) coastal alteration from developments, and (4) nutrient and toxin overload (Anderson et al., 2019; Morrison et al., 2014).

2.4 Research methods for seagrass and wild oyster reef

Over time, researchers have developed many techniques using remotely sensed (aerial and satellite) imagery and *in-situ* (also referred to as traditional technique) to map and monitor seagrass meadows and wild oyster reefs. These techniques were essential for monitoring the status of these habitats but had limitations. This section reviewed remotely sensed, and traditional methods used for mapping and monitoring seagrass and wild oyster reefs and identified their limitations.

2.4.1 Seagrass research methods: remotely sensed and traditional

Initially, aerial photographs and satellite imagery were the primary data sources for mapping seagrass meadows (Phinn et al., 2017). Using aerial photos, Haegele (1975) mapped underwater seagrass vegetation in Ganges Harbour and the French Creek. Haegele's research established that underwater seagrass mapping was more straightforward during low tides when combined with a coloured-infrared film. However, this research did not mention the water clarity during high tide, and classification was performed manually from the infrared photographs using a mirror stereoscope and validated from scuba surveys Haegele (1975).

Mumby et al., 1998 in the British West Indies used an airborne platform with a compact airborne spectrographic imager (CASI) to assess seagrass meadows, coral, and algae. Based on *in-situ* field survey information, these habitats were categorized into coarse and fine habitats. Seagrass was classified as a coarse habitat, and the accuracy ranged from 81- 89% for all habitat types. Although a high classification accuracy was achieved, this airborne platform could only detect limited seagrass, coral, and algae species, limiting its effectiveness.

The Landsat satellite missions have one of the most extensive satellite imagery archives that researchers have used to map seagrass over extensive spatial extents (Dekker et al., 2007; Ferguson and Korfmacher, 1997). Roelfsema et al., 2009 mapped seagrass meadows using a combination of Landsat-5 thematic mapper multispectral imagery and *in-situ* field surveys

conducted from a towed camera and spot surveys in Morten Bay, Australia. Although classification accuracy was 83%, the field surveys were complicated and time-consuming. Additional support and a boat were required to tow the camera, and experienced personnel were needed for video interpretations. In contrast, Phinn et al., 2017, used Medium Resolution Imaging Spectrometer (MERIS) and Moderate Resolution Imaging Spectroradiometer (MODIS) satellite imagery to understand the physical, biochemical, and environmental variables associated with seagrass meadows. One of the limitations of this study was that due to low spatial resolution, researchers could not estimate the spatial extent of seagrass meadows.

For mapping seagrass meadows globally, researchers have also used high spatial resolution satellite imagery that ranged from 5 to 50cm, such as SPOT 5 and 7 (Pasqualini et al., 2005; Siregar et al., 2018), IKONOS (Pu and Bell, 2017), Geo-Eye (Chayhard et al., 2018), WorldView-2 and 3 (Collin et al., 2019; Poursanidis et al., 2018), Quick-Bird (Hisabayashi et al., 2018), KOMPSAT-2 (Choi et al., 2018), Rapid-Eye (Traganos and Reinartz, 2018) and Planet-Scope (Traganos et al., 2017). However, the limitations of atmospheric and spectral band attenuation continue to persist.

Field-based traditional methods for seagrass research typically involved transects and quadrats in quantifying and identifying seagrass species (Morrison et al., 2014). Often for species-level discrimination and to measure their morphological features, e.g., stem size in a heterogeneous ecosystem, *in-situ* samples were used (Veettil et al., 2020). In addition, researchers collected *in-situ* spectral reflectance samples of seagrass meadows from a Spectro-radiometer (Veettil et al., 2020). However, the spectral reflectance information may vary with seasonal changes and water depth, and the Spectro-radiometer requires a recalibration after a shift in illumination (Veettil et al., 2020). *In-situ* field sampling tasks are tedious and physically challenging in mudflats, increasing the chances of error and data inconsistency resulting from fatigue (Morrison et al., 2014). Researchers can collect high-resolution data on the ground, but sampling over large spaces can be challenging (Johnston, 2019).

2.5 Oyster research methods: remotely sensed and traditional

Over time, aerial photographs and satellite imagery were developed more effectively to map and monitor wild oyster reef habitats (Schill et al., 2006). Initially, researchers used aerial photographs and different interpretation techniques to detect the presence of dead and live oyster reefs, such as image illumination differences (Grizzle et al., 2002; Kater and Baars, 2004). Researchers have also used aerial imagery to (1) assess long-term spectral characteristics of oysters, (2) identify anthropogenic and environmental impacts on the distribution of oysters, and (3) quantify loss over time (Grizzle et al., 2002; Garvis et al., 2015; Seavey et al., 2011). The spectral properties in aerial photographs at different wavelengths were insufficient to distinguish between live and dead

oysters over extensive areas (Power et al., 2010). Other challenges for oyster research included (1) dimensions of the oysters being variable in size to being mapped and differentiated, (2) variations in the spectral signature during exposure and seasonal changes such as rewetting, drying out, algal growth, and different species composition, and (3) tidal influences and sediments at varying water depths during image capture (Power et al., 2010; Schill et al., 2006). Researchers have established that low spatial resolution aerial imagery can only do a marginal estimation of oyster reef habitat and fails to assess loss consistently (NOAA, 2003; Power et al., 2010).

In 2003, the Marine Resources Division of the South Carolina Department of Natural Resources (SCDNR) and The National Oceanic and Atmospheric Administration (NOAA) Coastal Remote Sensing Programmes focused on developing new techniques using remotely sensed imagery for mapping intertidal oyster reefs (NOAA, 2003). The NOAA project focused on providing researchers at SCDNR with potential and efficient methodologies to assess wild oyster reefs through high-resolution aerial imagery digitization (NOAA, 2003). Their project examined the effectiveness of the following analysis techniques: (1) manual delineation using supervised and unsupervised spectral clustering, (2) spectral and feature analysis, (3) image-derived data, and (4) image segmentation. In the SCDNR research, feature analysis and image-derived data performed better than other techniques that identified the spatial extent, perimeter attributes, and wild oyster reef conditions (strata). Although the high-resolution imagery provided accurate results, one of the limitations in this research was difficulty discriminating wild oyster reefs from mud (NOAA, 2003). Likewise, Schmidt, 2000 used multispectral satellite imagery to classify wild oyster reefs but had limited success. This was primarily due to the broad spectral bandwidths in the satellite imagery used, leading to misclassifications between wild oyster reefs and mud (Schmidt, 2000). It is important to note that discrepancies occurred because of different satellite sensors, atmospheric and radiometric correction, day and time of data capture, sun angle, and seasonal changes between the habitats being sensed (Nieuwhof et al., 2015; Schill et al., 2006). Even if seasonal variables are kept constant during data capture, obtaining resemblance between datasets can be challenging (Le Bris et al., 2016). Moreover, temporal lags between satellite imagery acquisition and low spatial resolution can create oversight to detect rapid changes in wild oyster reef habitats (Windle et al., 2019).

Traditional wild oyster reef research methods included collecting data from global positional systems (GPS) and *in-situ* field surveys with transects and quadrats (Windle et al., 2019). The traditional techniques used for shellfish resource mapping have also been challenging due to the rugged and muddy environments where wild oysters are located (Nieuwhof et al., 2015). Traditional oyster reef monitoring techniques are subject to (1) errors, (2) human inconsistencies, (3) cause damage to the reef environment, and (4) are time intensive (Windle et al., 2019). In addition, traditional techniques can be constrained to a small spatial extent, limiting the

technique's applicability (Power et al., 2010). For example, on the Meola reef, Auckland, New Zealand, the Pacific oyster population had a gradual decline that was not detected until 2012 (Foley and Shears, 2019).

The limitations presented above using satellite and aerial imagery, including *in-situ* techniques for seagrass and wild oyster reefs research, are being addressed by the scientific community through the application of remotely piloted aircraft systems (Chand and Bollard, 2021 – see Chapters 3 and 5; Duffy et al., 2018; Ridge et al., 2020; Windle et al., 2019). RPAS technology can be used for rapid assessments and has been identified as an accurate method for spatial assessment of intertidal seagrass and oyster reefs, allowing for replicability overtime at a low cost (Duffy et al., 2018; Windle et al., 2019).

2.6 RPAS for marine ecology and conservation

In marine ecology and conservation, the application of lightweight RPAS (<25kg) has been used for various applications (Garrett et al., 2018). Anderson and Gaston, 2013 claimed that RPAS would revolutionise marine spatial ecology, and their applications have extended to atmospheric sampling Greatwood et al., 2017; mapping coral reefs Casella et al., 2017; mapping and monitoring of ecologically delicate marine habitats Ventura et al., 2018; monitoring and mapping wetlands vegetation Chabot et al., 2018; mussel demographics Gomes et al., 2018; intertidal reef monitoring Murfitt et al., 2017; humpback whale behavioural responses Fiori et al., 2020; and remote environment monitoring (Trasvina-Moreno et al., 2017).

RPAS low altitude remote sensing has allowed researchers to identify fine-scale changes in marine ecosystems, which was not previously possible with other remotely sensed products (Dronova, 2015; Seymour et al., 2017). For example, multi-rotors RPAS have been used for real-time surveying, monitoring, mapping coral reef health, georeferencing satellite and crewed aircraft data covering ± 5km^2 (Casella et al., 2016; Ventura et al., 2016). In contrast, fixed-wing RPAS have been used for their ability to survey large spatial extends (>10 km^2) and flight efficiency (45 minutes) (Konar and Iken, 2018)

2.7 RPAS sensors

A specialised range of sensors can be integrated onto RPAS platforms, but researchers need to understand sensor limitations and operational specifications (Espriella et al., 2020). One crucial aspect for researchers is evaluating and understanding sensor specifications to capture quality datasets for their research (Aasen et al., 2018). Without considering this specification, it may lead to poor quality datasets and unacceptable aerial survey expectations (Collin et al., 2019). Another specification to consider is whether the sensor can be remotely triggered to activate image capture. If not, recording data before take-off would require additional storage capacity and extra data

post-flight editing (Reus et al., 2018). Some sensors allow for an intervalometer function or time-lapse through the flight planning software, while others do not (Hassanalian and Abdelkefi, 2017). Although in some instances, this can be modified through a firmware modification.

Sensor sensitivity during aerial surveys relative to RPAS flight characteristics is essential for high-quality data capture (Aasen et al., 2018). Signals from RPAS motors, vibrations, and propeller wash can affect imagery, leading to distorted images and artifacts in the imagery (Rieucau et al., 2018). Therefore, a system with gimbals or other forms of stabilization with adjustable shutter speeds is desired (Aasen et al., 2018).

RPAS snapshot and push-broom sensing systems can satisfy the demand for an extensive array of marine applications (Collin et al., 2019; Marcello et al., 2015; Reus et al., 2018). However, choosing a sensor that meets all the research requirements can be challenging. Depending on the application, a high spatial resolution sensor will lead to a narrow wavelength for a particular band (Aasen et al., 2018). Higher altitudes RPAS flights covering large spatial extents will result in a low spatial resolution. Moreover, to block a specific spectrum of light, an additional filter can be put on the sensor (Rieucau et al., 2018). These add-on filters provide researchers flexibility and specific bands required to discriminate between co-occurring plant species in the marine environment (Lomax et al., 2005). A comprehensive review of sensors for marine applications are presented in **(Table 2)**. Furthermore, the increasing availability of miniaturized hyperspectral sensors requires innovative analytical techniques for data analysis (Lopez and Mulero-Pazmany, 2019).

Generally, a sensor can be distinguished by the number of bands and arrangements (Lopez and Mulero-Pazmany, 2019). In addition, sensors can be classified based on their spectral differentiation and the technique by which they achieve their spatial differentiation (Aasen et al., 2018; Sellar and Boreman, 2005). The following sections (2.7.1 to 2.7.5) reviewed the most common types of sensors used on RPAS platforms and their applications.

2.7.1 Spectro-radiometers, also referred to as Point Spectrometers

Spectro-radiometer sensors are becoming commercially available as a miniaturized version fully compatible with RPAS. Researchers have developed an ultra-lightweight RPAS spectrometer system for field spectroscopy (Burkart et al., 2015). The spectral information collected from this spectro-radiometer ranged from 338nm to 824nm wavelengths that measured vegetation's bidirectional reflectance distribution function (Burkart et al., 2015). Their spatial coverage is dependent on distance to the object and field of view (FOV) (Aasen et al., 2018). Recently, Shang et al., 2017, used a spectro-radiometer to monitor phytoplankton blooms in Taiwan. The main advantage of this sensor was its ability to capture very high-resolution spectral data and is

lightweight. However, they required extra GPS instruments for spatial referencing (Burkart et al., 2015).

2.7.2 Push-broom spectrometers

Push-broom hyperspectral sensors record a line of spectral information (Aasen et al., 2018). These sensors are operated by repeatedly recording individual lines with all spectral information about the object (Aasen et al., 2018). In the image, each pixel represented the object's spectral signatures within its instantaneous field of view (IFOV) (Burkart et al., 2015). Researchers have used a Push-broom sensor on a fixed-wing RPAS platform at altitudes of 330 to 575m from the surface and achieved a spatial resolution of 0.3m (Aasen et al., 2018). Moreover, Lucieer et al., 2014; Malenovsky et al., 2017 used a Headwall Photonics Micro-Hyper-spec VNIR (Headwall Inc., USA) push-broom sensor to map Antarctic moss beds with multi-rotors and achieved less than ten-centimetre per pixel ultra-high spatial resolution imagery. The limitations of this sensor are that they are heavy, so they can only be flown at slow speeds, making it challenging to map more extensive areas and requires a powerful onboard computer (Aasen et al., 2018). They also need additional GPS equipment onboard the RPAS for accurate georeferencing (Aasen et al., 2018).

2.7.3 Multi-Sensor: 2 Dimensional (2D) Imagers

These sensors, at every exposure, collected spectral information in 2D (Aasen et al., 2018). A 2D imager system uses many integrated sensors to record either hyper or multispectral images (Turner et al., 2014). Additional spectral information can be achieved by putting filters with specific wavelength configurations before the sensor (Aasen et al., 2018). Recently compact mini-multi-sensor array systems available in the market are MicaSense RedEdge M and Parrot Sequoia with spectral range 550nm to 790nm wavelength and RedEdge (-M) spectral range 475nm to 840nm wavelength with blue, green, red, red-edge, and near-infrared bands (MicaSense, 2017) Their applications ranged from agricultural crop health monitoring, and mangrove leaf area index (LAI), seagrass change detection (Chand and Bollard, 2022; Dash et al., 2017; Turner et al., 2014).

2.7.4 Sequential: 2D Imagers

Sequential 2D Imagers capture spectral bands chronologically, with a time gap between two sequential spectra bands (Nasi et al., 2018). Their spectral resolution ranged from ~500nm to 900nm wavelengths (Aasen et al., 2018). An example of this sensor is Rikola hyperspectral imager by Seno Oy (Nevalainen et al., 2017). These sensors are primarily used in remote environmental sensing, such as tree species classification, biodiversity assessment, and mineral exploration (Jakob et al., 2017; Nevalainen et al., 2017; Nasi et al., 2018).

2.7.5 RGB sensors and modified RGB sensors

RGB sensors capture the subject's reflectance along three spectral bands, red, green, and blue (RGB), along the visible electromagnetic spectrum, and their spectral resolution range from 400nm to 700nm wavelengths. RGBS sensors are low-cost to capture imagery at a very high spatial resolution but limited spectral resolution. To overcome limited spectral resolution, researchers have modified RGB sensors with an additional infrared band, RGBN extending the spectral resolution up to 840nm wavelengths (Aasen et al., 2018). For example, the Canon s110 NIR (near-infrared), green (560nm, FWHM: 50nm), red (625nm, FWHM: 90nm), and NIR (850nm, FWHM: 100nm) (Aasen et al., 2018). The main limitation of this sensor is an overlap between spectral bands, low radiometric resolutions, and images are stored in raw data format, e.g., digital negative (DNG) (Aasen et al., 2018).

2.7.6 Limitation of RPAS sensors for marine applications

The rapid advancement in technology has introduced new types of sensors. This diversity makes data quality assurance critical for researchers, particularly for spectral remote sensing and quantitative methodology, given the challenges associated with radiometric and geometric correction required for precise spectroscopy-focused marine environment remote sensing. For example, in the Gulf of Mexico, Florida, researchers used an RGB imaging system mounted on an RPAS to classify intertidal habitats (e.g., oyster reefs, saltmarsh, and mudflats) (Espriella et al., 2020). This study achieved a classification accuracy of 79%; however, misclassifications occurred between oysters and saltmarsh due to low spectral and textual separation. In New Zealand, Oaro reef, in Kaikoura, researchers tested three RPAS imagery, (1) three-band RGB imagery, (2) multispectral six band imagery, and (3) a composited nine bands imagery to assess macroalgae (Tait et al., 2019). Their results showed for biodiversity assessments in shallow habitats, six-band imagery achieved an 81% accuracy compared to 79% accuracy for the three-band RGB imagery. In contrast, the composite nine-band imagery achieved 90% overall accuracy (Tait et al., 2019). Although the multispectral imagery had better classification accuracy, the RGB imagery had better results for broad habitat classification. Using hyper and multispectral sensors, researchers can yield higher classification accuracy and taxonomic variations (Tait et al., 2019).

2.8 Method for RPAS image processing

2.8.1 Structure-from-Motion (SfM) Photogrammetry

Photogrammetry has its earliest origin in surveillance and reconnaissance to gather information about different locations from aerial photographs (Duffy et al., 2020; Pettorelli et al., 2018). SfM provides a solution for RPAS onboard sensor integration. The high geometric fidelity of the block bundle adjustment during SfM processing uses the camera angle that determines the orientation and position of the sensor (Aasen et al., 2018). SfM technique integrates a sequence of 2D

geotagged photographs to reconstruct into a 3D structure of a feature or landscape (D'Urban Jackson et al., 2020). SfM technique automatically transforms digital photos from a vantage point using three main steps to be transformed into a textured 3D model. First, during processing SfM algorithm relocates individual pixels to their spatial locations to account for a collective error from angular terrain effects and lens distortion (D'Urban Jackson et al., 2020). The process is as follows: initially, the algorithm (SfM) detects and identifies geometrically similar feature points in all the input images at different angles. This information is then used as inputs, and the position of the feature points is predicted and translated into a sparse x, y, and z three-dimensional (3D) point cloud (Verhoeven, 2011). Second, the facade of the 3D model is constructed. Third, the photogrammetry software uses a compact, multi-view stereo-matching algorithm to produce a polygonal mesh illustrated on the computer screen as a shaded, solid wireframe mode (Ventura et al., 2016). Finally, the polygonal mesh is textured with the initial geotagged photographs (Verhoeven, 2011) **(Figure 8)**. There is no guarantee that high-resolution data from RPAS will necessarily be processed in the SfM photogrammetric without errors, especially images captured over water (Oleksyn et al., 2021).

Furthermore, the point cloud generated by SfM is generally in an arbitrary reference frame (Oleksyn et al., 2021). This point cloud needs to be registered to an absolute world location coordinate system to increase the positional/spatial accuracy of the orthomosaic (Harwin et al., 2015). An absolute location in the world coordinate system can be registered by identifying key features such as surveyed marks or ground control points (GCPs) in the point cloud to known real-world coordinates. However, in marine environments, GCPs are not available. The solution is to distribute highly visible GCPs during low tides manually. The following section summarizes the expected RPAS spatial accuracy using different positional accuracy equipment and techniques.

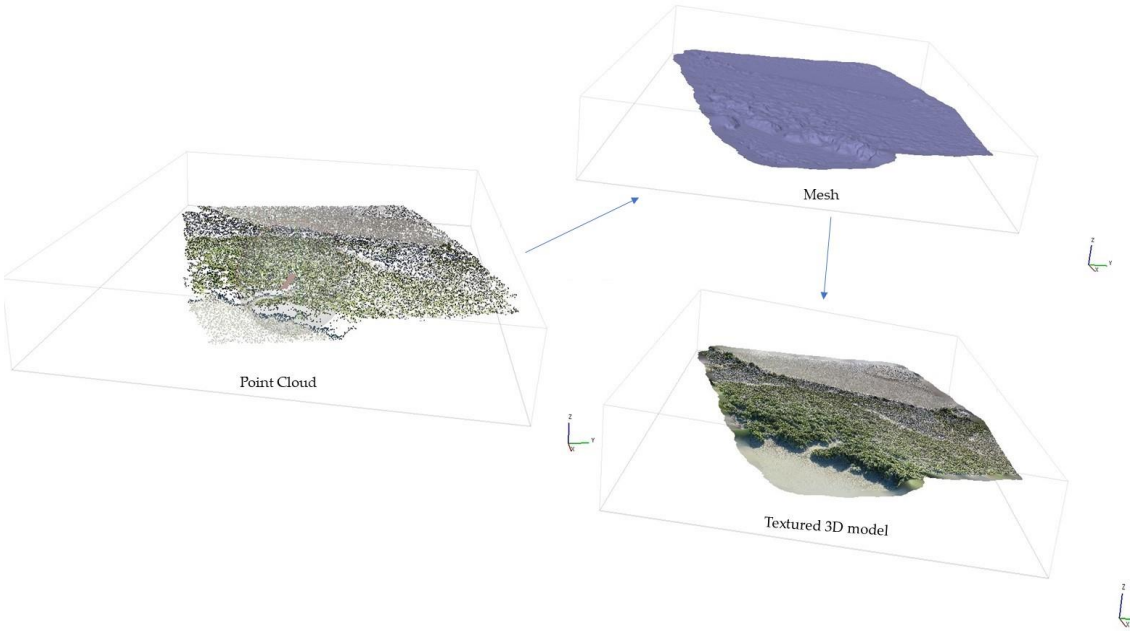

Figure 8. An overview of the SfM photogrammetry workflow during image processing in Pix4D. Initially, a point-cloud is generated from the geotagged RPAS images. The polygonal mesh is generated as a shaded, solid wireframe mode, and finally, the mesh is filled with texture. Image source Pix4D (2019).

2.9 RPAS spatial accuracy

Spatial accuracy is how accurately aerial imagery aligns with other datasets or reference maps obtained from the absolute latitude and longitude coordinates. For example, if satellite imagery is used, the final product's spatial accuracy will depend on the spatial accuracy of that satellite imagery. Consumer-grade RPAS are equipped with built-in Global Positioning Systems (GPS) to provide users an expected spatial/positional accuracy in X (longitude) and Y (latitude), typically ranging from ± 2 to 5 meters or as low as ± 10 meters (Gomes et al., 2018). The main advantage of this approach is that researchers can collect enough data for complete orthorectification and georeferencing based on onboard data alone and limited fieldwork.

The advancement in technology has allowed survey-grade GPS to be integrated into RPAS. For example, the DJI Phantom 4 RTK system can deliver an average vertical accuracy of 2cm and horizontal accuracy of 1.2cm without ground control points (GCPs) (Oleksyn et al., 2021). The other option for improved positional accuracy is the post-processing kinematic (PPK) global navigation satellite system (GNSS) solution, which is highly comparable to the RTK system but requires post-processing of flight logs (Giones and Brem, 2017). Users can also do a differential correction from a known base station for precise positional accuracy.

2.9.1 Ground control points (GCPs)

GCPs are usually used for non-direct georeferencing results. For example, in marine environments, there are no fixed surveyed markers; hence, researchers have typically used 5-13 randomly distributed ground control points to improve spatial accuracy (Chand and Bollard,

2021; Windle et al., 2019). To achieve an absolute geospatial accuracy ranging from 2-4cm, these GCPs markers are generally surveyed with a real-time kinematic (RTK) Global Navigation Satellite System (GNSS) or a total station (accuracy up to 1cm and better) to get accurate coordinated for the GCPs **(Figure 9)**. These GCPs can be identified in the RPAS imagery, and during bundle adjustment, a geometric transformation is performed through photogrammetric modelling (Aasen et al., 2018).

Figure 9. The image shows ground control points collected and surveyed at Meola Reef, Auckland, with a rover and a ground-based station Septentrio ® RTK survey system. Image captured by Subhash Chand

2.10 Remote sensing application challenges in marine environments

Nearshore marine environments are highly complex and dynamic (Pettorelli et al., 2014). The variations across the marine environment create a high level of spectral divergence, further challenging classification algorithms (Schwantes et al., 2018). Therefore, to increase classification accuracy, researchers mainly rely on spatial resolution and image texture to enhance features that can be discriminated between different cover types (Laba et al., 2010). Texture in remotely sensed imagery is the spatial distribution of colours/tones across the pixels (Pettorelli et al., 2014) used to increase classification accuracy in multispectral imagery (Schwantes et al., 2018). The spatial resolution in remotely sensed imagery can be referred to as the size of the smallest feature being detected by a sensor (Laba et al., 2010).

The USGS provides researchers free access to a collection of aerial and high-resolution satellite imagery such as OrbView3, past SPOT, and IKONOS-2 through Earth-Explorer (Pettorelli et al.,

2014; Turner et al., 2013). Despite high-resolution satellite imagery, marine applications' challenges still exist, such as a trade-off between the signal-to-noise ratio (SNR) and spatial resolution (Pettorelli et al., 2014). This trade-off implies that the sensor's spatial resolution could not be increased to match the researcher's application requirements unless paid (Schwantes et al., 2018). Still, if the spatial resolution is improved, it could decrease radiometric and spectral resolutions (Nagendra and Rocchini, 2008). The other challenge with high-resolution satellite imagery often leads to spectral mixing and creates segmentations that are difficult to discriminate between cover types, eventually decreasing classification accuracy (Schwantes et al., 2018).

Further challenges are desired tidal datasets availability and coverage, in-house capacity to process aerial and satellite datasets further, and security concerns that limit access to high spatial resolution imagery, e.g., South Asia (Nagendra and Rocchini, 2008; Pettorelli et al., 2014). The other challenge for marine research is acquiring *in-situ* ground truth data in inaccessible areas, which is integral for accuracy assessments. Besides, it can be challenging for novice researchers to integrate *in-situ* field datasets with remotely sensed products (Pettorelli et al., 2014).

Casella et al., 2017 have established that remote imaging through clear tropical waters within a few meters can be effortless for mapping coral reefs because the wavelengths can penetrate water much deeper in clear waters. For example, the blue spectral band with a 400nm wavelength passing through 100m of water will be half-bright (Purkis, 2018). However, spectral band attenuation increases with wavelength. For example, the wavelength of the red spectral band with 620nm to 750nm can only penetrate a few meters in clear water, and infrared bands 840nm can only penetrate a few centimetres (Purkis, 2018).

Another critical challenge for marine applications is comparing *in-situ* field data with satellite and aerial imagery (Pettorelli et al., 2014). However, this is restricted by an ecologist's knowledge of remote sensing products and application protocols (Nagendra et al., 2013). Limited knowledge of remote sensing products leads to underused, unappreciated datasets (Pettorelli et al., 2014). Usually, this challenge leads to difficulty understanding the benefits of remotely sensed products and their shortcomings. For example, poorly referenced remotely sensed imagery cannot be fully integrated with *in-situ* datasets and inability to locate time-relevant remote sensing datasets (Schwantes et al., 2018). Finally, the limited access to multi-temporal remotely sensed datasets is another challenge marine researchers face (Pettorelli et al., 2014).

On the contrary, temperate marine environments can also be challenging for RPAS surveys due to increased suspended particles in the water column (Espriella et al., 2020). Regardless of the imaging system's spectral resolution, spectral dampening (electromagnetic signals weakens) increases with depth at 2-3m, and detection is only possible for broad classes of submerged vegetation (Tait et al., 2019). In contrast to aerial and satellite imagery, researchers have the

option to operate RPAS for marine applications at optimum conditions during low tides (Chand and Bollard, 2022; Duffy et al., 2018).

2.10.1 Cost challenges

The costs that originate from operating an RPAS for extended periods are complicated to compute but depend on many components' collaboration (Pettorelli et al., 2018). The challenges arising from cost are primarily reliant on acquiring sophisticated instruments onboard, such as sensors, advanced telemetry communications systems, long-endurance, and heavy payload capability aircraft (Pettorelli et al., 2014). Usually, the payload is the most expensive part of the aircraft, which unfortunately breaks down (Lopez and Mulero-Pazmany, 2019).

Today there is no definite solution covering all conservation applications, as there are trade-offs between the cost of the sensors and the RPAS platform (Pettorelli et al., 2018). To be cost-effective, researchers have tried and tested different methods. For example, Ventura et al., 2018 modified and successfully used a Go-Hero Black edition sensor on a quadcopter to investigate and map seagrass meadows, a rocky coast containing juvenile fish, and two sandy beaches locations with biogenic reefs.

In addition, the upsurge in cost can be directly related to the significant volume of data accumulated, processed, and then stored, often requiring competent information technology personnel and infrastructure (Pettorelli et al., 2018). A large quantity of data collected during aerial surveys will create a bottle-neck effect in operation or research if they are not processed, passed on for classification, and moved to storage effectively (Lopez and Mulero-Pazmany, 2019). The marine environment is a space filled with uncertainty. For example, wind conditions could change suddenly and are occupied by low flying shorebirds where accidents could happen during RPAS operations. Also, breakdowns would compromise the project's viability, consequently increasing cost (Lopez and Mulero-Pazmany, 2019).

Nevertheless, it is universally agreed that the cost connected with RPAS applications is lower than some recognized techniques in the scientific community (Lopez and Mulero-Pazmany, 2019). For example, for seagrass and wild oyster reefs research, *in-situ* fieldwork can be (1) laborious and costly, (2) often there is a trade-off between frequency and sample size, (3) target habitat can be situated in inaccessible isolated areas, and (4) *in-situ* field sampling may cause disturbance to flora and fauna (Duffy et al., 2015). In contrast, RPAS surveys (1) are cheaper, costing around 1200 NZD for a consumer-grade RPAS with an RGB sensor, (2) ability to calculate leaf area index (LAI) and above-ground biomass (3) is less invasive, and (4) can cover large spatial extents at higher altitudes (not exceeding 120m from surface) (Ventura et al., 2017).

2.10.2 Environmental challenges

Turbidity remains a constant environmental challenge in temperate coastal marine waters (Lopez and Mulero-Pazmany, 2019). For example, runoff during heavy rainfall increase sedimentation flow into the ocean during extreme weather, reduce sensor visibility, and increase spectral complexity, making detection challenging (Oleksyn et al., 2021). This challenge is significant because it restricts RPAS surveys and research within habitats that do not exceed 5-meter depths unless water clarity is 100 percent (Oleksyn et al., 2021) **(Figure 10)**.

Furthermore, remote detection of submerged vegetation through turbid waters is challenging, irrespective of the high-quality sensing system (Tait et al., 2019). This challenge often leads to the misclassification of different submerged vegetations. For example, in the Oaro reef, in Kaikoura, New Zealand, researchers used an Airphen six-band multispectral sensor and a Sony mirrorless RGB sensor to classify macroalgae (Tait et al., 2019). However, spectral dampening occurred at 2-3m depths in both sensors, limiting detection for a broadly submerged algal group (Tait et al., 2019).

Researchers have also encountered environmental challenges when using RPAS in terrestrial environments, for example, wildlife census (Seymour et al., 2017b). However, computer vision and machine learning techniques have automated such tasks if delivered and analysed by highly qualified personnel (Andrew and Shepard, 2017). Nevertheless, computer vision and machine learning techniques only apply to reasonably easy-to-locate species in clear shallow turbid waters (Oleksyn et al., 2021). Therefore, manual counting and identifying individual species is highly recommended for more reliable and accurate results but takes a substantial investment in costs and time (Seymour et al., 2017).

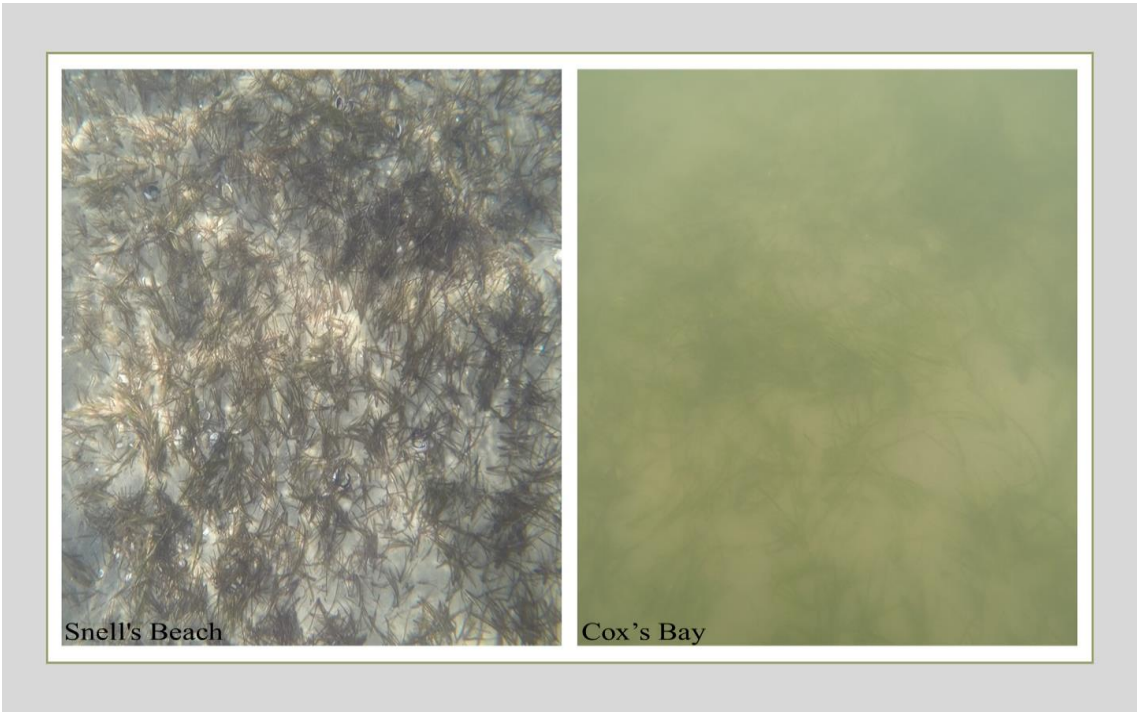

Figure 10. Images showing submerged seagrass meadows and water clarity at two locations in New Zealand during high tide. The image on the left with 100% visibility is from Snell's beach ~64km away from Auckland, and the right image is from Cox's Bay adjacent to Meola Reef, close to Auckland city. Kavita Prasad captured the images with a Go-Pro camera.

2.10.3 Motion blur challenge and solution

Motion blur is a crucial image quality-degrading challenge in all remotely sensed imagery (Pettorelli et al., 2018). Motion blur occurs during aerial image capture because the feature being captured moved during the time it took to expose the image, and the movement will be recorded as a blur. The introduction of motion blur in aerial images increases the severity of artifacts in the imagery and creates a uniform texture (Seymour et al., 2017b). Motion blur in RPAS imagery is mainly caused by the degradation effect of blur caused by sensor instability or poorly mounted sensors (Seymour et al., 2017). These poorly mounted sensors vibrate during image acquisition and produce blurry images (Oleksyn et al., 2021). In addition, a poorly mounted sensor can change its viewing angle during flights (Nahirnick et al., 2018). Motion blurred images create errors during SfM automatic image processing (Ventura et al., 2016).

Moreover, another source of motion blur is correlated to dynamic-wind speeds. For example, Lehmann et al., 2017, used two consumer-grade RGB sensors to detect and monitor invasive plants. During flights, turbulence from high wind speeds in marine environments and flight altitude contributed to image blur and artifacts in the imagery. For example, Breckenridge and Dakins (2011) discovered that imagery captured from 305 to 153 meters altitudes were too blurry to distinguish plant cover but significantly improved at 76m altitudes.

Not only do the factors mentioned above contribute to motion blur in imagery, but a sudden input from the operator is yet another source of motion blur in RPAS imagery. However, motion-

blurred images can now be automatically filtered before image processing to minimize errors and complete SfM processing automation (Ribeiro-Gomes et al., 2016).

To prevent motion blur, aircraft speed should match the shutter speed to maintain consistency among the captured photos (Watts et al., 2010). For example, an aircraft speed of 3m/s should be compatible with the shutter speed and exposure time at 1/2000s to acquire images without motion blur (Rosnell and Honkavaara, 2012; Watts et al., 2010). Sensors with a variable aperture depending on the light intensity and shutter speeds of 1/1250s to 1/1600s would be optimum to minimize motion blur (Turner et al., 2015).

2.10.4 Spectral confusion challenges

Spectral confusion or spectral mixing is a unique challenge in remote sensing (Seymour et al., 2017). High-resolution aerial imagery contains homogenous spectral pixels with comparable radiance creating spectral confusion (Pettorelli et al., 2018). Features with spectral similarity are challenging to separate or extract pure training samples for supervised classification and further reduce accuracy (Ventura et al., 2017). Spectral mixing is more prevalent in imagery capture within the visible electromagnetic spectrum ranging from 400-700 nanometres (Arona et al., 2018; Ventura et al., 2018). Apart from spectral mixing, confusing the classification model is the sub-pixel blending of homogenous hues (Seymour et al., 2017b). For example, guano droppings and dried sediments on rocks resemble pixels of blank wild oyster shells on the ground (Chand et al., 2020). Sub-pixel confusion depends on the target's scale relative to the image pixel size (Espriella et al., 2020). The challenge of spectral confusion further increases in ecosystems with a spatial overlap between two habitats and establishes a diverse, transitional area (Chand and Bollard, 2021). For example, in Meola rocky reef, wild oysters can be partly or entirely obscured in areas covered with mangroves.

2.10.5 Shadows and sunglint challenges

Using RPAS for low-altitude aerial surveys in marine environments is a routine (Oleksyn et al., 2021). Aerial imagery is best captured in marine environments when comparatively consistent lighting conditions (Casella et al., 2017; Duffy et al., 2018;). But capturing consistent data might be challenging in regions with structured surfaces spread with vegetation such as mangroves, saltmarsh, and rough sediment areas creating temporary variation shadows (Ventura et al., 2018).

Sunglint in remotely sensed imagery has been a long-standing challenge in airborne remote sensing in marine environments (Kay et al., 2009) **(Figure 11)**. Commonly sunglint occurs when the sun incidence angle is equivalent to the reflection angle, which causes a specular reflection from the water surface onto the sensor (Muslim et al., 2019). This specular reflection creates high intensity in the images, reducing the signal-to-noise ratio (SNR), and decreasing acceptable

observations and imagery usefulness (Joyce et al., 2018). In an estuary, sunglint would be dependent on tidal variations (Kay et al., 2009). During high tides, sunglint is dependent on depth, benthic structure, wind direction, and water entering the estuary from adjacent streams (Muslim et al., 2019). While during low tides, sunglint can be caused by moisture trapped between seagrass meadows, rock pools, and sediments with high specular reflectance (Chand and Bollard, 2021). For example, seagrass meadows resurface once submerged at low tides, covered with scum and cyanobacteria sticking to their blades (Muslim et al., 2019). This scum and bacteria create a high specular reflection in the short-wave infrared (SWIR) and NIR regions of the electromagnetic spectrum (Muslim et al., 2019). Meadows with a glossy surface can create a homogeneous landscape on the substrate background, masking other land cover features true colour and making it difficult to distinguish in the imagery (Muslim et al., 2019).

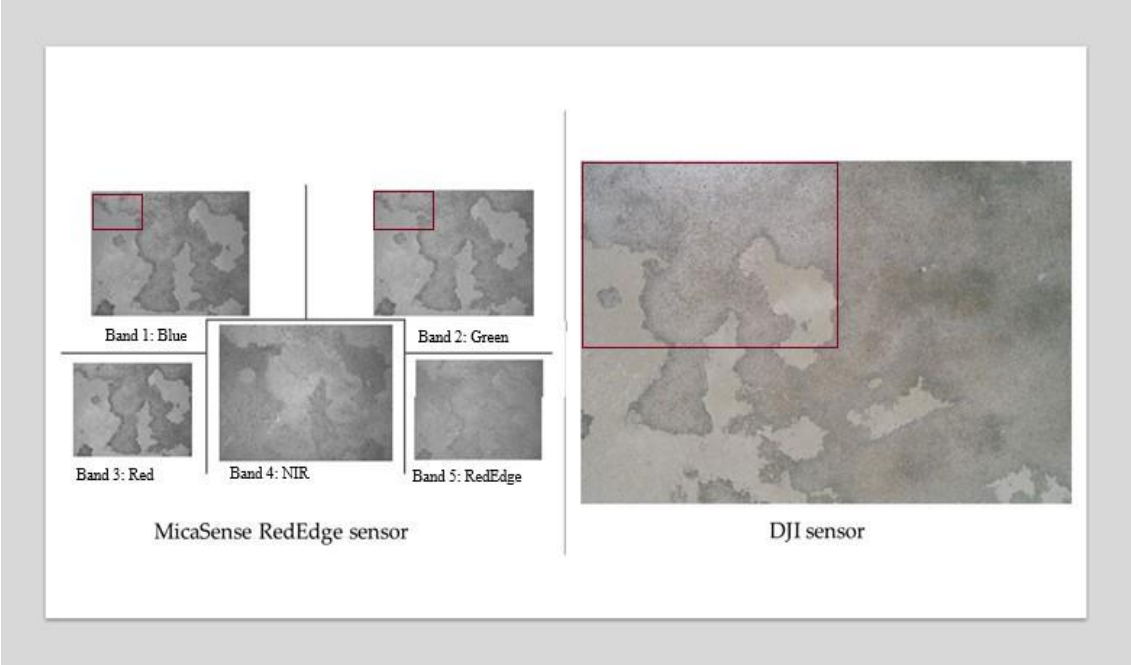

Figure 11. RPAS imagery captured during aerial survey at Meola reef with MicaSense RedEdge (VIS+NIR) and DJI (VIS) sensors. Despite sensor specification and model, both imageries had the presence of sunglint, shown by the red square outline.

2.10.6 Operational challenges

For marine ecology applications, the advent of RPAS aerial surveys was an extraordinary addition to data collecting protocols (Joyce et al., 2019). Although many applications have established high-quality imagery collection guidelines, operational challenges still create barriers (Oleksyn et al., 2021). A simple example of the operational challenge is that RPAS flights are restricted for most marine applications during light hours and reasonably good weather.

Operational challenges often result in hardware and data trade-offs (Oleksyn et al., 2021). For example, an increase in the size of the RPAS platform with a heavy payload will translate into increased expenses but will be spatially and spectrally more efficient (Hassanalian and Abdelkefi,

2017). Another challenge for a large RPAS is taking-off and landing from a boat (Joyce et al., 2019). Operating a large and heavy RPAS can be operationally challenging as it requires additional personnel support and a piloting licence (Muslim et al., 2019).

A battery powers most RPAS components responsible for the aircraft's endurance and is the most critical element for RPAS operations but has the most prevalent challenges (Joyce et al., 2019). For example, (1) poor battery management by novice users could crash the aircraft during flights Oleksyn et al., 2021, (2) the batteries included with off-the-shelf RPAS have a maximum flight time of fewer than 30 minutes, restricting aerial surveys to smaller spatial extents Castellanos-Galindo et al., 2019, (3) taking additional batteries in the field can be logistically and physically challenging (considering only two personnel out to collect data) and require proximity to recharge these batteries Oleksyn et al., 2021, (4) with short intervals (2-4 hrs) between tides, valuable time would be lost without extra fully charged batteries during habitat mapping surveys Castellanos-Galindo et al., 2019, (5) logistical challenges for overseas projects associated with battery transportation on airlines researchers need special hardware and permission (Joyce et al., 2019).

Another critical operational challenge is satellite range and connection, depending on the satellite position and the survey location (Joyce et al., 2019). RPAS needs to be connected to at least three satellites for flight stability, control, and prevent fly-offs (Castellanos-Galindo et al., 2019). The telemetry from satellites needs to be consistent between RPAS and the ground station to provide horizontal, vertical, and positional accuracy (Duffy et al., 2018).

Furthermore, extended manual RPAS operations could result in low overlap between images and pilot fatigue (Oleksyn et al., 2021). Novice RPAS pilots can be less precise with drone commands/controls if telemetry is lost and are less attentive to hazards, creating safety risks to other airspace users and the public (Gregory et al., 2010). On the contrary, poor flight planning associated with automated flights can risk compliance and loss of expensive equipment (Joyce et al., 2019). For example, flight altitudes above the regulatory levels could lead to a collision with other aircraft.

2.10.7 Radiometric resolution challenges and solution

RPAS offers a unique platform for researchers to advance their understanding of spatio-temporal environmental sciences research globally (Manfreda et al., 2018). RPAS platforms allow researchers to operate under different environmental conditions, during clear weather and below clouds. But changing environmental conditions such as cloud cover create shadows that impact the radiometric resolution of the imagery (Oleksyn et al., 2021). Surface reflectance in marine environments creates a continuous challenge for all remote sensors affecting radiometric resolution during image capture (Manfreda et al., 2018). This challenge from reflectance values varies depending on the type of sensor. For example, vignetting (is a reduction of an image's

brightness or saturation toward the periphery compared to the image centre) is caused by the focal length of the sensor or the aperture along with the sensor's wavelength and the image acquisition procedure (Sharma et al., 2019). A sensor's viewing angle and distance from the ground, surface type, or environmental conditions such as topology and bidirectional reflectance also affect the radiometric resolution in the imagery (Manfreda et al., 2018). During image classification, variables such as vignetting and bidirectional reflectance distribution introduce further uncertainties (Joyce et al., 2019). For high-resolution RPAS imagery, inconsistent reflectance values due to diversity in the optical properties and the three-dimensional surface structure translate into various geometric distortions (Stark et al., 2016).

RPAS captured imagery has little influence from atmospheric conditions, flying at low altitudes. Still, the imagery can be influenced by the atmospheric effect from wind spraying higher aerosol concentrations during evaporation (Joyce et al., 2019). Another factor affecting the RPAS imagery's radiometric properties is downwelling lighting conditions (is the process of accumulation and sinking of higher density material beneath lower density material, such as cold or saline water beneath warmer or fresher water or cold air beneath warm air) and transmittance from target to sensor distortion (Stark et al., 2016).

Generally, radiometric correction (RC) is applied to remotely sensed imagery to calibrate the pixel values (MicaSense, 2017). Radiometric correction improves the quality and interpretability of the remotely sensed data (Lu and He, 2017). RC calibration is straightforward, where the digital numbers from the raw data are converted into surface reflectance (Joyce et al., 2019). RC calibration involves *in-situ* field measurements of reference from a field spectroradiometer or a calibration panel target before and after RPAS flights (Joyce et al., 2019). Multispectral sensors such as MicaSense RedEdge and Parrot Sequoia setups consist of a downwelling irradiance sensor and a standardized reflectance panel for radiometric correction (MicaSense, 2017) **(Figure 12)**.

2.11 Overcoming environmental, shadows, and sunglint challenges

The environmental conditions are the primary reason for many of the challenges associated with RPAS aerial surveys for marine habitat mapping and classification (Joyce et al., 2019). However, there are solutions to overcome these environmental challenges. For example, planning aerial surveys to avoid extreme environmental conditions, such as high wind speed and bright illumination, is the most effective strategy for acquiring quality aerial imagery (Casella et al., 2017; Hodgson et al., 2013).

For best RPAS aerial survey results, Kay et al., 2009 have advocated avoiding significant shadows and illumination fluctuations. It is better to conduct aerial surveys close to solar noon or avoid it. Duffy et al., 2018 suggested that collecting images at nadir (the point on a sphere directly below the observer) in marine waters and maintaining the viewing zenith at 90 degrees to the sun can

reduce sunglint off the water surface. Flights should be planned in a lawnmower pattern (i.e., forming a pattern moving through the starting waypoint moving down, then from left to right, then up and continuing the motion until the last waypoint) and such that the RPAS is either flying directly towards or away from the sun azimuth, ± 180 degrees (Chand and Bollard, 2021; Joyce et al., 2019). RPAS aerial surveys on days with unpredictable cloud cover and continuous illumination changes created radiometric inconsistency and affected spectral signatures impacting classification accuracy (Manfreda et al., 2018). Radiometric errors may require a standardized correction (depending on the sensor) because cloud cover may filter out different spectral wavelength components (Hodgson et al., 2013).

Moreover, Chirayath and Instrella (2019) have demonstrated that the fluid lensing technique can be valuable rather than looking at water surface ripples as a distortion for habitat mapping. A well-planned mission and understanding of the effects of reflection from the water surface and the structured ground surface and sensor viewing angle could improve mapping outcomes (Joyce et al., 2019). Currently, to enhance spatial accuracy, DJI's Phantom RPAS range is integrated with onboard real-time kinematic (RTK) (is a technique used to improve the precision of position data derived from satellite-based positioning systems such as GPS), a survey-grade GNSS (is a system that uses satellites to provide autonomous geo-spatial positioning) system gives users survey-grade accuracy (Ridge et al., 2020). This high-precision equipment affordability will improve cross-reference accuracy with other datasets and mapping products (Oleksyn et al., 2021). However, it is desirable to ensure the networks necessary to operate the system in the area of interest before procurement (Joyce et al., 2019). Advancements in computing power and machine learning algorithms further boosted the identification and automatic detection power for habitat classification and mapping of submerged habitats such as wild oysters, coral reefs, and seagrass meadows (Bakirman and Gumusay, 2020; Chirayath and Instrella, 2019; Ridge et al., 2020).

2.11.1 Overcoming operational challenges

Aerial survey limitations due to battery capacity could be eased by monitoring the battery percentage levels and landing the aircraft before battery levels are below ~25% charge (Oleksyn et al., 2021). This battery level monitoring procedure will ensure that these batteries will have a long life and prevent early deterioration (Duffy et al., 2018). There is an increase in demand for longer RPAS flight times; hence manufacturers have developed larger off-the-shelf RPAS with increased battery capacity and flight endurance over 30 minutes (Oleksyn et al., 2021). The other incentive designers are introducing is the concept of automatic battery change-over, reducing the recall of the aircraft during flights (Abd-Elrahman et al., 2005).

Moreover, additional support is recommended to reduce pilot fatigue during extended manual operations to protect expensive equipment and ensure safety for the crew and the public (Joyce et

al., 2019). Also, pre-programmed automated flight planning is encouraged to reduce pilot fatigue (Joyce et al., 2019). Most automated flight planning software is open source, allowing the pilot to maintain a visual line of sight with the aircraft and focus on general safety (Oleksyn et al., 2021). A support person can be a good option during flights to communicate hazards to the pilot, such as identifying low-flying aircraft (Joyce et al., 2018). Besides, an automated flight planner will allow users to create good overlaps (front and side, > 80%) for high positional accuracy for marine habitat mapping (Duffy et al., 2018).

Before any RPAS aerial survey, planning should include a precheck of weather conditions (Oleksyn et al., 2021). Depending on the model, the aircraft's capacity to withstand wind speeds. For example, a DJI Phantom IV's maximum wind tolerance capacity is 10m/s (Duffy et al., 2018). For RPAS operation and tracking in windy conditions, users should calculate wind-induced error by calculating the movement distance of the RPAS at the proposed survey altitude while hovering over a fixed position for a particular time (Oleksyn et al., 2021). If wind conditions are too unstable, avoid flights.

Furthermore, deep learning has emerged as a powerful research technique for marine environments (Gray et al., 2019). Datasets from remotely sensed imagery and deep learning models, such as belief networks (are graphical models that communicate causal information and provide a framework for describing and evaluating probabilities when we have a network of interrelated variables), convolution neural network (CNN) (is a class of neural networks that specialises in processing data that has a grid-like topology, such as an image), and stacked autoencoder, are combined to investigate and automatically identify biogenic habitats (Vayssade et al., 2019). Researchers have integrated deep learning techniques and remotely sensed datasets for wild oysters and seagrass research. For example, (1) Reus et al., 2018 used underwater videography and CNN features to define seagrass meadows patches and pixels, and (2) Hoque et al ., 2018 used satellite imagery to automatically detect damages to seagrass beds from boat propeller scars using a CNN deep learning technique, (3) Moniruzzaman et al., 2019 used underwater camera imagery and a faster regional convolutional neural network (Faster R-CNN) method to detect seagrass, (4), Perez et al., 2020 used WorldView 2 satellite imagery and applied a deep capsule network (DNC) together with a CNN technique to evaluate deteriorated seagrass and distribution areas (5) Ridge et al., 2020 have used a CNN technique to automatically delineate and detect wild oyster reefs in Rachel Carson Reserve in America.

A strategic solution to high-resolution RPAS data analysis challenges is to push the boundaries further for developing and applying machine learning and computer vision for pattern recognition in marine ecosystems (Joyce et al., 2018). Developing these pattern-recognition algorithms would

diversify their applications in different ecosystems and narrow down species-level identification effectively (Oleksyn et al., 2021).

2.11.2 Overcoming radiometric challenges

In remote sensing, radiometric corrections improve image quality and ensure that the imagery is ready for geospatial analysis (Gray et al., 2019). Researchers have created linear calibration equations for radiometric correction of RPAS datasets from calibration targets that converted digital numbers to reflectance for every band (Laliberte et al., 2011). This model assumed a linear relationship between surface reflectance and the calibration targets. In contrast, Wang and Myint, 2015 used grey levels from more than two calibration targets that increased calibration precision. However, these studies have not considered that the reflection from the ground features varies with wavelength.

Furthermore, with rapid sensor technology advancements, organizations such as MicaSense have an automatic radiometric calibration process integrated into Pix4D Mapper and Agisoft Metashape photogrammetry software (MicaSense, 2017). This radiometric correction algorithm from MicaSense accounts for sensor sensitivity, exposure, gain, vignetting effects, and black-level adjustments (MicaSense, 2017). The equation for computing surface reflectance L from raw pixel value P is shown below.

$$L = V(x, y) * \frac{a_1}{g} * \frac{P - P_{BL}}{t_e + a_2 y - a_3 t_e y}$$

P = raw pixel value

P_{BL} = normalized black level value

a_1 a_2 and a_3 = radiometric calibration coefficients

V (x, y) = vignette polynomial function locations of pixels

t_e = image exposure time

g = sensor gain

x, y = pixel column and row numbers

L = spectral radiance

Equation source: MicaSense (2017).

The radiometric correction algorithm incorporates the sun and sensor position and the irradiance data from the reflectance calibration panel **(Figure 12)**. For example, during the calibration process in Pix4D, the radiometric correction algorithm considers the camera gain and exposure values. Also, the radiometric correction process converts digital numbers from raw multispectral

imagery into sensor reflectance and absolute surface reflectance values (MicaSense, 2017).

Figure 12. Showing a MicaSense reflectance (centre) panel with the images taken for each band before an RPAS flight. Each band has a unique reflectance correction value supplied by the manufacturer with this reflectance panel used for radiometric correction during image processing. Images captured by Kavita Prasad.

2.12 Summary

New Zealand has more than 400 intertidal estuaries, which vary in shape and size and are connected to the sea (Hume et al., 2007). Researchers have indicated that some estuaries health is neglected and is in poor condition, but their health and value can be restored, given an opportunity (MfE, 2019). The poor condition of these estuaries is due to the cumulative effects of excessive sediment discharge from developments, overloading nutrients, and pollutants, including climate change (Davies et al., 2018). Consequently, these cumulative effects significantly impact the intertidal estuaries, which hold incredible diversity and species turnover, making them vulnerable (Dudley et al., 2017). The challenge is that these intertidal species, for example, seagrass meadows (*Zostera muelleri)* affected, may recover from these cumulative effects at different rates (Davies et al., 2018). The solution could be continuous ecosystem monitoring, identifying the impacts, mitigating them, creating baseline habitat maps, and detecting fine-scale changes.

Furthermore, in New Zealand, there is a significant knowledge gap in the scale and the spatial extent of habitat loss (MfE, 2019). This knowledge gap is mainly due to the cost of monitoring and mapping submerged habitats (MfE, 2019). There is a national inventory gap in New Zealand for most biogenic habitats, except datasets, which are primarily available for seagrass meadows and mangroves (Anderson et al., 2019). However, these available datasets have temporal gaps and missing metadata on their spatial extent, abundance, and distribution (Morrison et al., 2014).

For example, a spatial query on 1 November 2021 from the Department of Conservation's SeaSketch website on seagrass point feature class showed the following result:

The Department of Conservations (DOC) SeaSketch project (https://www.seasketch.org/) conducts a national-scale assessment of seagrass extent using datasets captured from the local councils and digitized layers from other agencies and universities (Anderson et al., 2019). These datasets are from unreliable data sources with gaps in years, and authorities have difficulty accessing different spatial layers (Anderson et al., 2019). Meanwhile, researchers have focused on density changes and threats to seagrass and mangrove habitats. The focus should have been on how extensive changes are and how productive these habitats could be (Anderson et al., 2019; MfE, 2019).

For mapping and monitoring intertidal estuaries in New Zealand, researchers have used satellite, crewed aerial imagery, and *in-situ* field measurements (Anderson et al., 2019; Foley and Shears, 2019; Lundquist et al., 2018; Morrison et al., 2014; MfE, 2019). Satellite imagery still has challenges such as cloud contamination and revisit time, e.g., 18 days for free downloadable Landsat satellite imagery with low spatial resolution (Casella et al., 2017; Gomes et al., 2018). Although satellite technology has advanced in capturing high spatial resolution imagery, datasets for marine applications are insufficient for studying small and medium coastal dynamics and identifying fine-scale changes (Ventura et al., 2018). On the other hand, crewed aerial imagery also has revealed some operational limitations, mainly due to aircraft speed and flight altitude. Crewed aerial imagery costs are high because they include the cost of well-trained personnel operating expensive data acquisition sensors and specialised equipment (Windle et al., 2019). Traditional *in-situ* field measurements provide high-resolution ground sampling distance but have limited spatial extents and are challenging to monitor and map large spatial extents of marine habitats such as wild oyster reefs (Windle et al., 2019). These limitations can affect the collection of high-quality marine datasets, especially when time-saving and low-cost datasets are required. RPAS are well adapted to provide researchers with a high standard of mapping for nearshore marine environments and inaccessible areas, or those highly spectrally complex in the structure, such as wild oyster reefs at Meola Intertidal reef. RPAS allows for multi-temporal aerial surveys

and consistent monitoring over large spatial extents at fine as decimetre scales (Duffy et al., 2018). These resolutions are essential for understanding the spatial dynamics of nearshore marine environments.

Table 2. Comprehensive review of sensors and RPAS for marine applications

Year	Sensor type	Sensor Specification	RPAS type	Spectral and Spatial resolution	Applications and Endurance	References
Summary of applications using RPAS for marine research						
2010	2D Multispectral Sensor	Nikon® D90 12-megapixel digital single-lens reflex (SLR)	ScanEagle: Warragul Fixed Wing. Price USD 67480.00 including ground station and training	Three bands RGB 1024*768 pixels GSD acquired 3cm/pixel	Mapping, surveying, and monitoring of Dugongs and humpback whales in Australia. 60-90minutes	Hodgson et al., 2013
2012	2D Multispectral Sensor	miniMCA Tetracam	Oktocopter	Six bands multispectral 490nm-800nm	Mapping coastal salt marsh vegetation In Ralphs Bay, Australia	Kelcey and Lucieer, 2012
2012	2D Multi-spectral Sensor	Canon 550D (SLR)	TerraLuma, OktoKopter Payload: 1kg Overlap= 70%-90%	Photogrammetry: PMVS2 GSD: <1-3cm/pixel	Coastal monitoring in Southeast Tasmania, Australia Flight time: 6m @30-50m altitude	Harwin et al., 2015
2013	2D Multispectral Sensor	Canon EOS 55D	Hexacopter	Photogrammetry: Agisoft Photoscan GSD: 0.6cm/pixel	Reconstruction of coastal topography in Marina di Ravenna, Italy Flight time 20m	Mancini et al., 2013
2015	2D Multispectral Sensor	Olympus E-PM2 25 mm F1.8 lens,	APH-22 Hexacopter Payload = 0.13 kg	Three-bands RGB	Collecting images to measure killer whales (Orcinus orca) at Vancouver Island, Western Canada 60 flights each at ~13 -15 minutes	Durban et al., 2015

Table 2. Comprehensive review of sensors and RPAS for marine applications

Year	Sensor type	Sensor Specification	RPAS type	Spectral and Spatial resolution	Applications and Endurance	References
2015	2D Multispectral Sensors	3 Sensors on Predator: MTS-B Skyball, SeaVue Radar andAutomatic identification system 2 Sensors on Puma: Gimbaled and infrared	MQ-9 Predator B and Puma All-Ecosystem	Multispectral	Marine surveillance and resource monitoring in the Hawaiian Islands. Area: 30ha Distance: 1500km	Brooke et al., 2015
2016	HD Sensor (Mobius)	GoPro Hero 3 Black Edition	Home-made prototype quadcopter Flight planning: ArduPilot Mega <100USD.	Three-bands RGB 3000 *2250 pixels GSD= 1.01cm/pixel	Identify and map coastal fish nursery grounds in Giglio Is. Mediterranean Sea	Ventura et al., 2016
2016	2D Multispectral Sensor	GoPro Hero 4	Aeryon Scout	Three-bands RGB	Monitoring mid and low intertidal communities in Kachemak, Northern Gulf of Alaska	Konar and Iken, 2016
2016	2D Multispectral Sensor	Go Hero 3+ Silver edition	DJI Phantom II <USD 2500	Three-bands RGB	Investigate shark and Ray densities in Moorea (French Polynesia). Depth 1.5-2m.	Kiszka et al., 2016
2016	2D Multi-spectral Sensor	Nikon D700	DS6 hexacopter. Payload 1.6kg	Photogrammetry: Agisoft Photoscan. GSD = 1-2cm/pixel @ 50m -100m altitude	Monitoring mudflats in Seine France. Flight time 20m	Jaud et al., 2016

Table 2. Comprehensive review of sensors and RPAS for marine applications

Year	Sensor type	Sensor Specification	RPAS type	Spectral and Spatial resolution	Applications and Endurance	References
2017	2D Multi-spectral Sensor and Spectrometer	CMOS Ocean Optics STS-VIS	DJI Phantom II Vision+ and DJI Spreading Wings S800 Payloads 1.4 and 1.6kg Flight Planner: DJI GO	Three-bands RGB and1024 Spectral bands 350nm -800nm 1.5nm optical resolution	Examine ecosystem variable that affects ocean data acquisition	Zeng et al., 2017
2017	Hyperspectral	AvaSpec-dual spectroradiometer	LT-150 RPAS	360–1000 nm with a spectral resolution of 1 nm	Phytoplankton bloom in Taiwan. Flight Altitude:300m	Shang et al., 2017
2017	2D Multispectral Sensor	GoPro Hero 4 Black Edition	DHI Phantom II <USD1650.00	Photogrammetry: Agisoft Photoscan. GSD=0.78-1.56cm/pixel	Mapping shallow coral reefs near Tiahura, in Moorea, French Polynesia Flight time 10m	Casella et al., 2017
2017	2D Multispectral Sensor	Waterproof Canon D30	Swell-pro Splash drone quadcopter Flight planner: Mission Planner software (v. 1.3.35) Payload: 2.5kg	3band RGB GSD: <1cm/pixel Photogrammetry: Pix4Dmapper software (v. 2.1.53)	Intertidal reef monitoring in Victoria Australia Flight time: 15 minutes	Murfitt et al., 2017

Table 2. Comprehensive review of sensors and RPAS for marine applications

Year	Sensor type	Sensor Specification	RPAS type	Spectral and Spatial resolution	Applications and Endurance	References
2017	2D Multispectral Sensor	Sony DSC-WX220	SenseFly eBee RTK Payload: 0.73kg	3 band RGB GSD: ~2cm/pixel SfM: Pix4Dmapper	Coastal morphology assessment and management in south of Beaufort, North Carolina. Flight altitude: 70m	Seymour et al., 2017
2017	2D Multispectral Sensor	CMOS DJI Sensor	DJI Phantom III Pro	Photogrammetry: Autostitch GSD: 30-160mm/pixel	Measure jellyfish aggregates in Pruth Bay, Canada. Manual flight	Hunt et al., 2017
2017	2D Multispectral Sensor	Go Her Pro 4	DJI Phantom II	Photogrammetry: Agisoft Photoscan GSD: 3cm/pixel	Very high-resolution mapping of the state of coral reefs in northern lagoon Moorea Is. Flight altitude:30m	Collin et al., 2017
2018	2D Multispectral Sensor	Zenmuse X5 Sensor	Matrice 600 Max payload: 15.1kg Flight planner: Altizure®	Photogrammetry: Agisoft Photoscan. GDS: 7.5cm/pixel @ 80m altitude	Elevation monitoring of intertidal mudflats in Jiangsu Province, China Max flight time 30m	Dai et al., 2018
2018	2D Multispectral Sensor	Sony A6000 (DSLR)	T-Motor U5 RPAS Flight planner: MikroKopter Payload:8kg	Photogrammetry: Agisoft Photoscan (V1.2.1) GSD: 2cm/pixel	Investigate Aboriginal intertidal fish traps in the South Wellesley Islands, Australia	Kreij et al., 2018

Table 2. Comprehensive review of sensors and RPAS for marine applications

Year	Sensor type	Sensor Specification	RPAS type	Spectral and Spatial resolution	Applications and Endurance	References
2018	2D Multispectral Sensor	Sensor 1: SJ4000 wifi (CMOS) Sensor 2: SJ4000 modified with IRPro	DJI Phantom II Flight planner: DJI Ground Station v.04 software	Photogrammetry: Agisoft Photoscan GSD: 2.8cm/pixel Spectral band RGB: 450nm-675nm and IR:875nm-11000nm	Mapping of mangrove forest in the State of Terengganu on Peninsular Malaysia	Ruwaimana et al., 2018
2018	2D Multispectral Sensor	Canon IXUS 127HS senseFly S.O.D.A.	eBee SenseFly Payload 0.7kg USD 2600	Photogrammetry: Terra Version 4.0.1 Area covered: ~60000m2	Assessing the potential disturbance of RPAS on grey seals in Nova Scotia, Canada. Flight time: 20-25m	Arona et al., 2018
2018	2D Multispectral Sensor	GoPro Hero 3	DJI Phantom II, Quadcopter	Three-bands RGB Photogrammetry: Agisoft Photoscan 70% side and front overlap	Assessing coral bleaching in Kane Ohe Bay, Hawaii Flight time: 15m	Levy et al., 2018

Table 2. Comprehensive review of sensors and RPAS for marine applications

Year	Sensor type	Sensor Specification	RPAS type	Spectral and Spatial resolution	Applications and Endurance	References
2018	2D Multispectral Sensor	Nikon D810	ScanEagle®	GSD: 7cm/pixel	Estimating arctic cetacean density and associated uncertainty northeastern Chukchi and the western Beaufort SeaFlight altitude: 122m @ 1.6-6hr	Ferguson et al., 2018
2018	2D Multispectral Sensor	GoPro Hero 3+	DJI Phantom II	1920*1080 pixels	Exploring blacktip reef sharks in Moorea, French Polynesia Flight altitude 12m	Rieucau et al., 2018
2018	2D imager: Multi-spectral Sensor	Sensor-1. Parrot Sequoia Sensor-2. Sense Fly thermo Map thermal sensor	SenseFly eBee Flight planner: senseFly eMotion 3	1. Five bands: Blue, Green, Red, Red Edge, and NIR (530nm -810nm). GSD: 6-9cm/pixel 2. Thermal IR radiation: 7.5-13.5µm Photogrammetry: Pix4D mapper	To map intertidal sediments in S. Wales and SW England	Fairley et al., 2018
2018	2D Multispectral Sensor	CMOS DJI Sensor (14 megapixels) With Polarized Lens	DJI Phantom Vision 2+ (quadcopter) Payload 1.2kg	3 band RGB Video recording @720-1080p 4384*3288	Monitor marine mega-fauna in Great Abaco Is. Bahamas Endurance: 12m Manual flight @7.6m	Hensel et al., 2018

Table 2. Comprehensive review of sensors and RPAS for marine applications

Year	Sensor type	Sensor Specification	RPAS type	Spectral and Spatial resolution	Applications and Endurance	References
2018	2D Multispectral Sensor	Sony NEX 5N (16 megapixels)	V-Form Octocopter	Photogrammetry: Agisoft Photoscan GSD: 8cm/pixel	Estimate rocky shore mussel's distribution in Portuguese west coast Flight altitude: 30m	Gomes et al., 2018
2018	2Dimager: Multispectral Sensor	MicaSense Parrot Sequoia	SenseFly eBee (fixed wing)	Photogrammetry: Pix4D mapper Four bands (Green, Red, Red Edge and NIR)	Map suspended sediment concentration in Maumee River, Ohio. Depth intervals: 15,61,91 and 182cm)	Larson et al., 2018
2019	2D Multi-spectral Sensor	Sensor-1. Ultra-Cam-Xp Sensor-2. UltraCam-XpWA	Unknown	1. Three bands RGB 2. IR, Red Green GSD= 0.5m/pixel	Mapping of emerging biogenic reef in Sainte-Anne reef in French Polynesia	Collin et al., 2019
2019	2D Multispectral Sensor	Canon IXUS 127HS (16 megapixels) sense Fly SODA.	eBee Sensefly Flight Planner: eMotion3	Photogrammetry: Pix4D Mapper Pro GSD: <5cm/pixel	Assessment of estuarine ecosystems in Rachel Carson Reserve in North Carolina, USA	Gray et al., 2019
2019	2D Multispectral Sensor	Sesnor-1.X3- FC350 912.4 megapixel Sensor-2.X5S	1.DJI Inspire 1 Payload @2.9kg 2.DJI Inspire II Payload @3.4kg	Photogrammetry: Pix4D Mapper Pro GSD: 1.20-2.38cm/pixel 1. 4000 * 3000 pixels	Freshwater fish habitat mapping Xingu River basin, Brazil Flight altitude: 30m	Kalacska et al., 2019

Table 2. Comprehensive review of sensors and RPAS for marine applications

Year	Sensor type	Sensor Specification	RPAS type	Spectral and Spatial resolution	Applications and Endurance	References
				2. 5280*3956 pixels		
Summary of recent application of RPAS for seagrass and oyster research						
2016	2D Multispectral Sensor	Canon ELPH 130.	Multirotor Flight planning: Pixhawk <1000USD Payload 0.4kg	Three-bands RGB 4608*3456 pixels GSD=2.96cm-2.41cm/pixel	OBIA. for coastline identification and 3D coastal mapping in Lesvos Is. Grece and Eressos beach Flight time 15 minutes	Papakonstantinoub et al., 2016
2016		RPAS system not specified	The synergy between ground-based survey and Sentinel 2 satellite data		Performed a supervised seagrass classification	Topouzelis et al., 2018
2017	Hyperspectral sensor	Ultra-compact spectrometer (C12880MA)	Hexacopter with water landing capability	Flight height was 20m	Performed a pattern matching technique, using cross-correlation for detecting seagrass and algae in Izu Oshima, Japan.	Uto et al., 2017
2017	2D Multispectral Sensor	Ricoh GR II (CMOS) 16.2 Megapixels	3D Robotics Solo Payload 7kg Flight Planner: Pixhawk 2	Photogrammetry: Agisoft Photoscan (V1.2.5). GSD= ~4mm/pixel 70% side and front overlap	Spatial assessment of intertidal seagrass in Wales, UK Flight altitude: 50m	Duffy et al., 2018

Table 2. Comprehensive review of sensors and RPAS for marine applications

Year	Sensor type	Sensor Specification	RPAS type	Spectral and Spatial resolution	Applications and Endurance	References
2018	2D Multispectral Sensor	Go Pro Hero 3 12 megapixels	Aeryon Scout (Quadcopter)	Used Nonmetric multidimensional scaling to visualize the data and determine the difference between the sampling methods	Low taxonomic intertidal monitoring and classification of seagrass meadows in the northern Gulf of Alaska Flight altitude: 5m	Konar and Iken, 2018
2018	2D Multispectral Sensor	GoPro Hero 4 Black Edition	Quantum Nova Cheerson CX-20 (Quadcopter). Payload: 1.2kg. USD<658 Flight Planning: Ardu Pilot Mega	Three-bands RGB Photogrammetry: Agisoft Photoscan (V1.2.6) GSD: ~3cm/pixel	Mapping ecological sensitive marine habitats in Giglio Island, Italy Flight Altitude: 40m	Ventura et al., 2018
2018	2D Multispectral Sensor	1/2.3 CMOS (12 megapixels)	DJI Phantom III Flight planner: MapPilot Overlap 75% of both axes	Photogrammetry: Pix4D mapper (V2.1.61) GSD: 2cm/pixel	Delineating seagrass habitats in British Colombia, Canada Flight altitude: 80-120m	Nahirnick et al., 2018
2018	2D Multispectral Sensor	RPAS and sensor not specified	Studied the synergy between WorldView 2, GeoEye, and aerial imagery	Tha Mai district Chanthaburi province Thailand.	Performed spectral NDVI and supervised classification for seagrass detection	Chayhard et al., 2018

Table 2. Comprehensive review of sensors and RPAS for marine applications

Year	Sensor type	Sensor Specification	RPAS type	Spectral and Spatial resolution	Applications and Endurance	References
2019	2D Multispectral Sensor	GoPro Hero + RBG digital	Quadcopter	Assessed sun angle and theoretical visibility influencing mapping accuracy in temperate estuaries	Multivariate linear regression analysis and OBIA.	Nahirnick et al., 2019
2019	2D Multispectral Sensor	1/2.3 CMOS	DJI Phantom 4 Pro	Structure from motion. UAS sandbox	Investigated the reliability of RPAS data for seagrass mapping under different environmental conditions.	Doukari et al., 2019
2020	2D Multispectral Sensor	Parrot Sequoia		Agisoft Photoscan GSD: 2cm/pixel	Change mapping of intertidal seagrass	Martin et al., 2020

Chapter 3 Low-cost remotely piloted aircraft system (RPAS) with multispectral sensor for mapping and classification of intertidal biogenic oyster reefs

A version of this Chapter is published as:

Chand, S., Bollard, B., and Gillman, L. (2020). Low-cost remotely piloted aircraft system (RPAS) with multispectral sensor for mapping and classification of intertidal biogenic oyster reefs. 4(4), 148–154. https://doi.org/10.15406/AAOAJ.2020.04.00116

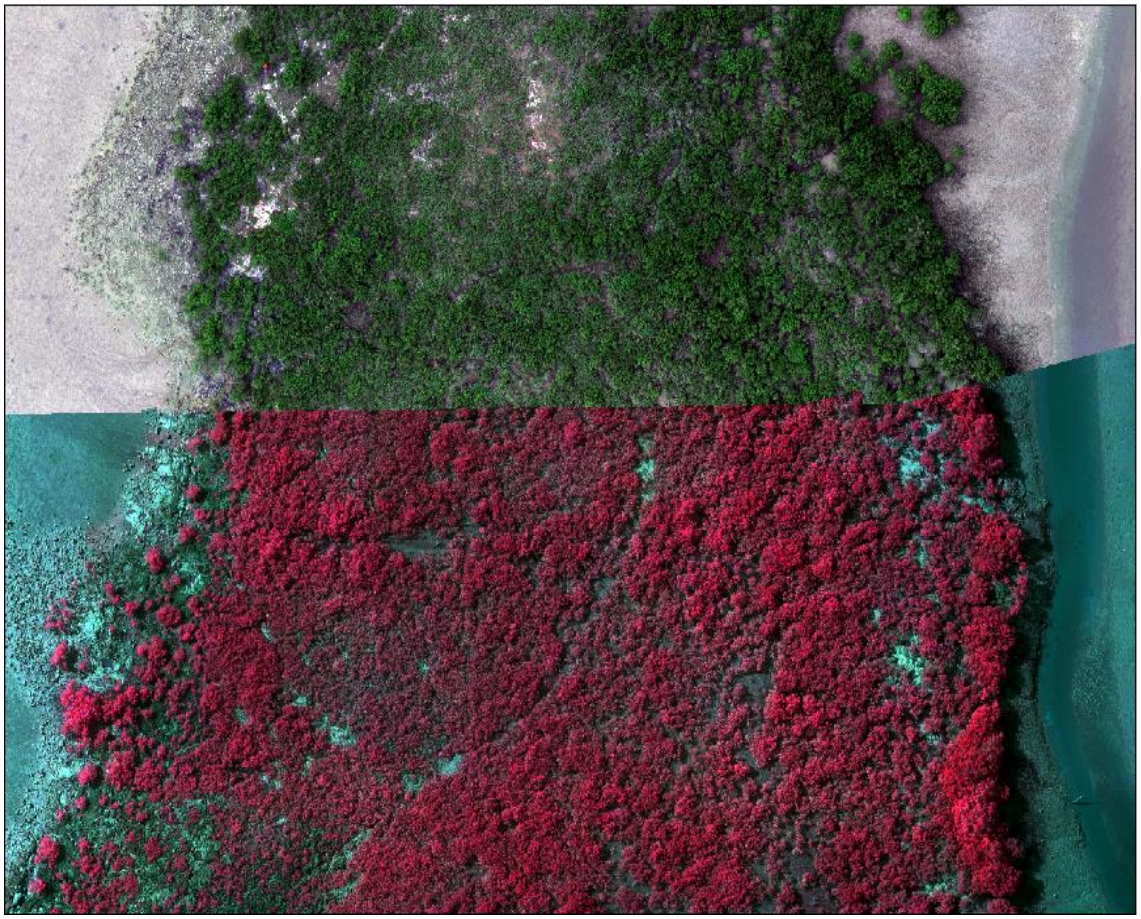

Cover image. A remote sensed aerial imagery is displayed in two different electromagnetic spectrums. The top part of the imagery is displayed in the VIS spectrum, and the bottom half is in the NIR spectrum.

In this chapter, we demonstrated the potential of structure from motion photogrammetry and low altitude remotely sensed imagery for thematic mapping**,** characterisation, and identification of wild oyster reefs (Thesis objective a). We also demonstrated the accuracy of the Object-based image analysis (OBIA) technique and a rule-based classification approach for detecting wild oyster reefs in a heterogeneous intertidal ecosystem (Thesis objective b). This chapter presented an essential first step towards low-altitude aerial surveys that successfully detected and characterised wild oyster reefs in the study area. The main contributions from this chapter were (1) supplement time-intensive *in-situ* surveys and (2) mitigate challenges from other remotely sensed imagery such as satellite and crewed aerial imagery for monitoring and mapping wild oyster reefs. The results showed that having spectral bands beyond the visible electromagnetic spectrum enhanced feature detection on the imagery and increased the potential to delineate

targeted features within a heterogeneous marine ecosystem. The findings also established that monitoring and mapping of turbid exposed intertidal rocky reefs present unique challenges but can be mitigated using RPAS datasets.

3.1 Introduction

Shellfish (e.g., oyster reefs) are biogenically structured landscapes and are challenging for manual field surveys. These habitats are economically and ecologically valuable, but they are depleted due to numerous anthropogenic and natural hazards (Grabowski et al., 2012). These habitats can be referred to as "biogenic habitats," formed by plants (e.g., salt marshes, mangroves, seagrass meadows, and kelp forest) and animals (e.g., shellfish) occurring from the intertidal out to the deep ocean (Butchart et al., 2010; Newell and Koch, 2004). Oyster reefs are a subset of "biogenic habitats" with hard and rugged structures, sometimes visually imposing, creating a discrete and unique habitat from the surrounding area (Kellogg et al., 2014). Wild oysters[1] deliver many ecosystem services to support and protect biodiversity by creating three-dimensional structures, sediment accumulation, nutrient recycling, water filtration, and carbon sequestration. These ecosystem services are important to sustain environmental changes in the Anthropocene era (Beck et al., 2011; Halpern et al., 2008; Thorngren et al., 2017). Restoration of this resource is of local and global importance, and restoration management will require accurate spatial mapping to monitor ecological status.

Recent advances in spaceborne (e.g., satellite) and airborne (e.g., crewed aerial) imagery have been successful in mapping and assessing the spatial extent of oyster reefs (Grizzle, 2002; NOAA, 2003). The increase in spatial (31cm, panchromatic and 1.24m, visible and near-infrared), spectral resolution (8 multispectral), and revisit time (<1 day) provided by WorldView- 3/4 satellites have improved the accuracy of capturing ecological changes in the dynamic marine environment (Reshitnyk et al., 2014; Schill et al., 2006). However, spaceborne imagery is affected by cloud cover and atmospheric aerosol interference, and surface reflectance is not always synchronized with desired oceanographic conditions. Consequently, high-resolution imagery often translates into high costs due to increased storage and processing time taken to orthorectify the imagery to the required accuracy (Schill et al., 2006). According to Digital Globe, the price of a 30-cm georeferenced + natural colour or 4-band WorldView 3/4 satellite imagery is approximately USD22.50/sq.km[2]. Due to financial constraints, high-resolution imagery may not be easily accessible to all researchers (NOAA, 2003; Reshitnyk et al., 2014).

[1] May read differently from published article as I have replaced "they" to "Wild oysters"

Mapping biogenic intertidal rocky reefs in temperate waters during high tides were challenging due to turbidity and suspended sediment concentration (SSC), which attenuates light penetration through the water column water (Casella et al., 2017). Even with high-resolution hyperspectral data (4.0 x 4.0m and 126 bands), oysters (~15cm long) require higher spatial resolution imagery to be effectively detected and mapped, and narrow bands are required to penetrate the water (Casella et al., 2017). Therefore, to apply remote sensing techniques to map and detect features effectively, the sensor and platform must be appropriate to the feature being sensed. The issue of spectral band attenuation in the water column and spatial resolution can be averted by surveying intertidal biogenic habitats at low tide.

In Europe, during low tide, researchers successfully classified intertidal biogenic reefs, built by the honeycomb worm (*Sabellaria alveolate)*[2], from an RPAS derived multispectral (red-edge) (RE) and near-infrared (NIR) very-high-resolution (0.17m/pixel) imagery (Collin et al., 2019). Additional spectral bands (e.g., RE and NIR) provided further opportunities to identify and map biogenic habitats based on their spectral characteristics (e.g., water appears dark in the NIR band). Another airborne survey of oyster reefs in Rachel Carson Reserve, North Carolina, USA, tested the quality of three different RPAS platforms with RGB cameras and ultra-high resolution (<5 cm) imagery for mapping and delineating oyster boundaries (Schwantes et al., 2018). These researchers concluded that RPAS-based fieldwork was quicker than traditional fieldwork (e.g., quadrats) and provided more validation points for accuracy assessment than satellite imagery.

For the classification of high-resolution (e.g., <5 cm/pixel) RPAS imagery, an object-based image analysis (OBIA) performs better than a pixel-based technique (e.g., maximum likelihood) because each pixel is smaller than the feature of interest (Chabot et al., 2018; Nahirnick et al., 2019; Ventura et al., 2018)[3]. The benefit of this technique is its ability to delineate ecological features into meaningful image objects and extract spatial, spectral, and contextual information from these objects (Blaschke, 2010; Horning, 2004).

RPAS in the most diverse fields of science has established itself as a new tool capable of providing unprecedented scientific applications (Manfreda et al., 2018; Ventura et al., 2018). At the same time, recent studies suggested that RPAS may provide better sampling efficiency and data quality for studying intertidal marine ecology in the visible spectrum (Nahirnick et al., 2019; Ventura et al., 2018). To our knowledge, there are no published studies that have explored the potential of a low-cost RPAS coupled with a multispectral sensor to map and classify biogenic oyster reefs.

[2] May read differently from published article as I have added the scientific name honeycomb worm (*Sabellaria alveolate)*

[3] May read differently from published article as I have, removed some in-text citations

Here, we demonstrate the potential of a low-cost RPAS coupled with a miniaturized multispectral sensor (MicaSense® RedEdge™) and use structure from motion photogrammetry to deliver very high-resolution maps useable for identification and characterization of biogenic oyster reefs. We show the benefits of enhanced spectral bands for remote sensing of biogenic habitats and report on time taken and area covered from the RPAS flights. In addition, it demonstrates the suitability of RPAS imagery and the accuracy of OBIA combined with rule-based classification for detecting and delineating oyster reefs from a heterogeneous intertidal rocky reef ecosystem.

3.2 Materials and Methods

3.2.1 Study Site

The study area for the RPAS survey and mapping of oysters was Meola Reef (Te Tokaroa) on the North Island of New Zealand. Located at -36.853981S and 174.710194E of the Waitemata Harbour in Auckland **(Figure 13)**. This Harbour is bordered by New Zealand's major city, Auckland, and one of New Zealand's busiest ports (Foley and Shears, 2019). Human activities, pollution, and urbanization have altered the Harbour and have become a hotspot for non-indigenous species (Foley and Shears, 2019; Hayward, 1997). The Te Tokaroa Meola Reef is a 28,000-year-old basalt volcanic rocky reef that extends over 2 km into the central Waitemata Harbour (Foley and Shears, 2019). It is the most prominent and most visible by satellite natural rocky reef system in Waitemata Harbour (LINZ, 2019). This rocky reef ecosystem supports high biodiversity of habitats, including saltmarsh (*Plagianthius divaricatus*) and mangroves (*Avicennia marina*) along the landward edge of the reef (Hayward et al., 1999). Pacific oysters (*Crassostrea gigas*) dominate the outer reef, and kelp forests dominate the subtidal zone of the reef (Foley and Shears, 2019). It also provides shelter and a breeding ground for fifty bird species (e.g., black swan (*Cygnus atratus*), Tui (*Prosthemadera novaeseelandiae*), and Oystercatcher (*Haematopus unicolor*)[4] (e-bird, NZ).

The hydrodynamics in this area is controlled by two high (~1.9 - 2.9m) and two low tides (~0.7-1.0 m) daily, which flush the Harbour from the Hauraki Gulf (Foley and Shears, 2019). This hydrodynamics is critical for biogenic benthic ecosystems such as oyster beds and larvae distribution; tides bring in larvae. This reef structure withstands environmental and human impacts, such as discharge effluent and trampling while setting fish nets during low tides and shell-fishing, and it is a popular spot for bird watchers, hikers, and dogs walkers.

[4] May read differently from published article as I have added the scientific names: black swan (*Cygnus atratus*), Tui (*Prosthemadera novaeseelandiae*), and Oystercatcher (*Haematopus unicolor*)[4]

3.2.2 Flight Safety

Flights were logged on the Airshare website, and all flights were within the visible line of sight (VLOS). The pilot was certified with Part 101 RPAS Civil Aviation Authority of New Zealand (CAANZ) and was always accompanied by a trained observer.

3.2.3 Aerial Survey Data

The RPAS aerial survey was conducted on 23 March 2019 (0.30m water level at 16:08 NZST) using a multispectral, MicaSense® RedEdge™ senor at nadir mounted on a Phantom 4 Pro® multi-rotor. Pix4D capture® autonomous flight planner was used to plan the fights at 50 m altitudes. The MicaSense® sensor, initially designed for agricultural purposes, leverages a digital RGB DJI camera, 4000 x 3000-pixel imagery, with the following distinct bands: Blue (475 nanometres (nm)), Green (560 nm), Red (668 nm), Near IR (840 nm), and Red Edge (717 nm) and 1280 x 960-pixel imagery. One of the benefits of using this sensor is to perform a radiometric correction during processing in Pix4D software (Pix4D, 2019), and using the following equation allows reflectance to be computed for all the bands:

$$Reflectance = \frac{Radiance}{Irradiance}$$

The images were mosaicked and rendered into absolute reflectance maps for each spectral band; pixel values ranged from 0-1. The cost of a consumer-grade Phantom 4 Pro RPAS used in this study was 1452.50 NZD (USD 866.70). Flight planning was done using an open-source flight planner, Pix4D capture®.

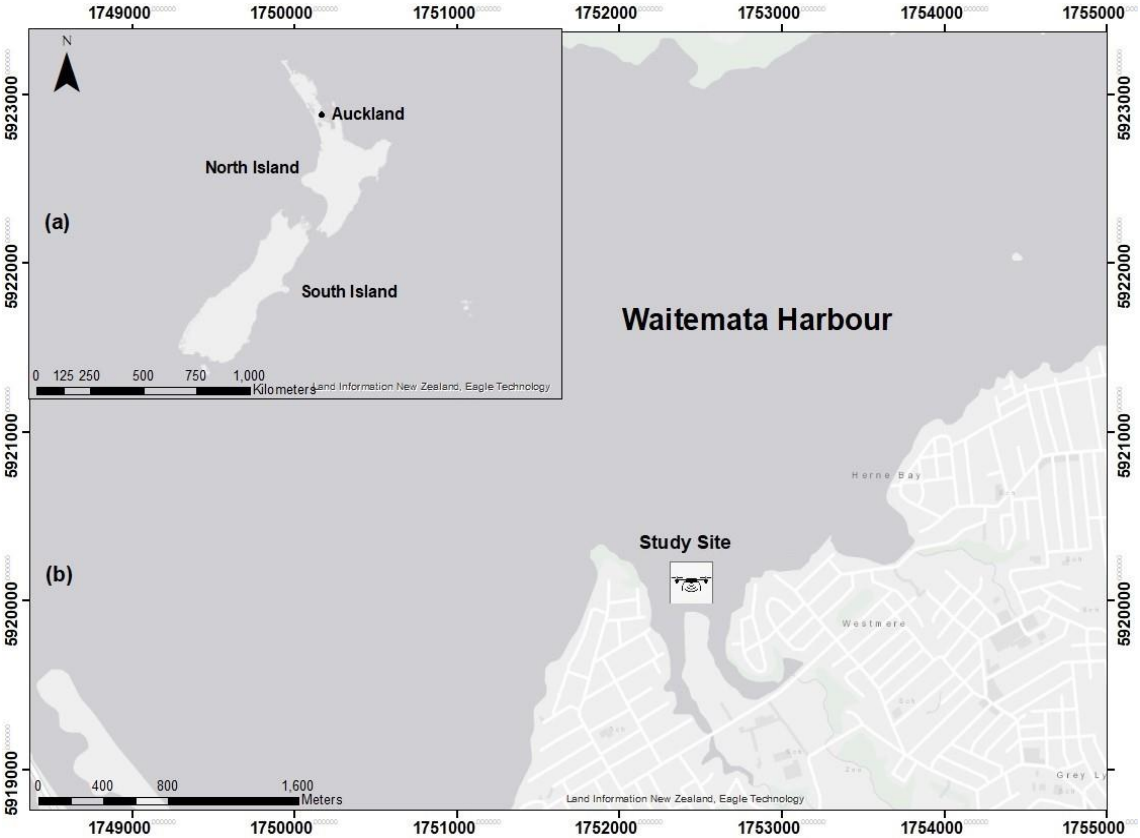

Figure 13. (a) Location of study site in Auckland, New Zealand. (b) Zoomed-in view of the study area within the Waitemata Harbour. Satellite imagery was sourced from LINZ (2019).

3.3 Aerial Image Processing and Classification

3.3.1 Structure from Motion Photogrammetry

RPAS aerial images were mosaicked using Pix4D® mapper (V 4.4.12 Educational edition). Pix4D® is a professional structure using motion photogrammetry software to transform images into digital spatial models (Pix4D, 2019). Pix4D® creates an orthomosaic from geotagged images, initially recreating a 3D scene and projecting the orthomosaic to the target coordinate system. Structure from motion (SFM) is a well-established concept for photogrammetry of high-resolution RPAS imagery (Johnston, 2019; Murfitt et al., 2017; Ventura et al., 2018). The general workflow used in Pix4D® includes (1) initial processing, adding multispectral imagery to the software here, the algorithm extracts meta-data information from the geotagged photographs (e.g., altitude, camera model, etc.); (2) detecting automatic tie points between the overlapped images to create a point cloud and mesh; (3) final processing option produces a digital surface model (DSM), orthomosaic and reflectance map of all available bands (only for multispectral) after radiometric processing and calibration (Pix4D, 2019).

3.3.2 Geo-reference and Radiometric correction

To geo-reference the orthomosaic accurately, ten ground control targets were laid out evenly across the study area. These targets were made similar to a section of a checkerboard, printed on A3 paper,

and laminated. All targets were surveyed using high accuracy RTK-GPS/GNSS (Septentrio®). After initial processing in Pix4D®, 3D GCPs were added to improve the accuracy of the project. Radiometric correction information was added from a reflectance panel provided by MicaSense® with calibrated values for each band, added in the final step of processing in the Pix4D® mapper. This option in Pix4D® produces a reflectance map for each band where the value of each pixel represents a true reflectance of the features on the ground.

3.3.3 Image Segmentation

To examine the potential of high-resolution imagery and the accuracy of the OBIA technique to extract targeted features from a heterogeneous ecosystem, one RPAS flight was used. This section of the reef is covered with mixed vegetation, and oysters are present along the northwest section of the reef. Initially, image segmentation was performed using the Feature Extraction module (FEM) within ENVI® version 5.3 (Exelis Visual Information Solutions, Co, USA). The benefit of this module is that the segmentation results can be previewed and refined before the final segmentation. Following segmentation, attributes/characteristics are calculated for all the objects in the imagery (1) spectral attributes (e.g., mean, standard deviation, maximum and minimum); (2) texture attributes (e.g., range, mean, variance, and entropy) and (3) fourteen spatial attributes including an adjustable texture kernel size (Warner, 2011). Through an iterative process, we found that the optimal segmentation result was achieved at a scale level of 50 (Edge algorithm) and merge level 80 (Full Lambda Schedule). The FEM consisted of two techniques (1) find object, (a) segment, (b) merge, (c) refine, (d) compute attributes, and (2) extract objects, (a) rule-based classification, (b) exporting results to a shapefile (ENVI).

3.3.4 Rule-Based Classification

ENVI's feature extraction module uses an object-based approach to extract land cover features with spatial, spectral (brightness and colour), and textural characteristics from imagery. The benefit of this module is that multiple features can be extracted simultaneously. In addition, the classification results can be previewed and further refined through the ENVI Zoom preview portal (ENVI). Rules were built for classification based on the object's attributes calculated during segmentation and appearance. The following land cover classes were defined: (1) mangroves and saltmarsh are vegetation that reflects most NIR spectrum, the rule assigned using their mean spectral attribute in band 4 (NIR); (2) shadows, bare rocks, and sediments appeared very dark in the NIR band, so spectral mean values attributes were used to create a rule for these objects and were merged; (3) finally, using spatial and spectral attributes of oyster reefs in band 1 (blue), rules were created based on, the mean spectral attribute, pattern of distribution, their shape and appearance (light or dark).

3.3.5 Principle to discriminate wild oyster reefs

One of the objectives of this study was to discriminate oyster reefs in the multispectral orthomosaic from other land cover features. To achieve this, we capitalised on the spectral reflective properties of different objects on the ground. The following remote sensing principles were followed: (1) most vegetation (mangroves and saltmarsh) absorbs red and blue light for photosynthesis, and a plant with chlorophyll reflects near-infrared light, spectral reflectance: 0.47 – 1.84 in band 4 (NIR-840nm wavelength). Shadows, bare rock (at a higher elevation than oyster reefs), and sediment (lower elevation than oyster reefs) have dark texture and appearance, spectral reflectance 0.16 – 0.47 in band 4 (NIR). Oyster reefs have spectral reflectance: 0.13 – 0.29 in band 1 (blue – 475nm wavelength).

3.3.6 Accuracy assessment

For accuracy assessment, used 2,772 random regions of interest (ROI) and an equalized stratified random sampling strategy to create ground truth ROI in the orthomosaic for each class in the total land cover area. The reliability of ground truth points is greater with a high-resolution (3.5 cm/pixel) orthomosaic (Lechner et al., 2012). Consequently, a confusion matrix was generated, which evaluates the accuracy of the OBIA classification. To assess the accuracy of the final classifications, including (1) overall accuracy from the referenced site, what percentage were mapped correctly, (2) kappa coefficient is calculated from a statistical test of the accuracy of a classification, (3) producer's accuracy is the map accuracy from the perspective of a mapmaker; how often real features on the ground are correctly shown on the classified map (4) user's accuracy is the accuracy from the perspective of a map user, often referred as the reliability of classification, i.e., the classes on a map will actually be present on the ground.

We also conducted an on-foot survey on 2 May 2019 to confirm the visual interpretation of oysters in the land cover from the classification map. For this purpose, we used an e-Trex® 20 Garmin handheld GPS with a positional accuracy of ± 1-2 m. Along with taking GPS waypoints, a Huawei P30 Pro mobile was used to collect geotagged ground photographs. The waypoint and geotagged photos were imported in ArcGIS and projected to WGS 1984 UTM Zone 60S datum for visual classification against the classified imagery.

3.3.7 Visual Analysis

To evaluate RPAS, high-resolution imagery can fill the gap in spatial resolution for monitoring marine ecosystems, an RGB (3 bands) satellite imagery year 2015 of resolution 75 cm/pixel was used from Land Information New Zealand (LINZ, 2019). After exploring the LINZ and Auckland Council aerial imagery archive (primary sources of imagery in New Zealand), this was the only imagery available at low tide. The spatial accuracy is ± 15cm. Here we zoomed in on both imagery

until they were blurred to show the scale at which we can view the imagery without any modification or classification.

3.4 Results

3.4.1 Intertidal rocky reef high-resolution orthomosaic

This study does not distinguish between different species of oysters, including vertical heights, and refers to all oyster structures as oyster reefs (including patches and string, clumps of oysters, and those attached to mangroves). The most basic need for oyster reef conservation is suitably scaled maps with sufficient information to identify ecological change (Gomes et al., 2018). Therefore, to evaluate the potential of a low-cost RPAS with a miniaturized multispectral sensor along a rocky intertidal reef characterized by oyster reefs, seven missions were conducted along Meola Reef in Auckland Harbour. Flights were performed between ~9 to 12 minutes, capturing a total of 18,760 geotagged images were selected after clean-up (involved removing blurred photos before processing), and the total reef area covered was 0.253 km^2 **(Table 3)**. The orthomosaic has a spatial resolution of 3.5cm/pixel.

Table 3. RPAS flight detail, including the area covered and photos used for photogrammetry

Flight number	Time for data capture	Area covered (km^2)	Number of geotagged photos used after clean-up
1	10 minutes	0.040	2840
2	10 minutes	0.033	2570
3	12 minutes	0.053	2740
4	11 minutes	0.046	3230
5	11 minutes	0.046	3520
6	10 minutes	0.035	2595
7	9 minutes	0.026	1265
Total	73 minutes	0.253 km^2	18,760

The high spatial resolution thematic map generated map **(Figure 14)** illustrates some important features such as the spatial extent of mangroves and spatial distribution of oyster reefs and provides a valuable dataset for mapping and monitoring intertidal biogenic habitats. In addition to, the dominating vegetation, such as mangroves and sections of saltmarsh, were distinguishable. Since all the images captured were in the late afternoon, shadows from mangroves were reflected in the northeast direction and had no impact on oyster reefs located in the northwest section.

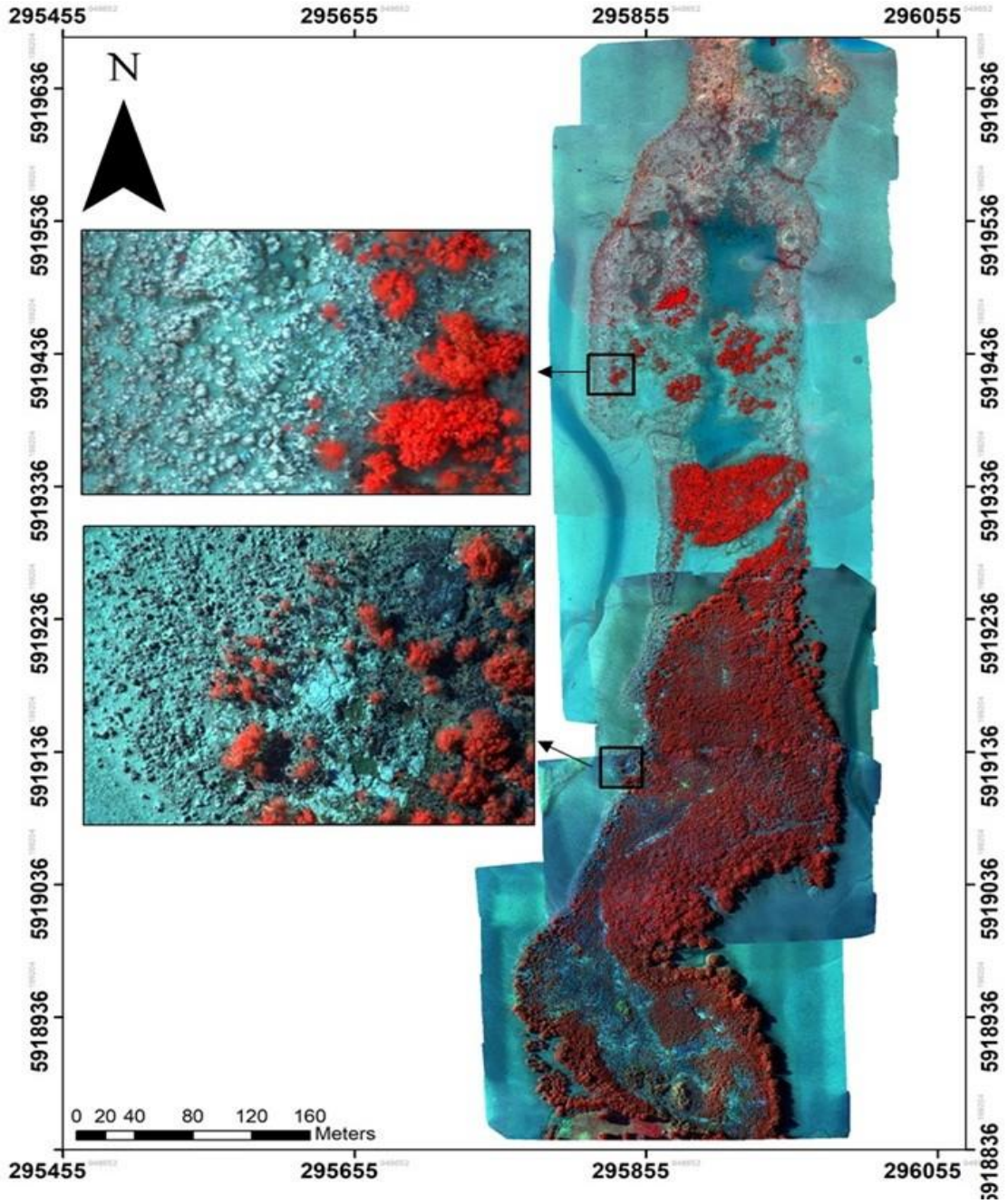

Figure 14. High-resolution false colour orthomosaic (3.5cm/pixel) of Meola Reef. The imagery, texture, and hue were used to distinguish different land cover features such as mangroves.

The segmentation of the orthomosaic is a fundamental step during thematic map production through OBIA since the characteristics of many objects can be used in the classification process. In ENVI, segmentation separates objects into real-world features, and the results from segmentation determine the geometry of objects **(Figure 15)**. Another benefit of using this classification technique is that the final classification results and their associated geometry can be exported as vector shapefiles, which can be subsequently used for other statistical analyses **(Figure 16)**.

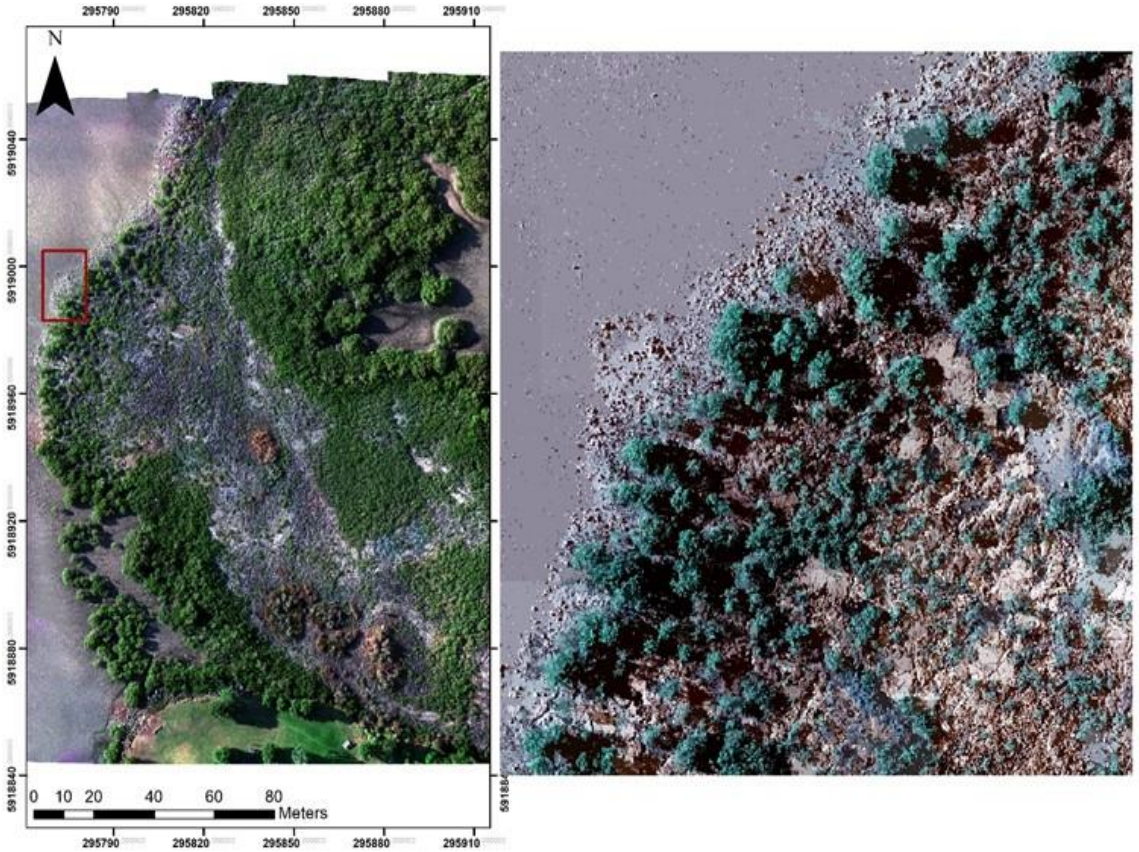

Figure 15. Figure on the right shows a zoomed-in segmentation result, where land cover features are segmented into different real-world (e.g., mangrove) objects.

Figure 16. The result of OBIA classification is exported as vector shapefiles with their geometric properties.

3.4.2 Thematic map

In this part of the reef, closer to the landward side, thematic map generation to highlight the characteristics of oysters was difficult due to bird droppings and wet/dry sediments that resembled the spectral properties of oysters. However, despite these limiting factors, satisfactory classification accuracy was achieved following OBIA feature extraction and rule-based classification workflow. A classified map **(Figure 17)** delineating oysters demonstrated a good match between the classified land cover and the original RPAS imagery leading to an overall accuracy of 83.9% and a Kappa Coefficient of 69.8% **(Table 4)**. The Producer's accuracy for the oyster class was 62.89%, while the user's accuracy was 95.0%. This can be interpreted as 62.89% of the reference oyster areas have been correctly identified as "oysters," and 95.0% of the areas identified as "oysters" in the classification were oysters. The reason for this reliability was the contribution of the high-resolution imagery (3.5 cm/pixel), enabling oyster reefs to be distinguishable.

Table 4. Classified imagery accuracy assessment and absolute accuracy of imagery.

Classified Imagery				
Classes	Producers Accuracy (%)	User's Accuracy (%)	Overall Accuracy	Kappa Coefficient
Mangrove	85.85	87.62		
Oysters	62.89	95	83.94%	69.80%
Saltmarsh	53.25	89		
Merged classes (shadows, bare rock, and sediments	100	84.98		

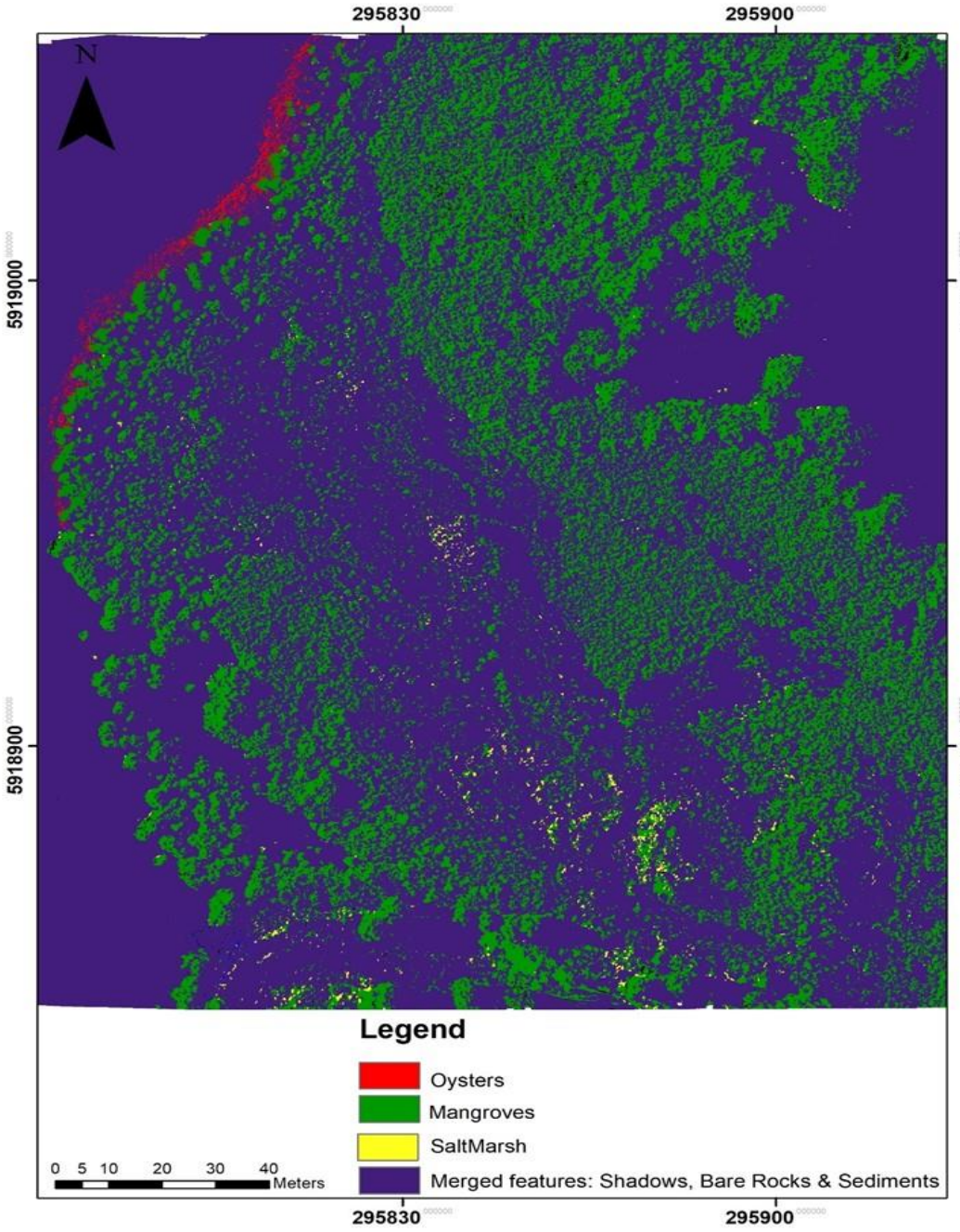

Figure 17. A high-quality thematic map generated after segmentation and rule-based classification, classified into three main land cover classes.

3.4.3 Visual Analysis

Visual analysis was conducted to examine the potential of RPAS imagery to fill the gap in spatial resolution for remote sensing of oyster reefs. The RPAS imagery has a 3.5cm/pixel resolution compared to the 7.5cm/pixel resolution satellite imagery. We interpreted the result using visual cues (e.g., texture, tone, shape, distribution pattern) from both imageries. At a map scale of 1:200, it was difficult to digitize and locate oysters from the satellite imagery manually, and at 1:100, the image became pixelated **(Figure 18a)**, whereas, from the RPAS imagery, oysters were evident at a scale of 1:100 **(Figure 18b)**.

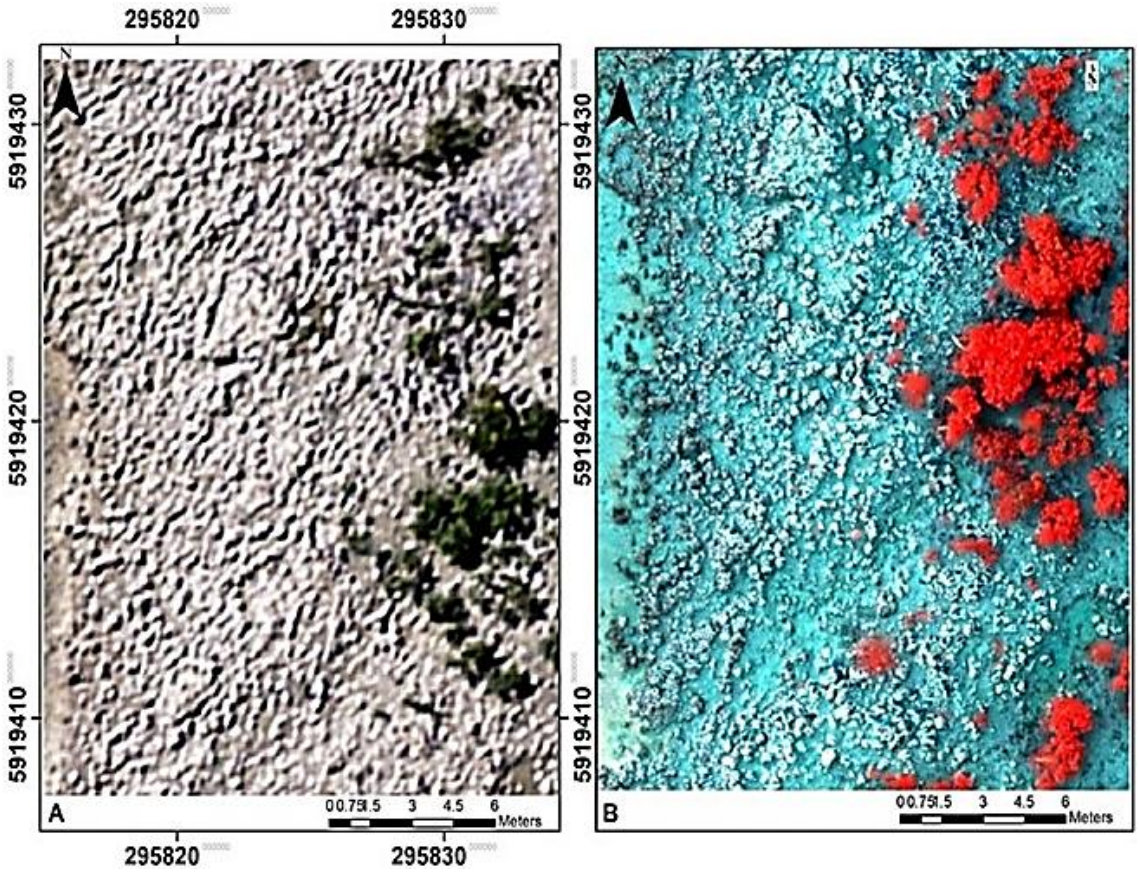

Figure 18. (a) satellite imagery zoomed to a map scale of 1: 100, and **(b)** is an RPAS imagery zoomed to a map scale of 1:100. For visual analysis of remotely sensed oyster reefs. Satellite imagery was sourced from LINZ (2019).

3.5 Discussion

Oysters are fundamental ecosystem engineers, where they also function as nutrient recyclers to filter sediments from water, increasing water clarity to thrive in additional biogenic habitats (e.g., seagrass) (Grabowski et al., 2012, Newell, 2005). Removing excess nutrients from water is a priority for marine management (Newell and Koch, 2004). However, once a dominant feature in many temperate marine environments, oyster reefs around the world have shown a marked decline in response to natural (e.g., predation, temperature) and anthropogenic stressors (e.g., sedimentation, housing expansion) (Grabowski et al., 2012; Thorngren et al., 2017).

While remote sensing (e.g., satellite and aerial imagery) in the marine environment is usually difficult to target optimum tidal and meteorological conditions, the availability of RPAS as a survey tool has met this need (Nahirnick et al., 2019; Ventura et al., 2018). RPAS bridges the difference between satellites and high-resolution ground surveys (Anderson and Gaston, 2013). However, ground surveys have a limited window of time for sampling between tides and can be destructive (e.g., trampling) to biodiversity. Our RPAS-derived image results produced high-resolution orthomosaic with a ground sampling distance of 3.5 cm/pixel, were captured within a smaller timeframe (~10 minutes flight time) and were obtained in a non-destructive manner.

High spatial and temporal resolution using low altitude remote sensing with multispectral RPAS has the benefit of detecting changes preceding ecological collapse (e.g., tipping points) (Gomes et al., 2018). Researchers have conducted manual ecological field surveys using quadrat sampling on the Meola intertidal reef (Foley and Shears, 2019). Between 2001 and 2017, Pacific oysters (*Crassostrea gigas*) and New Zealand rock oysters (*Saccostrea glomerate*) were the most abundant species on the reef. However, a subsequent increase in the population of predatory oyster borer snails has reduced the population of both species of oysters (Foley and Shears, 2019; Hayward, 1997/1999). Although in this study, we evaluated the potential of a multispectral sensor coupled with a low-cost RPAS from a 50 m altitude, future studies can use this technique to monitor and map the distribution of predatory borer snails from an altitude of ~20-30m. A lower flying altitude would improve the detail provided for directing mitigation measures or eradicating the predators.

Our results validated that RPAS platforms are a valuable tool for identifying intertidal marine biogenic habitats (Konar and Iken, 2018; Murfitt et al., 2017; Ventura et al., 2018). To our knowledge, this research initiated the application of multispectral sensors on an RPAS for high-resolution has been used to map oysters in temperate marine environments. In this study, a high resolution (3.5 cm/pixel) multispectral orthomosaic demonstrated that the use of spectral bands beyond the visible electromagnetic spectrum enhanced feature detection and increased the ability to delineate targeted features within a heterogeneous marine ecosystem. In temperate marine environments, turbidity and SSC usually make remote sensing of marine habitats challenging (Nagelkerken et al., 2015). We used RPAS on-demand capability to capture targeted habitats at low tide and optimum meteorological conditions to overcome this. Although data capture was after the solar noon, the flights were planned so that shadows from vegetation had no impact on the targeted feature, oyster reefs.

To maintain biodiversity, pivotal habitats such as oyster reefs provide quality breeding and feeding grounds for many fish and bird species that must be protected (Thorngren et al., 2017). This research showed that high-resolution RPAS-derived imagery and OBIA with a rule-based classification (based on spectral attributes of target features) have the potential to delineate targeted features within a heterogeneous marine ecosystem accurately. The segmentation of different features, such as oysters and mangroves, can be exported as vector shapefiles and used for other geo-analytics. RGB camera images are often suitable for revealing where a feature is on the ground. In contrast, the multispectral imagery allowed us to capture a target's reflectance from each wavelength (e.g., RedEdge and NIR) for enhanced target discrimination. Future studies can explore these parameters to classify oyster reefs into more categories, including shell density,

mean size, alive versus dead (dead/black oyster shells are brighter in colour), reef complexity, and oyster species.

3.6 Conclusions

As anthropogenic impacts, including climate change, continue to exert pressure on marine biogenic habitats, innovative methods for deriving useful information from multiple remote sensing imagery will be increasingly valuable as a tool to monitor this change. The technologies we have deployed in this study will provide a critical source of information to marine managers for conservation and planning. RPAS remote sensing enables the conduct of surveying on-demand during low tides and over a broad spatial scale. Flying low enables the capture of high-resolution imagery ranging from 50cm to 4 mm. Despite limitations for classifying features of similar spectral reflectance, OBIA for segmentation with a rule-based classification was sufficient for object identification and delineation of oyster reefs from other habitats. Our study showed that the deployment of RPAS coupled with a multispectral sensor for mapping and identifying oyster reefs in a heterogeneous marine environment increased the classification accuracy. The overall accuracy of 83.9% and a Kappa Coefficient of 69.8% were achieved. Our method enables long-term monitoring of marine environments at a lower cost than ground-based methods and at higher accuracy than other remote sensing methods. Therefore, a valuable tool for conservation and restoration management.

Chapter 4 Low altitude spatial assessment and monitoring of intertidal seagrass meadows beyond the visible spectrum using a remotely piloted aircraft system

A version of this Chapter is published as:

Chand, S., and Bollard, B. (2021). Low altitude spatial assessment and monitoring of intertidal seagrass meadows beyond the visible spectrum using a remotely piloted aircraft system. Estuarine, Coastal and Shelf Science, 255(February), 107299. https://doi.org/10.1016/j.ecss.2021.107299

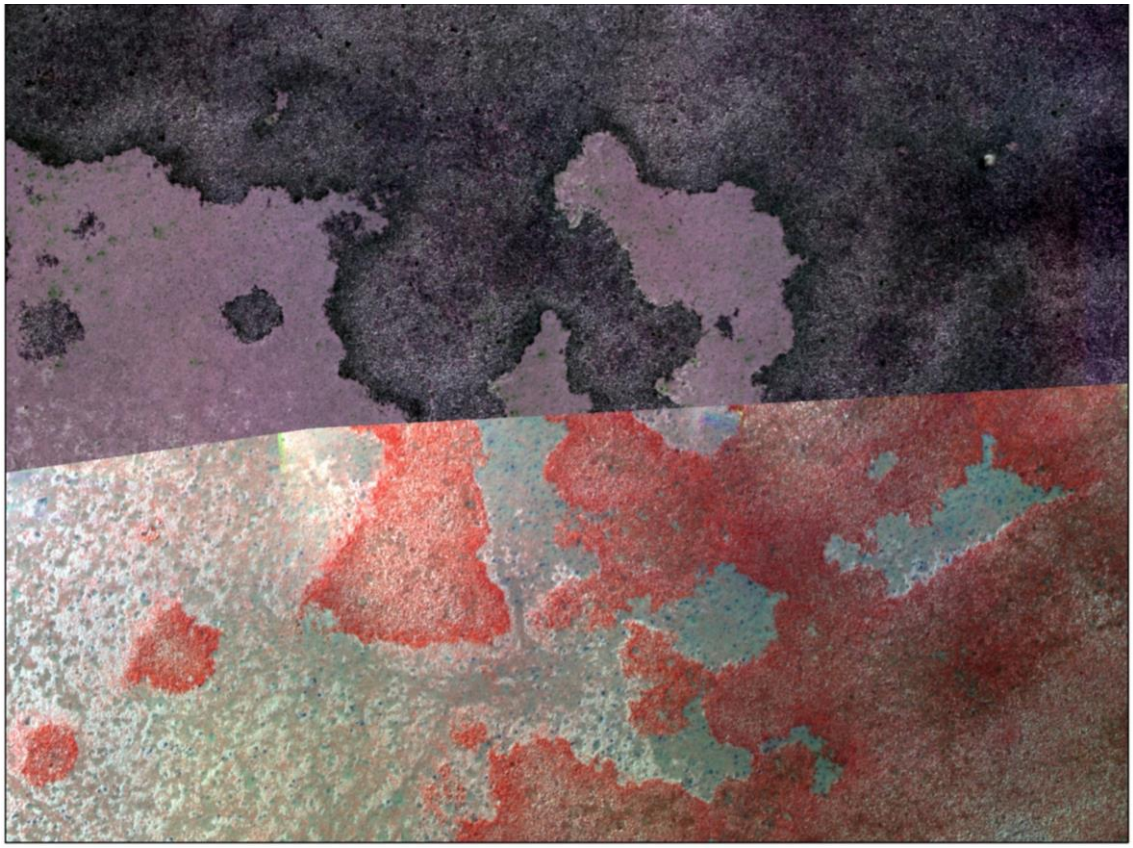

Cover image. RPAS aerial imagery showing seagrass meadows in the different electromagnetic spectrums. The top half of the image is shown in the VIS region, and the bottom is in the NIR region.

This chapter assessed the potential of an RPAS with a VIS+NIR sensor for low altitude mapping and high-resolution spatial assessment of intertidal seagrass meadows (Thesis objective c). We also modified a spectral index to distinguish seagrass meadows from other land cover features in the study area (Thesis objective d). Seagrass, a habitat under pressure from climate change-related and human activities often lead to continual decline over time, has provided an opportunity to research and develop empirical techniques for spatial assessment of this invaluable habitat. The results established that low altitude (50 m) combined with a VIS+NIR sensor (1) captured most information in the study area while providing high-resolution data for thematic map production, (2) coincided with field measurements, and (3) improved identification of different density of seagrass. The finding also showed that RPAS for data capture with a miniaturized VIS+NIR sensor was a significant step in identifying the drivers of change and improved our understanding of seagrass meadow spatial dynamics for conservation and planning.

4.1 Introduction

Seagrass ecosystems occur globally (except in Antarctica) and are essential ecological habitats that deliver multiple ecosystem services to the marine environment (Barbier et al., 2011; Bertelli and Unsworth, 2014). These services include (1) acting as an *in-situ* indicator to assess the relative health of marine ecosystems (Wood and Lavery, 2001), (2) absorbing and storing carbon referred to as carbon sequestration (e.g., contributing 15% of total carbon deposited in the ocean) (Fourqurean et al., 2012; Macreadie et al., 2014), and (3) pathogen reduction by producing natural biocides (Lamb et al., 2017). Despite their ecological importance, seagrass habitats globally have shown a significant decline. According to The International Union for Conservation of Nature (IUCN) Red List, 14% of all seagrass habitat-associated species are at some risk of extinction (Waycott et al., 2009; Short et al., 2016). To make things worse, anthropogenic activities and climate change (e.g., ocean warming) have been shown to affect seagrass meadow growth rates (Waycott et al., 2009; Grech et al., 2012). Consequently, globally 29% of seagrass meadows are either lost or gradually degraded (Waycott et al., 2009; Orth et al., 2006). To mitigate seagrass habitat degradation or loss, rapid assessment and monitoring are crucial for research to conserve this critical resource. For assessment, mapping, and monitoring, remote sensing from satellite and aerial photographs has provided datasets to researchers over the years.

Recent improvements, plus a lower cost of remote sensing airborne and spaceborne technologies, are advancing research ability to map seagrass habitats at various spatial and spectral scales (Marcello et al., 2015; O'Neill and Costa, 2013). The availability of aerial photos and satellite imagery often supplement traditional *in-situ* field surveys (Roelfsema et al., 2014; Traganos and Reinartz, 2018; Topouzelis et al., 2018). The widely available Landsat (e.g., 30m spatial resolution) or SPOT (15m spatial resolution) satellites provide researchers with time-series data to assess seagrass change detection trends. However, they might lack spatial resolution (e.g., 30 m) to delineate confidently heterogeneous seagrass habitats (Hossain et al., 2015a; Topouzelis et al., 2018). Satellite and field data do not always coincide, which could lead to false detection of temporal differences in the benthic composition and could consequently affect the accuracy of the maps produced (Hedley et al., 2016; Lyons et al., 2012; Pu and Bell, 2017; Peneva et al., 2008). Nevertheless, satellite remote sensing has successfully mapped seagrass in clear tropical waters with depths ranging from 1.4m to 16.5m (Tranganos and Reinartz, 2018). This capability is restricted, and the ability to penetrate water is reduced in temperate turbid coastal environments (McCarthy et al., 2018). However, with the advent of remotely piloted aircraft systems (RPAS) (also known as drones), marine applications with this technology have reached a new level of resolution.

Over the past two decades, the miniaturization of optical sensors used on small portable, low-cost aerial RPAS is increasingly being used by researchers to rapidly acquire high-resolution aerial imagery for many marine ecosystems (Anderson and Gaston, 2013; Duffy et al., 2018; Nahirnick et al., 2019). RPAS and remote sensors' integration has revolutionised marine science and conservation, filling the gap between *in-situ* field surveys and traditional remote sensing techniques (Colefax et al., 2018; Johnston, 2019). The integrity of RPAS, coupled with three-band RGB, 5-band multispectral to 200-bands hyperspectral sensor, is becoming more prevalent for marine applications (Chayhard et al., 2018; Hensel et al., 2018). With RPAS technology, (1) imagery can be captured directly for the desired marine ecosystem at scales relevant to management, (2) data can be captured at user-defined intervals, (3) data can be obtained at optimum meteorological and oceanographic conditions (e.g., early mornings when there is little or no wave action and low wind speed), and (4) spatial resolution of the imagery ranges from centimetre to millimetre per pixel resolution (Konar and Iken, 2018; Seymour et al., 2017b) and (5) spectral resolution can range from high to ultra-high, thus improving classification accuracy by using additional spectral bands (e.g., near infra-red (NIR) (Duffy et al., 2018).

Given the current status of seagrass meadows as critical habitat under pressure and with the status "At Risk-Declining" (Matheson et al., 2017; Matheson and Manley-Harris, 2018)[5]. Pragmatic solutions need to be designed for these meadows to mitigate further declines before reaching a tipping point. Nevertheless, according to the Ministry for the Environment (MfE), vast progress has been made to understand better the marine environment (Ministry for the Environment, NZ, 2019). Still, there are gaps in temporal data consistency, limiting the full potential of understanding drivers of change. These gaps can be bridged by developing new scale-appropriate techniques for rapid assessment and monitoring changes in the seagrass ecosystem. This technique will improve how drivers of change are identified and understood for conservation and planning.

This study uses a lightweight consumer-grade RPAS with a MicaSense® RedEdge multispectral sensor to survey and capture aerial imagery of intertidal seagrass (*Zostera muelleri*) meadows at low tide. There are no published studies aimed at exploring the potential of an RPAS with a multispectral sensor for low altitude monitoring and mapping intertidal seagrass meadows to the best of our knowledge. Therefore, we demonstrate the potential of an RPAS with a multispectral sensor for low altitude mapping and high-resolution spatial assessment of intertidal seagrass meadows. Next, we create a spectral index and demonstrate its potential to distinguish seagrass

[5] May read differently from published article as I have added another in-text citation to the sentence: Given the current status of seagrass meadows as critical habitat under pressure and with the status "At Risk-Declining" (Matheson et al., 2017; Matheson and Manley-Harris, 2018)

meadows from other land cover features. Finally, we use an object-based image analysis technique to segment the orthomosaic and perform a supervised classification.

4.2 Materials and Methods

4.2.1 Study site

The Waitemata Harbour, North Island, New Zealand, is a drowned river valley located in New Zealand's largest city Auckland and one of New Zealand's busiest ports, The Port of Auckland (Foley and Shears, 2019). Over time this Harbour has been modified by human activities and urbanization. Other pollution sources contaminating the Harbour waters are stormwater outflows and wastewater overflows. These sources include three freshwater inputs from the Rangitopuni stream, Henderson creek, Motion's creek, and Whau-river (Green et al., 2004). Continuous monitoring of contaminants (e.g., copper and zinc) by researchers around this Harbour found that contaminants' levels are above normal thresholds (Green et al., 2004; Matheson et al., 2011; Turner and Schwarz, 2006). Other concerns for the Harbour are pesticides, plastics, and pharmaceutical containments, including non-indigenous species from foreign ships (Aguirre et al., 2016; Hayward, 1997; Stewart et al., 2016).

The study site is located (-36.848 S, 174.714 E) along the eastern intertidal flat of Te Tokaroa Meola Reef **(Figure 19)**. The Waitemata Harbour estuary is 36% intertidal, with a mean depth of 4.28m (Foley and Shears, 2019). The hydrodynamics in this area is controlled by two high and low tides daily, which bring nutrient-rich waters from the Hauraki Gulf (Foley and Shears, 2019). Only one seagrass species, *Zostera muelleri*, exists in New Zealand and is predominantly found in the intertidal zones, mostly exposed during low tides (Lundquist et al., 2018). Worms and small crustaceans that live among these meadows are food sources for most reef birds (e.g., oystercatcher (*Haematopus unicolor*), pied stilt (*Himantopus leucocephalus*), and royal spoonbill (*Platalea regia*) (Morrison et al., 2007). Fish (e.g., juvenile snapper (*Pagrus auratus*), mullet garfish (*Mugil cephalus*), parore (*Girella tricuspidata*), and trevally (*Pseudocaranx dentex*)[6] were also found in the intertidal meadows during high tides (Parsons et al., 2014).

[6] May read differently from published article as I have added the scientific names: oystercatcher (*Haematopus unicolor*), pied stilt (*Himantopus leucocephalus*), and royal spoonbill (*Platalea regia*) (Morrison et al., 2007). Fish (e.g., juvenile snapper (*Pagrus auratus*), mullet garfish (*Mugil cephalus*), parore (*Girella tricuspidata*), and trevally (*Pseudocaranx dentex*)

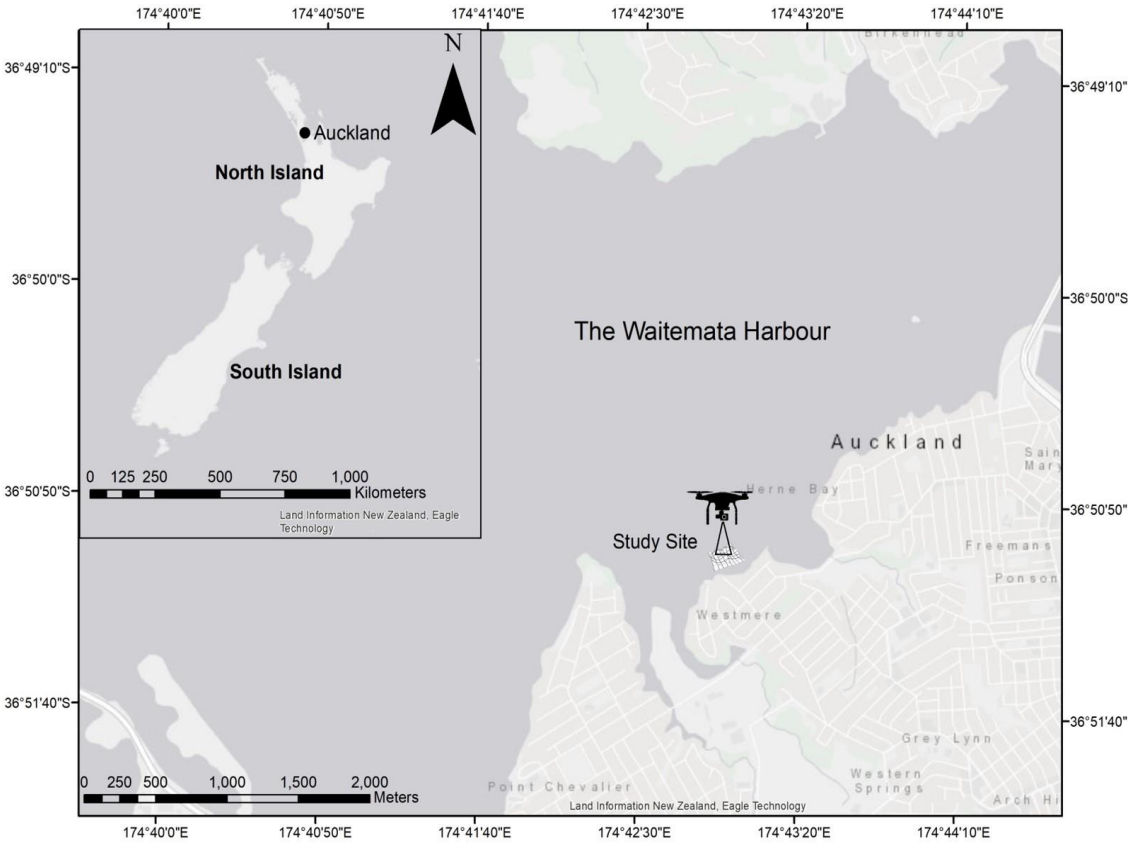

Figure 19. Location of study site in Auckland, North Island of New Zealand. Imagery source: Land Information New Zealand (LINZ, 2019).

4.2.2 Aerial image acquisition and sensor

A DJI Phantom 4 Pro with a custom mounted MicaSense RedEdge multispectral sensor was used for image acquisition. The flight was conducted from 50 m altitude at a speed of 3 m/s during a mean lower low water level (MLLW) (0.3m water level at 15:17 NZDST on March 22, 2019). We had fine weather during the image acquisition with no cloud cover and a 10 km/hr wind speed. Low visibility, measuring 70 cm from the Secchi disk, and turbidity were obstacles to data acquisition during high tide at this site. Nevertheless, a large section of the intertidal seagrass bed is exposed at low tides at this site.

From Pix4D© capture, 85 % front and 85 % side overlaps were selected between each image capture to optimize image matching and mosaicking. The flight was planned in the direction parallel to the sun to avoid surface reflection in the imagery. During the flight mission, taking approximately 10-12 min, we collected 3088 geotagged photos.

The MicaSense RedEdge sensor has five bands **(Table 5)** with a resolution of 1.2 megapixels and an image resolution of 1280 X 960 pixels for each band (MicaSense, 2017). Ground sampling distance with this sensor can produce imagery of 8cm/pixel (per band) from 120m altitude (MicaSense, 2017). The system also included a global navigation satellite system (GNSS) to geotag photos. A downwelling light sensor (DLS) is connected directly to the MicaSense

RedEdge sensor. The DLS is a 5-band incident light sensor used to correct lighting conditions during flights if covered by clouds.

Table 5. MicaSense RedEdge sensor band specifications (MicaSense, 2017).

Band No.	Band Name	Wavelength (nm)	Bandwidth (FWHM) (nm)
1	Blue	475	20
2	Green	560	20
3	Red	668	10
4	RedEdge	717	10
5	Near Infra-Red (NIR)	840	40

4.2.3 Field ground survey

We used ten ground control points (GCPs) that were evenly distributed across the seagrass mudflat to georeference the orthoimages. These GCPs were checkerboard style designed on white A3 paper and laminated. All GCPs were surveyed with a high accuracy RTK-GNSS (Septentrio®) system. Later these GCPs were imported in Pix4D® mapper as 3D GCPs to georeference the imagery.

4.2.4 Image processing and orthomosaic generation

Structure from motion and photogrammetric workflow has emerged as the scientific standard to stitch RPAS low-altitude aerial images into georectified orthomosaic (Ventura et al., 2018; Gomes et al., 2018; Casella et al., 2017). For this study, Pix4D® mapper (Education v 4.4.12) was used to produce georectified orthomosaic from RPAS imagery collected and projected to WGS 1984 UTM Zone 60S. Pix4D® mapper is an advanced photogrammetry software that converts images captured by RPAS to generate 2D and 3D maps and digital spatial models for each of the multispectral bands (Pix4D, 2019). In Pix4D, the interior and exterior orientation parameters were initially determined, followed by bundle block adjustment (Pix4D, 2019). Based on computer vision, the software matches key points between overlapping images. Followed by calculating the focal length, principal point, lens distortion (interior orientation parameters), position of the camera, and attitude (exterior orientation parameters) (Pix4D, 2019). The initial image georeferencing was based on the onboard GNSS and was further refined by adding GCPs from the RTK survey and reoptimized. In the second step, while finalizing the block bundle adjustment, additional tie points were generated based on automatic tie points. The result was the densified point cloud (DPC) (Pix4D, 2019). Based on the DPC, a 3D textured mesh was created. The third step, the dense point cloud, was filtered and interpolated to create an orthomosaic based on orthorectification. Finally, a reflectance map for all five bands with a true reflectance of the imagery objects was generated (Pix4D, 2019).

Radiometric calibration was applied using a calibrated reflectance panel and calibration information provided by MicaSense. The final product generated by Pix4D was reflectance orthomosaic containing reflectance values for the five individual bands (blue, green, red, NIR, and RedEdge), with the pixel values ranging from 0 to 1. Next, using the seamless mosaic tool in ENVI® Version 5.3 (Exelis Visual Information Solutions, Co, USA), the five individual bands were combined to create a five-band composite multispectral orthomosaic.

4.2.5 Determining a suitable spectral index for seagrass detection

Researchers have previously used satellite imagery such as Quick-Bird 4m multiband, Landsat TM 30m, and China-Brazil Resources Satellite 20m to explore the relationship between Leaf Area Index (LAI) and Normalized Difference Vegetation Index (NDVI) (Yang and Yang, 2009). The following spectral indexes were used:

(1) NDVI = (NIR – Red) / (NIR + Red)

(2) GreenNDVI = (NIR – Green) / (NIR + Green)

(3) BlueNDVI = (NIR – Blue) / (NIR + Blue)

This study compared the spectral reflectance from a field spectroradiometer and RPAS orthomosaic and created a spectral index that can easily distinguish seagrass meadows from other land cover features.

4.2.6 Seagrass spectral reflectance graph

We used a handheld ASD® (Analytical spectral devices Inc) spectroradiometer to capture seagrass spectral reflectance. This hyper-spectrometer can capture the reflectance of wavelengths ranging from 325nm to 1075nm. A white panel (Spectralon®) was used for calibration before the measurements and between measurements if the illumination changed. A GNSS was attached to the spectrometer to capture the geolocation when the samples were taken. This spectrometer has a target laser pointer to shoot directly on the seagrass. Seagrass spectral samples were collected simultaneously with the RPAS flight at low tide. An average of 20 samples was collected from homogeneous targets to provide an average spectrum. A wooden ruler was used for height adjustment to maintain all the samples at 15cm, yielding a field of view (FOV) of 22cm. The spectral file (.asd) from the field were downloaded from the spectrometer, visually inspected for quality, and imported into ENVI 5.3 spectral library viewer **(Figure 20a)**. Similarly, we trained and extracted the spectral reflectance samples of seagrass from the RPAS orthomosaic to create a spectral profile in ArcGIS Pro 2.5 **(Figure 20b)**. Both graphs were inserted together for comparison.

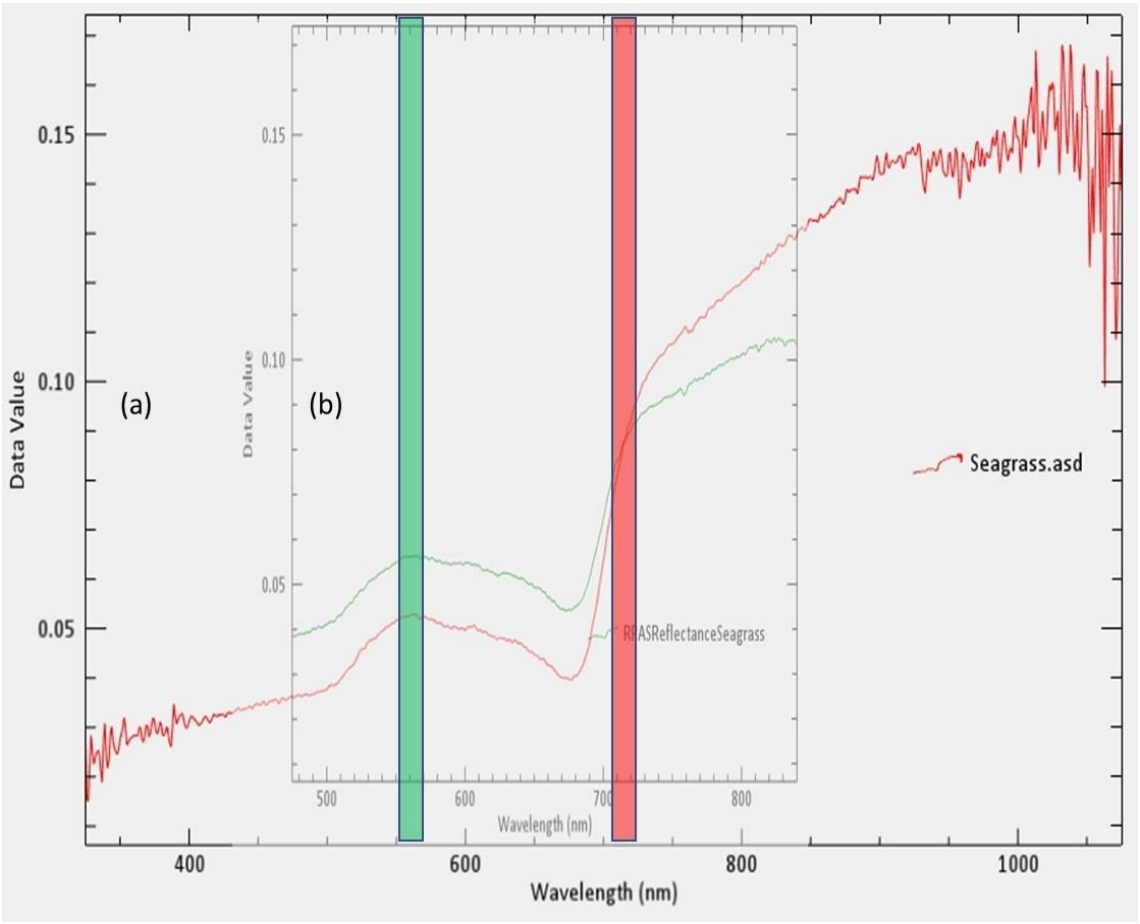

Figure 20. (a) Seagrass reflectance graph from field spectroradiometer (red curve) and (b) (green curve) an insert seagrass spectral reflectance from RPAS orthomosaic. In both graphs, the seagrass reflectance spectrum shows absorption along the blue and red wavelengths and reflectance along the green and steep curve in reflectance after the NIR region. We explored this spectral index to distinguish seagrass meadows from other land cover features.

4.2.7 Seagrass spectral index

The MicaSense RedEdge sensor captured the electromagnetic spectrum in the range of 475nm to 840nm wavelength. From the spectral signatures[7], we selected Green and the RedEdge bands to create the spectral index because of reflection along with the Green band and exponential hike after the red band. After an iterative process of evaluating different spectral index combinations from Green, RedEdge, and NIR bands, the final band math expression that explicitly distinguished seagrass meadows from other land cover features was:

$$RENDVI = (RE - Green) / (RE + Green)$$

[7] May read differently from the published article as I have replaced “graphs” with “spectral signatures”

4.2.8 Create a spectral index image

We used the Band Algebra toolbox from ENVI (Harris Geospatial Solutions, 2018), selected the band math tool, and entered the (B5 – B2) / (B5 + B2) expression. Here B5 corresponds to the RedEdge band, and B2 is the Green band.

4.2.9 Image Segmentation and classification scheme

Due to the high spatial resolution (3.4 cm/pixel) of the imagery, we used the ENVI® version 5.3 Feature Extraction module. This feature extraction module uses an object-based approach to classify imagery. There is more flexibility in the types of features extracted with the object-based method (Harris Geospatial Solutions, 2018). The benefit of this module is that multiple features can be extracted simultaneously, and the results for each step can be viewed in the Preview window. The feature extraction module combines these processes (1) segmentation of the image into different regions of pixels, (2) computing attributes for each region to create objects, and (3) classifying the objects with a supervised classification algorithm.

Initially, for image segmentation, the edge segmentation method was used. Edge segmentation is a valuable edge detector method that creates lines along with the most substantial intensity gradients (Harris Geospatial Solutions, 2018). Depending on the feature of interest, an appropriate scale level is required to delineate features in the imagery accurately. Therefore, after an iterative process, a Scale Level of 50.0 was selected to delineate the targeted features. The scale level can be further refined using the merge set to control over-segmentation. The merge level of 80.0 was used at this instant to merge segments.

For seagrass classification, we used a scheme developed and used by the United States Geological Survey (USGS) mapping projects (Handley et al., 2007). This scheme is a simple hierarchical system with consistency and improved accuracy in the mapping results. The scheme starts by determining the presence or absence of seagrass. Next, the scheme is further divided into two classes, continuous and patchy beds. Patchy beds are defined here as scattered units of seagrass. Patchy class is further subdivided into subclasses, dense, moderate, sparse, and very sparse classes. We used the regions of interest tool to create the training sample endmembers. The following region of interest was created (1) sparse seagrass, (2) very sparse seagrass, (3) water, and (4) sediment (named here to combine sand and mud).

4.2.10 Supervised classification

For image classification, we selected a supervised image classification technique. Supervised classification is a process of using training endmembers to assign objects to one or more known identities (Harris Geospatial Solutions, 2018). A supervised classification required at least two bands to be present in the input raster. Here we edited the metadata information and added a null

band so that the software could read this as a two-band raster image. After an iterative process of evaluating various supervised classification algorithms, Support Vector Machine, Minimum Distance, Spectral Angle Mapper, and Maximum Likelihood classification from the supervised classification toolbox in ENVI 5.3, Maximum Likelihood classification produced a better classification result. The input file, RENDVI segmented raster, was selected in the Maximum Likelihood window. Next, the four endmember classes were selected to create classified raster imagery.

4.2.11 Accuracy assessment and confusion matrix

For accuracy assessment, we used ArcMap v10.6. The Spatial Analyst toolbox was used to Create the Accuracy Assessment Points (ESRI, 2019). This tool creates randomly sampled points for the post-classification assessment. Initially, we used an equalized stratified random (ESR) sampling strategy to create 500 random points (distinct from training areas) in spectral index imagery (ESRI, 2019). The ESR sampling strategy creates randomly distributed points within each class, and each class has the same number of points (ESRI, 2019). The result was an accuracy assessment points shapefile with an attribute table that lists all the random points with a recorded field for classified and ground truth information. All ground truth points in the imagery were assessed visually to remove any bias during the accuracy assessment. Due to the high spatial resolution of the orthomosaic, visual inspection is very reliable for determining accuracy (Lechner et al., 2012). Next, from the Spatial Analyst toolbox, we used an update accuracy assessment points tool. This tool updates the ground truth field in the attribute table to compare reference points to the classified image. The input is the classified image and the previously created accuracy assessment points shapefile. The last target field was set to the classified field. This table was updated in both fields. The output was an updated accuracy assessment points shapefile, ready to compute a confusion matrix. Finally, we used the Compute Confusion Matrix geoprocessing tool from the Spatial Analyst toolbox to create a confusion matrix (ESRI, 2019). This confusion matrix was calculated to evaluate the accuracy of the classified imagery. This tool used the updated accuracy assessment points shapefile to calculate the confusion matrix. The confusion matrix contained the following information: (1) The Overall Accuracy from the referenced region shows what percentage was mapped correctly, (2) The Kappa Coefficient is the statistical test of the accuracy of the classification (3) The Producer's Accuracy shows the frequency of real features on the ground is corrected reflected on the classified map, and (4) The User's Accuracy shows the reliability of classification classes on the map that are actually present on the ground.

4.3 Results

4.3.1 High-resolution orthomosaic for remote observation

In the study site, the generated orthomosaic of the *Zostera muelleri* meadows had a spatial resolution of 3.5 cm/pixel **(Figure 21a)**. The high-level detail generated in the map clearly showed some essential features in the land cover. Other than the seagrass meadow, other features on the ground, e.g., blank clam (*Austrovenus stutchburyi*) shells (live clams are often locally collected at low tide), small swimmer crab (*Pagurus novizealandiae*)[8] burrows, were distinguishable **(Figure 21b)**. This high-level detail can be invaluable for monitoring and low altitude observation of coastal intertidal environments. The area covered in this intertidal zone with one flight was 0.04 km^2.

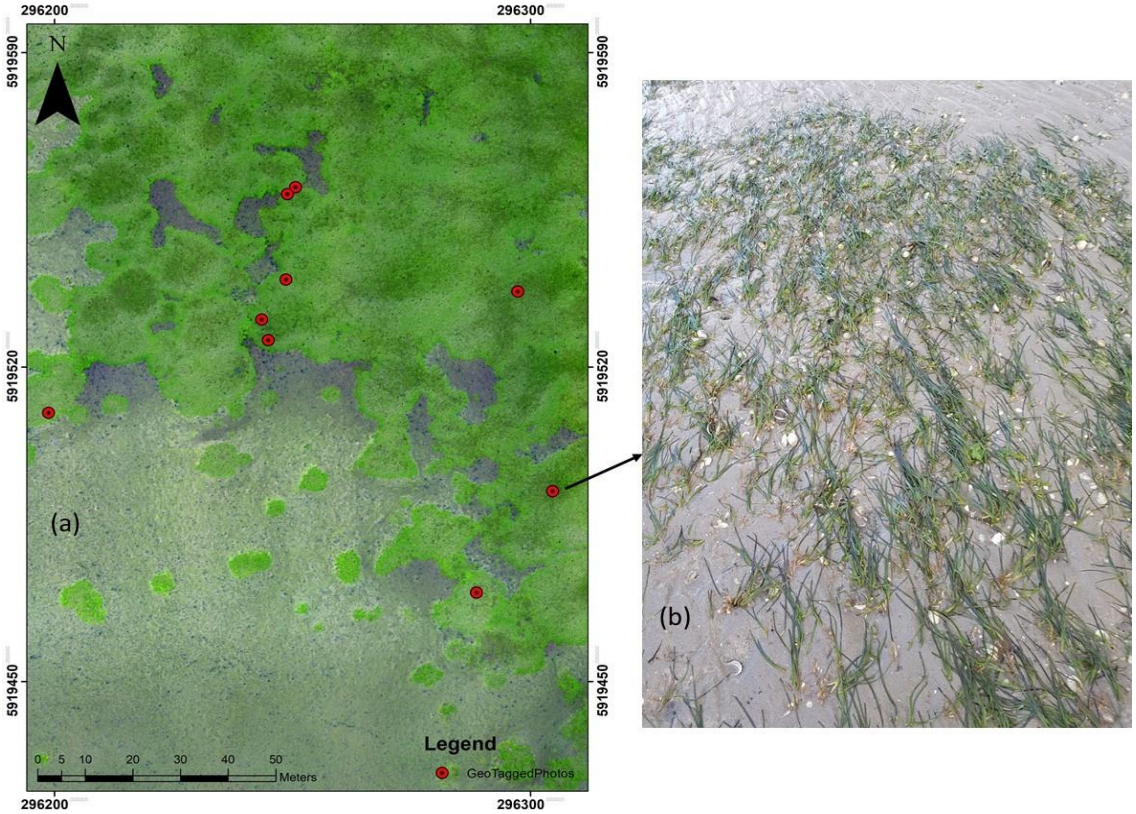

Figure 21. (a) High-resolution false colour orthomosaic (3.5 cm/pixel) showing the distribution of *Zostera muelleri*, the red dots on the map are GCPs (b), A geotagged photo showing sparse seagrass density and clamshells among the meadows.

4.3.2 Spectral index map

The spectral index map was created using the band math expression RENDVI. Through visual assessment of the spectral index map, seagrass meadows were spectrally distinguishable from water and other land cover features **(Figure 22)**. Other identifiable features were New Zealand

[8] May read differently from published article as I have added the scientific names: clam (*Austrovenus stutchburyi*) shells (live clams are often locally collected at low tide), small swimmer crab (*Pagurus novizealandiae*)

hermit crab (*Pagurus novizealandiae*), polychaetes (*Heteromastus filiformis*) burrows among the seagrass meadows. This provides evidence that biodiversity still exists among seagrass meadows, despite their sparse distribution.

In remotely sensed imagery, different land cover features reflect and absorb electromagnetic radiation differently. The high level of detail in the generated index map shows a reflectance value of ~1.03 for *Zostera muelleri* reflected from the Green and RedEdge bands. This information is depicted by the texture and hue of seagrass, ranging from light to dark green. Higher reflectance from seagrass meadows indicates healthy meadows that have higher chlorophyll content. Apart from meadows, water has a low reflective value of (~0.08), and sediment (~0.26) has different reflective values easily delineated in the imagery.

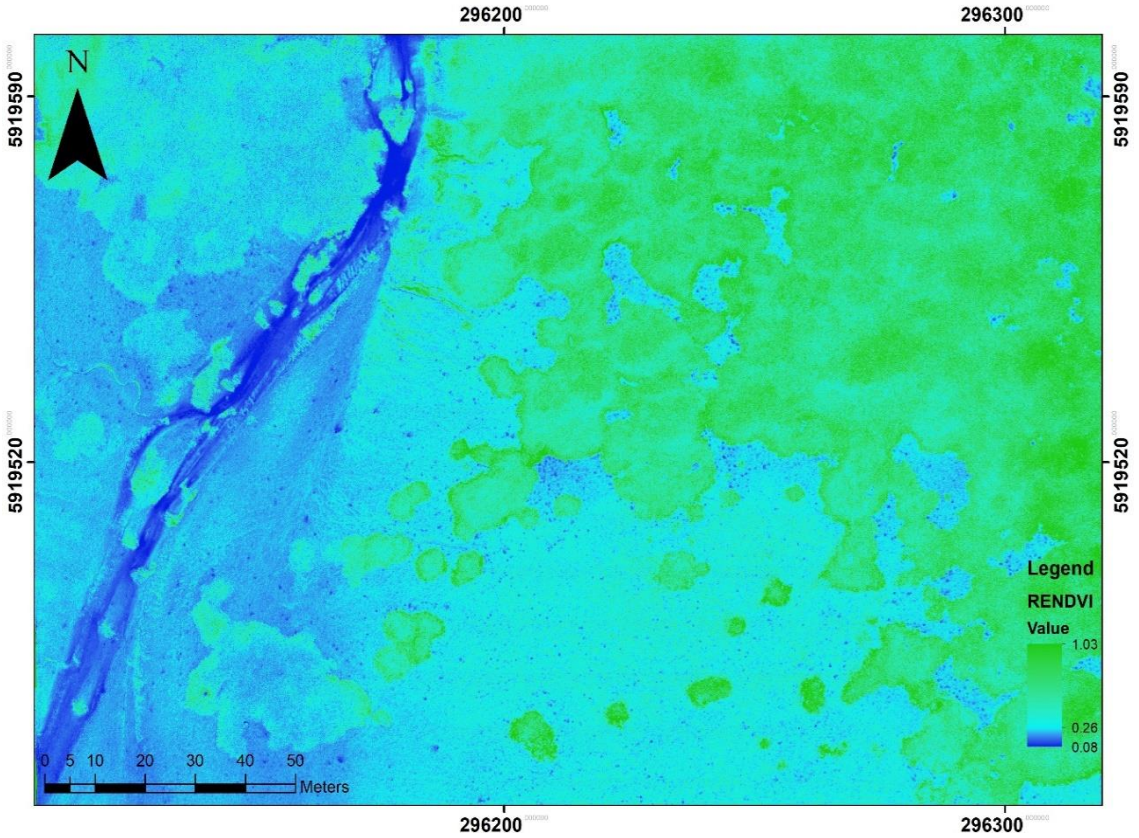

Figure 22. RENDVI spectral index map. In the index map, we applied a coloured ramp to distinguish between features.

4.3.3 Supervised classification map

The orthophoto segmentation was a critical step during thematic map production through OBIA. All the objects' characteristics could be used in the supervised classification process. For this reason, the segmentation results that determine the geometry of the land cover features in the edge-based segmentation algorithm and merge level settings should be carefully assessed before performing classification. The insert **(Figure 23a)** shows the result of segmentation to delineated

meadows based on their texture and spectral intensity using different hues, distinct from other land cover features.

The classified map **(Figure 23b)** exhibited a good match between classified land cover and the orthomosaic leading to an overall classification accuracy of 95% and a Kappa Coefficient of 0.81. From the classified imagery, 0.0015km^2 is occupied by sparse seagrass, and 0.0112km^2 is occupied by very sparse seagrass.

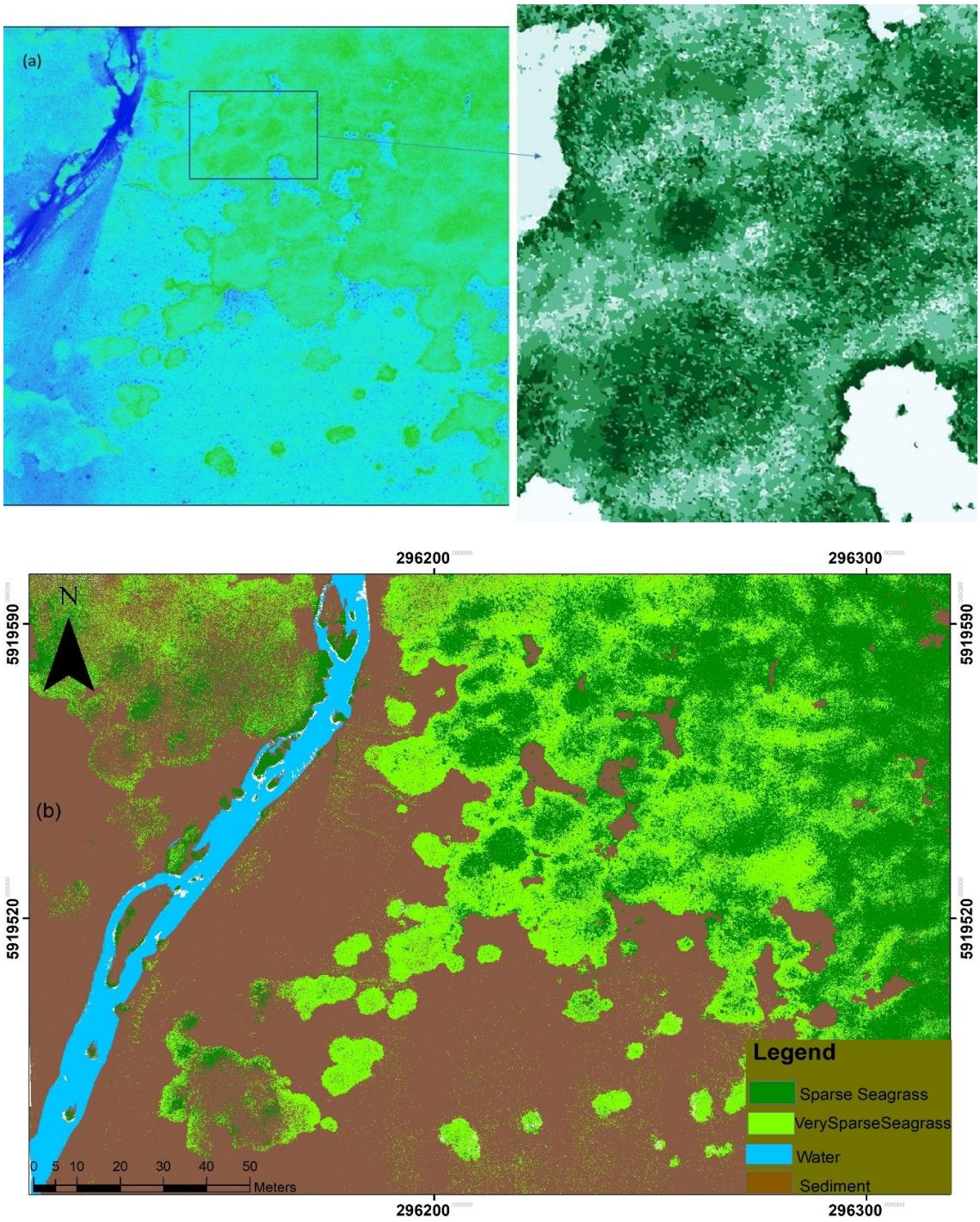

Figure 23. (a) Segmentation results after OBIA show that seagrass meadows areas have been successfully segmented into different image objects, and (b) Thematic map of correctly classified land cover features.

4.3.4 Accuracy assessment

The results of the accuracy assessment for the classified imagery are shown as a confusion matrix in **(Table 6)**, including the accuracy of each feature class (User accuracy and Producer accuracy), the combined agreement between classified data and referenced data (Overall accuracy), and the Kappa Coefficient estimate of accuracy. Values close to 1 indicate that classification is better than random. Accuracy was assessed from validation samples collected directly from remote imagery.

Table 6. Confusion matrix for accuracy assessment

Classified Imagery				
Classes	Producer accuracy	User accuracy	Overall accuracy	Kappa Coefficient
Dense seagrass	0.96	0.91	95%	0.81
Sparse seagrass	0.95	0.58		
Sediment	0.98	0.99		
Water	1	1		

4.4 Discussion

Remote sensing from satellite, aerial imagery, and *in-situ* field-based techniques are well established for mapping and monitoring seagrass meadows (McCarthy et al., 2018; Roelfsema et al., 2014; Tait et al., 2019). However, these techniques could have limitations that are not always feasible for many marine projects. Marine field surveys could be problematic (e.g., accessibility and terrain) and time-consuming (e.g., tidal variations) (Duffy et al., 2019; Tait et al., 2019). Simultaneously, satellite and aerial imagery can be challenging in optically complex turbid marine environments and lack spatial resolution (Koedsin et al., 2016; Wicaksono and Lazuardi, 2018). The timing of satellite overpasses such as Landsat 8 or Sentinel-2A/2B could be timed with an upcoming field survey. However, the time of satellite overpass may not always be favourable to all locations such as (1) an overpass may be at night, (2) no image capture at that location, (3) obstruction of the feature by high tides, and (4) image capture could be obstructed with an increased cloud cover (Amran, 2010; Konar and Iken, 2018).

In this aspect, RPAS has considerable potential to radically improve intertidal marine surveys and remove many limitations mentioned above (Manfreda et al., 2018). Our research has established that the combination of low altitude (50m) with a multispectral sensor can capture most information from a targeted area. Concurrently coincide with field measurements, providing high-resolution data for thematic map production. This high resolution can be attributed to the structure from motion photogrammetry technique to produce a five-band multispectral orthomosaic of ground sampling distance of 3.5 cm/pixel. Where positional accuracy is concerned, integration of surveyed GCPs with a GNSS rendered a positional accuracy of 0.02m. From this orthomosaic,

seagrass meadows were visually distinguished from other features such as water and sediments. For spatial assessment and mapping of seagrass meadows, a multispectral sensor has not been used in a turbid intertidal estuary to the best of our knowledge. Our results have established that RPAS with a multispectral sensor could fill the multi-temporal data gap with consistency. From this technique, marine managers can quickly identify the drivers of change and restore this crucial resource before reaching their tipping point.

Furthermore, it is challenging for an RPAS survey to target ideal wind and solar conditions in the marine environment. During flights, mixed meteorological (e.g., clouds) conditions usually interfere with the RPAS sensor viewing angle and produce sunglint and shadows in the imagery (Nahirnick et al., 2019). This change in environmental conditions during RPAS flights often results in inconsistent radiometric resolution in the imagery (Nahirnick et al., 2019). The flexibility of RPAS (e.g., deployed anytime) was capitalised on targeting optimum meteorological and oceanographic conditions during data capture. Although the images were captured in the afternoon, sunlight was consistent with no cloud cover. Nevertheless, a radiometric calibration was applied during processing to improve the quality of the imagery. Plus, flights were planned to fly parallel to the sun to minimize surface reflection in the imagery. Since individual seagrass meadows were not visible in the imagery from a 50 m altitude, future studies should consider collecting data at a lower altitude, possibly ranging from ~20-30m. In other marine environments, low altitude could also benefit from demarcating heterogeneous vegetation among seagrass meadows. Two individuals completed flight planning and RPAS data capture in less than 20 minutes. The setup and collection of GCPs with a real-time kinematic (RTK) system took the most time. However, all the fieldwork, including the flight and GCP survey, were completed in less than two hours. More time can be saved by using an RPAS with a survey-grade RTK system.

Spectral index using the Green and NIR band had been explored to detect seagrass distribution and identify long-term changes (Xue and Su, 2017). The seagrass spectral index showed the most reflectance in the Green and RedEdge bands from the spectral graphs. From this information, we computed a spectral index, RENDVI. Our result showed the ease of use and the ability of RENDVI to identify areas of seagrass meadows and distinguish other land cover features in the imagery. On the other hand, the spatial scale is an essential factor that influences the rules assigned for image segmentation (Hulet et al., 2014; Ventura et al., 2018). During image segmentation, land cover features are segmented using spectral heterogeneity of image objects on the ground. They are correlated to their spatial and textural attributes. Achieving a good segmentation result is one of the essential steps for the success of further classification. A good segmenting of the imagery resulted in an overall accuracy of 95% and a Kappa Coefficient of 0.81. Apart from seagrass meadows, water and sediments showed good spectral differences and were easily

distinguished. This was confirmed by getting a higher user and producer accuracy for sediment and water.

The high spatial resolution and ability of RPAS to capture multi-temporal data at low altitudes have allowed researchers to detect local changes and have been proven to be a valuable tool for marine research (Kalacska et al., 2019; Ventura et al., 2018). The use of RPAS for data capture with a multispectral sensor is a significant step in gaining insights to identify the drivers of change in the marine environment and improve our understanding of the spatial dynamics of seagrass meadows for conservation and planning.

4.5 Conclusion

Seagrass meadows are located in a dynamic marine environment where they consistently deal with changes and challenges from human activities and climate change. Seagrass habitats are also challenging habitats to investigate, map, and monitor because of (1) widespread distribution, (2) primarily established in mudflats, which are difficult for on-foot survey over large areas, (3) the danger of trampling biodiversity sheltering among meadows, and (4) are exposed for short periods for *in-situ* samplings over large distances. To monitor and map these meadows, RPAS is a well-established tool with low altitude capability and high-resolution ground sampling distance. The other obvious benefit of this technology is that flight planning can be done on the fly with minimum effort and maximum results. Our work validates this perspective and its application to improve our understanding of seagrass dynamics and identify change drivers. Consequently, rapidly identifying changes is vital for the management of this critical resource. Plus, the long-term sustainability of other marine resources, such as fisheries, is dependent on seagrass meadows at different stages of their life cycle.

Depending on the project's size, small multi-rotors are reasonably better for mapping remote areas. In contrast, winged RPAS would better suit large extensive seagrass beds. Different sensors, with three-band (RGB) and five-bands (multispectral), can be exploited for various applications. As explored in the study, the multispectral sensor increased the ability to distinguish meadows from other land cover features from Green and RedEdge spectral bands with high accuracy. Lastly, for long-term, multi-temporal monitoring and identification of changes to many important intertidal marine biogenic habitats, researchers could benefit from a well-planned deployment of RPAS with suitable sensors.

Chapter 5 Multispectral low altitude remote sensing of wild oyster reefs

A version of this Chapter is published as:

Chand, S., and Bollard, B. (2021). Multispectral low altitude remote sensing of wild oyster reefs. Global Ecology and Conservation, 30(August), e01810. https://doi.org/10.1016/j.gecco.2021.e01810

Cover image. Aerial imagery of Meola intertidal reef captured at low tide. The top half is displayed in the VIS+NIR spectrum, and the bottom half is shown in the VIS spectrum. Wild oyster reefs dominate this section of the rocky reef.

This chapter investigated the potential of VIS and VIS+NIR sensors and low altitude aerial imagery for distinguishing wild oyster reefs in a heterogeneous intertidal rocky reef ecosystem (Thesis objective e). We assessed the spectral signatures collected from RPAS against an *in-situ* handheld Spectro-radiometer (Thesis objective f). We also evaluated the accuracy of an object-based image analysis technique (OBIA) and a Support Vector Machine (SVM) to classify high-resolution multispectral RPAS imagery (Thesis objective g). Spatial assessment and mapping of wild oyster reefs can be challenging due to complex and rugged structures that are challenging to access using conventional *in-situ* and time-extensive techniques. The application of remote sensing for ecology and conservation of benthic habitats has emerged as a powerful technique to expedite many of these challenges. The results established that the spectral resolution from the VIS+NIR was more critical to successfully detect and accurately classify wild oyster reefs in this rocky intertidal reef. The findings also showed that extracting spectral reflectance signatures from the RPAS orthomosaic was more time-efficient than the *in-situ* Spectro-radiometer, which had to be recalibrated after an illumination change. This remote sensing technique for ecology and

conservation offers scale-appropriate spatial assessment, monitoring, and mapping of benthic habitats in challenging and inaccessible marine environments.

5.1 Introduction

In New Zealand, wild oyster reefs distribution and spatial location vary across temperate estuaries (Morrison et al., 2014). The Rock Oyster (*Saccostera commercialis*) and the Bluff oyster (*Ostrea edulis*) were two primary native species of oysters in New Zealand spatially located either on muddy sediments or established on rocky reefs (Morrison et al., 2014). During the 1970s, Pacific oysters (*Crassostrea gigas*) presence were detected in New Zealand. Since their introduction, Pacific oysters have replaced the Rock Oyster on Meola intertidal reef and in the Kaipara Harbour (Foley and Shears, 2019; Morrison et al., 2014). However, on the Meola intertidal reef, Pacific oysters are a foundation species to support biodiversity (Foley and Shears, 2019). Seagrass meadows[9] also provide ecosystem services such as spawning and nursery grounds for many local fish species and provide long-term removal and storage of atmospheric carbon dioxide through carbon sequestration (Barbier et al., 2011; Lefcheck et al., 2019). The abundance of oysters on the Meola rocky reef gradually declined but was detected during an *in-situ* survey in 2012 due to an increase in the quantity of predatory oyster borer snail (*Haustrum scobina*) (Foley and Shears, 2019). This decline calls attention that as pressures on oyster reefs exaggerate, it will become critical to identify dynamic changes from spatial assessments to monitor their ecological status (Grabowski et al., 2012; IPCC, 2014). Apart from *in-situ* techniques, remotely sensed datasets are essential for effective monitoring and mapping of coastal estuarine environments (Anderson et al., 2019; Baggett et al., 2014).

Researchers have used time-series satellite imagery to (1) assess spatio-temporal changes in intertidal habitats due to natural or anthropogenic pressures using spectral attributes, (2) distinguish sediment from intertidal oysters, and mapping (3) and digitize oyster reefs (Grizzle et al., 2002; Garvis et al., 2015; NOAA, 2003). However, the limitations of satellite imagery with cloud cover and atmospheric correction persist. Open-source satellite data could have low and medium resolutions and more extended revisit periods (Seavey et al., 2011). In addition, satellite datasets may not always be synchronized with the desired tides and *in-situ* works (Schill et al., 2006). Consequently, pre-processed imagery with high accuracy translates into increased costs (Schwantes et al., 2018). Unfortunately, it is challenging to assess and monitor their vulnerability from remotely sensed datasets hidden underwater due to the spatial complexity of oyster reefs. Challenges are further exacerbated when different sensors collect aerial imagery with spectral and radiometrically inconsistent (Windle et al., 2019)—also captured at undesired spatial and

[9] May read differently from published article as I have replaced, “they” to “seagrass meadows”

temporal resolutions (Schwantes et al., 2018). Furthermore, researchers explored brightness differences in aerial imagery to detect dead and live oyster reefs (Grizzle et al., 2002). Moreover, mapping wild oyster reefs and quantifying population density assessments within intertidal estuarine environments remain challenging (Windle et al., 2019). These challenges are due to the environmental conditions wild oyster reefs reside in and the expansive estuarine conditions, e.g., saline to brackish to intertidal. Despite challenges, researchers have used satellite imagery over the years, e.g., the Landsat series and crewed aerial imagery, to assess, map, and monitor oyster habitats (Grizzle et al., 2002). Advancements in satellite sensors have improved spatial resolution ranging from 30 to 50cm imagery with better spectral resolution ranging from 8 to 11 spectral bands (Espriella et al., 2020). Besides, commercial satellites such as WorldView 3 and 4 have improved their revisit time to less than a day, an essential feature to align with *in-situ* work in the marine environments (NOAA, 2003; Reshitnyk et al., 2014).

While technical challenges persist with other techniques, remotely sensed aircraft system (RPAS) applications have increased to alleviate many of the challenges mentioned above (Anderson and Gaston, 2013; Manfreda et al., 2018). These RPAS are off-the-shelf systems that include components necessary to operate the aircraft and can be retrofitted with desired sensors, e.g., near-infrared (NIR) capability (Murfitt et al., 2017; Taddia et al., 2019). For example, researchers in the USA Rachel Carson Reserve surveyed wild oyster reef areas ranging from 30 to 300m^2 (Windle et al., 2019). Windle et al., 2019 used two visible (VIS), red, green, and blue (RGB), sensors that produced 5cm orthomosaic for delineating oyster boundaries and thematic mapping. They revealed that RPAS platforms could accurately monitor intertidal oyster reefs surveyed with a real-time kinematic global positioning system (RTK-GPS) and improved reef morphology measurement (Windle et al., 2019). In addition, RPAS applications provide a baseline for studying oyster reefs and have been more efficient than conventional *in-situ* techniques. Moreover, RPAS aerial imagery provided a more significant number of validation points than satellite imagery for accuracy assessments.

Furthermore, researchers in the Gulf of Mexico in Florida used a multi-rotor RPAS equipped with a VIS sensor to survey intertidal habitats (Espriella et al., 2020). This study used a geographic object-based image analysis (GOBIA) technique that distinguished three habitats, mudflats, saltmarsh, and oyster reefs, and resulted in an overall accuracy of 79%. However, one of the limitations of this research was little spectral and textural separability. Moreover, broadband resolution from many multispectral satellite sensors may restrict the detection of oyster reefs (Girouard et al., 2004). Therefore, this limitation could be mitigated by using additional spectral bands in the near-infrared region. In addition, there is a gap in exploring RGB (VIS) and

multispectral (VIS+NIR) for spatial assessments, monitoring, and mapping of wild oyster reefs from proximal low altitude remote sensing.

This study aimed to produce a spatial distribution map of wild oyster reefs in a rocky intertidal reef at low tide using multispectral (VIS+NIR) low altitude RPAS. In addition, answer the following questions (1) How effective is multispectral (VIS+NIR) imagery for distinguishing wild oyster reefs in a heterogeneous ecosystem dominated by vegetation? (2) Are spectral reflectance signatures collected from RPAS orthomosaic equally effective to *in-situ* spectral signatures collected using a handheld spectro-radiometer? In addition, aim to evaluate an OBIA workflow's accuracy with a Support Vector Machine (SVM) to classify high-resolution multispectral RPAS imagery.

5.2 Materials and Methods

5.2.1 Study area background

The coastal system studied was Meola rocky reef (36° 51' 14.3316" S and 174° 42' 36.6984" E), located within the Waitemata Harbour in Auckland **(Figure 24)**. This rocky reef is one of the most visible features of satellite imagery, especially during low tides in the Waitemata Harbour (Land Information New Zealand (LINZ), 2019). The Waitemata Harbour is surrounded by New Zealand's largest city, Auckland, and comprises the busiest port. This rocky basalt reef was formed from volcanic eruptions 28,000 years ago and extended over 2km from the landward edge into Waitemata Harbour (Foley and Shears, 2019). Over time, the Waitemata Harbour has been and continues to be impacted by increased urban development, human waste, and vessel wastewater discharges. Consequently, this Harbour has become a hotspot for invasive species (Foley and Shears, 2019; Hayward, 1997).

Despite changes over time, the Meola reef ecosystem has rapidly maintained its biodiversity of benthic habitats vegetation: e.g., seagrass, algae, kelp, saltmarsh, mangroves, microhabitats, such as rockpools and shellfish, e.g., oysters (*Crassostrea gigas*). This reef also includes a widespread breeding and nesting spot for South Oystercatcher, Tui, and Black swan (Foley and Shears, 2019; Hayward et al., 1999; NZ, e-Bird, 2019). It is important to note that this reef is fully submerged during high tides, while most reef sections are exposed during low tides. For oyster larvae distribution, this is a critical process, where this reef is flushed with nutrient-rich waters from the Hauraki Gulf with two high (ranging from ~1.9 - 2.9m) and low tides (ranging from ~0.7- 1.0 m) daily (Foley and Shears, 2019).

Research over time by the local council has revealed that this reef has endured many environmental and anthropogenic impacts. Consequently, a decline in the oyster population has been detected (Foley and Shears, 2019). The decline of oysters can be associated with a rapid expansion of

adjacent urban areas. Effluent discharge increases water toxicity and interrupts oysters normal growth and survival rates (Newell et al., 2005). Locals, setting fish traps on the reef during low tides, tramp on live oyster shells, while other impacts on the reef are from hikers and bird watchers.

5.2.2 RPAS system and *in-situ* data collection

RPAS aerial data was captured at 14:30 NZST during Mean Lower Low Water (0.6m) on June 19, 2019, using a Phantom 4 Pro® multi-rotor. The Phantom RPAS was equipped with a multispectral MicaSense® RedEdge™ sensor at a slightly off-nadir viewing angle using a ready-to-use quick-mount integration kit from MicaSense and an off-the-shelf DJI sensor. The advantage of using this integration kit from MicaSense is that the DJI RGB sensor on the RPAS can be used simultaneously without any interference. Together they weigh ~1.62kg with a battery and other accessories **(Figure 25)**. The slightly off-nadir sensor does not affect the final orthomosaic, as the sensor position information was included during the photogrammetry process.

To capture low-altitude (50m from surface) images over Meola Reef, we used Pix4D Capture © 2019, an open-source autonomous flight planner. In the software, a mission was planned by selecting a grid-style mission, which is like a lawnmower-style flight path. After the solar noon, the flight path was planned to fly the RPAS directly towards or away from the azimuth ±180 degrees to avoid any sunglint in the imagery. Other settings included: (1) picture trigger mode set to fast as this allowed the RPAS to fly through the waypoints taking images without stopping in a continuous motion maintaining the orientation of the sensor during flights; (2) with a typical speed of 3m/s; (3) white colour balance set to auto; and (4) side and front overlaps set at 80% respectively. All civil aviation regulations of New Zealand were followed, including the Part 101 Pilot certificate. All hazards were anticipated before the flights, including having an observer. The flight times were logged on Airshare to notify other airspace users (NZ, Airshare, 2019).

Mangroves dominate the landward edge of this rocky intertidal reef, and oyster reefs are only in the Northwest section. It is essential to point out that we have referred to all oyster structures as oyster reefs irrespective of their establishment. There was no attempt to differentiate between Pacific and New Zealand oysters, their vertical height, and determine where they are dead or alive in this study.

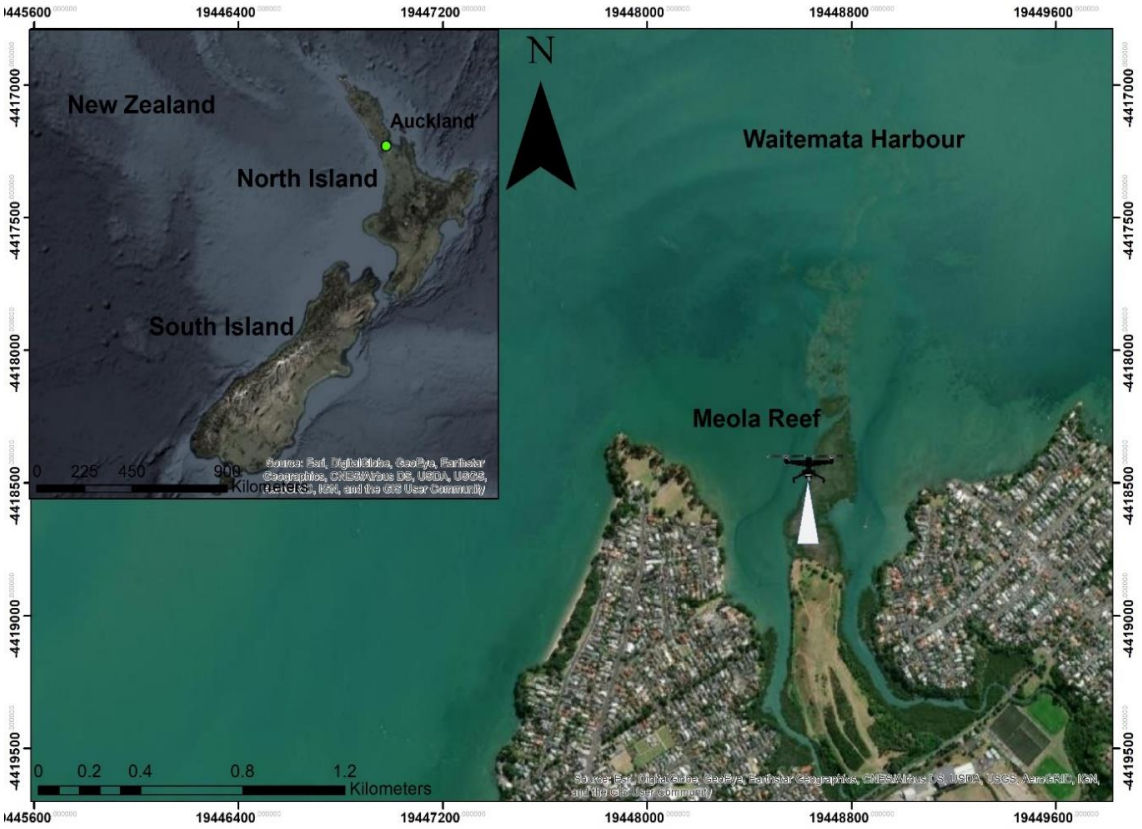

Figure 24. The Meola intertidal rocky reef was a coastal system studied within the Waitemata Harbour. Source of imagery, Land Information New Zealand (LINZ, 2019).

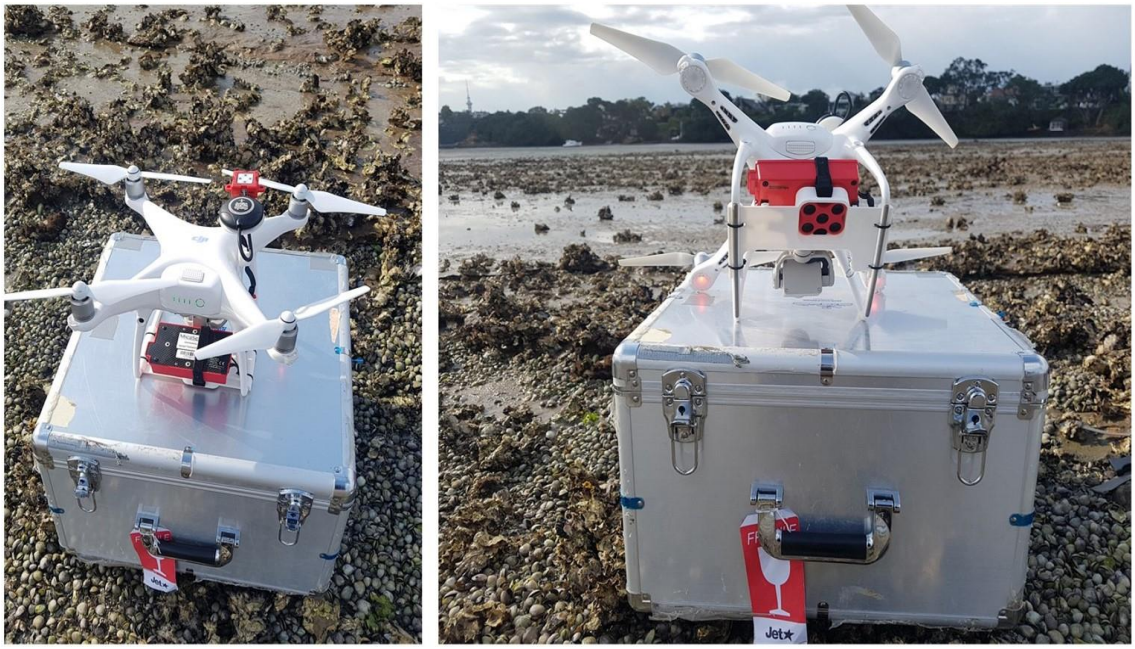

Figure 25. The RPAS setup with DJI VIS and MicaSense RedEdge-M VIS+NIR sensors, including a downwelling light sensor (DLS) and a GPS. Images courtesy of Kavita Prasad.

The MicaSense® VIS+NIR sensor has the following distinct bands: Band 1 is Blue (475 nanometres (nm), Band 2 is Green (560 nm), Band 3 is Red (668 nm), Band 4 is the Red Edge (717 nm), Band 5 is near infra-red (NIR) (840 nm), and image resolution is 1280 x 960 pixels per band (MicaSense, 2017). To improve the image quality, we applied a radiometric correction during image processing

in Pix4D Mapper ®. Reflectance was calculated by dividing Radiance over Irradiance for individual bands to give each spectral band a pixel value ranging from 0-1 to improve the images' quality and normal viewing. In contrast, the VIS sensor has Red (660nm), Blue (450nm), and Green (520nm) (RGB) bands.

5.2.3 Ground reference data

For georeferencing the aerial imagery, ten checkerboard-style ground control points were randomly scattered along the study area. To get an absolute spatial accuracy for the orthomosaic, these ground control points were surveyed using high accuracy Septentrio® GPS RTK base station and rover, and 4 of the ground control points (GCPs) were utilized as checkpoints in Pix4D® Mapper educational edition (V 4.4.12). After initial processing in Pix4D, the GCP information was imported using GCP/MTP Manager. These GCPs and checkpoints were marked using the raycloud and reoptimized.

5.2.4 VIS and VIS+NIR orthomosaic

To generate a high-resolution orthomosaic, all aerial photographs were processed in Pix4D® Mapper SfM photogrammetry software. Pix4D has been a popular choice for RPAS users to transform aerial photos into 2D and 3D digital spatial models (Espriella et al., 2020; Pix4D, 2019). SfM algorithm works by utilizing a series of 2D overlapped geotagged aerial photographs to reconstruct the 3D structure of a scene. SfM photogrammetry used meta-data information such as sensor model and flight altitude to determine the interior and exterior orientation parameters before performing a bundle block adjustment (Ventura et al., 2018). Bundle block adjustment was performed using matching key points from the overlapped photos to create a point cloud and 3D textured mesh. The image georeferencing was determined from the onboard RPAS global positioning system (GPS). This georeferencing was further refined using the RTK surveyed GCPs after initial processing and reoptimized. The projection used for the output orthomosaic was WGS 1984 UTM Zone 60S. Bundle block adjustment produced a densified point cloud which was then filtered and interpolated to generate orthomosaic and reflectance maps for all five multispectral bands with all the features on the ground with their actual reflectance. Radiometric calibration was applied on the fly using the reflectance panel and calibration information provided by MicaSense (MicaSense, 2017). Finally, we used the composite bands geoprocessing tool in ArcGIS Pro v2.5 to create a 5-band image composite from the individual reflectance maps.

5.2.5 Classification schema and RPAS spectral signature

Remotely sensed imagery has been presented as a powerful tool for distinguishing different land cover features and objects in marine environments (Joyce et al., 2018). All features have distinctive spectral signatures that can be used to identify and differentiate them quantitatively. The spectral

reflectance allows selecting regions of relevance or land cover features on the remotely sensed imagery and reviews the spectral profile information of all bands from the chart (ESRI, 2019). The spectral graph contains geometry to define the pixel selection and an image with vital metadata to train samples for supervised classification (ESRI, 2019). A classification schema was created based on six classes (1) bare rocks, (2) oyster reefs, (3) sediment (combined mud and sand), (4) mangroves, (5) saltmarsh, and (6) shadows. Training Samples Manager (TSM) in ArcGIS Pro v2.5 (ESRI Inc., Redlands, CA, USA) (ESRI, 2019) was used to collect training samples based on the classification schema from the orthomosaic. To inspect the spectral signatures of all the samples collected in all the bands, we visualized their spectral signatures using the spectral profile tool in ArcGIS Pro v2.5. The samples were visualized to explore the geometry and key metadata information for all the available bands and identify the samples' separability for a good classification result. These training samples were saved as a feature dataset used during supervised classification.

5.2.6 *In-situ* hyperspectral spectral reflectance

To collect an *in-situ* spectral reflectance dataset, an ASD Spec® Handheld spectro-radiometer was used. This radiometer was calibrated with a Spectralon® white panel before sampling and recalibrated after an illumination change in the field. Reflectance samples for bare rock, mangrove, oyster reef, and saltmarsh were collected. Reflectance samples for shadows and sediments were not collected due to technical issues with the spectro-radiometer. All the reflectance samples collected were geotagged and simultaneously gathered with the RPAS flights to maintain consistency. The wavelengths captured with this spectrometer ranged from 325nm to 1075nm. *In-situ* spectra samples were evaluated and visually inspected for quality, and average samples for each class were plotted in ENVI spectral library viewer.

5.2.7 Image Segmentation

The techniques used for image classification will be applied to the VIS and VIS+NIR domains. Initially, for image segmentation, we used an object-based image analysis (OBIA) in ArcGIS Pro v2.5. Segmentation of high-resolution RPAS imagery using an OBIA technique has been proven effective over a pixel-based approach for marine applications (Blaschke, 2010; Fallati et al., 2020). The principle behind an OBIA approach is that this technique segments the image into clusters of neighbouring pixels with analogous spatial details, spectral detail, and minimum segment size (ESRI, 2019). For example, the target land cover feature can be differentiated by its spectral reflectance signatures in the remotely sensed imagery **(Figure 28)**. Also, the texture used for image segmentation is built on the spatial distribution of tones across the pixels of the remotely sensed imagery. The amount of detail can be varied during segmentation that characterizes a land cover feature of interest (ESRI, 2019). For example, the spatial detail can be adjusted to a smaller number resulting in more smoothing and minor detail. Moreover, the spectral detail refers to a sensor's

ability to capture a specific wavelength of the electromagnetic spectrum; the narrower the wavelength range, the finer the spectral resolution (Fallati et al., 2020). After an iterative process, the spectral detail was set to 20 to discriminate between the different land cover features. The spatial detail was set as 15, considering the smallest feature to be identified were oysters. The minimum segment size in pixels was set to 20, where smaller segments than 20 were merged with their best fitting neighbour segments.

5.2.8 Supervised classification

In this study, a Support Vector Machine (SVM) classification was performed to identify and map wild oyster reefs. SVM is a supervised machine learning algorithm selected because proven research shows that SVM classifiers can handle large images, are not dependent on a standard distribution of reflectance values, and are less exposed to image noise (Dronova, 2015). In addition, the SVM classifier is an advanced machine learning classification technique and a binary classifier that functions by recognizing the best hyperplane and correctly dividing the data points into two classes (Bahari et al., 2014). Moreover, if there are more hyperplanes, SVM will select a hyperplane with maximum margin (Bahari et al., 2014). Besides, SVM is beneficial for classifying the data linearly and non-linearly and is often used for supervised classification applications (Mountrakis et al., 2011; Shi and Yang, 2012). Our contribution to the body of knowledge lies in differentiating oysters from a heterogenous rocky reef habitat mainly dominated by vegetation. Also, the following segmented attributes: (1) active chromaticity colour, which describes the colour of different features in the land cover as seen by the human eye in the imagery, (2) mean digital number, the numerical value assigned to each pixel in individual bands and (3) standard deviation (SD) shows higher information content within that band such as for oysters the range of SD from visible to NIR wavelength increased.

5.2.9 Validation

The accuracy assessments of SVM classifications were performed using a confusion matrix. We compared the reported land cover of randomly selected points (different from training samples) to the actual land cover to generate a confusion matrix (Foody and Mathur, 2004). The purpose of accuracy assessments is to evaluate the OBIA image analysis technique and SVM classification efficiency. A confusion matrix provides results that can describe a classification model's performance and a thematic map's accuracy. The result of a confusion matrix can be used to question the appropriateness of the datasets or methods used in deriving the classification (Foody, 2002). We used a stratified random sampling strategy to create 400 accuracy assessment points different from the classified imagery training areas. All the random points were manually classified. The classified imagery's accuracy was assessed on the screen without any visible aid using the high-resolution orthomosaic. High spatial resolution (<5 cm/pixel) has been proven to be a reliable source for

assessing accuracy (Lechner et al., 2012; Ventura et al., 2018). Finally, a confusion matrix to determine the accuracy of the final classification was calculated, which included: (1) Overall Accuracy can be explained as a percentage (ranging from 0 to 100%) of all correctly classified values proportional to the total sample size, (2) Kappa Coefficient is similar to classification accuracy where this parameter measures a consensus between classification and ground truth values, (3) producers accuracy is described as the probability that a given value in a feature class is correctly classified, (4) user's accuracy is defined as the likelihood that a value predicted to be in a specific feature class is actually that feature class.

5.3 Results

5.3.1 VIS and VIS+NIR orthomosaic

The aerial survey took approximately 11 minutes, capturing 2954 geotagged photos, covering a spatial extent of 0.067 km^2. In addition, the SfM photogrammetry technique produced a VIS orthomosaic of 1.3 cm/pixel spatial resolution and VIS+NIR orthomosaic of 3.5 cm/pixel spatial resolution. In this section of the rocky reef, mangroves are a dominant feature. However, the different spectral band combinations could visualize more detailed information about the land cover features and their attributes. For example, a true-colour image composite Red, Green, and Blue (3, 2, 1) band combination displays the landscape in the imagery in a natural colour. The wild oyster reefs can be visualized along the northwest part of the imagery, established on basalt volcanic rocks **(Figure 26a)**. In contrast with a false-colour image composite (4, 3, 2), NIR, Red, and Blue band combination **(Figure 26b)** represent mangroves in red colour from high NIR reflectance. The imagery was collected in winter when the chlorophyll content in leaves was low, and vegetation appeared yellow if the green band was used. Basalt volcanic rocks in the middle of the imagery appear dark, and sediments are various shades of blue. In addition, wild oyster reefs located along the northwest corner of the imagery reflect more NIR spectrum and can be visually identified by their formation and high reflection.

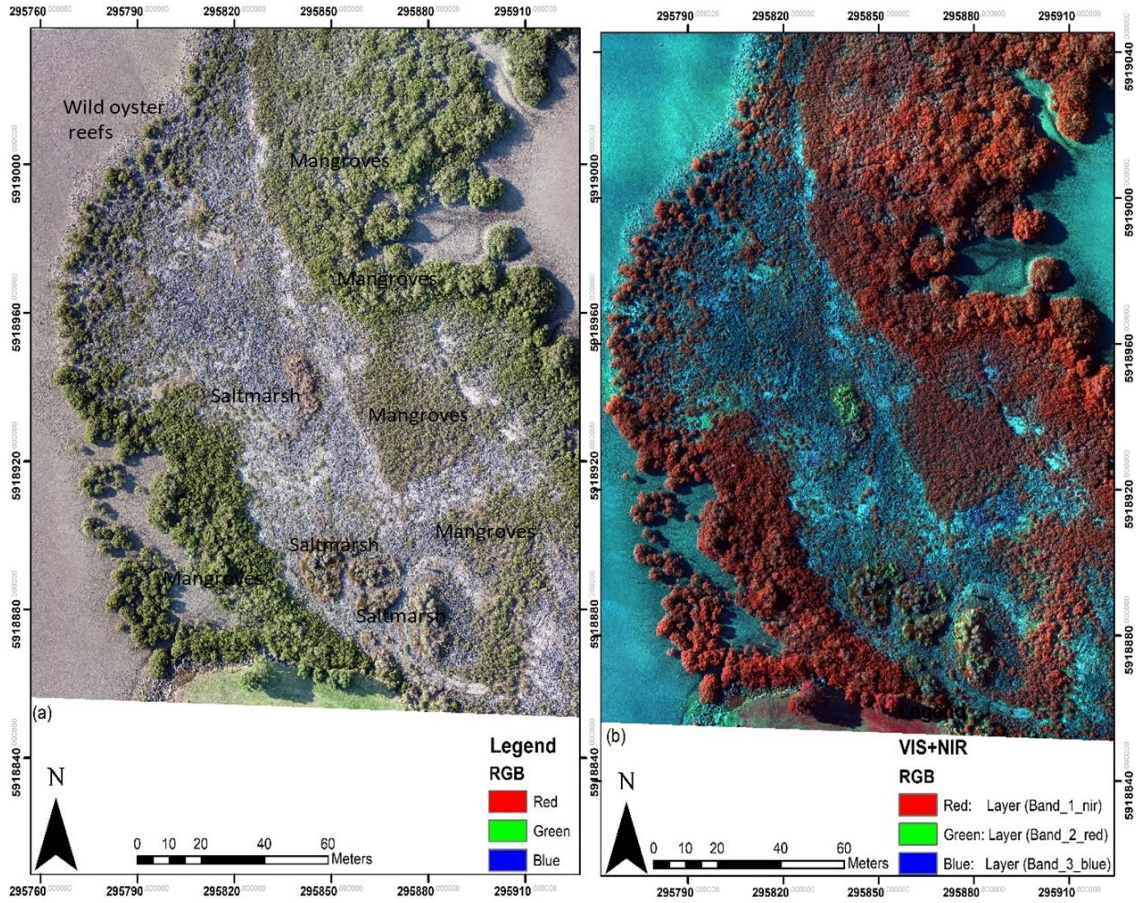

Figure 26. (a) True-colour VIS image composite, mangroves dominate the outer fringes, saltmarsh in shades of brown in the centre, basalt rocks in black, and oyster reefs are in the northwest corner. (b) A false-colour image composite, mangroves in red, saltmarsh in green, bare rocks are black, sediment in shades of blue, and a strip of oysters with high reflectance in the northwest fringe.

Figure 27. *In-situ* feature classes of mangroves, wild oyster reefs, and saltmarsh.

5.3.2 Spectral signature from orthomosaic and *in-situ* hyper-spectrometer

The spectral reflectance signatures of wild oyster reefs are generally within a similar range in the VIS spectrum (400nm to 700nm), with a slightly steeper slope along the blue and green wavelengths **(Figure 28a and b)**. In contrast, absorption in the 668nm Red band indicates photosynthetic vegetative material chlorophyll-*a* on the blank oyster shells, similar to the spectral reflectance of mangroves and saltmarsh. This spectral feature of chlorophyll-*a* on the blank oyster shells was only detected from the orthomosaic. In addition, no macroalgal epibionts were visualized during ground-truthing on the surfaces of oyster shells **(Figure 27)**. The growth of macroalgal epibionts can be attributed to an increase in the population of predatory oyster borer snails that decompose oyster shells in this ecosystem. The decomposed oyster shells favour micro-benthos growths, which develop biofilms on sediments. In the NIR region, the spectral reflectance of oyster reefs was higher because of surface reflection from the horizontal smooth polished surface.

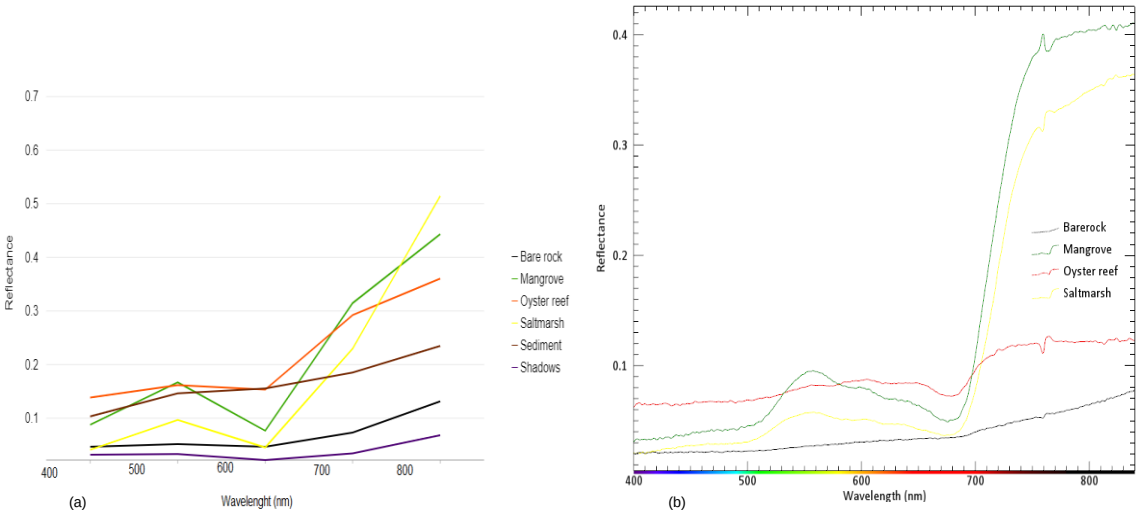

Figure 28. (a) spectral signatures acquired from VIS+NIR imagery of six feature classes. (b) spectral signatures acquired from *in-situ* hyper-spectrometer, only four feature classes are displayed on the graph due to technical problems during data collection in the spectrometer.

5.3.3 Oyster identification

The thematic map obtained with the SVM classification is presented in **(Figure 29)**. With the VIS+NIR image, it was possible to detect wild oyster reefs and detect the presence of the growth of macrobenthos in the spectral reflectance. Most land-cover misclassification errors occurred due to spectral reflectance confusion or spectral mixing between wild oyster reefs, bare rock with dried sediments, and guano droppings in the blue and red bands (Chand et al., 2020)[10]. During winter, low chlorophyll content in the land cover vegetation and high reflection also confused the classification model, where saltmarsh vegetation was confused with mangroves. However, image

[10] May read differently from published article as I have added a reference (Chand et al., 2020)

segmentation was essential for delineating feature classes to create a thematic map of the study area. Moreover, the segmentation technique allowed the feature attributes to be used during classification. The image segmentation results determined the land cover geometry and should be carefully evaluated before the classification.

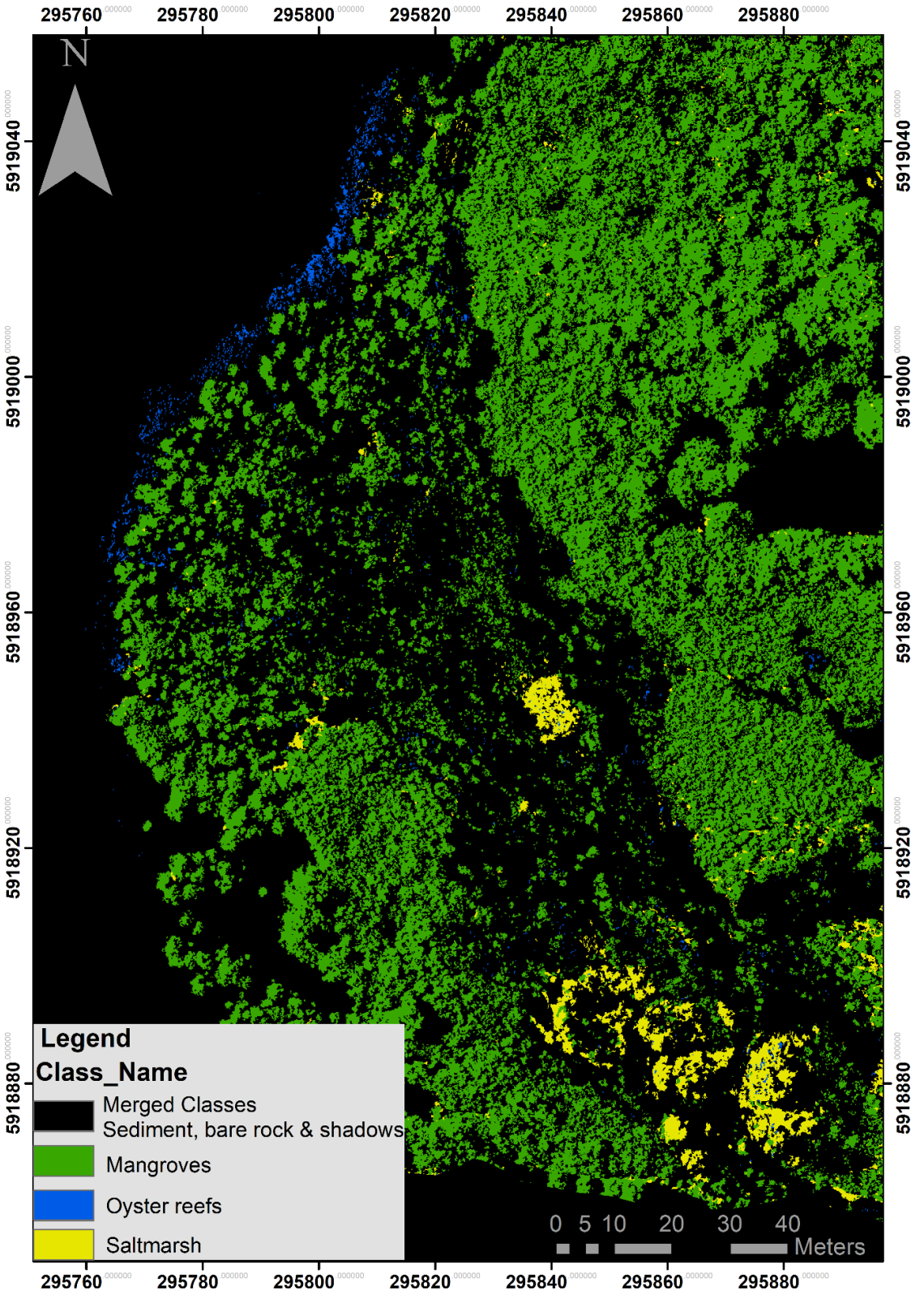

Figure 29. SVM classified thematic map based on RPAS spectral reflectance, sediment, bare rock, and shadows were merged to show spectral mixing and misclassified pixels of wild oyster reefs and saltmarsh.

5.3.4 SVM classification accuracy

The overall classification accuracy and Kappa Coefficient calculated from the confusion matrix confirm the best results using the VIS+NIR orthomosaic. With a high spatial resolution, the lower spectral VIS had a Kappa Coefficient of 0.60 **(Table 8)** compared to 0.74 **(Table 7)** for the VIS+NIR orthomosaic. For oyster reef classification from the VIS+NIR orthomosaic, a Producers accuracy of 0.78 and User's accuracy of 0.96 was achieved. These results can be translated into the User had identified 0.96 of oysters successfully compared to 0.78 referenced oysters. When comparing spatial and spectral resolution, it was evident that VIS+NIR orthomosaic spectral resolution was more significant than the spatial resolution to correctly identify wild oyster reefs and other features.

Table 7. Multispectral classified imagery accuracy assessment

Multispectral				
Classes	Producer's Accuracy	User's Accuracy	Overall Accuracy	Kappa Coefficient
*Merged classes	100	0.87	*Sediment, bare rock and shadows	
Mangrove	0.87	0.89	85%	0.74
Oyster reefs	0.78	0.96		
Saltmarsh	0.55	0.91		

Table 8. RGB classified imagery accuracy assessment

RGB				
Classes	Producer's Accuracy	User's Accuracy	Overall Accuracy	Kappa Coefficient
*Merged classes	0.85	0.73	*Sediment, bare rock and shadows	
Mangroves	0.79	0.76	70%	0.60
Oyster reefs	0.60	0.72		
Saltmarsh	0.45	0.63		

5.4 Discussion

The ecological importance of wild oyster reefs on the Meola intertidal reef is that they support a wide range of biodiversity and provide essential services. Hence, spatial assessments, monitoring, and mapping of wild oyster reefs are necessary to maintain an ecological balance within this rocky reef ecosystem. The OBIA and SVM classification analysis obtained from VIS+NIR processing revealed that wild intertidal oyster reefs could be distinguished. The technique to extract spectral reflectance signatures from RPAS orthomosaic was proven effective considering the technical

issues encountered during *in-situ* spectral data collection. Spectral reflectance information could be beneficial when it is challenging to obtain ground truth data (Rosso et al., 2005).

Although, researchers over time have used satellite (multispectral and hyperspectral) and aerial imagery to map wild oyster reefs (Le Bris et al., 2016; NOAA, 2003). The application of these techniques still has spatial and temporal limitations (Grizzle, 2002; NOAA, 2003; Newell et al., 2005). Furthermore, *in-situ* techniques can be spatially challenging and time-extensive. However, these techniques cannot be replaced but integrated with other datasets to get better results. In addition, the application of RPAS remote sensing of wild oyster reefs was restricted within the VIS electromagnetic spectrum (Espriella et al., 2020; Windle et al., 2019). Hence, it was challenging to distinguish oyster reefs from mud from the VIS spectrum, limiting the classification accuracy (Espriella et al., 2020). Therefore, this study tested an RPAS with VIS and VIS+NIR sensors for spatial assessment and thematic mapping of wild oyster reefs to minimize this gap. The spatial distribution map of wild oyster reefs obtained from multispectral (VIS+NIR) RPAS orthomosaic SVM classification revealed that it could distinguish wild oyster reefs in a heterogeneous intertidal rocky reef ecosystem dominated by vegetation.

5.4.1 Spectral reflectance signatures of wild oyster reefs

In this study, two spectral reflectance samples were tested for wild oyster reefs, and both graphs showed absorption along with the red spectral band (600nm to 700nm). This absorption indicates the existence of unicellular photoautotroph organisms which could not be detected visually (Le Bris et al., 2016). The absorption in the red band is a characteristic of colonizing macroalgae on oyster shells, which were not detected visually during ground-truthing. In addition, a higher spectral reflectance from oyster reefs was observed along with the NIR spectrum range (700nm to 840nm).

Although the hyperspectral data had a spectral reflectance from 325nm to 1075nm wavelengths, collecting spectral samples was time-consuming as the machine needed to be calibrated with a change in illumination every time. In addition, during data collection, the Spectro-radiometer had technical issues, and no further readings were taken. In contrast, spectral samples compiled from RPAS orthomosaic outweighed the hyperspectral *in-situ* data in the following aspects: (1) many samples from the land cover can be collected simultaneously, (2) it is less time consuming, (3) high-resolution multispectral imagery allows the analyst to collect pure training samples, (4) no further calibration was required, (5) spectral signatures are not weather dependent, (6) samples can be visualized and resampled as desired, and (7) samples are in harmony with the RPAS flight whereas to collect *in-situ* samples additional personnel can be required.

5.4.2 SVM classification accuracy

In this study, the classification accuracy depended on distinguishing wild oyster reefs from RPAS spectral signatures. It was low for wild oyster reefs in the VIS orthomosaic, for which the overall accuracy was 70% due to misclassification from spectral mixing. The overall accuracy was higher in the VIS+NIR orthomosaic with 85% due to pure training samples and spectral unmixing. Furthermore, this study demonstrated the application of OBIA and SVM classification techniques to produce a thematic map of wild oyster reefs. The accuracy of SVM is attributed to an efficient hyperplane searching method to develop efficient decision boundaries that reduce misclassification even with few training samples and speed up processing time (Candade and Dixon, 2004). Although OBIA was a critical step in segmenting attributes of various land features based on their geometry, they are a powerful technique for high-resolution image classification when combined with the SVM classifier. The SVM classifier's advantage is that it produces accurate classification results even with fewer training samples (Foody and Mathur, 2004). In addition, the spectral reflectance from the high-resolution VIS+NIR orthomosaic was used to evaluate the spectral separation from each feature class. Moreover, apart from spatial assessment of wild oyster reef and monitoring the ecological status of biodiversity on this rocky reef, this technique can be used to accurately map benthic vegetation such as mangroves and saltmarsh.

5.4.3 Comparing VIS and VIS+NIR data

The VIS orthomosaic had a higher spatial resolution than the VIS+NIR orthomosaic, but the VIS orthomosaic had less spectral variability, increasing the number of mixed pixels among the land cover features. Similarly, Espriella et al., 2020 reported that VIS spectral bands did not have the spectral separability to map shellfish habitats. In contrast, the VIS+NIR orthomosaic had more spectral variability allowing for better discrimination of wild oyster reefs than spatial resolution. Other studies have also emphasized acceptable discrimination obtained for wild oyster reefs, wetland vegetation, benthic macroalgae, and coral reefs from narrow spectral bands in contrast to broadband resolution imagery (Botha et al., 2013; Collin et al., 2019; Le Bris et al., 2016). Nevertheless, in this study, better results for detecting were observed by using VIS+NIR five spectral bands. For marsh vegetation, spatial resolution affected classification accuracy more than spectral resolution due to mixed vegetation.

5.4.4 Challenging marine environments

When satellite imagery is used to research marine environments targeting optimum tidal conditions for intertidal species could sometimes be difficult due to cloud cover and tidal variations (Schwantes et al., 2018). To overcome these challenges, low-altitude multi-rotor RPAS with vertical take-off and landing capability allows researchers to target optimum tidal and meteorological conditions for surveying intertidal benthic habitats. Moreover, it is crucial to note

that RPAS flights below the clouds do not require atmospheric corrections, but cloud shadows could impact certain imagery portions (Konar and Iken, 2018; Nagelkerken et al., 2015).

In temperate marine environments, the visibility of target species from the air can be obscured by turbidity; hence data collection during low tides are the best option (Duffy et al., 2018; Konar and Iken, 2018). In addition, increased turbidity from sediments along the water column also attenuates most spectral bands (Nahirnick et al., 2019). The optimum time to collect RPAS aerial imagery is early morning or late afternoons (Collin et al., 2019). The aerial data collected after the solar noon had minimal artifacts or sunglint on the imagery due to good flight planning, 80% overlaps, and consistent aircraft speed. One of the limitations of this study from collecting data after the solar noon was that oyster reefs under mangroves were obscured from shadows. However, this shadow limitation can be mitigated by collecting data during solar-noon to avoid shadows and integrating *in-situ* datasets to improve classification accuracy.

5.4.5 Remote sensing for ecology and conservation

On the Meola rocky intertidal reef studied between 2001 and 2017, Rock oysters (*Saccostrea glomerata*) and the Pacific oysters (*Crassostrea gigas*) were most abundant. However, during an *in-situ* survey, a decline in the population of oysters was discovered in 2012 from an increase in oyster borer snails (Foley and Shears, 2019). A decline in the wild oyster population has negative consequences in many functional aspects, such as reduced support to other biodiversity and affecting the ecosystem's ecological processes. Habitat loss and species fragmentation are some of the most severe threats to marine ecosystems (Belluco et al., 2006). Therefore, complementing *in-situ* surveys with high spatial and temporal resolution remotely sensed imagery can effectively be used to identify ecological changes in an ecosystem from natural invaders such as predatory borer snails and anthropogenic activities. Data integration benefits ecology and conservation to prevent preceding tipping points of the broader ecosystem. One of the limitations of this study was the inability to identify and locate borer oyster snails in the orthomosaic. Future studies could use RPAS flights at lower altitudes to identify predatory oyster borer snails with near-perfect camouflage during low tides.

An essential attribute of remote sensing of wild oyster reefs is identifying the different species and differentiating between alive and dead oysters, including oyster stock inventory. Therefore, future studies should consider researching the aspects mentioned above. Other benthic habitats are crucial for marine ecosystems, such as mangroves and saltmarsh, apart from research on oysters. Further research applications to study these habitats can be undertaken using RPAS multispectral imagery. Multispectral low-altitude imagery is beneficial because different band combinations can be applied, and information such as mangrove health and cover can be extracted.

5.5 Conclusion

The application of VIS+NIR (visible + near-infrared) low altitude proximal remote sensing can be a valuable tool for spatial assessment and mapping wild oyster reefs in intertidal estuaries. In contrast, acquiring comprehensive *in-situ* data could be challenging. This study showed that VIS+NIR remotely sensed orthomosaic could be used successfully to detect and map wild oyster reefs in a heterogeneous environment. In addition, low altitude remote sensing capability for monitoring biogenic habitats with high-resolution, 3.5cm/pixel multispectral imagery. Moreover, spectral resolution from the five bands of VIS+NIR imagery was more valuable than the spatial resolution to effectively detect and classify wild oyster reefs. In addition, the OBIA and SVM classification techniques achieved an overall accuracy of 85% and a Kappa Coefficient of 0.74.

Furthermore, marine managers can use proximal low altitude remote sensing for ecology and conservation planning to create high-resolution baseline maps and use this technique for multi-temporal monitoring of intertidal benthic habitats. As benthic habitats are under consistent anthropogenic activity pressure, environmental change alters ecosystems at alarming rates. Furthermore, remotely sensed high spatial resolution datasets could be a critical source of information for restoring and improving the overall health of benthic habitats and understanding the spatial dynamics of intertidal marine environments.

Chapter 6 Detecting the spatial variability of seagrass meadows and their consequences on associated macrofauna benthic activity using novel drone technology

A version of this Chapter has been published as:

Chand, S., Bollard, B. (2022). Detecting the Spatial Variability of Seagrass Meadows and Their Consequences on Associated Macrofauna Benthic Activity Using Novel Drone Technology. RemoteSens. 14, 160. https://doi.org/10.3390/rs14010160

Cover image. A flock of black swans feeding on seagrass meadows during autumn in the study area.

This chapter tested the performance of VIS and VIS+NIR sensors to detect fine-scale seasonal time-series seagrass changes in a dynamic nearshore marine environment using spectral indices and a supervised machine learning classification technique (objective h). We also answered the following research question: could the abundance and distribution of macrofauna benthic activity among seagrass meadows be determined from proximal low altitude remotely sensed drone aerial imagery? (objective i). Although seagrass meadows from both sensors were successfully detected, it was challenging to identify seasonal seagrass density (low, medium, high). Hence, the spectral indices technique was evaluated to determine seasonal seagrass density and quantify change. Based on this technique and the supervised classification method, both sensors produced 90-98% classification accuracy. Furthermore, the feeding burrows of macrofaunal benthic activity were used as a proxy for identifying changes in their abundance and distribution. It was established from the quantified results from the drone imagery that the population of macrofaunal benthic activity increases with the abundance of seagrass in summer and declines with the loss of seagrass meadows during autumn and winter.

6.1 Introduction

New Zealand and the southern parts of Australia have only one indigenous species of seagrass, *Zostera muelleri* (Anderson et al., 2019). In New Zealand, these meadows are recognized to provide a diverse range of ecological services, which include (1) nutrient recycling (Matheson and Wadhwa, 2012), (2) primary productivity to detrital micro-organisms, and grazing marine fauna, (3) dissipate wave energy (Calleja et al., 2017), (4) stabilize and trap sediment flow (Duarte et al., 2013), and (5) increase species (Turner and Schwarz, 2006). In addition, most juvenile fish utilize seagrass beds as a nursery and prey on small organisms living within seagrass meadows (Duarte, 2002). It is an important habitat for juvenile fisheries of snappers (*Pagrus auratus*)[11] for recreational and commercial fisheries (Grech et al., 2012). Also, seagrass meadows are exceptional bio-indicators of ecosystem conditions for monitoring the impacts of human activities and global climate change (Duarte et al., 2013; Lin et al., 2018; Orth et al., 2006).

Furthermore, *Zostera muelleri* is primarily an intertidal species but extends into sub-tidal zones where water clarity and quality are high (Morrison et al., 2014). However, the spatial distribution and occurrence of seagrass meadows along the nearshore marine environments make them highly vulnerable to anthropogenic activities such as (1) increased sedimentation, (2) increased nutrient overload from septic tank leachate, allowing overgrowth of algae, and increased suspended solids concentration (SSC), reducing water clarity and quality (Fourqurean et al., 2012), and (3) coastline modification and developments (Matheson et al., 2017). In particular, New Zealand seagrass meadows are also vulnerable to natural impacts from (1) intensive grazing by black swans (*Cygnus atratus*)[12] in both the Waitemata Harbour (Chand and Bollard, 2021) and Tauranga Harbour (Matheson et al., 2012), (2) vulnerable to diseases such as the slime mould (*Labyrinthula zosterae*) (Inglis, 2003), and (3) are vulnerable to increased temperatures and sea-level rise from climate change impacts (Kettles and Bell, 2016).

Moreover, the conservation status of seagrass in New Zealand is "At Risk of Declining" (de Lange et al., 2017). This seagrass decline affects associated species and their vital linkage with the adjacent habitats, igniting a broader degradation and long-lasting impacts on other habitats and biodiversity dependent on seagrass within the ecosystem (Waycott et al., 2009). Besides, the possibility of identifying subtle fine-scale changes goes undetected and undocumented (Kettles and Bell, 2016). Therefore, a flexible and repetitive technique to inventory seagrass meadows is in high demand (Ha et al., 2021; Hobley et al., 2021). To supplement data collection and detect fine-scale changes that would otherwise go undetected and undocumented, a holistic perspective

[11] May read differently from published article as I have added the scientific name to snapper (*Pagrus auratus*).
[12] May read differently from published article as I have added the scientific name to black swans (*Cygnus atratus*)

of an ecosystem provides a comprehensive understanding of system change (Orth et al., 2006; Unsworth et al., 2018). Conventionally, passive remote sensing provided by satellite imagery was used to provide regional to global observational datasets for applications at regular intervals (Johnston, 2019). However, oblique views, cloud cover, tidal variations, and the costs for high spatial and spectral resolution datasets are problems that satellite imagery struggles to overcome (Anderson et al., 2013). In addition, historical airplane captured aerial imagery was also used extensively for seagrass research; however, this imagery is expensive to procure, the spatial resolution is not sufficient to discriminate fine-scale features, and it cannot record multiple bands (Hossain et al., 2015b). The transition to autonomous remotely piloted aircraft systems (RPAS) or drones and commercially available miniaturized sensors has solved many challenges associated with satellite datasets. RPAS allows aerial surveys (1) at low-altitude with (2) high spatial resolution, (3) cloud-free remotely sensed imagery, (4) at the researcher's desired timeframe, and (5), most importantly, increased sampling frequency within the tidal range (Chand and Bollard, 2021; Duffy et al., 2018; Joyce et al., 2018).

Meanwhile, there have been attempts at mapping and monitoring seagrass meadows using RPAS with different classification techniques reported (Chayhard et al., 2018; Chand and Bollard, 2021; Duffy et al., 2018; Hobley et al., 2021; Konar and Iken, 2018; Nahirnick et al., 2019; Riniatsih et al., 2021; Ventura et al., 2018; Yang et al., 2020). In New Zealand, Martin et al., 2020, assessed an *in-situ* survey technique for measuring seagrass density change in Wharekawa Harbour using a multirotor RPAS with a Parrot Sequoia sensor. While different RPAS mapping monitoring techniques have been applied for seagrass research, there is a gap in simultaneously testing VIS (visible spectrum) and VIS+NIR (visible and near-infrared spectrum) domains to detect fine-scale seasonal seagrass changes in a dynamic nearshore marine environment. The reason for this gap may be related to applying this technology to detect fine-scale changes and the need for imagery to develop robust models for the classification of seagrass in a nearshore ecosystem to be captured at the optimal time to allow classification techniques to be applied.

Therefore, this research will test the performance of VIS and VIS+NIR sensors to detect fine-scale seasonal time-series seagrass changes in a dynamic nearshore marine environment using spectral indices and a supervised machine learning classification technique. Moreover, macrofauna benthic activity is directly associated with habitat diversity. The loss of structurally intricate habitats such as seagrass is a significant threat to the marine environment that would subsequently interrupt typical ecosystem functioning (Rodil et al., 2021). In addition, researchers from *in-situ* surveys had determined that well-established seagrass beds translated into an increased abundance in macrofauna benthic activity compared to unvegetated areas (Lundquist et al., 2018). Also, researchers have investigated the impacts of seagrass on benthic fauna diversity

are based on comparative surveys between vegetated seagrass beds and unvegetated areas (Micheli et al., 2008). However, no attempt has been made to identify and quantify the abundance and distribution of marine macrofauna benthic activity from proximal low altitude remotely sensed drone imagery. Hence, this research tested whether macrofauna benthic activity abundance and distribution amongst seagrass meadows be determined from proximal low altitude remotely sensed drone aerial imagery? Therefore, this study also aimed to identify and quantify the abundance and distribution of macrofauna benthic activity through their feeding burrows across the time-series seasonal imagery within the study area. We also investigated the effect of seagrass gain and loss on the abundance and distribution of macrofauna benthic activity.

6.2 Materials and Methods

6.2.1 Study site

The study site, Cox's Bay, is located on the intertidal mudflat on the Eastern side of Motions Creek and Te Tokaroa Meola intertidal rocky reef along the Waitemata Harbour (36° 50′ 45″ S, 174° 43′ 02″ E) **(Figure 30)**. This estuary is 36% intertidal, with a semidiurnal tidal regime ranging between 1.9 m during neap tides and 2.9 m during spring tides (Foley and Shears, 2019). Mostly exposed during low tides, the seagrass beds have expanded to more than 40 hectares (Lundquist et al., 2018). Reproduction of *Zostera muelleri* is primarily vegetative as flowering, and seed production is rare in New Zealand. As a result, the patch dynamics are gradual (Turner and Schwarz, 2006; Turner, 2007). The general trend of *Zostera muelleri* attains its highest biomass during austral summer to autumn, and most declines are during winter, reaching a minimum cover in early spring (Martin et al., 2020; Turner, 2007).

In addition, Cox's Bay is ~6 kilometres from Auckland, one of New Zealand's largest cities, and The Port of Auckland and this Bay has been increasingly influenced by urban expansion, pollution, forestry, and over-fishing, altering the dynamics of marine biodiversity and the ecosystem (Foley and Shears, 2019). In wider Waitemata Harbour, The Research and Evaluation Unit (RIMU) of the Auckland Council has identified an increase in sediment concentration levels (Matheson et al., 2017). Increased sedimentation has been implicated as a primary reason for declining seagrass density by smothering and blocking sunlight (Saunders et al., 2017). Besides, a water quality report from a nearby Motions Creek (a primary freshwater creek upstream of the seagrass bed) indicates an increasing concentration of extractable metal content such as Copper, Lead, and Zinc (Lundquist et al., 2018).

6.2.2 Data collection

The seasonal RPAS imagery was collected using a DJI Phantom 4 Pro during Summer, Autumn, and Winter of 2019. **(Figure 31)** displays very high-resolution VIS (True-colour) and VIS+NIR

(False-colour) orthomosaic of the study area created using Pix4D® mapper and structure from motion (SfM) photogrammetry technique (Pix4D, 2019). The SfM photogrammetry technique estimates extrinsic and intrinsic camera parameters from overlapping imagery (Cunliffe et al., 2016). The high quality of the orthomosaic produced is dependent on appropriate flight planning, the flight altitude, aircraft speed, and the sensor's field of view (Joyce et al., 2018). For data collection, two sensors were integrated on the same aircraft (1) a DJI 1/2.3" (Complementary Metal Oxide Semiconductor) CMOS sensor with VIS (Red (564-580nm), Green (535-545nm), and Blue (420-440nm) bands) with a ground sampling distance of approximately 1.35cm/pixel **(Figure 31a)** and (2) a MicaSense RedEdge-M sensor with VIS+NIR, Green (475nm), Blue (560nm), Red (668nm), RedEdge (717nm) and Near Infrared (840nm) bands and a ground sampling distance of approximately 3.47cm/pixel from an altitude of 50m **(Figure 31b)**. The VIS+NIR images were radiometrically corrected using the MicaSense Calibration panel and correction values for each band.

6.2.3 On-site survey and classification schema

All the seasonal time-series orthomosaic were orthorectified (Geometric corrected) using respective Global Position System (GPS) logs of camera positions and ten ground control points (GCPs) distributed across the site. A sample of the ground control point is shown in **(Figure 31)**. These GCPs were checkerboard style printed on an A3 paper and laminated to identify the target's centre accurately, and all the GCPs were surveyed using a high accuracy RTK-GNSS system, Septentrio®. During the image process in Pix4D, these GCPs were identified in the dense point cloud and their surveyed waypoints to enhance the positional accuracy. The orthorectification process ensures that both orthomosaic are well aligned to show the same features on the ground and attain high positional accuracy. A classification schema was created based on a U.S. Geological Survey seagrass classification schema that recommends a simple system has a better chance of reliability and enhanced accuracy during the mapping results (Hanlon, 2019). The purpose of the classification schema is to describe the morphology of the seagrass present as absent, low density, medium density, and high density in the defined spatial extent, not the shoots per square meter (biomass density) **(Figure 32)**.

6.2.4 Identification of macrofauna benthic activity from feeding burrows

The following species were observed in the study area during ground-truthing: *Aricidea sp*. (polychaetes), *Boccardia syrtis* (polychaetes), *Heteromastus filiformis* (polychaetes), *Prionopsio aucklandica*, *Austrovenus stutchburyi* (cockle), *Linucula hartvigiana* (clam), *Macomona liliana* (clam), *Colurostylis lemurum*, *Notoacmea scapha* (limpet), *Diloma subrostrate* (snail). In addition, we observed and photographed many feeding burrows in the study area among seagrass meadows and unvegetated areas **(Figure 33)**. We didn’t know which species was responsible for

the feeding burrows, so we dug up a minimum of 20 burrows and mostly found *Heteromastus filiformis* (polychaetes) in the study area. These polychaetes were unharmed and returned safely to their habitats. In the drone aerial imagery, these feeding burrows were identifiable as dark-coloured spots with low reflectance among seagrass meadows and unvegetated sediment **(Figure 34)**. Moreover, the location of each feeding burrow in the study area was manually digitized in ArcMap (version 10.8) from the VIS and VIS+NIR time-series seasonal imagery to evaluate the trend of increase or decline.

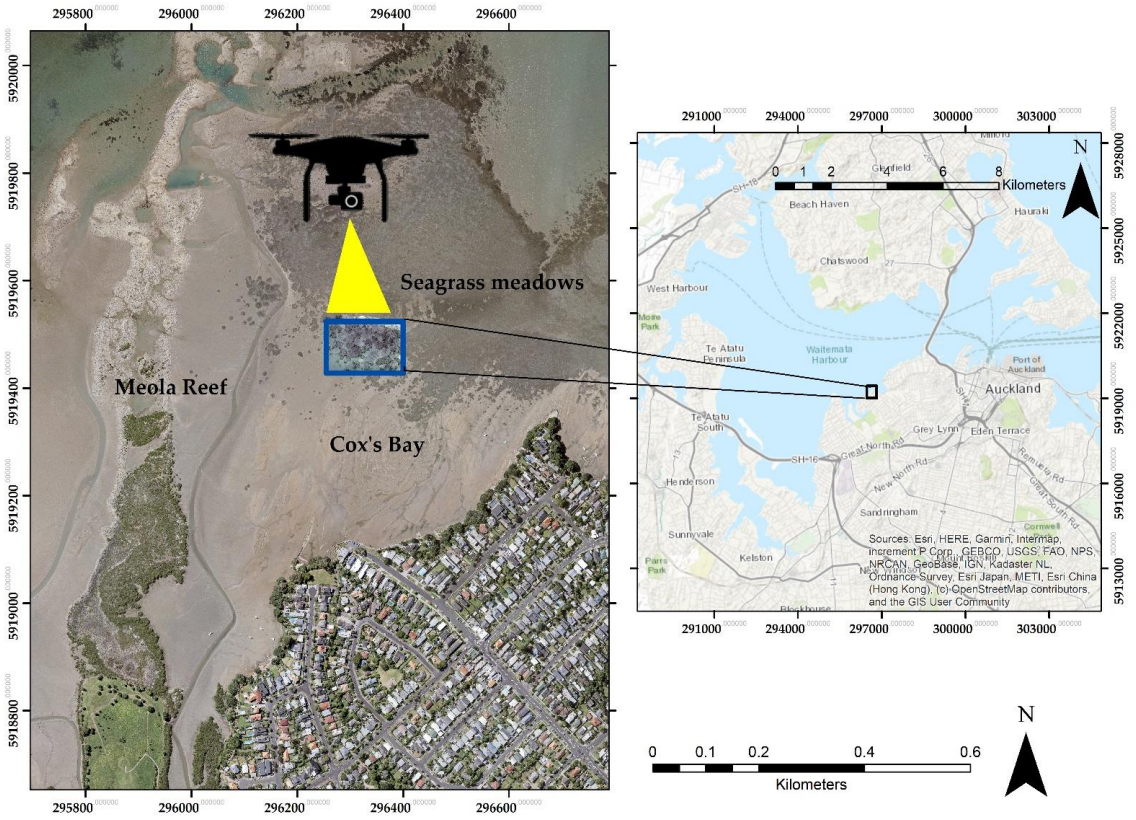

Figure 30. Location of the study site, North Island of New Zealand. Seagrass meadows are spatially located adjacent to The Meola intertidal reef, where wild oyster reefs and mangroves dominate this intertidal reef. Source Land Information New Zealand (LINZ, 2019).

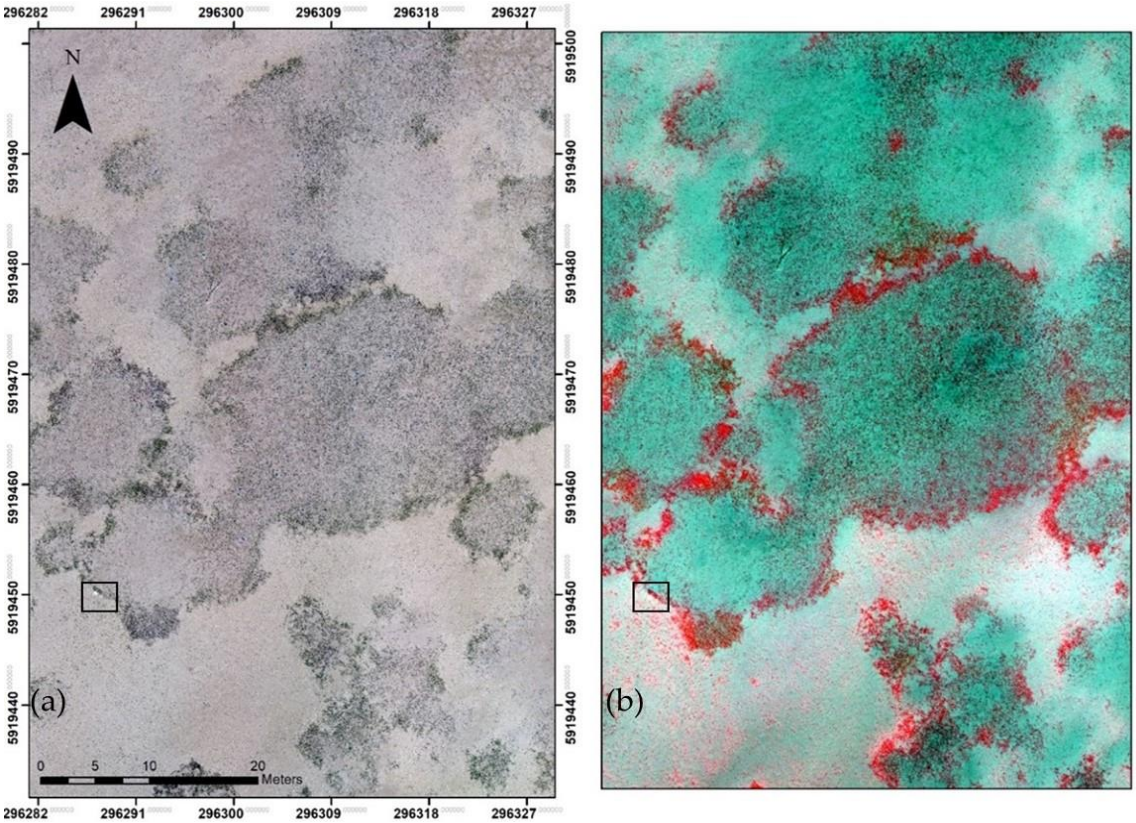

Figure 31. (a) VIS true-colour image composite and (b) VIS+NIR false-colour image composite. The black square in both imageries reveals one of the ground control points from the ten used for Geometric correction.

Figure 32. Seagrass classification schema to map their distribution across the study area. Seagrass density on the ground is referred to absent as 0%, low as 1-40%, medium as 40-70% and high density as 70-100%. Seagrass images courtesy of Kavita Prasad.

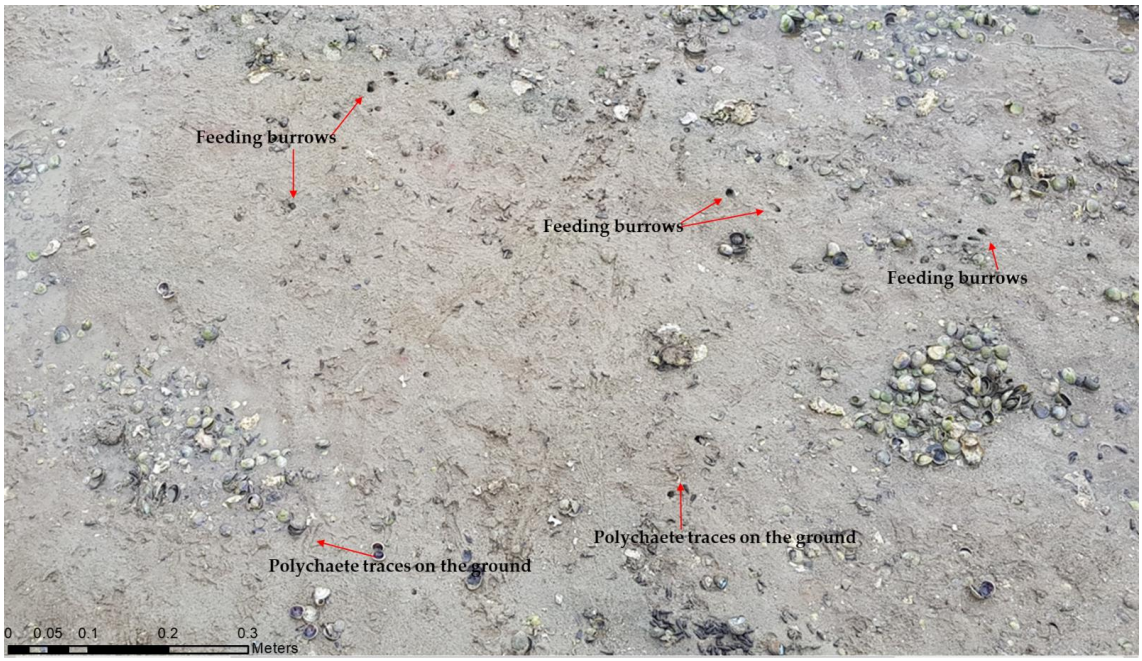

Figure 33. A ground truthing image shows macrofauna benthic activity from feeding burrows and traces of polychaetes crawling in the sediment.

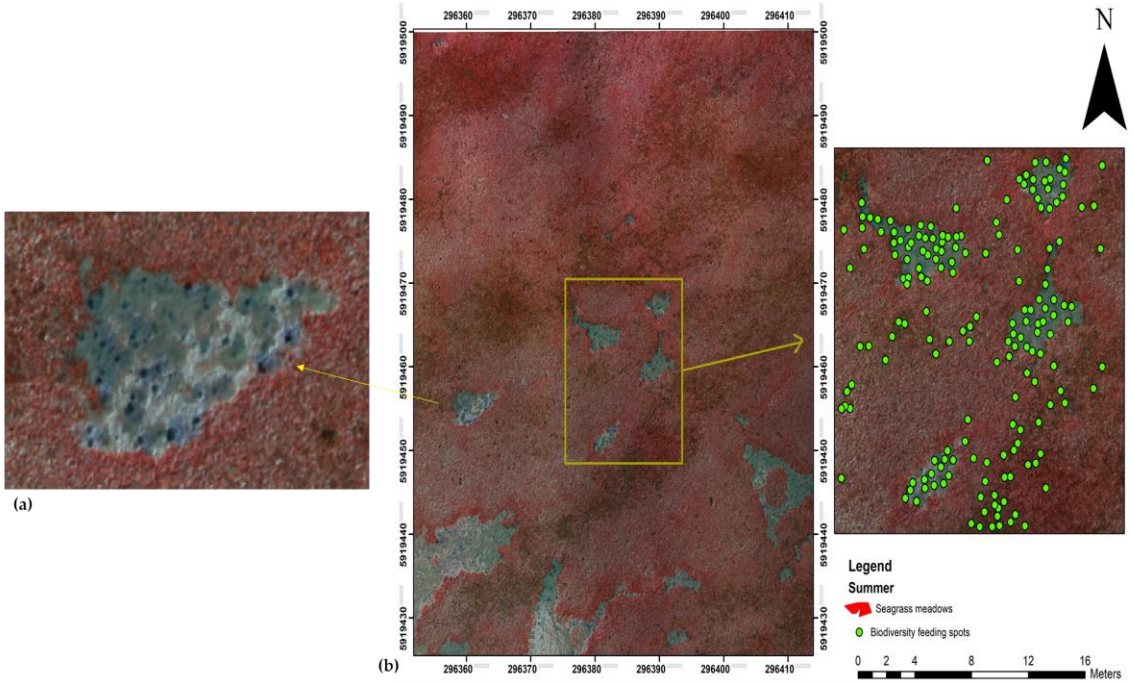

Figure 34. (a) a zoomed-in section from the summer aerial imagery showing an example of feeding burrows. (b) digitized feeding burrows symbolized as green dots in ArcMap.

6.2.5 Vegetation indices for supervised classification

Vegetation indices are derivatives calculated from VIS and VIS+NIR spectral bands to identify multiple vegetation classes and densities (Xue and Su, 2017). The VIS+NIR spectral bands from the MicaSense RedEdge-M sensor were used to compute and test indices for seagrass detection. The vegetation indices evaluated were (1) normalized difference vegetation index (NDVI) (Lebourgeois et al., 2008), (2) green normalized difference vegetation index (GNDVI) (Gitelson

and Merzlyak, 1998), (3) difference vegetation index (DVI) (Tucker, 1979), and (4) enhanced vegetation index (EVI) (Huete et al., 2002). After evaluation, NDVI, with its normalized difference formula from reflectance and highest absorption in chlorophyll-a, makes it robust over other indices. Moreover, the VIS spectral band from the DJI sensor was used to compute (1) visible atmospherically resistant index (VARI) (Gitelson et al., 2002) and sum green index (SGI) (Lobell and Asner, 2003). For the VIS sensor, the SGI was used as this is one of the most detailed vegetation indices used to detect changes in vegetation greenness reflected across the 500nm to 600nm spectrum.

6.2.6 Support vector machine classification

ArcGIS Pro v2.7 software was used for pixel-based supervised classification and accuracy assessments after assessing Binary Encoding, Mahalanobis Distance, Maximum Likelihood, Minimum distance, Spectral Angle Mapper, and Support Vector Machine classifiers (ESRI, 2019). For pixel-based supervised classification, both orthomosaics were classified with a support vector machine (SVM) learning classifier. This SVM classifier is less susceptible to noise and needs fewer training samples. Spectral reflectance signature files for both imageries were generated by collecting pure training samples in the Training Sample Manager Toolbox. The assigned feature class schemas were absent, low-density, medium-density, and high-density. Using an equalized stratified random sampling strategy, fifty random samples were taken across the study area based on the features pixel spectral for every class. These samples were polygons selected around the seagrass classes containing several hundred pixels. The classification model was repeated for the time-series imagery to determine the different densities of seagrass meadows.

6.2.7 Accuracy assessment

A confusion matrix was utilized as the quantitative technique for characterizing the image classification accuracy assessments (ESRI, 2019). The results presented the correspondence between the classification result and a reference image (Foody, 2002). The result of the pixel-based supervised classification of the seasonal time-series VIS and VIS+NIR orthomosaics were assessed for accuracy using randomly generated referenced points in the high-resolution multispectral orthomosaic. For accuracy assessments, 500 random points were used, and an equalized stratified random sampling strategy was applied so that each class would have an equal number of random points.

Accuracy assessments were conducted for VIS and VIS+NIR orthomosaics to produce a confusion matrices table. The confusion matrix included: an overall accuracy (defined as the percentage of all correctly classified values), a Kappa Coefficient (measured the agreement between ground truth values and classification), Producer's accuracy (defined as the likelihood

that an assigned class was correctly classified), User's accuracy (defined as the likelihood that a predicted value in a specific class is truly that class) (Foody, 2002).

6.2.8 Habitat maps: Post classification detecting change

A technique for change detection between multi-temporal remotely sensed image uses Multivariate Alteration Detector (MAD) transformation. This technique for pixel-based change detection is based on the theory of canonical correction analysis (CCA) to transform the data into new images with layers corresponding to each canonical variate (Nielsen et al., 1998). The CCA was developed to improve image differencing techniques by making the images similar or correlated before taking their difference (Nielsen et al., 1998). Images were transformed into new images with layers representing each canonical variate. The primary variate represented a linear combination containing the most correlation in the image, with successive layers containing decreasing correlations. The theory behind the MAD transformation is that by conducting this linear transformation on seasonal time-series imagery, the difference between two or more embodiments will highlight areas of change in the image. The MAD transformation analysis for change detection was executed in Geospatial Free and Open-Source Software (GFOSS) using Orfeo Toolbox, available in the QGIS environment through the Processing Toolbox. The change maps were computed based on the general growth and decline trend of *Zostera muelleri* in New Zealand by subtracting time-series raster imageries to show growth from summer to autumn and loss of seagrass meadows from autumn to winter.

6.3 Results

The VIS+NIR sensor produced a 3.5 cm/pixel spatial resolution orthomosaic, in contrast to the VIS sensor had a finer spatial resolution orthomosaic of 1.3 cm/pixel. However, detecting seagrass meadows directly from the orthomosaic was technically challenging due to the difference in density and length of seagrass blades. Hence, the spectral indices technique was applied to solve this challenge and achieved consistent classification accuracy from VIS and VIS+NIR sensors, as the results **(Table 9)** attest. Moreover, for proximal low-altitude aerial surveys of seagrass meadows in the study area, winter was identified as the best season because of consistent lighting conditions and less spectral reflection from the land cover.

6.3.1 The performance of the SVM classifier

6.3.1.1 VIS classification

SVM classification produced an average overall class accuracy of 93% and an average Kappa of 0.90. The absent feature class scored an average user accuracy of 0.98 **(Table 9)**. Low seagrass density cover achieved an average user class accuracy of 0.79. At the same time, the medium-density seagrass cover scored an average user class accuracy of 0.72. The high seagrass density

cover scored an average user accuracy of 0.97. The average high-density class has established that high-density seagrass coverage was easy to detect and is less susceptible to spectral mixing compared to other classes.

6.3.1.2 VIS+NIR classification

SVM classification produced an average overall class accuracy of 95% and an average Kappa of 0.93. The absent feature class scored an average user accuracy of 1 **(Table 9)**. Low seagrass density cover achieved an average user class accuracy of 0.73. In contrast, the medium density seagrass cover scored an average user class accuracy of 0.69. Besides, the high seagrass density cover scored an average user class accuracy of 0.98. In addition, the high-density seagrass class coverage achieved a better classification accuracy than other classes because of their unique spectral reflection in the NIR region, increasing their ability to be distinguished effectively from other features classes, for example, in **(Figure 31)**.

Table 9. The accuracy assessment of seasonal time-series seagrass classification for VIS and VIS+NIR orthomosaic, including the user accuracy "U-acc" and producer accuracy "P-acc," and the Overall Accuracy for the classified features versus referenced data ("Overall Accuracy") and the Kappa Coefficient. Kappa Coefficient estimates of zero indicate a random association and increasing values towards one showing an increasingly no-random result.

Data	**VIS orthomosaic**						**VIS+NIR orthomosaic**					
Seasonal time-series	Summer		Autumn		Winter		Summer		Autumn		Winter	
Density classes	**U-acc**	**P-acc**	**U-acc**	**P-acc**	**U-acc**	**P-acc**	**U-acc**	**P-acc**	**U-acc**	**P-acc**	**U-acc**	**P-acc**
Absent	0.99	0.99	0.98	0.99	0.97	0.99	1	0.99	1	0.99	1	0.99
Low	0.76	0.88	0.78	0.90	0.85	0.82	0.81	0.75	0.80	0.86	0.90	0.97
Medium	0.82	0.66	0.63	0.69	0.72	0.41	0.66	0.88	0.86	0.79	0.89	0.85
High	0.99	0.99	0.97	0.93	0.95	0.97	0.99	0.97	0.98	0.97	0.96	0.94
Overall accuracy	90%		91%		98%		92%		94%		98%	
Kappa	0.92		0.87		0.90		0.95		0.88		0.95	

6.3.2 Identification of macrofauna benthic activity feeding burrows

The analysis of abundance and distribution of feeding burrows from remotely sensed imagery showed a high abundance of macrofauna benthic activity during summer **(Figure 35)**. However, as seagrass meadows declined towards autumn, macrofauna benthic activity abundance decreased. The quantified statistical results show that the transition from autumn to winter had significantly affected the macrofauna benthic activity, with a significant decrease in macrofauna

benthic activity feeding burrows **(Figure 35)**. These statistical results of macrofauna benthic activity feeding burrows are directly related to seagrass abundance and distribution (**Figure 37**).

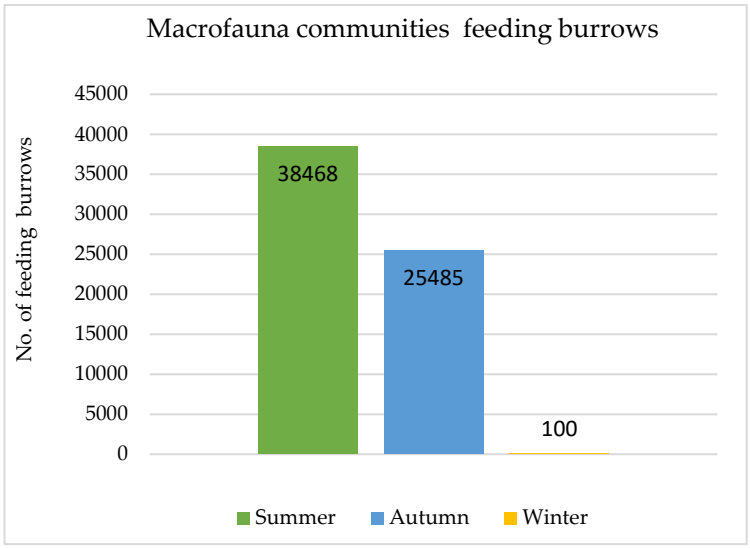

Figure 35. A graph showing macrofauna benthic activity by identifying their feeding burrows from the time-series seasonal imagery.

6.3.3 Habitat maps: Post classification change detection

The supervised classification model applied to the seasonal time-series imageries revealed distinct absent, low-density, medium-density, and high-density seagrass coverage areas across summer towards winter. Furthermore, the calculated difference between the classified maps illustrated seagrass gain and loss areas across the study area in the seasonal time series imagery **(Figure 36)**. The quantitative change analysis revealed a trend of overall loss across summer to autumn and gain in abundance and distribution from autumn to winter **(Figure 37)**. Although the quantitative values calculated from VIS and VIS+NIR sensors produce different results, loss and gain trends across summer to autumn and autumn to winter were consistent. This result means that an average loss across summer to autumn was 17%, and an average gain was 15% from the VIS imagery. In contrast, the VIS+NIR revealed a loss across summer to winter of 39% and an average gain of 12%.

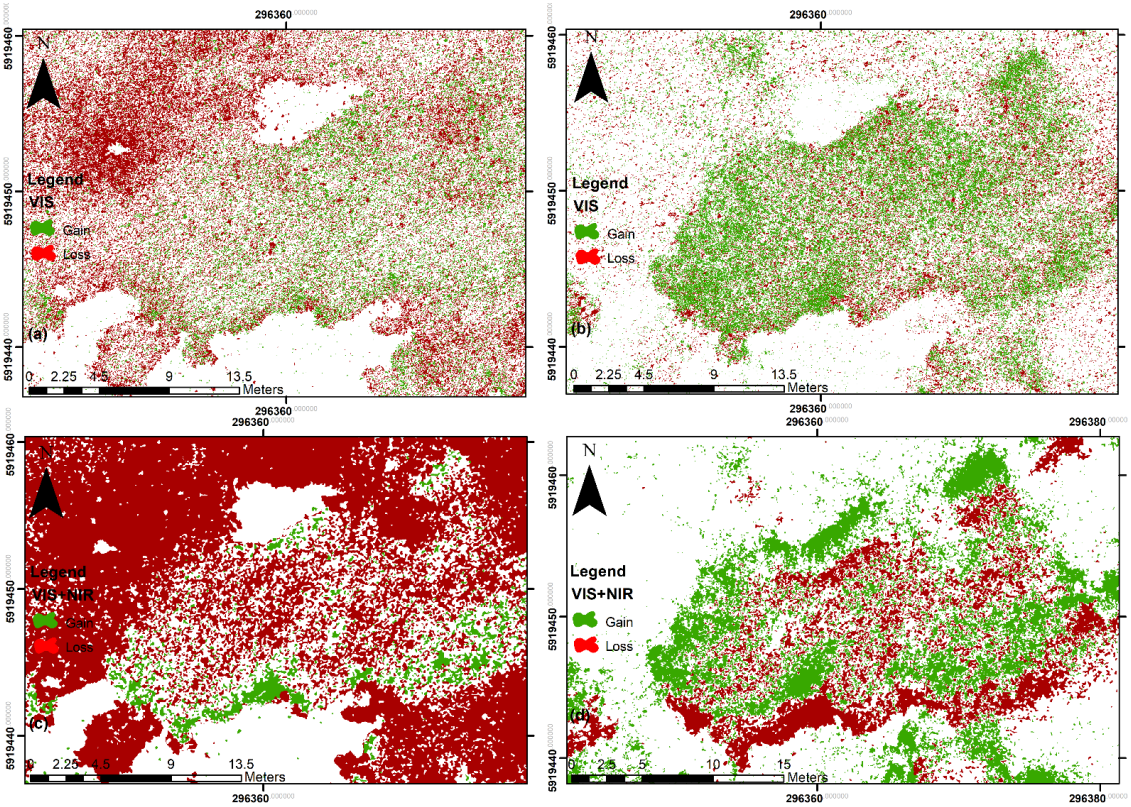

Figure 36. Seasonal time-series density changes in seagrass meadows. Using VIS imagery (a) gain and loss of seagrass across summer to autumn and (b) gain and loss across autumn to winter. Using VIS+NIR imagery (c) gain and loss of seagrass from summer to autumn (d) gain and loss across autumn to winter.

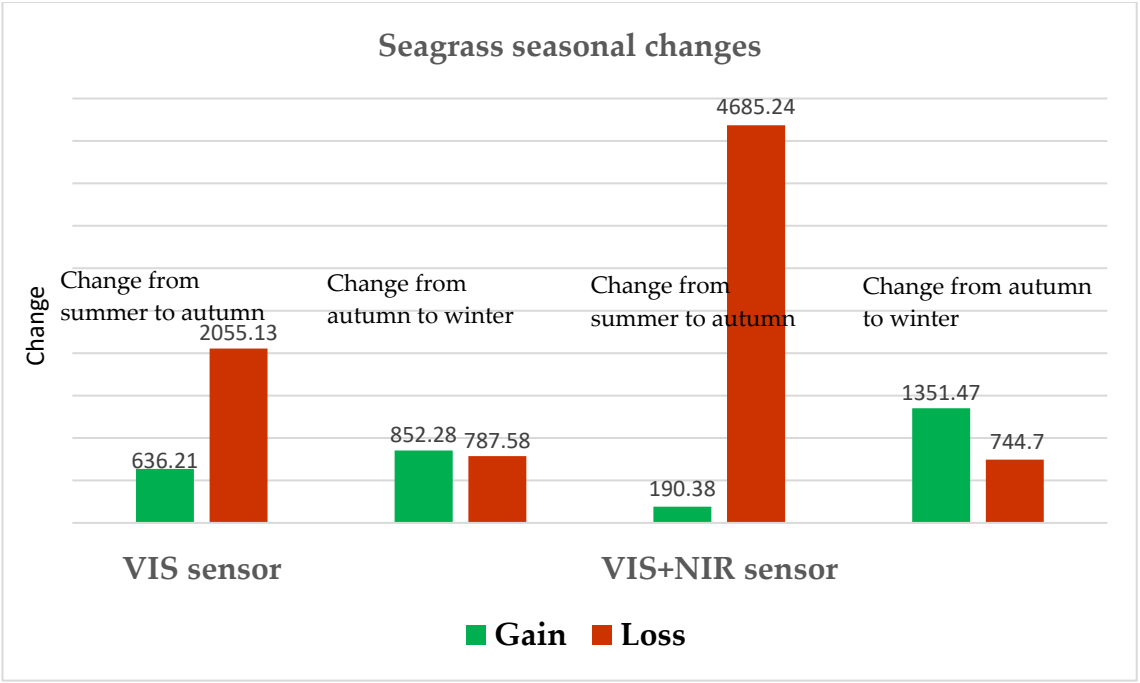

Figure 37. (a) graph of seasonal time-series density changes in seagrass meadows using VIS and VIS+NIR imagery across summer to autumn and autumn to winter.

6.4 Discussion

Seagrass meadows are a crucial part of many marine ecosystems (Lamb et al., 2017; Wernberg et al., 2016). However, seagrass loss from anthropogenic pressure such as discharge of sediments and pollutants from local runoffs and global climate change are concerns that need to be mitigated to protect this critical resource. Hence, this study tested the performance of VIS and VIS+NIR sensors to detect fine-scale seasonal time-series seagrass changes in a dynamic nearshore marine environment using spectral indices and a supervised classification technique. In addition, answer the following ecological question: What effect does seagrass gain and loss have on the abundance and distribution of macrofauna benthic activity by quantifying an increase or decrease in macrofauna benthic activity feeding burrows from drone imagery?

The results had established that the supervised classification technique produced accurate thematic maps for seasonal surveys, indicating its feasibility for mapping and monitoring dynamic changes in seagrass density along the intertidal zone during low tide. In addition, this research has built on previous knowledge and advanced on the following: (1) established the efficacy of a cost-effective VIS sensor and compared a VIS+NIR sensor for mapping fine-scale seagrass seasonal density changes, (2) ability to quantify fine-scale seasonal density changes in an open-source geoprocessing software, QGIS, (3) achieved a repeatable technique for quantitative ecological assessments and monitoring with high spatial resolution and revisit positional accuracy.

6.4.1 The performance of the sensors and the SVM classifier

Although the VIS imagery had a high spatial resolution, the VIS+NIR imagery had a better spectral resolution of five spectral bands. Hence, it was evident in this study that spectral resolution was more important in identifying different densities of seagrass meadows. The spectral resolution was more important due to the presence of the NIR band, which is highly reflected by seagrass meadows. Furthermore, the results from the ground truth datasets were 99% in agreement with the VIS+NIR sensor compared to 90% from the VIS sensor. Moreover, the classification accuracies are attributed to the training of the classification model, SGI vegetation index, and NDVI spectral index. In addition, the application of a machine learning classifier SVM performed better with these spectral indices and produced a high classification accuracy. Other researchers also had established that advanced machine learning classifiers like SVM are more trusted algorithms for coastal remote sensing (Mountrakis et al., 2011; Traganos et al., 2017).

Furthermore, in a related study for mapping seagrass *Zostera marina* with a VIS sensor, the classification accuracy was higher for dense seagrass cover (Nahirnick et al., 2019). Similarly researchers using Parrot Sequoia multispectral sensor in the Coromandel Peninsula in New

Zealand for change seagrass detection achieved high classification accuracy with dense seagrass than other classes (Martin et al., 2020). Also, this research achieved similar results, showing higher classification accuracy with dense seagrass than in other classes. The primary reason for achieving high classification accuracy results is spectral unmixing, which increases the ability of the classification model to predict high-density seagrass successfully while avoiding false positive and false negative pixel classification.

6.4.2 VIS+NIR classification analysis

The VIS+NIR sensor produced an orthomosaic of 3.5 cm/pixel spatial resolution. In addition, the positional accuracy in longitude and latitude for the georectified orthomosaic was 0.02m. The VIS+NIR imagery achieved an overall classification accuracy of 92% in summer, 94% in autumn, and 98% in winter **(Table 9)**. Sediment feature class and high-density feature class with the supervised classification technique scored well, achieving user's accuracy scores ranging from 0.96 to 1. These results indicate that the SVM classification technique successfully predicted sediment and high-density training polygons while avoiding false positive and false negative pixels during classification. In contrast, low and medium density classes with the supervised classification technique scores were satisfactory, achieving user's accuracy scores ranging from 0.66 to 0.90. These results indicate that the SVM classification technique had errors in successfully predicting medium and low-density training polygons while excluding true-positive and true-negative pixels during classification.

Furthermore, winter was the optimum season for aerial surveys of seagrass meadows in the study area. In addition, the high density of seagrass meadows across the time-series seasonal achieved high classification accuracy. Moreover, these results achieved from this study are harmonized with other studies (Chand and Bollard, 2021; Nahirnick et al., 2019; Ventura et al., 2018; Yang et al., 2020) that low altitude proximal remote sensing with RPAS is a valuable tool for identifying seasonal changes and for monitoring of intertidal seagrass meadows.

6.4.3 Identification of macrofauna benthic activity feeding burrows

Researchers have established that to understand the importance of landscape patterns on seagrass meadows, it is essential to comprehend the connection between seagrass distribution dynamics and the abundance of macrofauna benthic activity (Hughes et al., 2009; Turner and Schwarz, 2006). Hence, this research also aimed to answer the question: ***What is the effect of seagrass gain and loss on the abundance and distribution of macrofauna benthic activity?*** The results from time-series imagery showed that the abundance of macrofauna benthic activity feeding burrows during summer was higher than in autumn. This high abundance is associated with the high abundance and distribution of seagrass meadows during summer. This high benthic activity is

more centralized in the middle of seagrass meadows than in other locations because seagrass meadows protect from predators. This statement is justified by quantifying benthic activity and its association with seagrass gain and loss from the high spatial resolution orthomosaic.

During autumn, the abundance and distribution of seagrass meadows were low, mainly from black swans grazing on seagrass beds during their moulting season. As a result, the macrofauna species lost protection, and the benthic activity began to decline as at-tested by quantifying the high spatial resolution orthomosaic. Furthermore, during winter, the abundance and distribution of seagrass meadows were very low, with seagrass meadows regenerating in the study area. As a result of the abundance of macrofauna benthic activity, feeding burrows were highly impacted and reduced to a hundred as attested and quantified from the high spatial resolution drone orthomosaic.

Furthermore, researchers have used *in-situ* datasets and satellite aerial imagery to map *Zostera's* expansion of seagrass meadows associated with an abundance of macrofauna benthic activity diversity (Lundquist et al., 2018). Similar conclusions were made by Alderson, 1997; Bell and Hicks, 1991; Berkenbusch et al., 2000; Hicks, 1986, 1989; Inglis, 2003; Turner et al., 1999; Van-Houte Howes et al., 2004; Wood and Schiel, 1997. These studies have highlighted more diversity and abundance of macrofauna and various functional groups within *Zostera* beds than the neighbouring unvegetated sediments in New Zealand estuaries. Other macrofauna studies (e.g., oysters, mussels, clams, and cockles) of benthic activity among seagrass beds in Manukau Harbour have also supported the spatial density of seagrass at landscape scales. For example, patch isolation and fractal dimension can influence community structure (Turner and Schwarz, 2006). These studies have revealed the importance of landscape variation patterns on seagrass meadows. Hence, researchers need to comprehend seagrass dynamics and spatial distribution for monitoring and mapping changes in an estuary. But complexity in mapping and monitoring seagrass habitats arises when they are collectively impacted by anthropogenic and climate change (Duarte et al., 2013; Fourqurean et al., 2012). Furthermore, the meadows reaction to these impacts may not have been anticipated, and the response may differ spatially, making detecting change challenging. Therefore, this research could be a frontier to expedite many challenges associated with mapping and monitoring seagrass meadows in dynamic marine environments.

6.4.4 Habitat maps: Post classification change detection

Apart from the techniques used, high spatial information of the drone orthomosaic was a critical factor for detecting seagrass meadows in the study area. Hence, the results achieved from the classification model showed an overall loss of seagrass meadows across summer towards autumn (**Figure 36a and c)** and overall gain, abundance, and distribution across autumn towards winter (**Figure 36b and d)**. Moreover, both VIS and VIS+NIR achieved high classification accuracy,

but the VIS+NIR sensor showed high accuracy during ground-truthing. This sensor is more dependable because of the availability of a NIR wavelength that the seagrass meadows highly reflect. However, the results from the VIS cannot be dismissed as the difference was not significant during ground-truthing, and the advantage of this sensor was a very high spatial resolution orthomosaic for fine-scale ground sampling. In addition, this study established a repeatable technique for the spatial assessment of seagrass meadows in a dynamic marine environment in the study area.

Furthermore, as established from this study, time-series change detection enables resource managers to take counteractive action to mitigate further deterioration quickly. Such subtle changes identified included: (1) a shift in species density, richness, and distribution, (2) identification of wasting disease, (3) sudden decline in distribution and abundance of macrofauna benthic activity, and (4) rapid monitoring allows resource managers to evaluate and amend policies that avoid adverse effects to an ecosystem from the loss a ketone species. Moreover, marine ecologists and executives can use repeatable high-resolution datasets to extract invaluable information on seagrass ecology and, consequently, determine ecosystem health (Anderson et al., 2019). This continuous information flow will improve understanding of seagrass dynamics, associate macrofauna benthic activity movement within the ecosystem, and, most importantly, is applicable for conservation and planning (Lundquist et al., 2018). For example, early detection of fine-scale seasonal changes allows resource managers to quickly take remedial actions to mitigate further loss and deterioration of habitat and adapt management practices for conservation and planning.

Moreover, identifying drivers of change is essential for marine managers to establish a connection between natural and environmental conditions (Anderson et al., 2019; Matheson et al., 2017). However, method limitations for this study included aerial survey datasets restricted for a year due to Covid-19 lockdowns and were limited to a single seagrass species. Hence, future studies should monitor and quantify seagrass density fluctuations and trends for two years or more to establish a direction in density change. In addition, answer the following research question: Are seagrass abundance and distribution changes related to environmental or natural elements? For example, seagrass bed size may reduce after heavy rainfall inundated with coastal erosion sediment and simultaneously flooded with sewage waste discharge (Matheson et al., 2017).

6.5 Conclusion

This research used VIS and VIS+NIR sensors to detect fine-scale seasonal time-series seagrass changes in a dynamic nearshore marine environment using spectral indices and a supervised classification technique. The supervised classification results showed a high level of accuracy from both sensors. The VIS sensor achieved an overall accuracy of 90-98%, while the VIS+NIR

sensor achieved 92-98%. Furthermore, the classification model was used to detect time-series change detection. The time-series seasonal change detection results showed an overall loss of seagrass meadows across summer towards autumn, whereas an overall gain in abundance and distribution across autumn towards winter. In addition, both sensors, VIS, and VIS+NIR, show consistent results, i.e., loss across summer to autumn and gain from autumn to winter in the abundance and distribution of seagrass meadows. Moreover, the abundance and distribution of macrofauna benthic activity feeding burrows were higher during summer as they are associated with the high abundance and distribution of seagrass meadows. This change analysis using time-series seasonal RPAS imagery combined with supervised machine learning demonstrated the valuable contribution for documenting spatial ecological changes in a dynamic marine environment.

Chapter 7 Discussion and Conclusion

7.1 Introduction

This thesis has detailed new contributions to scientific knowledge regarding spatial dynamics of nearshore marine habitats from proximal low-altitude remote sensing. Each of the empirical studies described pioneering techniques, namely (Chapter 3), RPAS mapping and classification of wild oyster reefs with a VIS+NIR sensor in a temperate heterogenous estuary, (Chapter 4) proximal low altitude remote sensing for spatial assessment of temperate intertidal seagrass meadows from a VIS+NIR sensor, (Chapter 5) VIS and VIS+NIR low altitude multispectral remote sensing of wild oyster reefs, and (Chapter 6) detecting seasonal seagrass variability from novel drone technology using VIS and VIS+NIR sensors and their consequences on associated macrofauna benthic activity. Each of these chapters contains detailed discussion sections. Hence, Chapter 7 highlights the main findings, discusses common themes emerging across the mentioned chapters and discusses challenges and opportunities for future research using low-altitude remote sensing in marine environments.

7.2 Research aim

The overarching aim of this thesis, as stated in Chapter 1, was primarily to use the novel remotely piloted aircraft system with multi-sensors to supplement spatial and temporal data collection in a nearshore marine environment. The focus of the empirical techniques was to (1) assist marine managers in understanding the spatial dynamics of nearshore marine habitats, (2) increase the ability to capture high-quality aerial datasets, and (3) quantify fine-scale changes for conservation and planning. Through empirical investigations within a temperate intertidal estuary, Meola Rocky Reef (intertidal wild oyster reefs) and Cox's Bay (seagrass meadows) answered the aim. The more focused purpose relating to each chapter was to:

Chapter 3. aimed to demonstrate the potential of RPAS with a miniaturized multispectral sensor to deliver very high-resolution maps useable for the identification and characterization of wild oyster reefs. This study also evaluated the accuracy of OBIA and rule-based classification geospatial analysis techniques.

Chapter 4. aimed to explore the potential of an RPAS with a multispectral sensor for low altitude spatial assessment, monitoring, and mapping of intertidal seagrass meadows. In this study, a spectral index was modified to demonstrate its potential for distinguishing seagrass meadows from other land cover features using an object-based image analysis technique to segment the orthomosaic and perform a supervised classification.

Chapter 5. aimed to produce a spatial distribution map of wild oyster reefs in a rocky intertidal reef at low tide using multispectral (VIS+NIR) low altitude RPAS and evaluated an OBIA

workflow's accuracy with a Support Vector Machine (SVM) to classify high-resolution multispectral RPAS imagery.

Chapter 6. aimed to test the performance of VIS and VIS+NIR sensors to detect fine-scale seasonal time-series seagrass changes in a dynamic nearshore marine environment using spectral indices and a supervised machine learning classification technique. This study also aimed to identify and quantify the abundance and distribution of macrofauna benthic activity through their feeding burrows across the time-series seasonal imagery within the study area.

The proceeding sections will cover general remarks (with methodological consideration drawn from the thesis), followed by a discussion of each empirical chapter. Lastly, discuss the limitations and recommendations.

7.3 The rationale for this research

Benthic habitats are under pressure from anthropogenic and natural impacts, with increased declines identified throughout New Zealand's marine environment (Anderson et al., 2019; Morrison et al., 2014). For example, the declining status of seagrass meadows and the introduction of invasive species in local ecosystems (Foley and Shears, 2019; Matheson et al., 2017). However, it is essential to accentuate that many of the declines in benthic habitats such as seagrass and wild oysters have gone unrecorded and have been poorly documented (Anderson et al., 2019; Morrison et al., 2014). A lack of spatial datasets for mapping and monitoring was the primary reason for inconsistent records and poor documentation of declines. From reviewed literature (Chapter 2), it was established that (1) there are gaps in the national inventory for most biogenic habitats, (2) temporal inconsistency within spatial datasets, and (3) missing information on the condition and health of biogenic habitats, and their spatial extent, (4) knowledge gap on drivers of change that cause benthic habitat declines, (5) data gap from original baselines assessments which are essential for future assessments and predictions, and (6) contributions of wild oysters for fisheries production is Unknown.

Nevertheless, it is worth mentioning that New Zealand research in benthic habitats has expanded beyond *in-situ* surveys and manual imagery digitization (Anderson et al., 2019). Still, there is no universal solution for mapping and monitoring benthic habitats locally. Therefore, this research focused on developing practical techniques and applications to fill this inconsistent spatial and temporal datasets gap.

7.4 RPAS and Sensors

RPAS equipped with different sensors has profound attributes that make them advantageous for collecting high-resolution, remotely sensed data within the sea-land interface. These attributes

have been demonstrated with the empirical work in Chapters 3, 4, 5, and 6. For example, RPAS platforms are more flexible for proximal remote surveying with high positional accuracy than other platforms such as blimps and balloons, as attested in Chapter 3. In addition, a multi-rotor lightweight RPAS is well suited for capturing low-altitude aerial data than *in-situ* field sampling for seagrass meadows in mudflats (Chapters 4 and 6). At the same time, RPAS equipped with VIS and VIS+NIR sensors (Chapters 5) can capture electromagnetic spectrum at broad spectral ranges such as visible (VIS) (400nm to 700nm) and beyond the visible spectrum (VIS+NIR) (**Figure 38**). These spectral bands at different wavelengths capture spectral reflectance from the land cover features, which allowed the extraction of pure training samples to accurately classify wild oyster reefs and seagrass meadows (Chapters 3, 4, 5, and 6).

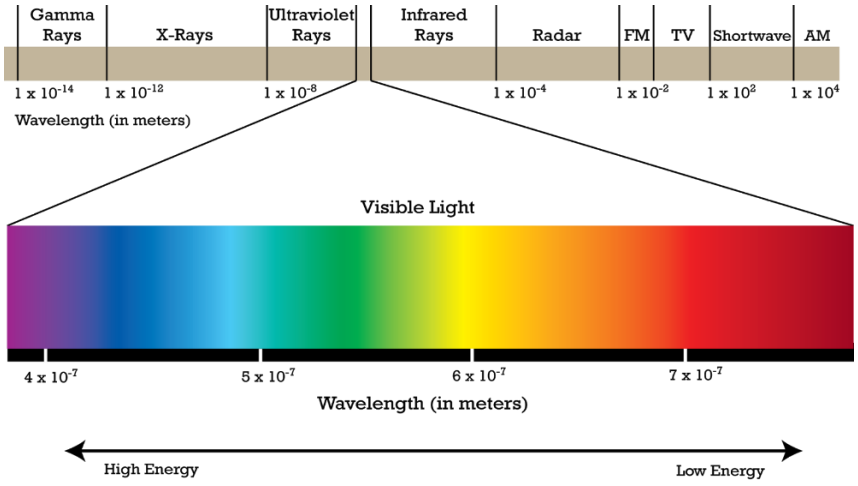

Figure 38. The electromagnetic spectrum. Free image sourced from clipartmax.com

7.5 The synergy between RPAS, remote sensing, and *in-situ* techniques

The synergy between RPAS remote sensing with other remote sensing products such as satellite and historical crewed aerial photographs provided new understandings and spatial scalability to intertidal estuarine research. For example, Gray et al., 2019, used the synergy between a 1.24m/pixel spatial resolution WorldView 3 and RPAS datasets to support and validate habitat classification in a heterogenous intertidal ecosystem. However, in Chapter 3, it was challenging to extract pure training samples from the 75cm satellite imagery as spectral mixing occurred between the pixels of wild oysters and other land cover features. This challenge was mitigated by including high-resolution RPAS imagery that enhanced feature detection and increased the potential to delineate wild oysters in an overlapped ecosystem. Similarly, as attested from Chapters 4 and 5, RPAS spectral signatures were comparable to the *in-situ* spectro-radiometer for seagrass meadows, wild oyster reefs detection, and the classification results achieved were 95% **(Table 6)** and 85% **(Table 7)**, respectively.

7.6 Will RPAS remotely sensed datasets replace other products?

RPAS platforms have revolutionized low altitude proximal remote sensing techniques for marine applications in the last decade. For example, Hodgson et al., 2010 pioneered the application of an RPAS to survey marine mammals in Australia. Since then, this technology has matured and offered researchers a stable, cost-effective, and flexible platform for marine remote sensing (Chapters 3, 4, 5, and 6). However, RPAS remote sensing overstatement to capture high spatial and temporal imagery could lead to discrepancies between the research question and the methodology (Anderson, 2016; Johnston, 2019). It is essential to accentuate that RPAS could not entirely replace aerial, satellite, and *in-situ* techniques (Tang and Shao, 2015). Although, researchers and marine managers could use RPAS captured datasets to supplement *in-situ* and other remotely sensed datasets, as discovered through the primary aim of this thesis. In addition, RPAS technology has offered researchers the opportunity to add complementary datasets for mapping and monitoring and answer specific research questions relating to marine and terrestrial ecosystems.

Nevertheless, depending on the research extent and application, selecting other remotely sensed datasets are more appropriate—for example, using satellite imagery for mapping coral reefs over an area of 100 km^2 (Roelfsema et al., 2018). Also, the research questions should reflect on data acquisition and platform capability. This selection of datasets calls attention that applications always get better with trial and error while developing new scientific research concepts. For example, Chapter 3 was used as a pilot study to test and assess RPAS low altitude proximal remote sensing capability to delineate and classify wild oyster reefs in a heterogenous estuary. Consequently, we developed other concepts through Chapters 4 to 6.

7.7 Spatial ecology from consumer-grade RPAS and challenges

Chapter 3 assessed the potential of a low-cost consumer-grade RPAS platform to map and identify wild oyster reefs. This assessment involved the RSAP platforms' performance from 50m altitude, flight time, and ability of the sensor to capture the spectral reflectance of different land cover features **(Table 3)**. The aircraft used was effectively stable at 50m altitude with wind speeds up to 12m/s (with only ten blurred photos). From seven flights taking 73 minutes, the multispectral sensor with a field of view (FOV) of 47.9 degrees captured an area of 0.253km^2. Generally, the imagery's pixel size is the primary component in detecting smaller objects on the ground. For example, the oyster shells size ranged from ~6-8cm, whereas the imagery produced had a ground sampling distance of 3.5cm/pixel. From the orthomosaic, wild oyster reefs were successfully demarcated from other land cover features and segmented for classification to achieve a user's accuracy of 0.95 **(Table 4).**

Chapter 4 evaluated and compared the spectral reflectance of seagrass meadows from *in-situ* and RPAS, VIS+NIR orthomosaic. Also, a spectral index was modified for spatial assessments to distinguish seagrass meadows from other land cover features accurately. The findings showed comparable results from *in-situ* and remote reflectance, and the supervised classification technique achieved an overall accuracy of 95% and a Kappa Coefficient of 0.81**(Table 6)**. The results achieved were significant, considering challenges in collecting *in-situ* datasets in mudflats and aerial surveys within the tidal range. For example, the *in-situ* data collection using a spectro-radiometer was time-extensive and required a re-calibration after an illumination change. Nonetheless, the results established that researchers could confidently use low altitude RPAS capability and high-resolution imagery to extract spectral reflectance for training samples and complement *in-situ* datasets.

Chapter 5 compared VIS and VIS+NIR sensors for the spatial assessment of intertidal wild oyster reefs in a heterogenous rocky reef setting. The topology in this ecosystem was physically challenging to collect *in-situ* datasets over large spatial extents. Hence, a multi-rotor RPAS was deployed from 50m altitude, VIS sensor produced a 1.3cm/pixel spatial resolution orthomosaic and achieved a user's accuracy of 0.72 for wild oyster reefs. In contrast, the VIS+NIR sensor from the same altitude had a spatial resolution of 3.5cm/pixel and achieved a user's accuracy of 0.96 for wild oyster reefs **(Table 7)**. Although spectral information was more important than spatial information in this study, the VIS sensor had a better ground sampling distance. This remote sensing technique for ecology and conservation offers scale-appropriate spatial assessment, monitoring, and mapping of benthic habitats in challenging and inaccessible marine environments.

Chapter 6 tested VIS and VIS+NIR sensors for fine-scale change detection of seasonal seagrass meadows using spectral indices. This study also quantified the abundance and distribution of macrofauna benthic activity through their feeding burrows across the time-series seasonal imagery within the study area. Survey times and *in-situ* data collected in mudflats are limited during the tidal variation because walking in the soft sediment is physically challenging. Thus, RPAS technology was presented as a practical solution to identify seasonal density changes to achieve a 90-98% classification accuracy. These results are essential for seagrass conservation because managers can quickly detect fine-scale seasonal changes and take mitigation actions before the decline of this keystone species affects associated species and the entire ecosystem.

The VIS+NIR sensor provided notable improvements in classification accuracy for accurately detecting and delineating features in this study. For example, the VIS+NIR sensor differentiated textures (the spatial allocation of tones across the pixels) in the imagery and increased the extraction of pure training samples, improving classification accuracy. The widely available

consumer-grade VIS sensor also produced accurate and dependable classification results (Chapters 5 and 6). This VIS sensor has a wider focal length of 20mm and a field of view of 94 degrees compared to VIS+NIR sensors, and it maintains the visual output (imagery) like a human eye for researchers with limited remote sensing knowledge. Researchers have also established that VIS sensors in turbid waters attenuate beyond 2-3 meters to detect broadly submerged taxonomic vegetation (Tait et al., 2019).

Mapping and monitoring any ecosystem requires consistent datasets (Gomes et al., 2018). However, consistent data collection can be challenging during a global pandemic lockdown such as the novel COVID-19. To mitigate this challenge, citizen scientists with consumer-grade RPAS can share and distribute raw geotagged photographs to a dedicated website (Ferguson et al., 2018).

7.8 Role of Citizen scientists in data contribution during pandemic lockdowns

Logistical challenges for aerial surveys during lockdowns due to the global pandemic: One increasingly common solution is the inclusion of citizen scientists in environmental monitoring and data collecting programmes (Dominquez-Tejo et al., 2016; Jarvis et al., 2015; Pinarbasi et al., 2017). The concept of citizen science is not new; since 1900, volunteers and non-scientists as part of the citizen science programmes have recorded scientific information (Koss and Kingsley, 2010). The advancement in technology, such as smartphones with high-resolution cameras and high-speed internet, has expanded the capacity for citizen science applications regardless of their physical locations (Newman et al., 2012). For example, universally recognized programmes like Zooniverse enrol online volunteers to detect changes in kelp forests from satellites and plankton species (Hyder et al., 2015). This programme has allowed marine ecologists to process large volumes of data than previously achievable.

However, a consistent data acquisition framework is required to collect high-quality data using off-the-shelf drones (Joyce et al., 2018). This framework can be based on a simple defined technique using drones and flight parameters with open-source flight planning software to form an easy-to-follow data acquisition protocol for non-experienced drone owners (Papakonstantinou et al., 2021). Open-source flight planning software is freely available for the most common (iOS and Android) devices. Through an easy-to-follow framework, citizen scientists can select fight details to create flight missions and capture high-quality data consistently (Papakonstantinou et al., 2021).

For citizen science programmes to succeed, a collaborative approach is needed. This approach means that people from various backgrounds such as (1) information technology, (2) data analysts, (3) boat owners, (4) local councils, (5) government organizations, (6) divers, (7) tour boat operators, (8) local communities, and (9) local anglers are encouraged to be involved. For

citizen science endeavours to be long-lived, these projects should be well designed, implemented, and managed (Vann-sander et al., 2016). Communication, good relationships, and understanding between stakeholders are integral in achieving a successful outcome from a citizen science programmes. This success is also dependent on the affordability and availability of consumer-grade, new, and refurbished RPAS, including open-source flight planning software. In New Zealand, the proliferation of UAVs for recreational activities and the availability of high-speed internet (to upload data) can contribute to high-quality datasets from marine environments. For example, citizen scientists can be engaged with RPAS platforms near Meola Reef to capture RPAS datasets and upload them to a designated web service, such as the newly launched Geo-Nadir website.

Geo-Nadir is an online website (geonadir.com) dedicated to citizen scientists globally sharing RPAS datasets and a place to reach out and collaborate with other researchers (Kovacs et al., 2018). The primary purpose of Geo-Nadir is to connect RPAS pilots, researchers, and land and sea managers to find solutions for environmental challenges that require spatial datasets. At the time of writing, we are the first researchers from New Zealand to share our RPAS VIS datasets and collaborate with other citizen scientists on Geo-Nadir **(Figure 39)**.

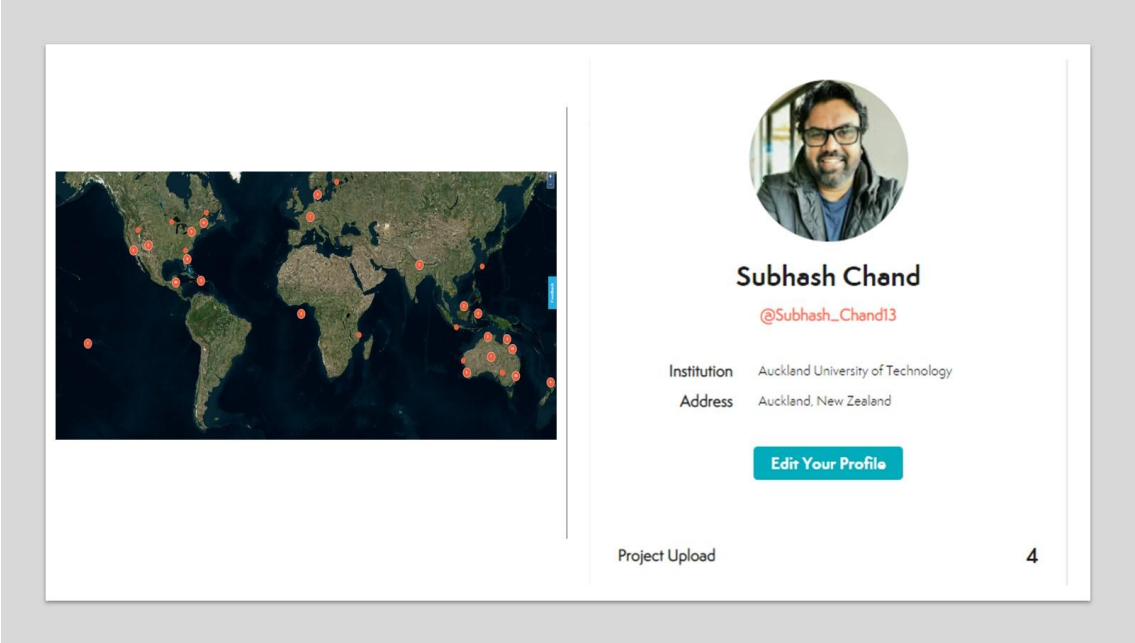

Figure 39. Global citizen scientists sharing their RPAS datasets on Geo-Nadir

7.9 Empirical discussion and potential research questions

7.9.1 Intertidal oyster reefs

The Auckland council in New Zealand has conducted *in-situ* surveys and researched Meola rocky reef since 2001. The standard technique used for sampling and quantifying oyster reefs were transects, quadrats, and GPS receivers (Foley and Shears, 2019). Chapter 3 presented the first

application of a low-cost multi-rotor RPAS that captured high spatial resolution multispectral imagery to map and characterise wild oyster reefs on this rocky intertidal reef. In this study, wild oyster reefs from RPAS imagery were better detectable than satellite imagery of 7.5cm/pixel **(Figure 17)** and achieved a user's accuracy of 0.95. Because of spectral mixing, the coarse spatial resolution satellite imagery was insufficient to delineate wild oyster reefs from other land cover features. Apart from wild oyster reefs, researchers could also identify fine-scale changes in vegetation (mangroves) cover from the false-colour composite **(Figure 14)**.

Chapter 5 investigated VIS and VIS+NIR sensors for spatial assessment and mapping wild oyster reefs in a rocky intertidal reef at low tide. Also, evaluated *in-situ* and RPAS spectral reflectance to reduce field survey times and reliance on expensive equipment such as the hyper spectro-radiometer and hyperspectral remote sensing of wild oyster reefs (Le Bris et al., 2016). Chapter 5 is a significant development working with VIS and VIS+NIR sensors for remote sensing of wild oyster reefs in the study area previously not anticipated. The VIS+NIR orthomosaics had a higher spectral and textural separation and achieved a user's accuracy of 0.96 compared to 0.72 for the VIS orthomosaic **(Figure 26a and b)**. Using a VIS sensor for mapping wild oysters, researchers achieved a similar classification result (users' accuracy of 0.72) due to minimal spectral and textural separation of wild oyster reefs from mud (Espriella et al., 2020).

Moreover, data collection on this rocky intertidal reef was methodologically challenging due to the rugged topology created by wild oyster reefs extending almost 2km seaward. This challenge was mitigated by identifying a suitable space for RPAS take-off and landing and considering the tidal variations before designing the flight plan. The other challenge was evenly distributing the GCPs, and associated D-GNSS work was time-extensive. Hence, Chapter 2 reviewed the literature on RPAS operation challenges and identified solutions to overcome these challenges.

7.9.1.1 Future research questions

Some of the critical research questions developed from the empirical work presented in Chapters 3 and 5 are:

a) Can RPAS imagery be used to conduct virtual quadrat sampling of wild oyster reefs at larger spatial extents and produce comparable results as *in-situ* quadrats?
b) Can RPAS imagery effectively locate and map oyster borer snails (*Haustrum scobina*) on the Meola rocky reef?
c) How can oyster density estimates be combined with environmental data such as sedimentation to predict changes in the wild oyster reefs population?
d) Would RPAS imagery be suitable to identify and differentiate between dead (blank shells) and alive, wild oysters?

e) Can the different species of wild oyster reefs on the Meola reef be determined from RPAS imagery?

7.10 Intertidal seagrass meadows

Chapter 4 demonstrated the potential of an RPAS with a multispectral sensor for low altitude mapping and spatial assessment of intertidal seagrass meadows. The VIS+NIR orthomosaic showed that different seagrass density was identifiable from the false-colour composite imagery and achieved an overall classification accuracy of 95% **(Table 6)**. Previous studies have explored different vegetation indices from satellite imagery, e.g., Landsat, to differentiate seagrass species from other benthic vegetation and quantify seagrass standing crop density (Barille et al., 2010; Kromkamp et al., 2006). Among the indices used, the Normalized Difference Vegetation Index (NDVI) is the most common vegetation index created to estimate above-ground seagrass meadows biomass (Bargain et al., 2012), followed by Leaf Area Index (LAI) to estimate above-ground biomass (Tamondong et al., 2018). It was also established that *in-situ* and RPAS spectral reflectance were comparable, and the meadows had peaked spectral reflectance along the Green and RedEdge bands. This spectral reflectance information was used to create a modified spectral index (RENDVI) to accurately distinguish seagrass meadows from other land cover features.

Chapter 4 is a significant achievement in creating a seagrass vegetation index that successfully differentiated seagrass from other land cover features **(Figure 22)**. The spectral index developed, RENDVI, is unique for detecting seagrass meadows previously not explored. Apart from the spectral index map, the high-resolution false-colour composite imagery **(Figure 23)** depicted areas of different seagrass densities, such as dense and sparse. As mentioned earlier, the seagrass mudflat was methodologically challenging to evenly distribute GCPs for positional accuracy. Researchers can mitigate this challenge by using RTK grade on-board RPAS.

Chapter 6 tested the performance of VIS and VIS+NIR sensors to detect fine-scale seasonal time-series seagrass changes in a dynamic nearshore marine environment using spectral indices and a supervised machine learning classification technique. This study aimed to identify and quantify the abundance and distribution of macrofauna benthic activity through their feeding burrows across the time-series seasonal imagery within the study area. The results established that using spectral indices increased the ability to detect seagrass meadows from both VIS and VIS+NIR sensors accurately **(Figure 36)**. This study's overall accuracy of supervised classification results ranged from 90-98%, with summer as the optimum season for consistent aerial surveys. It was also established from the aerial imagery that the abundance and distribution of macrofauna benthic activity decrease with seasonal seagrass meadows decline **(Figure 35)**.

Chapter 6 is a significant achievement in working with VIS and VIS+NIR sensors to detect fine-scale seasonal changes in seagrass meadows. Researchers have established that changes in

essential habitats such as seagrass in dynamic marine environments often go undetected and undocumented (Kettles and Bell, 2016). Therefore, the contribution to knowledge from this study is that fine-scale changes can be rapidly identified, quantified, and documented for marine managers to mitigate further deterioration of this critical habitat and identify the source of variability. The other contribution was identifying and quantifying macrofauna benthic activity through their feeding burrows, supplementing *in-situ* data collection.

7.10.1 Future research questions

Some of the critical research questions developed from the empirical work presented in Chapters 4 and 6 are:

f) Can VIS+NIR sensors onboard the RPAS platform be used to detect wasting disease (browning of seagrass leaf blade caused by a fungal infection of the internal tissues caused by the marine slime mould, *Labyrinthula zosterae*) on individual seagrass blades and monitor the overall health of seagrass meadows?
g) Is intra-annual or seasonal RPAS remote sensing optimal for monitoring the variations in seagrass density?
h) Can historical satellite and RPAS imagery be used in synergy to detect changes in seagrass density?
i) What effect will a total eradication of seagrass meadows have on the whole ecosystem?
j) Are seagrass abundance and distribution changes related to environmental or natural elements?
k) Boat anchorage is a primary threat to seagrass beds, disturbing and uprooting the seagrass meadows. Can seagrass regenerate from anchorage damage and their scars? For example, as shown in **(**Figure 40**)**.

7.11 Identifying drivers of change

Nearshore marine environments are most susceptible to natural and anthropogenic drivers of change than the open ocean (Griffen et al., 2016; Gunderson et al., 2016). These drivers of change are a concern because they typically act together, and their effects are more acute when combined (Halpern et al., 2019). Their interactions will highly influence habitat populations and impact other ecosystem functions and services. Therefore, understanding the spatial dynamics and identifying drivers of change will assist in conservation and planning and better management programmes to reinforce ecosystem resistance. The drivers of change identified during this study and reviewed literature are factors that adversely affect nearshore benthic habitats **(Table 10)**.

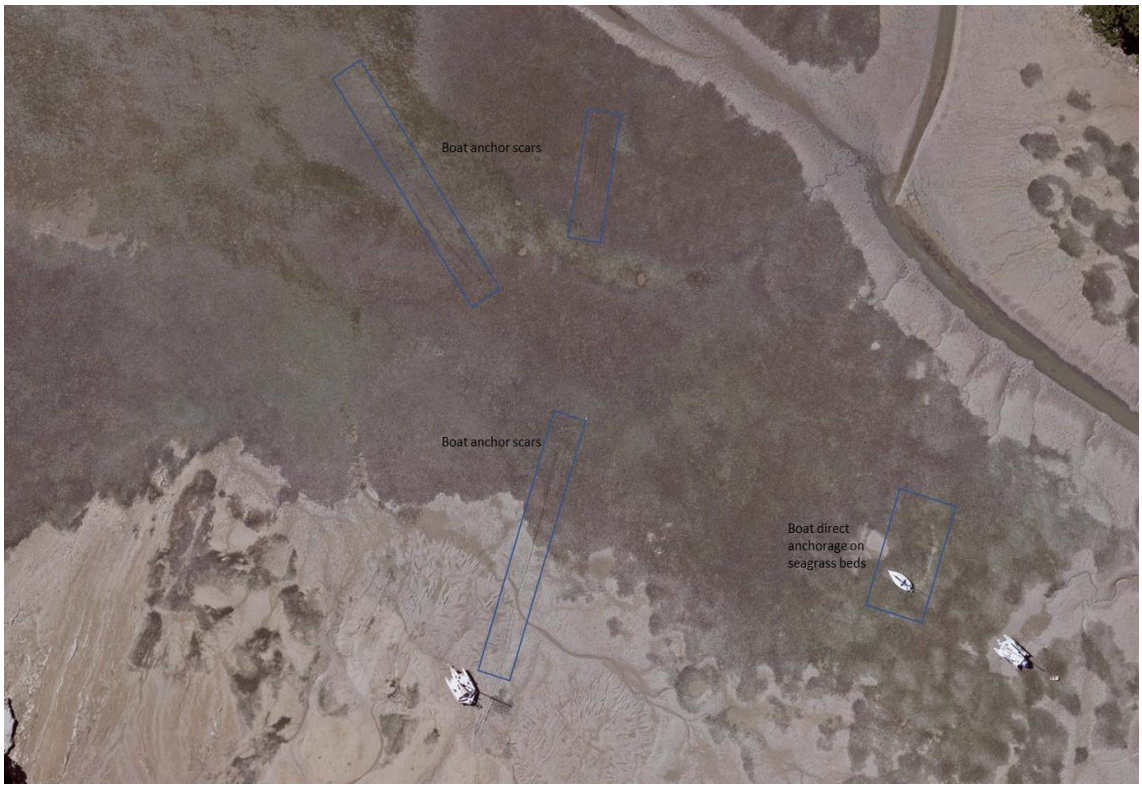

Figure 40. Showing boats sitting directly on seagrass beds and anchorage scars at Cox's Bay adjacent to Meola Reef. Satellite image source LINZ, 2019.

Table 10. The drivers of change identified impacting biogenic New Zealand's nearshore benthic habitats—source (Anderson et al., 2019; Morrison et al., 2014).

Classes	Drivers of change
Class 1: Degradation of water quality	Nutrient enrichments: from sedimentation and sewage discharge
	Chemical and pharmaceutical containments
	Pathogens
	Agricultural runoffs
Class 2: Impact on habitats	Urban expansion
	Coastline reclamation
	Excessive sedimentation
	Dredging
	Flux in infrastructure developments
Class 3: Change biotic communities	Overfishing
	Alterations in hydrological regimes
	Introduced and invasive species

	Marine debris such as plastics and other floatable
Class 4: Climate associated	Increase in Greenhouse gases
	Marine heatwaves
	Extreme precipitation and runoffs
	Extreme climatic events such as La Nino and El Nino, Hurricanes
Class 5: Natural drivers of change	Marine grazers such as black swan
	Wasting diseases
	Boat anchorage
	Trampling on seagrass by dogs and collecting shellfish during low tides
	Trampling live oysters while setting fishnets

7.12 The contribution of this study to marine management

Spatial inventory gaps in assessing biodiversity loss and gain in New Zealand's nearshore marine ecosystems are challenges marine managers frequently encounter (Anderson et al., 2019). For example, many benthic habitats locally form extensive areas but remain poorly represented, without national knowledge of their status, abundance, and distribution (Matheson et al., 2017). With rapid changes in dynamic marine environments, assessments should be frequent, including (1) information on impacts and threats that change the anatomy of the ecosystem and (2) data on the status of an ecosystem that can be used to predict the future trajectory of benthic habitats.

Furthermore, some of the policy contributions of this study ranged from the national to the regional level. From a national level perspective for surveying the marine environments, The Resource Management Act (RMA) 1991 and The Environmental Reporting Act (ERA) 2015 Under the RMA 1991, the mandated New Zealand Coastal Policy Statement (NZCPS) 2010 provides guidelines and policies for managing and monitoring the coastal environment (DOC, 2010). Under The RMA 1991, the function of the local councils is to manage coastal environments in association with The Department of Conservation (DOC). The local councils operate Under Section 30 (1) (d) to monitor the condition of the coastal environments. Under Section 35 (1), all local authorities must collect information, undertake research, and should monitor coastal environments to the appropriate extent effectively. The DOC currently complies with all spatial information about the extent of seagrass beds under their Sea-Sketch project initiative, mainly from local councils and universities in different formats (Anderson et al., 2019).

Moreover, regional level surveys and plans are directed and implemented from Catchment Management, Land Management plans, and Coastal Zone Management (O'Donell, 2009). Regional mapping of coastal estuaries provides quantitative information on habitat conditions for the local council's statutory responsibility under the scope of NZCPS, 2010. This scope allows the councils to maintain their coastal habitats from adverse effects on the ecological processes (DOC, 2010). Intertidal estuaries are a source of natural resources and hold cultural importance (Taonga species) for indigenous communities (iwi and hapū) in New Zealand (MfE, 2019). Local surveys of benthic habitats are essential to understand the status and predict future trends. For example, a long-term study on Otago's coast, New Zealand, showed an increase in ocean acidity by 7.1 percent (MfE, 2019). Benthic habitats in intertidal estuaries such as oysters (*Saccostrea glomerata*), paua (*Haliotis iris*), and green-lipped mussels (*Perna canaliculus*) will be highly vulnerable to this change. Increased ocean acidity will also impact local aquaculture productions and exports (MfE, 2019).

The development of an RPAS technique for spatial assessments of benthic habitats is applicable at regional levels, which will add value to the spatial information datasets at a Regional to National level. Researchers and marine managers can easily configure the technique according to the objectives for different estuaries. For example, suppose the project's objective is to identify and locate oyster borer snails (*Haustrum scobina*) along the Meola rocky intertidal reef. The researchers should plan the RPAS flights to be at least within an altitude of ~5-10 meters from the surface to locate oyster borer snails and get imagery where pixels of the imagery will be smaller than the object's size. Subtle fine-scale changes can be readily detected as the technique is scalable.

7.13 Limitations and Recommendations

This research used RPAS equipped with multi-sensors to supplement spatial and temporal data collection in the temperate estuarine ecosystem. The aerial imagery is captured to produce a high-resolution geographical layer such as an orthomosaic and analysed using geospatial workflows to extract quantitative or qualitative information to assist marine managers in (1) identifying fine-scale changes, (2) understanding the spatial dynamics of nearshore marine habitats, and (3) identifying drivers of change for conservation and planning and (4) supplement *in-situ* and remotely sensed datasets. The flexibility in flight planning allows RPAS surveys to be configured according to the project's objective and research needs. For example, in this study, most aerial photographs were captured from 50m altitude to balance the trade-off between the pixel size of the imagery and ground targets such as wild oyster reefs. However, flying at a low altitude yielded a finer spatial resolution and improved classification accuracy but compromised the spatial extent. Therefore, some of the key limitations of this research included:

a) Aerial surveys were logistically challenging along the Meola intertidal rocky reef and the mudflat. Because of resource constraints, it was time-extensive to distribute ground control points and simultaneously collect GPS data in the mudflat. Hence, aerial flights had to be reduced to account for the incoming tide, and good lightning conditions for aerial image capture were missed.
b) Flying at a low altitude compromised the spatial extent and required more fully charged batteries for additional flights.
c) The study site is popular and crowded with birds that attacked the drone regularly, which minimized aerial survey times and compromised battery charge.
d) Data collection was limited to a single year, 2019, due to COVID-19 lockdowns. It would have been optimum to compare the results of spatial assessments and identify environmental and natural drivers affecting these biogenic habitats for another two years (2020-2021).
e) The survey results were limited to a single seagrass species, *Zostera muelleri*. Further research is required to test this technique in a heterogeneous ecosystem with more than one seagrass species and different substrates.
f) The installation of underwater cameras at the study site would have been beneficial to visualise marine biodiversity presence during high tides. Nonetheless, during fieldwork, we had the opportunity to meet and observe a local collecting his catch at Meola Reef **(Figure 41)**.
g) Limited aerial coverage in Cox's Bay because houses are near seagrass beds.
h) The spatial resolution was insufficient in aerial imagery to detect and identify predatory oyster borer snails (*Haustrum scobina*) on Meola intertidal reef.

Figure 41. A local showing his catch at the Meola intertidal rocky reef. Image courtesy of Kavita Prasad taken with permission.

7.14 Recommendations

7.14.1 Placing information boards along important coastlines

The Meola rocky intertidal reef and Cox's Bay (adjacent to the Meola reef) are biodiversity hotspots that hold carbon-rich benthic habitats such as seagrass meadows and wild oyster reefs. Despite their ecological and economic importance, there is no information about these essential benthic habitats for the public at the Meola reef dog park entrance or Cox's Bay coastline. The only information found on the Auckland Council website was upgrading plans for the walkway and installing lights in this area. However, the Auckland Council has displayed an information board on seagrass meadows and mangroves along the Westmere Coastal walking track **(Figure 42)**.

Therefore, a recommendation to the Auckland council and marine managers would be to install information boards such as **(Figure 43)** and **(Figure 44)** along the coastlines where these vital benthic habitats are present. The significance of these information boards would be to create awareness, notify the public of the importance of benthic habitats and be extra vigilant when entering these biodiversity hotspots.

Figure 42. Information board displaying the importance of mangroves and seagrass meadows as fish nursery grounds. Source Auckland Council website.

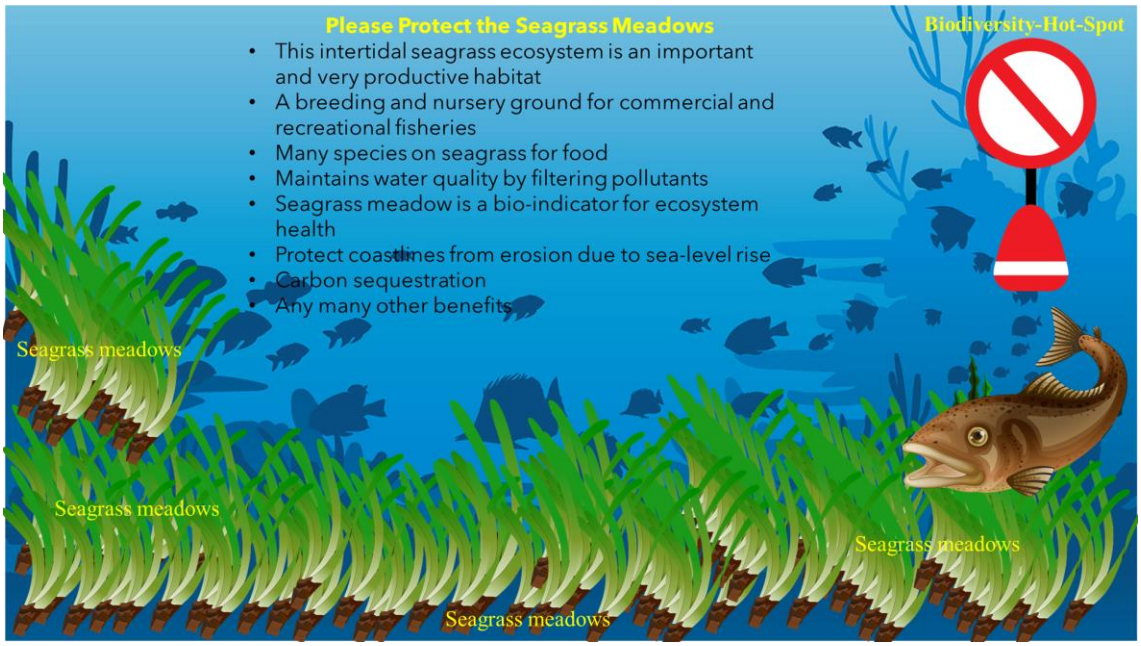

Figure 43. A sample information board displays the importance of seagrass meadows at Cox's Bay. Icons were downloaded free from https://ian.umces.edu/media-library/symbols/#_Resources

Figure 44. A sample information board to show biodiversity at Meola Reef. Icons were downloaded free from https://ian.umces.edu/media-library/symbols/#_Resources

7.14.2 Recommendation to Auckland and local Councils

7.14.2.1 Frequency of monitoring benthic habitats

In New Zealand, benthic habitats such as seagrass meadows occur across a broad range of cover from continuous to sparse seagrass beds. *Zostera muelleri* in New Zealand is mainly an intertidal species but is also found in sub-tidal locations across the North and South Island (Morrison et al., 2014). Therefore, not all seagrass areas behave the same, even under natural conditions; they would be highly stable (growing up to 40 hectares in the study site, Lundquist et al., 2018) to

those that might be highly variable (e.g., declines observed in Tauranga Harbour (Matheson et al., 2017). Consequently, the local council should not take a one size fits all approach to monitoring that would yield undesirable outcomes. Hence monitoring programs should be devised with a rationale about the location and nature of the meadow and the research question being answered.

A critical consideration is at what scale monitoring should monitoring be conducted. But seagrass landscapes are highly dynamic and present substantial shifts in the spatial footprint of the meadows (Anderson et al., 2019). Therefore, monitoring the overall state of seagrass and wild oysters in a region would be best addressed using the methods used in this study to integrate much greater spatial extents that are considered representative of an area—further duplicating in new regions to contextualise the changes observed locally.

Variables are another essential consideration that should be integrated into monitoring programmes. These variables should be the most suitable and are dependable on the questions being asked of the monitoring programmes. For example, if tracking changes in seagrass is the overarching goal, then these variables should be considered: (1) changes in seagrass and wild oyster cover in an area, (2) significant shift in species composition, (3) changes in sediment and water clarity, (4) movement of seagrass meadows toward the shoreline, (5) length of seagrass blades.

The frequency of monitoring is another critically crucial as seagrass in New Zealand is highly seasonal. Hence, the frequency of monitoring would depend on the project's objectives. For example, an annual assessment of seagrass conditions could be conducted during the peak season for assessing seagrass abundance during summer (typically between December and February). And evaluate the seagrass seed bank during spring (September to November). However, if monitoring seasonal change is vital to the programme, more frequent (ideally at least quarterly or seasonal) sampling will be the best option. An even higher sampling frequency (weekly or monthly) will be beneficial if the monitoring is expected to evaluate compliance or impacts of a particular development or discharge event.

7.14.3 Other recommendations

Boat anchorage directly on seagrass beds (Figure 40) is an essential threat to the meadows as the dragging of boat anchors uproots the rhizomes of seagrass meadows needed for regeneration. Hence, boat owners should be educated on the importance of seagrass meadows and advised on the consequences of boat anchorage on seagrass beds. A systematic approach that would benefit the boat owners and seagrass beds are needed to be devised, such as (1) a straightforward solution would be anchoring their boats away from seagrass beds or in a place where there is no seagrass,

(2) using mooring buoys instead of anchors, and (3) retrieve anchors by pulling it vertically and not dragging it across the seagrass bed. Auckland and local councils should also educate recreational boat users to take steps to mitigate the risk of accidentally spilling fuel or oil while operating their boats. If an accident has occurred, the Auckland or local Council needs to be notified immediately to take preventive action. Auckland and the local Council should have strict policies and fines for regular offenders that discharge harmful boat effluents such as used oil into the ocean. Waste from the boats should be discharged in deep waters as pumping them in shallow water would harm shellfish and recreational beach users.

Excessive sedimentation and nutrient overload are detrimental to seagrass beds, and wild oysters as excessive sediment accumulation affects their growth. Auckland Council should identify the point source of sediments (for example, from construction sites) and, where possible, advise the public to take the necessary steps to cover loose sediments or bag them to avoid run-off during heavy rain. Another solution would be planting trees or shrubs along the coastline edges to catch eroding soil and control excessive sediments entering waterways.

Other recommendations where RPAS with specialized sensors can be used for spatial assessment and for continuous monitoring could be: (1) assessing and quantifying wild oyster stock (2) detecting alive and dead oysters, (3) detect and locate predatory oyster borer snails (*Haustrum scobina*) (4) assess human impact on Meola reef (5) determine sediment levels from digital surface models (6) detecting kina barrens (sea urchins), (7) identifying and detecting non-native, brown laminarian kelp (*Undaria pinnatifida*), (8) monitoring algal boom in local estuaries and streams, (9) assessing landslides and coastal erosion, (10) evaluating coastline change detection, (11) assessing above-ground seagrass biomass and seagrass health, (12) detecting marine litter among mangroves and nearshore marine environments, (13) species-level mapping and monitoring, (14) evaluating changing morphology of estuarine mudflats, (15) assessing long-term changes in vegetation cover for major metropolitan cities in New Zealand, (16) evaluating mangrove health and changes, (17) assessing the safety of breeding and nesting grounds for shorebirds from predators.

7.15 Concluding remarks

In New Zealand, all coastal systems are currently experiencing different magnitudes of changes. These changes and processes are interrupted and exacerbated by anthropogenic-driven activities and climate change and result in negatively impacting marine ecosystems. Changes from these combined impacts in marine ecosystems are more frequent than anticipated and occur at fine spatial scales. Many of these changes go undetected and undocumented, or the authorities lack resources for consistent mapping and monitoring of these habitats because coastal systems present technical and logistical challenges regarding data capture, both remotely and *in-situ*. Therefore,

this research has combined proximal low altitude remote sensing and spatial ecology to provide a technique for consistent, low-cost spatial assessment, mapping, and monitoring of benthic nearshore marine habitats. This research attests that RPAS has outstanding potential for baseline mapping of the natural nearshore marine environments and offers flexibility for on-demand surveying and data capture. Moreover, these RPAS platforms can be integrated with bespoke sensors for advanced research. In contrast, many consumer-grade RPAS platforms are available with sensors ready to fly and create novel aerial datasets. Furthermore, geographical layers produced, such as orthomosaic and Geo-TIFFs, analysed within geospatial workflows, will increase our understanding of the spatial dynamics of benthic habitats at finer spatial resolutions and temporal scales than previously achievable with other technologies. By exploring different attributes of seagrass and wild oyster reefs, this work has demonstrated the potential of proximal low altitude RPAS remote sensing for spatial assessments and monitoring diverse landscapes in spectral and spatial domains. RPAS technology will have additional software and hardware advancements, so the implementation and applications of these techniques in coastal marine environments will progress rapidly. Besides, further notable improvements for research in nearshore marine environments will eventuate from integrated research and management programmes combined with *in-situ* and remotely sensed datasets.

Literature cited

Aasen, H., Honkavaara, E., Lucieer, A., and Zarco-Tejada, P. J. (2018). Quantitative remote sensing at ultra-high resolution with UAV spectroscopy: A review of sensor technology, measurement procedures, and data correction workflows. Remote Sensing, 10(7), 1–42. https://doi.org/10.3390/rs10071091

Abd-Elrahman, A., Pearlstine, L., and Percival, F. (2005). Development of pattern recognition algorithm for automatic bird detection from unmanned aerial vehicle imagery. Surv. Land Inf. Sci., 65, 37.

Aguirre, J.D., Bollard-Breen, B., Cameron, M., Constantine, R., Duffy, C.A.J., Dunphy, B., Hart, K., Hewitt, J.E., Jarvis, R.M., Jeffs, A., Kahui-McConnell, R., Kawharu, M., Liggins, L., Lohrer, A.M., Middleton, I., Oldman, J., Sewell, M.A., Smith, A.N.H., Thomas, D.B., Tuckey, B., Vaughan, M., and Wilson, R. (2016). Loved to Pieces: Toward the sustainable management of the Waitemata Harbour and Hauraki Gulf. Regional Studies in Marine Science 8, 220-233. https://doi.org/10.1016/j.rsma.2016.02.009

Airshare. https://www.airshare.co.nz. Accessed on 22nd March 2019.

Alderson, S.L. (1997). The analysis of ecological experiments in which overdispersion is present. Unpublished MSc. thesis, University of Auckland, Auckland, New Zealand

Amran, M. A. (2010). Estimation of seagrass coverage by depth invariant indices on Quickbird imagery. Biotropia, 17(1), 42–50. https://doi.org/10.11598/btb.2010.17.1.43

Anderson, K., and Gaston, K. J. (2013). Lightweight unmanned aerial vehicles will revolutionize spatial ecology. Front. Ecol. Environ, 11, 138–146. https://doi.org/10.1890/120150

Anderson, K., (2016). Integrating multiple scales of remote sensing measurement – from satellites to kites. Prog. Phys. Geogr. 40, 187–195. https://doi.org/10.1177/0309133316639175

Anderson, T. J., Morrison, M., MacDiarmid, A. B., Clark, M. R., Archino, R. D., Tracey, D. M., Wadhwa, S. (2019). Review of New Zealand's Key Biogenic Habitats. NIWA Client Report, (January), 190.

Andrew, M.E., and Shephard, J.M. (2017). Semi-automated detection of eagle nests: an application of very high-resolution image data and advanced image analyses to wildlife surveys. Remote Sens. Ecol. Conserv. http://dx.doi.org/10.1002/rse2.38

Arias-Oritz, A., Serrano, O., Masque, P., Lavery, P., Mueller, U., Kendirck, G.A., Rozaimi, A., Esteban, A., Fourqurean, J.W., Marba, N., Mateo, M.A., Murray, K., Rule, M.J., and Duarte, C.M., (2018). A marine heatwave drives massive losses from the world's largest seagrass carbon stocks. Nat. Clim. Change 8, 338–344. https://doi.org/10.1038/s41558-018-0096-y

Arona, L., Dale, J., Heaslip, S. G., Hammill, M. O., and Johnston, D. W. (2018). Assessing the disturbance potential of small unoccupied aircraft systems (UAS) on gray seals (*Halichoerus grypus*) at breeding colonies in Nova Scotia, Canada. PeerJ, 6, e4467. https://doi.org/10.7717/peerj.4467

Auckland 0.075m Urban Aerial Photos (2015-2016). Download from Land Information New Zealand. Accessed on 27th June 2019. https://data.linz.govt.nz/layer/88142-auckland-0075m-urban-aerial-photos-2015-2016/

Baggett, L. P., Powers, S. P., Brumbaugh, R., Coen, L. D., DeAngelis, B., Greene, J., and Morlock, S. (2014). Oyster habitat restoration monitoring and assessment handbook. The Nature Conservancy, 96pp.

Bahari, N. I. S., Ahmad, A., and Aboobaider, B. M. (2014). Application of support vector machine for classification of multispectral data. IOP Conference Series: Earth and Environmental Science, 20(1), 0–8. https://doi.org/10.1088/1755-1315/20/1/012038

Bakirman, T., and Gumusay, M.U. (2020). A novel GIS-MCDA-based spatial habitat suitability model for *Posidonia oceanica* in the Mediterranean. Environ Monit Assess 192, 231. https://doi.org/10.1007/s10661-020-8198-1

Barbier, E. B., S. D. Hacker, C. Kennedy, E. W. Koch, A. C. Stier, and B. R. Silliman. (2011). The value of estuarine and coastal ecosystem services. Ecol. Monogr. 81, 169–193. https://doi.org/10.1890/0012-9615-81.2.169

Bargain, A., Robin, M., Le Men, E., Huete, A., and Barille, L. (2012). Spectral response of the seagrass Zostera noltii with different sediment backgrounds. Aquat. Bot. 98, 45–56.

Barille, L., Robin, M., Harin, N., Bargain, A., and Launeau, P. (2010). Increase in seagrass distribution at Bourgneuf Bay (France) detected by spatial remote sensing. Aquat. Bot. 92, 185–194. https://doi.org/10.1016/j.aquabot.2009.11.006

Bauer, J. E., Wei-Jun C, Peter, A. R., Thomas S. B., Charles S. H., and Pierre A. G. R. (2013). The changing carbon cycle of the coastal ocean. Nature 504, 61–70. https://doi.org/10.1038/nature12857

Beck, M. W., Brumbaugh R. D., Airoldi, L., Carranza, A., Coen, L. D., Crawford, C., Defeo, O., Edgar, G. J., Hancock, B., Kay, M. C., Lenihan, H. S., Luckenbach, M. W., Toropova, C. L., Zhang G. F., and Guo X. M. (2011). Oyster reefs at risk and recommendations for conservation, restoration, and management. BioScience 61:107–116.

Beck, M. W., Brumbaugh, R. D., Airoldi, L., Carranza, A., Coen, L. D., Crawford, C. and Conservancy, T. N. (2009). Shellfish at risk: A global analysis of problems and pollutions. The Nature Conservancy, Arlington VA, 52. ISPRS Ann. Photogramm. Remote Sens. Spat. Inf. Sci. 2012, 4, 101–106.

Bell, S.S., and Hicks, G.R.F. (1991). Marine landscapes and faunal recruitment: a field test with seagrasses and copepods. Marine Ecology Progress Series 73: 61–68.

Belluco, E., Camuffo, M., Ferrari, S., Modenese, L., Silvestri, S., Marani, A., and Marani, M. (2006). Mapping saltmarsh vegetation by multispectral and hyperspectral remote sensing. Remote Sens. Environ. 105, 54–67. https://doi.org/10.1016/j.rse.2006.06.006

Berkenbusch, K., Rowden, A.R., and Probert, P.K. (2000). Temporal and spatial variation in macrofauna community composition imposed by ghost shrimp *Callianassa filholi* bioturbation. Marine Ecology Progress Series 192: 249–257.

Bertelli, C.M., and Unsworth, R.K.F. (2014). Protecting the hand that feeds us: seagrass (Zostera marina) serves as commercial juvenile fish habitatMar. Pollut. Bull., 83, pp. 425-429. https://doi.org/10.1016/j.marpolbul.2013.08.011

Blaschke, T. (2010). Object-Based Image Analysis for Remote Sensing. J. Photogramm. Remote Sens., 65, 2–16. https://doi.org/10.1016/j.isprsjprs.2009.06.004

Botha, E.J., Brando, V.E., Anstee, J.M., Dekker, A.G., and Sagar, S. (2013). Increased spectral resolution enhances coral detection under varying water conditions. Remote Sens. Environ. 131, 247–261. https://doi.org/10.1016/j.rse.2012.12.021

Breckenridge, R., and Dakins, M. (2011). Evaluating rangelands bare grounds using unmanned aerial vehicles: A case study. GIScience and R-Sensing, 48(1), 74-85.

Brooke, B. P., McArthur, M. A., Woodroffe, C. D., Linklater, M., Nichol, S.L., Anderson, T.J., MIeczko, R., and Sagar, S. (2012). Geomorphic features and infauna diversity of a subtropical mid-ocean carbonate shelf: Lord Howe Island, Southwest Pacific Ocean, Seafloor Geomorphology as Benthic Habitat, 375 –386. https://doi.org/10.1016/B978-0-12-385140-6.00025-6

Burkart, A., Aasen, H., Alonso, L., Menz, G., Bareth, G., and Rascher, U. (2015). Angular Dependency of Hyperspectral Measurements over Wheat Characterized by a Novel UAV Based Goniometer. Remote Sens7, 725–746. http://dx.doi.org/10.3390/rs70100725

Butchart, S.H.M., Walpole, M., Collen, B., Van-Strien, A., Scharlemann, J.P W., and Almond, R.E.A. (2010). Global Biodiversity: Indicators of Recent Declines. Science.; 328(5982):1164±8. https://doi.org/10.1126/science.1187512

Byers, J.E., Grabowski, J.H., Piehler, M.F., Hughes, R.A., Weiskel, H.W., Malek, J.C., and Kimbro, D.L. (2015). Geographic variation in intertidal oyster reef properties and the influence of tidal prism. Limnol. Oceanogr. 60, 1051–1063. http://dx.doi.org/10.1002/lno.10073

Brewin, R.J.W., de Mora, L., Jackson, T., Brewin, T.G., and Shutler, J. (2015). On the Potential of Surfers to Monitor Environmental Indicators in the Coastal Zone. PLoS One 10, e0127706. https://doi.org/10.1371/journal.pone.0127706

Bertelli, C.M., Robinson, M.T., Mendzil, A.F., Pratt, L.R., and Unsworth, R.K.F. (2018). Finding some seagrass optimism in Wales, the case of *Zostera noltii*. Mar. Pollut. Bull. 134, 216–222. https://doi.org/10.1016/j.marpolbul.2017.08.018

Calleja, F., Galvan, C., Silio-Calzada, A., Juanes, J. A., and Ondiviela, B. (2017). Long-term analysis of *Zostera noltei*: A retrospective approach for understanding seagrasses' dynamics. Marine Environmental Research, 130, 93–105. https://doi.org/10.1016/j.marenvres.2017.07.017

Candade, N. and Dixon, B. (2004). Multispectral classification of Landsat images: A comparison of support vector machine and neural network classifiers. ASPRS Annual Meeting Proc. Denver CO.

Haegele, C.W. (1975). Vegetation mapping of herring spawning grounds in British Columbia. In OCEAN 75 Conference. IEEE, 840–844.

Casella, E., Collin, A., Harris, D., Ferse, S., Bejarano, S., Parravicini, V., Hench, J.L., and Rovere, A. (2016). 493 Mapping coral reefs using consumer-grade drones and structure from motion photogrammetry 494 techniques. Coral Reefs. https://dx.doi:10.1007/s00338-016-1522-0

Casella, E., Collin, A., Harris, D., Ferse, S., Bejarano, S., Parravicini, V., and Rovere, A. (2017). Mapping coral reefs using consumer-grade drones and structure from motion photogrammetry techniques. Coral Reefs, 36(1), 269–275. http://doi.org/10.1007/s00338-016-1522-0

Castellanos-Galindo, G. A., Casella, E., Mejia-Renteria, J. C., and Rovere, A. (2019). Habitat mapping of remote coasts: Evaluating the usefulness of lightweight unmanned aerial vehicles for conservation and monitoring. Biological Conservation, 239(September). https://doi.org/10.1016/j.biocon.2019.108282

Chabot, D., Dillon, C., Shemrock, A., Weissflog, N., and Sager, E. (2018). An Object-Based Image Analysis Workflow for Monitoring Shallow-Water Aquatic Vegetation in Multispectral Drone Imagery. ISPRS International Journal of Geo-Information, 7(8), 294. https://doi.org/10.3390/ijgi7080294

Chand, S., and Bollard, B. (2022). Detecting the Spatial Variability of Seagrass Meadows and Their Consequences on Associated Macrofauna Benthic Activity Using Novel Drone Technology. Remote Sens. 2022, 14, 160. https://doi.org/10.3390/rs14010160

Chand, S., and Bollard, B. (2021). Low altitude spatial assessment and monitoring of intertidal seagrass meadows beyond the visible spectrum using a remotely piloted aircraft system. Estuarine, Coastal and Shelf Science, 255(February), 107299. https://doi.org/10.1016/j.ecss.2021.107299

Chand, S., and Bollard, B. (2021). Multispectral low altitude remote sensing of wild oyster reefs. Global Ecology and Conservation, 30(August), e01810. https://doi.org/10.1016/j.gecco.2021.e01810

Chand, S., Bollard, B. and Gillman, L. (2020). Low-cost remotely piloted aircraft system (RPAS) with multispectral sensor for mapping and classification of intertidal biogenic oyster reefs. 4(4), 148–154. https://doi.org/10.15406/aaoaj.2020.04.00116

Chayhard, S., Manthachitra, V., Naulchawee, K., and Buranapratheprat, A. (2018). Multitemporal mapping of seagrass distribution by using integrated remote sensing data in Kung Kraben Bay (KKB), Chanthaburi Province, Thailand. Int. J. Agric. Technol. 14, 161–170. http://refhub.elsevier.com/S1470-160X(20)30497-0/h0355

Chirayath, V., and Instrella, R. (2019). Fluid lensing and machine learning for centimetre-resolution airborne assessment of coral reefs in American Samoa. Remote Sensing of Environment, 235, 111475. https://doi.org/10.1016/j.rse.2019.111475

Chmura, G., Short, F., Torio, D., Arroyo-Mora, P., Fajardo, P., Hatvany, M., and van Ardenne, L. (2016). North America's Blue Carbon: Assessing Seagrass, Salt Marsh and Mangrove Distribution and Carbon Sinks. Montreal, Canada: Commission for Environmental Cooperation.

Choi, J.K., Kim, K., and Terauchi, G., (2018). Satellite-based seagrass mapping in Korean coastal waters. Proc. SPIE 10778, Remote Sensing of the Open and Coastal Ocean and Inland Waters, 107780J (15 November 2018). https://doi.org/10.1117/12.2326787.

Clements, J.C., and Chopin, T. (2017). Ocean acidification and marine aquaculture in North America: potential impacts and mitigation strategies. Reviews in Aquaculture, 9(4), 326–341. https://doi.org/10.1111/raq.12140

Colefax, A. P., Butcher, P. A., and Kelaher, B. P. (2018). The potential for unmanned aerial vehicles (RPAS) to conduct marine fauna surveys in place of manned aircraft. ICES Journal of Marine Science, 75(1), 1–8. https://doi.org/10.1093/icesjms/fsx100

Collin, A., Dubois, S., James, D., and Houet, T. (2019). Improving Intertidal Reef Mapping Using UAV Surface, Red Edge, and Near-Infrared Data. Drones, 3(3), 67. https://doi.org/10.3390/drones3030067

Collin, A., Etienne, S., and Feunteun, E. (2017). VHR coastal bathymetry using WorldView-3: colour versus learner. Remote Sens. Lett. 8, 1072–1081. https://doi.org/10.1080/2150704X.2017.1354261.

Costanza, R., de Groot, R., Sutton, P., van der Ploeg, S., Anderson, S.J., Kubiszewski, I., Farber, S., and Turner, R.K. (2014). Changes in the global value of ecosystem services. Global Environmental Change, 26: 152-158.

Cullen-Unsworth, L. C., and Unsworth, R. K. F. (2016). Strategies to enhance the resilience of the world's seagrass meadows. Journal of Applied Ecology https://10.1111/1365-2664.12637

Cullen-Unsworth, L. C., Nordlund, L. M., Paddock, J., Baker, S., McKenzie, L. J., and Unsworth, R. K. F. (2014). Seagrass meadows globally as a coupled social-ecological system: Implications for human well-being. Marine Pollution Bulletin, 83(2), 387-397. https://10.1016/j.marpolbul.2013.06.001

Cunliffe, A.M., Brazier, R.E., and Anderson, K. (2016). Ultra-fine grain landscape-scale quantification of dryland vegetation structure with drone-acquired structure-from-motion photogrammetry. Remote Sens. Environ. 2016, 183, 129–143. http://dx.doi.org/10.1016/j.rse.2016.05.019

D'Urban Jackson, T., Williams, G. J., Walker-Springett, G., and Davies, A. J. (2020). Three-dimensional digital mapping of ecosystems: A new era in spatial ecology. Proceedings of the Royal Society B: Biological Sciences, 287(1920), 1–10. https://doi.org/10.1098/rspb.2019.2383

Dash, J. P., Watt, M.S., Pearse, G.D., Heaphy, M. and Dungey, H.S. (2017). Assessing very high-resolution UAV imagery for monitoring forest health during a simulated disease outbreak. ISPRS J. Photogramm. Remote Sens, 131, 1–14. http://dx.doi.org/10.1016/j.isprsjprs.2017.07.007

Davies, K., Fisher, K., Foley, M., Greenaway, A., Hewitt, J., Le-Heron, R., and Lundquist, C. (2018). Navigating collaborative networks and cumulative effects for Sustainable Seas. Environmental Science and Policy, 83, 22–32. https://doi.org/10.1016/j.envsci.2018.01.013

Dawson, S. M., Bowman, M. H., Leunissen, E., and Sirguey, P. (2018). Corrigendum: Inexpensive Aerial Photogrammetry for Studies of Whales and Large Marine Animals. Frontiers in Marine Science, 5(November), 1–7. https://doi.org/10.3389/fmars.2018.00438

Dekker, A., Brando, V., Antsee, J., Fyfe, S., Malthus, T., and Karpouzli, A. (2007). Remote Sensing of Seagrass Ecosystems: Use of Spaceborne and Airborne Sensors. In: Larkum, T., Orth, R.J., Duarte, C.M. (Eds.), Seagrasses: Biology, Ecology and Conservation. Springer, Netherlands. http://refhub.elsevier.com/S1470-160X(20)30497-0/h0500

Dennison, W. C., Orth, R. J., Moore, K. A., Stevenson, J. C., Carter, V., Kollar, S., and Batiuk, R. A. (1993). Assessing Water Quality with Submersed Aquatic Vegetation Habitat requirements as barometers of Chesapeake Bay health. Retrieved from https://academic.oup.com/bioscience/article/43/2/86/239768

Department of Conservation (DOC). (2010). New Zealand Coastal Policy Statement. Department of Conservation, Wellington.

de Lange, P.J., Rolfe, J.R., Barkla, J.W., Courtney, S.P., Champion, P.D., Perrie, L.R., 607 Beadel, S.M., Ford, K.A., Breitwieser, I., Schönberger, I., Hindmarsh-Walls, R., Heenan, 608 P.B., and Ladley, K. (2017). Conservation status of New Zealand indigenous vascular 609 plants, 2017. New Zealand Threat Classification Series 22. 82 pp.

Dai, W., Li, H., Zhou, Z., Cybele, S., Lu, C., Zhao, K., Zhang, X., Yang, H., and Li, D. (2018). UAV Photogrammetry for Elevation Monitoring of Intertidal Mudflats. Journal of Coastal Research, 85(85), 236–240. https://doi.org/10.2112/SI85-048.1

Dominguez-Tejo, E., Metternicht, G., Johnston, E., and Hedge, L. (2016). Marine Spatial Planning advancing the Ecosystem-Based Approach to coastal zone management: A review. Marine Policy, 72, 115–130. https://doi.org/10.1016/j.marpol.2016.06.023

Dos-Santos, V. M., and Matheson, F. E. (2017). Higher seagrass cover and biomass increases sexual reproductive effort: A rare case study of *Zostera muelleri* in New Zealand. Aquatic Botany, 138, 29–36. https://doi.org/10.1016/j.aquabot.2016.12.003

Doukari, M., Batsaris, M., Papakonstantinou, A., and Topouzelis, K. (2019). A protocol for aerial survey in coastal areas using UAS. Remote Sensing, 11(16). https://doi.org/10.3390/rs11161913

Dronova, I. (2015). Object-based image analysis in wetland research: A review. Remote Sensing, 7(5), 6380–6413. https://doi.org/10.3390/rs70506380

Duarte, C.M., Losada, I.J., Hendriks, I.E., Mazarrasa, I., and Marba, N. (2013). The role of coastal plant communities for climate change mitigation and adaptation. Nat. Clim. Chang. 3, 961–968. https://doi.org/10.1038/nclimate1970

Duarte, C.M. (2002). The future of seagrass meadows. Environ. Conserv. 29, 192e206. http://refhub.elsevier.com/S0272-7714(15)30041-X/sref24

Dudley, B., Zeldis, J.R., and Burge, O. (2017). New Zealand Coastal Water Quality Assessment. NIWA Client Report no. 2016093CH. Prepared for the Ministry for the Environment. Christchurch, New Zealand. Retrieved from:https://www.mfe.govt.nz/publications/environmental-reporting/new-zealand-coastal-water-quality-assessment

Duffy, J. E., Benedetti-Cecchi, L., Trinanes, J., Muller-Karger, F. E., Ambo-Rappe, R., Bostrom, C., and Yaakub, S. M. (2019). Toward a coordinated global observing system for seagrasses and marine macroalgae. Frontiers in Marine Science, 6(JUL). https://doi.org/10.3389/fmars.2019.00317

Duffy, J. E., Reynolds, P. L., Bostrom, C., Coyer, J. A., Cusson, M., Donadi, S., and Stachowicz, J. J. (2015). Biodiversity mediates top-down control in eelgrass ecosystems: A global comparative-experimental approach. Ecology Letters, 18(7), 696–705. https://doi.org/10.1111/ele.12448

Duffy, J. P., Cunliffe, A. M., DeBell, L., Sandbrook, C., Wich, S. A., Shutler, J. D., Myers-Smith, I. H., Varela, M. R., and Anderson, K. (2018). Location, location, location: considerations when using lightweight drones in challenging environments. Remote Sensing in Ecology and Conservation, 4(1), 7–19. https://doi.org/10.1002/rse2.58

Duffy, J. P., Pratt, L., Anderson, K., L., and Shutler, J. D. (2018). Spatial assessment of intertidal seagrass meadows using optical imaging systems and a lightweight drone. Estuarine, Coastal and Shelf Science, 200, 169–180. https://doi.org/10.1016/j.ecss.2017.11.001

Duffy, J., Anderson, K., Shapiro, A., and Avino, F. S. (2020). Drone Technologies for Conservation. WWF Conservation Technology Series, 1(5).

Dunn, F. E., Nicholls, R. J., Darby, S. E., Cohen, S., Zarfl, C., and Fekete, B. M. (2018). Projections of historical and 21st century fluvial sediment delivery to the Ganges-Brahmaputra-Meghna, Mahanadi, and Volta deltas. Science of the Total Environment, 642, 105–116. https://doi.org/10.1016/j.scitotenv.2018.06.006

Durban, J. W., Fearnbach, H., Barrett-Lennard, L. G., Perryman, W. L., and Leroi, D. J. (2015). Photogrammetry of killer whales using a small hexacopter launched at sea. Journal of Unmanned Vehicle Systems, 3, 131–135. https://doi.org/10.1139/juvs-2015-0020

ENVI Zoom Tutorial: ENVI Feature Extraction with Rule-Based Classification. (n.d). Retrieved from http://read.pudn.com/downloads166/ebook/758099/Feature_Extraction_RuleBased.pdf

Espriella, M. C., Lecours, V., Frederick, P. C., Camp, E. V., and Wilkinson, B. (2020). Quantifying intertidal habitat relative coverage in a Florida estuary using UAS imagery and GEOBIA. Remote Sensing, 12(4). https://doi.org/10.3390/rs12040677

Environment Systems Research Institute (ESRI). (2019). The Image Classification Wizard. Accessed from https://pro.arcgis.com/en/pro-app/help/analysis/image-analyst/the-image-classification-wizard.htm

Environment Systems Research Institute (ESRI). Accuracy Assessment for Image Classification. (2019). Retrieved from https://desktop.arcgis.com/en/arcmap/latest/manage-data/raster-and-images/accuracy-assessment-for-image-classification.htm

Fallati, L., Saponari, L., Savini, A., Marchese, F., Corselli, C., and Galli, P. (2020). Multi-Temporal UAV Data and Object-Based Image Analysis (OBIA) for Estimation of Substrate Changes in a Post-Bleaching Scenario on a Maldivian Reef. https://doi.org/10.3390/rs12132093

Fairley, I., Mendzil, A., Togneri, M., and Reeve, D. E. (2018). The use of unmanned aerial systems to map intertidal sediment. Remote Sensing, 10(12). https://doi.org/10.3390/rs10121918

Ferguson, L.R., and Korfmacher, K. (1997). Remote sensing and GIS analysis of seagrass meadows in North Carolina, USA. Aquatic Botany 58, 3-4 (1997), 241–258. https://doi.org/10.1016/S0304-3770(97)00038-7

Ferguson, M., Angliss, R. P., Kennedy, A., Lynch, B., Willoughby, A., Helker, V. T., Brower, A. A., and Clarke, J. T. (2018). Performance of manned and unmanned aerial surveys to collect visual data and imagery for estimating arctic cetacean density and associated uncertainty. Journal of Unmanned Vehicle Systems, 154(May), juvs-2018-0002. https://doi.org/10.1139/juvs-2018-0002

Fiori, L., Martinez, E., Orams, M. B., and Bollard, B. (2020). Using Unmanned Aerial Vehicles (UAVs) to assess humpback whale behavioural responses to swim-with interactions in Vava'u, Kingdom of Tonga. Journal of Sustainable Tourism. **Error! Hyperlink reference not valid.**

Foley, M. M., and Shears, N. T. (2019). Te Tokaroa Meola Reef intertidal reef ecological monitoring programmes: 2001 to 2017. Auckland Council technical report, TR2019/004. Downloaded from http://www.knowledgeauckland.org.nz/publication/?mid=2817andDocumentType=1and (assessed on 3 September 2019).

Foody, G. M. (2002). Status of land cover classification accuracy assessment. Remote Sensing of Environment, 80(1), 185–201. https://doi.org/10.1016/S0034-4257(01)00295-4

Foody., G. M. and Mathur, A. (2004). A relative evaluation of multiclass image classification by support vector machines. IEEE Transactions on Geoscience and Remote Sensing, 42 (6), 1335–134

Ford, R., and M. D. M. Pawley. (2008). Meola Reef Ecological Monitoring: 2001 to 2008. Prepared by Auckland Uni-Services for Auckland Regional Council. Auckland Regional Council Technical Report 2009/020.

Fourqurean, J.W., Duarte, C.M., Kennedy, H., Marba, N., Holmer, M., Mateo, M.A., Apostolaki, E.T., Kendrick, G.A., Krause-Jensen, D., McGlathery, K.J. and Serrano, O. (2012). Seagrass ecosystems as globally significant carbon stock. Nat. Geosci. 5, 505–509. https://doi.org/10.1038/ngeo1477.

Frolicher, T., Fischer, E., and Grube, R. N. (2018). Marine heatwaves under global warming. Nature, 560(7718), 360–364. https://doi.org/10.1038/s41586-018-0383-9

Garner, K.L., Chang, M.Y., Fulda, M.T., Berlin, J.A., Freed, R.E., Soo-Hoo, M.M., Revell, D.nL., Ikegami, M., Flint, L.E., Flint, A.L., and Kendall, B.E. (2015). Impacts of sea-level rise and climate change on coastal plant species in the central California coast. Peer J 3(e958). https://doi.org/10.7717/peerj

Garrett, B., and Anderson, K. (2018). Drone methodologies: Taking flight in human and physical geography. Transactions of the Institute of British Geographers, 43, 341–3590.

Garvis, S. K., Sacks, P. E., and Walters, L. J. (2015). Formation, Movement, and Restoration of Dead Intertidal Oyster Reefs in Canaveral National Seashore and Mosquito Lagoon, Florida. Journal of Shellfish Research, 34(2), 251–258. https://doi.org/10.2983/035.034.0206

Gaw, S., Thomas, K.V., and Hutchinson, T.H. (2014). Sources, impacts, and trends of pharmaceuticals in the marine and coastal environment. Philosophical Transactions of the Royal Society B, 369. https://doi.org/10.1098/rstb.2013.0572

Gray, P. C., Bierlich, K. C., Mantell, S. A., Friedlaender, A. S., Goldbogen, J. A., and Johnston, D. W. (2019). Drones and convolutional neural networks facilitate automated and accurate cetacean species identification and photogrammetry. Methods in Ecology and Evolution, 10(9), 1490–1500. https://doi.org/10.1111/2041-210X.13246

Geange, S., Townsend, M., Clark, D., Ellis, J.I., and Lohrer, A.M. (2019). Communicating the value of marine conservation using an ecosystem service matrix approach. Ecosystem Services, 35, 150–163. https://doi.org/10.1016/j.ecoser.2018.12.004

Giones, F., and Brem, A. (2017). From toys to tools: The co-evolution of technological and entrepreneurial developments in the drone industry. Business Horizons, 60, 875–884.

Girouard, G., Bannari, A. E. l., Harti, A., and Desrochers, A. (2004). Validated spectral angle mapper algorithm for geological mapping: comparative study between Quick-Bird and Landsat-TM. In: XXth ISPRS Congress, Geo-imagery Bridging Continents, Istanbul, Turkey, pp. 12e23. http://refhub.elsevier.com/S0272-7714(16)30039-7/sref24

Gitelson, A., and Merzlyak, M. (1998). Remote Sensing of Chlorophyll Concentration in Higher Plant Leaves. Advances in Space Research 22, 689-692

Gitelson, A.A., Kaufman, Y.J., Stark, R., and Rundquist, D. (2002). Novel algorithms for remote estimation of vegetation fraction. Remote Sens. Environ. 80, 76–87. http://dx.doi.org/10.1016/S0034-4257(01)00289-9

Gomes, I., Peteiro, L., Bueno-Pardo, J., Albuquerque, R., Perez-Jorge, S., Oliveira, E. R., and Queiroga, H. (2018). What's a picture really worth? On the use of drone aerial imagery to estimate intertidal rocky shore mussel demographic parameters. Estuarine, Coastal and Shelf Science, 213(August), 185–198. https://doi.org/10.1016/j.ecss.2018.08.020

Grabowski, J. H., R. D. Brumbaugh, R. F. Conrad, A. G. Keeler, J. J. Opaluch, and C. H. Peterson. (2012). Economic valuation of ecosystem services provided by oyster reefs. Bioscience 62, 900-909. https://doi.org/10.1525/bio.2012.62.10.10

Greatwood, C., Richardson, T. S., Freer, J., Thomas, R. M., Rob Mackenzie, A., Brownlow, R., Lowry, D., Fisher, R. E., and Nisbet, E. G. (2017). Atmospheric sampling on Ascension Island using multirotor UAVs. Sensors (Switzerland), 17(6), 1–24. https://doi.org/10.3390/s17061189

Grech, A., Chartrand-Miller, K., Erftemeijer, P., Fonseca, M., McKenzie, L., Rasheed, M., and Coles, R. (2012). A comparison of threats, vulnerabilities, and management approaches in global seagrass bioregions. Environmental Research Letters 7(2): 024006.

Green, E.P., and Short, F.T (Eds.). (2003). World Atlas of Seagrasses. University of California Press, Berkeley, USA. 324 pp.

Green, M., Timperley, M., Collins, R., Senior, A., Adams, R., and Swales, A. (2004). Prediction of contaminant accumulation in the Waitemata Harbour. NIWA Client Report: HAM2003-087/1. Report prepared by NIWA for Auckland Council.

Gregory, K.B., Winn, W., Johnson, K., and Rosekind, M.R. (2010). Pilot fatigue survey: Exploring fatigue factors in air medical operations. Air Med. J. 29, 309–319.

Griffen, B.D., Belgrad, B.A., Cannizzo, Z.J., Knotts, E.R. and Hancock, E.R. (2016). Rethinking Our Approach to Multiple Stressor Studies in Marine Environments. Marine Ecology Progress Series, 543, 273-281. https://doi.org/10.3354/meps11595

Grizzle, R. E., Adams, J. R., and Walters, L. J. (2002). Historical changes in intertidal oyster (*Crassostrea virginica*) reefs in a Florida lagoon potentially related to boating activities. Journal of Shellfish Research, 21(2), 749–756.

Grizzle, R., Ward, K., Geselbracht, L., and Birch, A. (2018). Distribution and condition of intertidal eastern oyster (*Crassostrea virginica*) reefs in Apalachicola Bay Florida based on high-resolution satellite imagery. J. Shellfish Res. 2018, 37, 1–12. http://dx.doi.org/10.2983/035.037.0514

Grizzle, R.E. (2002). Distribution and abundance of (Crassostrea virginica) (Gmelin,1791) (*Eastern oyster*) and (Mercenaria *spp. (Quahogs*) in a coastal lagoon. Journal of Shellfish Research 9,347-358.

Gunderson, A.R., Armstrong, E.J. and Stillman, J.H. (2016) Multiple Stressors in a Changing World: The Need for an Improved Perspective on Physiological Responses to the Dynamic Marine Environment. Annual Review of Marine Science, 8, 357-378. https://doi.org/10.1146/annurev-marine-122414-033953

Gattuso, J.P., Magnan, A., Bille, R., Cheung, W.W.L., Howes, E.L., Joos, F., Allemand, D., Bopp, L., Cooley, S.R., Eakin, C.M., Hoegh-Guldberg, O., Kelly, R.P., Portner, H.-O., Rogers, A.D., Baxter, J.M., Laffoley, D., Osborn, D., Rankovic, A., Rochette, J., Sumaila, U.R., Treyer, S., and Turley, C. (2015). Oceanography. Contrasting futures for ocean and society from different anthropogenic 7 CO_2 emissions scenarios. Science, 349 (6243), aac4722-aac4722, https://doi.org/10.1126/science.aac4722.

Ha, N.-T., Manley-Harris, M., Pham, T.-D., and Hawes, I. (2021) Detecting Multi-Decadal Changes in Seagrass Cover in Tauranga Harbour, New Zealand, Using Landsat Imagery and Boosting Ensemble Classification Techniques. ISPRS Int. J. Geo-Inf. 10, 371. https://doi.org/10.3390/ijgi10060371

Halpern, B.S., Frazier, M., Afflerbach, J., Lowndes, J.S., Micheli, F., and O'Hara, C. (2019) Recent Pace of Change in Human Impact on the World's Oceans. Science Reports, 9, Article No. 11609. https://doi.org/10.1038/s41598-019-47201-9

Halpern, B.S., Walbridge, S., Selkoe, K.A., Kappel, C.V., Micheli F, and D'agrosa C. (2008). A global map of human impact on marine ecosystem Science. 319(5865):948±52. https://doi.org/10.1126/science.1149345

Handley, L., Altsman, D., and DeMay, R., eds. (2007). Seagrass Status and Trends in the Northern Gulf of Mexico: 1940-2002: U.S. Geological Survey Scientific Investigations Report 2006-5287 and U.S. Environmental Protection Agency 855-R-04-003, 267 p.

Hanlon, D. (2019). Appendix 1. Upon a Stone Altar, 211–211. https://doi.org/10.2307/j.ctvp2n4g9.16

Harris Geospatial Solutions, I. (2018). Image Processing in IDL. IDL Version 6.2, (July), 293.

Retrieved from https://www.harrisgeospatial.com/docs/pdf/image.pdf

Harwin, S., Lucieer, A., and Osborn, J (2015). The Impact of the Calibration Method on the Accuracy of Point Clouds Derived Using Unmanned Aerial Vehicle Multi-View Stereopsis. Remote Sens. 7, 11933–11953. http://dx.doi.org/10.3390/rs70911933

Hassanalian, M., and Abdelkefi, A. (2017). Classifications, applications, and design challenges of drones: A review. Progress in Aerospace Sciences, 91(April), 99–131. https://doi.org/10.1016/j.paerosci.2017.04.003

Hayward, B.W., (1997). Introduced marine organisms in New Zealand and their impact in the Waitemata Harbor, Auckland. Tane 36, 197-223.

Hayward, B.W., Grenfell, H.R., Reid, C., and Hayward, K.A. (1999). Recent New Zealand shallow water benthic foraminifera - taxonomy, ecologic distribution, biogeography and use in paleoenvironmental assessment. Institute of Geological and Nuclear Sciences Monograph 21.

Hayward, B.W., Stephenson, A.B., Morley, M., Riley, J.L., and Grenfell, H.R. (1997). Faunal changes in Waitemata Harbour sediments, 1930s-1990s. Journal of the Royal Society of New Zealand 27, 1-20.

Hedley, J., Russell, B., Randolph, K., and Dierssen, H. (2016). A physics-based method for the remote sensing of seagrasses. Remote Sens. Environ. 174, 134–147. http://dx.doi.org/10.3390/rs8020118.

Hedley, J.D., Roelfsema, C., Koetz, B., and Phinn, S. (2012). Capability of the Sentinel 2 mission for tropical coral reef mapping and coral bleaching detection. Remote Sens. Environ. 120, 145–155. http://dx.doi.org/10.1016/j.rse.2011.06.028

Hedley, J.D., Roelfsema, C.M., Chollett, I., Harborne, A.R., Heron, S.F., Weeks, S.J., Skirving, W.J., Strong, A.E., Mark Eakin, C., Christensen, T.R.L., Ticzon, V., Bejarano, S., and Mumby, P.J. (2016). Remote sensing of coral reefs for monitoring and management: a review. Remote Sens. 8. https://doi.org/10.3390/rs8020118

Hensel, E., Wenclawski, S., and Layman, C. (2018). Using a small, consumer-grade drone to identify and count marine megafauna in shallow habitats. Latin American Journal of Aquatic Research, 46(5), 1025–1033. https://doi.org/10.3856/vol46-issue5-fulltext-15

Hicks, G.R.F. (1986). Distribution and abundance of meiofaunal copepods inside and outside seagrass beds. Marine Ecology Progress Series 31: 159–170.

Hicks, G.R.F. (1989). Does epibenthic structure negatively affect meiofauna? Journal of Experimental Marine Biology and Ecology 133: 39–55.

Hisabayashi, M., Rogan, J., and Elmes, A. (2018). Quantifying shorelines change in Funafuti Atoll, Tuvalu using a time series of Quickbird, Worldview and Landsat data. GIScience and Remote Sensing 55, 307–330. https://doi.org/10.1080/15481603.

Hobley, B., Arosio, R., French, G.; Bremner, J., Dolphin, T., and Mackiewicz, M. (2021). Semi-Supervised Segmentation for Coastal Monitoring Seagrass Using RPA Imagery. Remote Sens. 13, 1741. https://doi.org/10.3390/rs13091741

Hodgson, A. J., Noad, M., Marsh, H., Lanyon, J., and Kniest, E. (2010). Using unmanned aerial vehicles for surveys of marine mammals in Australia: test of concept. Report to Australian Marine Mammal Centre, November 2014. https://www.researchgate.net/publication/267827643

Hodgson, A., Kelly, N., and Peel, D. (2013). Unmanned aerial vehicles (UAVs) for surveying Marine Fauna: A 520 dugong case study. PLoS One 8, e79556. https://doi:10.1371/journal.pone.0079556

Horning, N. (2004). Land cover classification methods, Version 1.0. American Museum of Natural History, Centre for Biodiversity and Conservation.

Hossain, M. S., Bujang, J. S., Zakaria, M. H., and Hashim, M. (2015a). Application of Landsat images to seagrass areal cover change analysis for Lawas, Terengganu and Kelantan of Malaysia. Continental Shelf Research, 110, 124-148. https://doi.org/10.1016/j.csr.2015.10.009

Hossain, M.S., Bujang, J.S., Zakaria, M.H., and Hashim, M. (2015b). Application of Landsat images to seagrass areal cover change analysis for Lawas, Terengganu and Kelantan 647 of Malaysia. Cont. Shelf Res. 110, 124–148. https://doi.org/10.1016/j.csr.2015.10.009

Huete, A., Didan., K, Mirua., T, Rodriguez, E.P, Gao., X, and Ferreira., L.G. (2002). Overview of the Radiometric and Biophysical Performance of the MODIS Vegetation Indices. Remote Sensing of Environment 83, 195–213.

Hughes, T. P., Kerry, J. T., Alvarez-Noriega, M., Alvarez-Romero, J. G., Anderson, K. D., Baird, A. H., and Wilson, S. K. (2017). Global warming and recurrent mass bleaching of corals. Nature, 543(7645), 373–377. https://dx.doi.org/10.1038/nature21707

Hughes, A. R., Williams, S. L., Duarte, C. M., Heck, K. L., and Waycott, M. (2009). Associations of concern: declining seagrasses and threatened dependent species. Front. Ecol. Environ. 7, 242–246. https://doi.org/10.1890/080041

Hulet, A., Roundy, B.A., Petersen, S.L., Jensen, R.R., Bunting, S.C. (2014). Cover estimations using object-based image analysis rule sets developed across multiple scales in pinyon-juniper woodlands. Rangel. Ecol. Manag. 67, 318-327. http://dx.doi.org/10.2111/REM-D-12-00154.1

Hume, T.M., Snelder, T., Weatherhead, M. and Liefting, R. (2007). A controlling factor approach to estuary classification. Ocean and Coastal Management, 50, 905–929. https://doi.org/10.1016/j.ocecoaman.2007.05.009

Hunt, B., Schaub, J., Holmes, K., Quayle, L., Lu, Y., and Pakhomov, E. (2017). Using unmanned aerial vehicles (UAVs) to measure jellyfish aggregations. Marine Ecology Progress Series, 591(January), 29–36. https://doi.org/10.3354/meps12414

Hyder, K., Town hill, B., Anderson, L. G., Delany, J., and Pinnegar, J. K. (2015). Can citizen science contribute to the evidence-base that underpins marine policy? Marine Policy, 59, 112–120. https://doi.org/10.1016/j.marpol.2015.04.022

Inglis, G.J. (2003). The seagrasses of New Zealand. Pp. 148–157 in Green, E.P.; Short, F.T. (Eds): World atlas of seagrasses. University of California Press, Berkeley, California.

IPCC (Intergovernmental Panel on Climate Change) (2014). Climate Change Synthesis Report. Contribution of Working Groups I, II, and III to the Fifth Assessment Report of the Intergovernmental Panel on Climate Change. IPCC, Geneva, Switzerland.

Jarvis, R. M., Breen, B. B., Krageloh, C. U., and Billington, D. R. (2015). Citizen science and the power of public participation in marine spatial planning. Marine Policy, 57, 21–26. https://doi.org/10.1016/j.marpol.2015.03.011

Jakob, S., Zimmermann, R., and Gloaguen, R. (2017). The Need for Accurate Geometric and Radiometric Corrections of Drone-Borne Hyperspectral Data for Mineral Exploration:

MEPHySTo—A Toolbox for Pre-Processing Drone-Borne Hyperspectral Data. Remote Sens. 9, 88. http://dx.doi.org/10.3390/rs9010088

Jaud, M., Ammann, J., Verney, R., Le Dantec, N., Deloffre, J., Grasso, F., Delacourt, C., and Grandjean, P. (2016). Potential of UAVs for Monitoring Mudflat Morpho dynamics (Application to the Seine Estuary, France). ISPRS International Journal of Geo-Information, 5(4), 50. https://doi.org/10.3390/ijgi5040050

Johnston, D. W. (2019). Unoccupied Aircraft Systems in Marine Science and Conservation. Annual Review of Marine Science, 11(1), annurev-marine-010318-095323. https://doi.org/10.1146/annurev-marine-010318-095323

Joyce, K.E., Duce, S., Leahy, S.M., Leon, J., and Maier, S.W. (2018). Principles and practice of acquiring drone-based image data in marine environments. Mar. Freshw. Res. 70, 952. https://www.publish.csiro.au/mf/MF17380

Joyce, K.E., Duce, S., Leahy, S.M., Leon, J., and Maier, S.W. (2019). Principles and practice of acquiring drone-based image data in marine environments. Mar. Freshw. Res. 70, 952. http://doi.org/10.1071/MF17380

Kiszka, J. J., Mourier, J., Gastrich, K., and Heithaus, M. R. (2016). Using unmanned aerial vehicles (UAVs) to investigate shark and ray densities in a shallow coral lagoon. Marine Ecology Progress Series, 560, 237–242. https://doi.org/10.3354/meps11945

Kalacska, M., Arroyo-Mora, J., Sousa, L., Vieira, T., and Lucanus, O. (2019). RPAS-Based 3D Point Clouds of Freshwater Fish Habitats, Xingu River Basin, Brazil. Data, 4(1), 9. https://doi.org/10.3390/data4010009

Kater, B. J., and Baars, J. M. D. D. (2004). The potential of aerial photography for estimating surface areas of intertidal Pacific oyster beds (*Crassostrea gigas*). Journal of Shellfish Research, 23(3), 773+. https://www.scopus.com/inward/record.url?eid=2-s2.0-13544273981andpartnerID=10andrel=R3.0.0

Kay, S., Hedley, J.D., and Lavender, S. (2009). Sun Glint Correction of High and Low Spatial Resolution Images 538 of Aquatic Scenes: A Review of Methods for Visible and Near-Infrared Wavelengths. Remote Sens. 1, 539 697–730. https://doi.org/10.3390/rs1040697

Kellogg, M. L., Smyth A. R., Luckenbach, M. W., Carmichael, R. H., Brown, B. L., and Cornwell, J. C. (2014). Use of oysters to mitigate eutrophication in coastal waters. Estuarine, Coastal and Shelf Science 151, 156-168.

Kelly, S. (2009). Kaipara Harbour oyster reserves. Final research report for Ministry of Fisheries project OYS2008/02 March 2009. 31 p. (Unpublished report held by Ministry for Primary Industries, Wellington.)

Kelcey, J., and Lucieer, A. (2012). Sensor Correction of a 6-Band Multispectral Imaging Sensor for UAV Remote Sensing. Remote Sens, 4, 1462–1493. http://dx.doi.org/10.3390/rs4051462

Kettles, H., and Bell, R. (2016): Estuarine ecosyste Pages 24-30. In: Robertson, H., Bowie, S., White, R., Death, R., Collins, D. (Eds). Freshwater conservation under a changing climate. Proceedings of a workshop hosted by the Department of Conservation, 10-11 December 2013, Wellington. Department of Conservation, Christchurch. 86 pp.

Klemas V.V. (2016) Remote Sensing of Submerged Aquatic Vegetation. In: Finkl C., Makowski C. (eds) Seafloor Mapping along Continental Shelves. Coastal Research Library, vol 13. Springer, Cham. https://doi.org/10.1007/978-3-319-25121-9_5

Koch, M., Bowes, G., Ross, C., and Zhang, X.-H. (2013). Climate change and ocean acidification effects on seagrasses and marine macroalgae. Glob. Chang. Biol. 19, 103–132.

Koedsin, W., Intararuang, W., Ritchie, R. J., and Huete, A. (2016). An integrated field and remote sensing method for mapping seagrass species, cover, and biomass in Southern Thailand. Remote Sensing, 8(4). https://doi.org/10.3390/rs8040292

Konar, B., and Iken, K. (2018). The use of unmanned aerial vehicle imagery in intertidal monitoring. Deep-Sea Research Part II: Topical Studies in Oceanography, 147(April 2017), 79–86. https://doi.org/10.1016/j.dsr2.2017.04.010

Koss, R. S., and Kingsley, J. Y. (2010). Volunteer health and emotional wellbeing in marine protected areas. Ocean and Coastal Management, 53(8), 447–453. https://doi.org/10.1016/j.ocecoaman.2010.06.002

Kovacs, E., Roelfsema, C., Lyons, M., Zhao, S., and Phinn, S. (2018). Seagrass habitat mapping: how do Landsat 8 OLI, Sentinel-2, ZY-3A, and Worldview-3 perform? Remote Sensing Letters, 9(7), 686-695. https://doi.10.1080/2150704X.2018.1468101

Kromkamp, J.C., Morris, E.P., Forster, R.M., Honeywill, C., Hagerthey, S., and Paterson, D.M. (2006). Relationship of intertidal surface sediment chlorophyll concentration to hyperspectral reflectance and chlorophyll fluorescence. Estuar. Coasts 29, 183–196.

Kreij, A., Scriffignano, J., Rosendahl, D., Nagel, T., and Ulm, S. (2018). Aboriginal stone-walled intertidal fishtrap morphology, function and chronology investigated with high-resolution close-range Unmanned Aerial Vehicle photogrammetry. Journal of Archaeological Science, 96(July), 148–161. https://doi.org/10.1016/j.jas.2018.05.012

Krumhansl, K.A., Okamoto, D.K., Rassweiler, A., Novak, M., Bolton, J.J., Cavanaugh, K.C., Connell, S.D., Johnson, C.R., Konar, B., and Ling, S.D. (2016). Global patterns of kelp forest change over the past half-century. Proc. Natl. Acad. Sci. USA 113, 13785–13790 http://dx.doi.org/10.1073/pnas.1606102113

Laba, M., Blair, B., Downs, R., Monger, B., Philpot, W., Smith, S., Sullivan, P., and Baveye, P.C. (2010). Use of textural measurements to map invasive wetland plants in the Hudson River National Estuarine Research Reserve with IKONOS satellite imagery. Remote Sens. Environ. 114, 876–886. http://dx.doi.org/10.1016/j.rse.2009.12.002

Laliberte, A.S., Goforth, M.A., Steele, C.M., and Rango, A. (2011). Multispectral Remote Sensing from Unmanned Aircraft: Image Processing Workflows and Applications for Rangeland Environments. Remote Sens. 3, 2529–255. http://dx.doi.org/10.3390/rs3112529

Lamb, J.B., Van De Water, J.A.J.M., Bourne, D.G., Altier, C., Hein, M.Y., Fiorenza, E.A., Abu, N., Jompa, J., and Harvell, J. (2017). Seagrass ecosystems reduce exposure to bacterial pathogens of humans, fishes, and invertebrates Science, 355 (80), pp. 731-733. https://doi.org/10.1126/science.aal1956

Land Information New Zealand (LINZ). Accessed on November 1, 2020, from https://www.linz.govt.nz/

Le Bris, A., Rosa, P., Lerouxel, A., Cognie, B., Gernez, P., Launeau, P., Robin, M., and Barille, L. (2016). Hyperspectral remote sensing of wild oyster reefs. Estuarine, Coastal and Shelf Science, 172, 1–12. https://doi.org/10.1016/j.ecss.2016.01.039

Lebourgeois, V., Begue, A., Labbe, S., Mallavan, B., Prevot, L., and Roux B. (2008). Can commercial 247 digital cameras be used as multispectral sensors? A crop monitoring test. Sensors. 248 8(11):7300-7322

Lechner, A.M., Fletcher, A., Johansen, K., and Erskine, P. (2012). Characterizing Upland Swamps Using Object-Based Classification Methods and Hyper-Spatial Resolution Imagery Derived from an Unmanned Aerial Vehicle. ISPRS Ann. Photogramm. Remote Sens. Spat. Inf. Sci. 2012, 4, 101-106. http://dx.doi.org/10.5194/isprsannals-I-4-101-2012.

Lefcheck, J. S., B. B. Hughes, A. J. Johnson, B. W. Pfirrman, D. B. Rasher, and A. R. Smyth. (2019). Are coastal habitats important nurseries? A meta-analysis. Conserv. Lett. e12645, https://doi.org/10.1111/conl.12645

Lehmann, J. R. K., Prinz, T., Ziller, S. R., Thiele, J., Heringer, G., Meira-Neto, J. A. A., and Buttschardt, T. K. (2017). Open-Source Processing and Analysis of Aerial Imagery Acquired with a Low-Cost Unmanned Aerial System to Support Invasive Plant Management. Frontiers in Environmental Science, 5(July), 1–16. https://doi.org/10.3389/fenvs.2017.00044

Levy, J., Hunter, C., Lukacazyk, T., and Franklin, E. C. (2018). Assessing the spatial distribution of coral bleaching using small-unmanned aerial syste Coral Reefs 37, 373–87. https://doi.org/10.1007/s00338-018-1662-5

LINZ, (2019). NZ Coastlines. Retrieved from https://data.linz.govt.nz/layer/50258-nz-coastlines-topo-150k/

Lin, H., Sun, T., Zhou, Y., Gu, R., Zhang, X., and Yang, W. (2018). Which genes in a typical intertidal Seagrass (Zostera japonica) indicate pollution? Front. Plant Sci. 9. 664 https://doi.org/10.3389/fpls.2018.01545

Lobell, D., and Asner, G. (2003). Hyperion Studies of Crop Stress in Mexico." Proceedings of the 12th Annual JPL Airborne Earth Science Workshop, Pasadena, CA

Lomax, A.S., Corso, W., and Etro, J.F. (2005). Employing unmanned aerial vehicles (UAVs) as an element of the integrated ocean observing system. In Proceedings of OCEANS 2005 MTS/IEEE, pp. 184–90. New York: IEEE. https://doi: 10.1109/oceans.2005.1639759.

Lopez, J. J., and Mulero-Pazmany, M. (2019). Drones for conservation in protected areas: Present and future. Drones, 3(1), 1–23. https://doi.org/10.3390/drones3010010

Lu, B. and He, Y. (2017). Species classification using Unmanned Aerial Vehicle (UAV)-acquired high spatial resolution imagery in a heterogeneous grassland. ISPRS J. Photogramm. 128, 73–85. http://dx.doi.org/10.1016/j.isprsjprs.2017.03.011

Lucieer, A., Malenovsky, Z., Veness, T., and Wallace, L. (2014). Hyper UAS-Imaging Spectroscopy from a Multirotor Unmanned Aircraft System: Hyper UAS-Imaging Spectroscopy from a Multirotor Unmanned. J. Field Robot. 31, 571–590.

Lundquist, C. J., Jones, T. C., Parkes, S. M., and Bulmer, R. H. (2018). Changes in benthic community structure and sediment characteristics after natural recolonisation of the seagrass *Zostera muelleri*. Scientific Reports, 8(1), 1–9. https://doi.org/10.1038/s41598-018-31398-2

Lyons, M. B., Phinn, S. R., and Roelfsema, C. M. (2012). Long-term land cover and seagrass mapping using Landsat and object-based image analysis from 1972 to 2010 in the coastal environment of Southeast Queensland, Australia. ISPRS Journal of Photogrammetry and Remote Sensing, 71, 34–46. https://doi.org/10.1016/j.isprsjprs.2012.05.002

Larson, M. D., Simic Milas, A., Vincent, R. K., and Evans, J. E. (2018). Multi-depth suspended sediment estimation using high-resolution remote-sensing UAV in Maumee River, Ohio. International Journal of Remote Sensing, 1–18. https://doi.org/10.1080/01431161.2018.1465616

MacDiarmid, A., Bowden, D., Cummings, V., Morrison, M., Jones, E., Kelly, M., Neil, H., Nelson, W., and Rowden, A. (2013). Sensitive marine benthic habitats defined. NIWA Client Report WLG2013-18, 72 p.

Maavara, T., R. Lauerwald, P. Regnier and Van-Cappellen, P. (2017). Global perturbation of organic carbon cycling by river damming. Nature Communications, 8, 15347.

Macreadie, P. I., Baird, M. E., Trevathan-Tackett, S. M., Larkum, A. W. D., and Ralph, P. J. (2014). Quantifying and modelling the carbon sequestration capacity of seagrass meadows - A critical assessment. Marine Pollution Bulletin, 83(2), 430–439. https://doi.org/10.1016/j.marpolbul.2013.07.038

Malenovsky, Z., Lucieer, A., King, D.H., Turnbull, J.D., and Robinson, S.A. (2017). Unmanned aircraft system advances health mapping of fragile polar vegetation. Methods Ecol. Evol. 8, 1842–1857.

Manfreda, S., McCabe, M. F., Miller, P. E., Lucas, R., Madrigal, V. P., Mallinis, G., and Toth, B. (2018). On the use of unmanned aerial systems for environmental monitoring. Remote Sensing, 10(4). https://doi.org/10.3390/rs10040641

Mancini, F., Dubbini, M., Gattelli, M., Stecchi, F., Fabbri, S., and Gabbianelli, G. (2013). Using unmanned aerial vehicles (UAV) for high-resolution reconstruction of topography: the structure from motion approach on coastal environments. Rem. Sens. 5, 6880–6898. http://dx.doi.org/10.3390/rs5126880

Marcello, J., Eugenio, F., Marques, F., and Martin, J. (2015). Precise classification of coastal benthic habitats using high-resolution Worldview-2 imagery. International Geoscience and Remote Sensing Symposium (IGARSS), 2307–2310. https://doi.org/10.1109/IGARSS.2015.7326269

Martin, R., Ellis, J., Brabyn, L., and Campbell, M. (2020). Change-mapping of estuarine intertidal seagrass (*Zostera muelleri*) using multispectral imagery flown by remotely piloted aircraft (RPA) at Wharekawa Harbour, New Zealand. Estuarine, Coastal and Shelf Science, 246, 107046. https://doi.org/10.1016/j.ecss.2020.107046

Matheson, F. and Wadhwa, S. (2012). Seagrass in Porirua Harbour: preliminary assessment of restoration potential. NIWA report for Greater Wellington Regional Council. 35 p. (Unpublished report, available from Greater Wellington Regional Council).

Matheson, F. E., Reed, J., Dos Santos, V. M., Mackay, G., and Cummings, V. J. (2017). Seagrass rehabilitation: successful transplants and evaluation of methods at different spatial scales. New Zealand Journal of Marine and Freshwater Research, 51(1), 96–109. https://doi.org/10.1080/00288330.2016.1265993

Matheson, F. E., & Manley-Harris, M. (2018). Exploring sediment effects and associated thresholds for the New Zealand seagrass *Zostera muelleri*. November. Accessed from: https://www.researchgate.net/publication/343982192_Exploring_sediment_effects_and_associatedthresholds_for_the_New_Zealand_seagrass_Zostera_muelleri#fullTextFileContent

https://niwa.co.nz/freshwater-and-estuaries/freshwater-and-estuaries-update/freshwater-update-75-november-2017/protecting-and-restoring-seagrass-%E2%80%93 on 23 November 2018.

Matheson, F. E., Lundquist, C. J., Gemmill, C. E. C., and Pilditch, C. A. (2011). New Zealand seagrass – More threatened than IUCN review indicates. Biological Conservation, 144, 2749-2750. https://doi.org/ 10.1016/j.biocon.2011.08.020

Matheson, F. E., and Schwarz, A. M. (2007). Growth responses of *Zostera capricorni* to estuarine sediment conditions. Aquatic Botany, 87(4), 299-306. https://doi.org/j.aquabot.2007.07.002.

Matheson F, Dos Santos V, Inglis G, Pilditch C, Reed J, Morrison M, Lundquist C, van Houte-Howes K, Hailes S, Hewitt J 2009. New Zealand seagrass general information guide. NIWA Information Series No. 72.

McCarthy, M. J., Radabaugh, K. R., Moyer, R. P., and Muller-Karger, F. E. (2018). Enabling efficient, large-scale high-spatial-resolution wetland mapping using satellites. Remote Sens. Environ. 208, 189–201. https://10.1016/j.rse.2018.02.021

MicaSense, (2017). Best practices: Collecting Data with MicaSense RedEdge and Parrot Sequoia [WWW 547 Document]. Accessed from, https://support.micasense.com/hc/en-us/articles/224893167-Best-practices-548%20Collecting-Data-with-MicaSense-RedEdge-and-Parrot-Sequoia on 17 October 2020.

MicaSense-RedEdge. (2017). User Manual Multispectral Sensor. (May), 1–27. Retrieved from https://support.micasense.com/hc/enus/article_attachments/204648307/RedEdge_User_Manual_06.pdf

Micheli, F., Bishop, M.J., Peterson, C.H., and Rivera, J. (2008). Alteration of seagrass species composition and function over two decades. Ecol. Monogr. 78, 225–244. https://doi.org/10.1890/06-1605.1

Ministry for the Environment and Statistics New Zealand (2016). New Zealand's Environmental Reporting Series: Our marine environment 2016. Retrieved from www.mfe.govt.nz

Ministry for the Environment (MfE). (2019). Our marine environment 2019 summary. In Ministry for the Environment. Accessed from https://www.mfe.govt.nz/publications/marine/our-marine-environment-2019-summary

Michael, K. (2007). Summary of information in support of the Foveaux Strait Oyster Fishery Plan: The Foveaux Strait ecosystem and effects of oyster dredging. Final Research Report for Ministry of Fisheries Research Project ZBD200504, objectives 1–5. (Unpublished report held by Ministry for Primary Industries, Wellington.)

Moniruzzaman, M., Islam, S. M. S., Lavery, P., and Bennamoun, M. (2019). Faster R-CNN Based Deep Learning for Seagrass Detection from Underwater Digital Images. Digital Image Computing: Techniques and Applications, DICTA 2019. https://doi.org/10.1109/DICTA47822.2019.8946048

Morrison, M. A., Jones, E. G., Consalvey, M., and Berkenbusch, K. (2014). Linking marine fisheries species to biogenic habitats in New Zealand: a review and synthesis of knowledge. New Zealand Aquatic Environment and Biodiversity Report No. 130. In Aquatic Environment and Biodiversity Report No. 130. (Vol. 6480, Issue 130). http://fs.fish.govt.nz

Morrison, M. A., Lowe, M. L., Grant, C. M., Smith, P. J., Carbines, G., Reed, J., Bury, S. J., and Brown, J. (2014). Seagrass Meadows as Biodiversity and Productivity Hotspots New Zealand Aquatic Environment and Biodiversity Report No 137 (Vol. 6480, Issue 137). http://fs.fish.govt.nz

Morrison, M., Lowe, M., Spong, K., and Rush, N. (2007). Comparing seagrass meadows across

New Zealand. Water and Atmosphere 15 (1): 16-17.

Morrison, M.A., Lowe, M.L., Parsons, D.M., Usmar, N.R., and McLeod, I.M. (2009). A review of land-based effects on coastal fisheries and supporting biodiversity in New Zealand. New Zealand Aquatic Environment and Biodiversity Report No. 37. 100 p.

Mountrakis, G., Im, J., and Ogole, C. (2011). Support vector machines in remote sensing: a review. ISPRS J. Photogramm. Remote Sens. 66, 247–259. https://doi.org/10.1016/j.isprsjprs.2010.11.001

Mullerova J., Bruna J., Bartalos T., Dvorak P., Vítkova M., and Pysek P. (2017). Timing Is Important: Unmanned Aircraft vs. Satellite Imagery in Plant Invasion Monitoring. Front Plant Sci 8:887

Mumby, P., Green, E.P., Clark, C.D and Edwards, A.J. (1998). Digital analysis of multispectral airborne imagery of coral reefs. Coral Reefs 17, 1 (1998), 59–69.

Murfitt, S.L., Allan, B.M., Bellgrove, A., Rattray, A., Young, M.A., and Lerodiaconou, D. (2017). Applications of unmanned aerial vehicles in intertidal reef monitoring. Sci. Rep. 7, 10259. http://dx.doi.org/10.1038/s41598-017-10818-9

Muslim, A. M., Chong, W. S., Safuan, C. D. M., Khalil, I., and Hossain, M. S. (2019). Coral reef mapping of UAV: A comparison of sun glint correction methods. Remote Sensing, 11(20). https://doi.org/10.3390/rs11202422

Nagelkerken, I., Sheaves, M., Baker, R., and Connolly, R.M. (2015). The seascape nursery: a novel spatial approach to identify and manage nurseries for coastal marine fauna. Fish Fish. Oxf. (Oxf) 16, 362–371. http://refhub.elsevier.com/S0006-3207(19)30809-2/sbref0215

Nagendra, H. and Rocchini, D. (2008) High-resolution satellite imagery for tropical biodiversity studies: the devil is in the detail. Biodiversity and Conservation, 17, 3431–3442.

Nagendra, H., Lucas, R., Honrado, J.P., Jongman, R.H.G., Tarantino, C., Adamo, M. and Mairota, P. (2013) Remote sensing for conservation monitoring: assessing protected areas, habitat extent, habitat condition, species diversity, and threats. Ecological Indicators, 33, 45–59

Nahirnick, N. K., Hunter, P., Costa, M., Schroeder, S., and Sharma, T. (2019). Benefits and Challenges of UAS Imagery for Eelgrass (*Zostera marina*) Mapping in Small Estuaries of the Canadian West Coast. Journal of Coastal Research, 35(3), 673. https://doi.org/10.2112/jcoastres-d-18-00079.1

Nahirnick, N.K., Reshitnyk, L., Campbell, M., Hessing-Lewis, M., Costa, M., Yakimishyn, J., and Lee, L. (2018). Mapping with confidence; delineating seagrass habitats using Unoccupied Aerial Systems (UAS). Remote Sens. Ecol. Conserv. 5, 121–135. http://dx.doi.org/10.1002/rse2.98

Nasi, R., Honkavaara, E., Blomqvist, M., Lyytikainen-Saarenmaa, P., Hakala, T., Viljanen, N., Kantola, T., and Holopainen, M. (2018). Remote sensing of bark beetle damage in urban forests at individual tree level using a novel hyperspectral camera from UAV and aircraft. Urban For. Urban Green, 30, 72–83. http://dx.doi.org/10.1016/j.ufug.2018.01.010

Nevalainen, O., Honkavaara, E., Tuominen, S., Viljanen, N., Hakala, T., Yu, X., Hyyppa, J., Saari, H., Polonen, I., and Imai, N. (2017). Individual Tree Detection and Classification with UAV-Based Photogrammetric Point Clouds and Hyperspectral Imaging. Remote Sens, 9, 185. http://dx.doi.org/10.3390/rs9030185

Newman, G., Wiggins, A., Crall, A., Graham, E., Newman, S., and Crowston, K. (2012). The future of citizen science: emerging technologies and shifting paradig Front Ecol n Environ, 10, 298–304. http://dx.doi.org/10.1890/110294

New Zealand e-Bird, (2019). https://ebird.org/newzealand/hotspot/L712931

Newell, R. I. E., and Koch. E.W. (2004). Modelling seagrass density and distribution in response to changes in turbidity stemming from bivalve filtration and seagrass sediment stabilization. Estuaries 27:793-806.

Newell, R. I. E., T. R. Fisher, R. R. Holyoke, and Cornwell. J. C. (2005). Influence of eastern oysters on nitrogen and phosphorus regeneration in Chesapeake Bay, USA. in R. F. Dame and S. Olenin, editors. The Comparative Roles of Suspension-Feeders in Ecosyste Springer, Netherlands.

Newell, R.I.E. (2004). Ecosystem influences of natural and cultivated populations of suspension-feeding bivalve mollusks: A review. Journal of Shellfish Research 23: 51–61.

Nielsen, A.A., Conradsen, K., and Simpson, J. J. (1998). Multivariate Alteration Detection (MAD) and MAF Postprocessing in Multispectral, Bitemporal Image Data: New Approaches to Change Detection Studies. Remote Sens Environ. 64:1–19.

Nieuwhof, S., Herman, P.M., Dankers, N., Troost, K., and Van-der Wal, D. (2015). Remote sensing of epibenthic shellfish using synthetic aperture radar satellite imagery. Remote Sensing. 7(4):3710±34.

National Oceanic and Atmospheric Administration (NOAA) Coastal Services Center. (2003). Pilot investigation of remote sensing for intertidal oyster mapping in coastal South Carolina: a methods comparison NOAA coastal services center noaa / csc / 20514-pub. methods, 1–32. https://coast.noaa.gov/data/digitalcoast/pdf/oyster-mapping.pdf (accessed on 16 March 2018).

Nowicki, R. J., Thomson, J. A., Burkholder, D. A., Fourqurean, J. W., and Heithaus, M. R. (2017). Predicting seagrass recovery times and their implications following an extreme climate event. Marine Ecology Progress Series, 567, 79–93. https://doi.org/10.3354/meps12029

Narayan, S., Beck, M. W., Reguero, B. G., Losada, I. J., Van Wesenbeeck, B., Pontee, N., Sanchirico, J. N., Ingram, J. C., Lange, G. M., and Burks-Copes, K. A. (2016). The effectiveness, costs and coastal protection benefits of natural and nature-based defences. PLoS ONE, 11(5), 1–17. https://doi.org/10.1371/journal.pone.0154735

O'Neill, J. D., and Costa, M. (2013). Mapping eelgrass (*Zostera marina*) in the Gulf Islands National Park Reserve of Canada using high spatial resolution satellite and airborne imagery. Remote Sensing of Environment, 133, 152–167. https://doi.org/10.1016/j.rse.2013.02.010

O'Donnell, E. (2009). Wharekawa Harbour and catchment management plan. Environment Waikato Technical Report 2009/12. Waikato Regional Council, Hamilton. Resource Management Act (1991). http://www.legislation.govt.nz/act/public/1991/0069/latest/DLM230265.html

Oleksyn, S., Tosetto, L., Raoult, V., Joyce, K. E., and Williamson, J. E. (2021). Going Batty: The Challenges and Opportunities of Using Drones to Monitor the Behaviour and Habitat Use of Rays. Drones, 5(1), 12. https://doi.org/10.3390/drones5010012

Oliver, E. C. J., Benthuysen, J. A., Bindoff, N. L., Hobday, A. J., Holbrook, N. J., Mundy, C. N., and Perkins-Kirkpatrick, S. E. (2017). The unprecedented 2015/16 Tasman Sea marine heatwave. Nature Communications, 8, 16101. https://dx.doi.org/10.1038/ncomms16101

Orth, R. J., Carruthers, T. J. B., Dennison, W. C., Duarte, C. M., Fourqurean, J. W., Heck, K. L., Hughes, A. R., Kendrick, G. A., Kenworthy, W. J., Olyarnik, S., Short, F. T., Waycott, M., and Williams, S. L. (2006). A Global Crisis for Seagrass Ecosyste BioScience, 56(12), 987. https://doi.org/10.1641/0006-3568(2006)56[987:agcfse]2.0.co;2

Parsons, D. M., Sim-Smith, C., Cryer, M., Francis, M., Hartill, B., Jones, E., and Zeldis, J. (2014). Snapper (*Chrysophrys auratus*): A review of life history and key vulnerabilities in New Zealand. New Zealand Journal of Marine and Freshwater Research, 48(2), 256–283. https://doi.org/10.1080/00288330.2014.892013

Pasqualini, V., Pergent-Martini, C., Pergent, G., Agreil, M., Skoufas, G., Sourbes, and L., Tsirika, A. (2005). Use of SPOT 5 for mapping seagrasses: an application to *Posidonia oceanica*. Remote Sens. Environ. 94, 39–45. https://doi.org/10.1016/j.rse.2004.09010.

Peneva, E., Griffith, J. A., and Carter, G.A. (2008). Seagrass mapping in the Northern Gulf of Mexico using airborne hyperspectral imagery: a comparison of classification methods. J. Coast. Res. 24 (4), 850–856. http://refhub.elsevier.com/S0303-2434(16)30168-4/sbref0260

Perez, D., Islam, K., Hill, V., Zimmerman, R., Schaeffer, B., Shen, Y., and Li, J. (2020). Quantifying seagrass distribution in coastal water with deep learning models. Remote Sensing, 12(10), 1–17. https://doi.org/10.3390/rs12101581

Peterson, C.H., Grabowski, J.H., and Powers, S.P. (2003). Estimated enhancement of fish production resulting from restoring oyster reef habitat: quantitative valuation. Marine Ecology Progress Series 264: 249–264.

Pettorelli, N., Laurance, W. F., O'Brien, T. G., Wegmann, M., Nagendra, H., and Turner, W. (2014). Satellite remote sensing for applied ecologists: Opportunities and challenges. Journal of Applied Ecology, 51(4), 839–848. https://doi.org/10.1111/1365-2664.12261

Pettorelli, N., Schulte to Buehne, H., Shapiro, A., and Glover-Kapfer, P. (2018). Satellite Remote Sensing Conservation Technology 4 Satellite Remote Sensing. WWF Conservation Technology Series, 1(4), 125.

Phinn, S.R., Kovacs, E.M., Roelfsema, C.M., Canto, R.F., Collier, C.J., and McKenzie, L.J. (2017). Assessing the potential for satellite image monitoring of seagrass thermal dynamics: for inter- and shallow sub-tidal seagrasses in the inshore Great Barrier Reef World Heritage Area, Australia. Int. J. Digital Earth 11, 803–824. https://doi.org/10.1080/17538947.2017.1359343

Pimm, S. L., Alibhai, S., Bergl, R., Dehgan, A., Giri, C., Jewell, Z., and Loarie, S. (2015). Emerging Technologies to Conserve Biodiversity. Trends in Ecology and Evolution, 30(11), 685–696. https://doi.org/10.1016/j.tree.2015.08.008

Pinarbasi, K., Galparsoro, I., Borja, A., Stelzenmuller, V., Ehler, C. N., and Gimpel, A. (2017). Decision support tools in marine spatial planning: Present applications, gaps, and future perspectives. Marine Policy, 83, 83–91. https://doi.org/10.1016/j.marpol.2017.05.031

Pinkerton, M.H., Sutton, P.J.H., and Wood, S. (2019). Satellite indicators of phytoplankton and ocean surface temperature for New Zealand. NIWA Client Report 2018180WN. Prepared for the Ministry for the Environment. Wellington, New Zealand.

Pix4D Radiometric correction documentation (2011-2020). Accessed on 30 March 2020. https://support.pix4d.com/hc/en-us/articles/202559509-Radiometric-corrections

Pix4D. www.Pix4D.com. Accessed on 30th April 2019.

Poursanidis, D., Topouzelis, K., and Chrysoulakis, N. (2018). Mapping coastal marine habitats and delineating the deep limits of the Neptune's seagrass meadows using very high-resolution Earth observation data. Int. J. Remote Sens. https://doi.org/10.1080/01431161.2018.1490974.

Power, A., Corley, B., Atkinson, D., Walker, R., Harris, D., Manley, J., and Johnson, T. (2010). A caution against interpreting and quantifying oyster habitat loss from historical surveys. J. Shellfish Res, 29, 927–937. https://dx.doi.org/10.2983/035.029.0425

Pu, R., and Bell, S. (2017). Mapping seagrass coverage and spatial patterns with high spatial resolution IKONOS imagery. International Journal of Applied Earth Observation and Geoinformation, 54, 145–158. https://doi.org/10.1016/j.jag.2016.09.011

Purkis, S. J. (2018). Remote Sensing Tropical Coral Reefs: The View from Above. Annual Review of Marine Science, 10(1), annurev-marine-121916-063249. https://doi.org/10.1146/annurev-marine-121916-063249

Reshitnyk, L., Costa, M., Robinson, C., and Dearden, P. (2014). Evaluation of WorldView-2 and acoustic remote sensing for mapping benthic habitats in temperate coastal Pacific waters. Remote Sens. Environ. 153, 7–23. https://doi.org/10.1016/j.rse.2014.07.016

Reus, G., Moller, T., Jager, J., Schultz, S. T., Kruschel, C., Hasenauer, J., Wolff, V., and Fricke-Neuderth, K. (2018). Looking for seagrass: Deep learning for visual coverage estimation. Oceans /IEEE Kobe Techno-Oceans, OCEANS - Kobe 2018, 18–23. https://doi.org/10.1109/OCEANSKOBE.2018.8559302

Rieucau, G., Kiszka, J. J., Castillo, J. C., Mourier, J., Boswell, K. M., and Heithaus, M. R. (2018). Using unmanned aerial vehicle (UAV) surveys and image analysis in the study of large surface-associated marine species: a case study on reef sharks *Carcharhinus melanopterus* shoaling behaviour. Journal of Fish Biology, 93(1), 119–127. https://doi.org/10.1111/jfb.13645

Ribeiro-Gomes, K., Hernandez-Lopez, D., Ballesteros, R., and Moreno, M. A. (2016). Approximate georeferencing and automatic blurred image detection to reduce the costs of UAV use in environmental and agricultural applications. Biosyst. Eng. 151, 308–327. https://doi.org/10.1016/j.biosystemseng.2016.09.014

Ridge, J. T., Gray, P. C., Windle, A. E., and Johnston, D. W. (2020). Deep learning for coastal resource conservation: automating detection of shellfish reefs. Remote Sensing in Ecology and Conservation, 6(4), 431–440. https://doi.org/10.1002/rse2.134

Riniatsih, I., Ambariyanto, A., Yudiati, E., Redjeki, S., and Hartati, R. (2021). Monitoring the seagrass ecosystem using the unmanned aerial vehicle (UAV) in coastal water of Jepara. IOP Conference Series: Earth and Environmental Science, 674(1). https://doi.org/10.1088/1755-1315/674/1/012075

Rodil, I. F., Lohrer, A. M., Attard, K. M., Hewitt, J. E., Thrush, S. F., and Norkko, A. (2021). Macrofauna communities across a seascape of seagrass meadows: environmental drivers, biodiversity patterns and conservation implications. Biodiversity and Conservation, 30(11), 3023–3043. https://doi.org/10.1007/s10531-021-02234-3

Roelfsema, C. M., Phinn, S. R., Udy, N., and Maxwell, P. (2009). An integrated field and remote sensing approach for mapping seagrass cover, moreton Bay, Australia. Journal of Spatial Science, 54(1), 45–62. https://doi.org/10.1080/14498596.2009.9635166

Roelfsema, C., Kovacs, E., Ortiz, J. C., Wolff, N. H., Callaghan, D., Wettle, M., and Phinn, S. (2018). Coral reef habitat mapping: A combination of object-based image analysis and ecological modelling. Remote Sensing of Environment, 208, 27–41. https://doi.org/10.1016/j.rse.2018.02.005

Roelfsema, C.M., Lyons, M., Kovacs, E.M., Maxwell, P., Saunders, M.I., Samper-Villarreal, J., and Phinn, S.R. (2014). Multi-temporal mapping of seagrass cover, species and biomass: a semi-automated object-based image analysis approach. Remote Sens. Environ. 150, 172–187. https://doi.org/10.1016/j.rse.2014.05.001

Rosnell, T., and Honkavaara, E. (2012). Point cloud generation from aerial image data acquired by a quadrocopter-type micro unmanned aerial vehicle and a digital still camera. Sensors, 12(1), 453-480. https://doi:10.3390/s120100453

Rosso, P.H., Ustin, S.L., and Hastings, A. (2005). Reflectance properties and physiological responses of *Salicornia virginica* to heavy metal and petroleum contamination. Environ. Pollut. 137, 241–252. http://refhub.elsevier.com/S2351-9894(21)00360-7/sbref26

Ruwaimana, M., Ibrahim, S., Syafiq A., M., Dahdouh-Guebas, F., Otero, V., M. Muslim, A., Koedam, N., Satyanarayana, B., and Raymaekers, D. (2018). The advantages of using drones over space-borne imagery in the mapping of mangrove forests. Plos One, 13(7), e0200288. https://doi.org/10.1371/journal.pone.0200288

Saunders, M.I., Atkinson, S., Klein, C.J., Weber, T., and Possingham, H.P. (2017). Increased Sediment Loads Cause Non-Linear Decreases in Seagrass Suitable Habitat Extent. PLoS ONE, 12, e0187284. http://doi.org/10.1371/journal.pone.0187284

Schill, S.R., Porter, D., Coen, L.D., Bushek, D., and Vincent, J. (2006). Development of an Automated Mapping Technique for Monitoring and Managing Shellfish Distributions. NOAA/UNH Cooperative Institute for Coastal and Estuarine Environmental Technology (CICEET), Durham NH. 88 p.

Schmidt, L. (2000). Classifying oyster reefs using high-resolution multispectral imagery. Unpublished graduate research. The University of South Carolina.

Schwantes, A., Poulin, S., Johnston, D., Ridge, J., Seymour, A., Swenson, J., and Gray, P. (2018). Integrating Drone Imagery into High-Resolution Satellite Remote Sensing Assessments of Estuarine Environments. Remote Sensing, 10(8), 1257. https://doi.org/10.3390/rs10081257

Seavey, J. R., Pine, W. E., Frederick, P., Sturmer, L., and Berrigan, M. (2011). Decadal changes in oyster reefs in the Big Bend of Florida's Gulf Coast. Ecosphere, 2(10), art114. https://doi.org/10.1890/es11-00205.1

Seebens, H., Schwartz, N., Schupp, P.J., and Blasius, B. (2016). Predicting the spread of marine species introduced by global shipping. Proceedings of the National Academy of Sciences of the United States of America, 113(20), 5646–5651. https://doi.org/10.1073/pnas.1524427113

Sellar, R.G., and Boreman, G.D. (2005). Classification of imaging spectrometers for remote sensing applications. Opt. Eng. 44, 013602. http://dx.doi.org/10.1117/1.1813441

Seymour, A.C., Dale, J., Hammill, M., Halpin, P.N. and Johnston, D.W. (2017). Automated detection and enumeration of marine wildlife using unmanned aircraft systems (UAS) and thermal imagery. Sci. Rep. 7, 45127. https://www.nature.com/articles/srep45127

Seymour, A.C., Ridge, J.T., Rodriguez, A.B., Newton, E., Dale, J., and Johnston, D.W. (2017b). Deploying fixed-wing unoccupied aerial systems (UAS) for coastal morphology assessment and management. J. Coast. Res. 34: 704–17. https://doi.org/10.2112/JCOASTRES-D-17-00088.1

Shang, S., Lee, Z., Lin, G., Hu, C., Shi, L., Zhang, Y., Li, X., Wu, J., and Yan, J. (2017). Sensing an intense phytoplankton bloom in the western Taiwan Strait from radiometric measurements on a UAV. Remote Sens. Environ. 198, 85–94. http://dx.doi.org/10.1016/j.rse.2017.05.036

Sharma, H. B., Panigrahi, S., Sarmah, A. K., and Dubey, B. K. (2019). UAV and satellite synergies for optical remote sensing applications: A literature review. Journal Pre of. Science of the Total Environment, 135907. https://doi.org/10.1016/j.srs.2021.100019

Shears, N.T. (2010). Meola Reef ecological monitoring programmes: 2001–2010. Prepared by Auckland Uni-Services for Auckland Regional Council. Auckland Regional Council Technical Report 2010/031.

Shi, D., & Yang, X. (2015). Support Vector Machines for Land Cover Mapping from Remote Sensor Imagery. 265–279. https://doi.org/10.1007/978-94-017-9813-6_13

Short, F.T., Polidoro, B., Livingstone, S.R., Carpenter, K.E., Bandeira, S., Bujang, J.S., Calumpong, H.P., Carruthers, T.J.B., Coles, R.G., Dennison, W.C., Erftemeijer, P.L.A., Fortes, M.D., Freeman, A.S., Jagtap, T.G., Kamal, A.H.M., Kendrick, G.A., Judson Kenworthy, W., La Nafie, Y.A., Nasution, I.M., Orth, R.J., Prathep, A., Sanciangco, J.C., van Tussenbroek, B., Vergara, S.G., Waycott, M., and Zieman, Stewart, M., Northcott, G., Gaw, S., and Tremblay, L.A. (2016). An update on emerging organic contaminants of concern for New Zealand with guidance on monitoring approaches for councils, Prepared by Streamlined Environmental Ltd., Northcott Research Consultants Ltd., University of Canterbury, Cawthron Institute and the University of Auckland for Auckland Council, Greater Wellington Regional Council and Environment Canterbury Regional Council. Auckland Council technical report, TR2016/006.

Siregar, V.P., Agus, S.B., Subarno, T., and Prabowo, N.W. (2018). Mapping shallow waters habitats using OBIA by applying several approaches of depth invariant index in North Kepulauan Seribu. IOP Conference Series: Earth and Environmental Science 149, 012052. https://doi.org/10.1088/1755-1315/149/1/012052.

Spalding, M. D., Mcivor, A. L., Beck M. W., Koch E. W., Mcoller I., and Reed D. J. (2014). Coastal ecosystems: A critical element of risk reduction. Conserv. Lett. 7, 293–301. https://doi.org/10.1111/conl.12074

Stark, B., Zhao, T., and Y. Chen. (2016). An analysis of the effect of the bidirectional reflectance distribution function on remote sensing imagery accuracy from Small Unmanned Aircraft Systems. International Conference on Unmanned Aircraft Systems (ICUAS), pp. 1342-1350, https://doi.org/10.1109/ICUAS.2016.7502566

Stats NZ (2019a). Environmental-economic accounts: Data to 2017. Wellington, New Zealand. Retrieved from www.stats.govt.nz

Stewart, M., Northcott, G., Gaw, S., and Tremblay, L.A. (2016). An update on emerging organic contaminants of concern for New Zealand with guidance on monitoring approaches for councils, Prepared by Streamlined Environmental Ltd., Northcott Research Consultants Ltd., University of Canterbury, Cawthron Institute and the University of Auckland for Auckland Council, Greater Wellington Regional Council and Environment Canterbury Regional Council. Auckland Council technical report, TR2016/006.

Stocker, C., Bennett, R., Nex, F., Gerke, and M., Zevenbergen, J. (2017). Review of the Current State of UAV Regulations. Remote Sens, 9, 459. http://dx.doi.org/10.3390/rs9050459

Strydom, S., Murray, K., Wilson, S., Huntley, B., Rule, M., Heithaus, and M. Zdunic, K. (2020). Too hot to handle unprecedented seagrass death driven by marine heatwave in a World Heritage Area. Global Change Biology, gcb.15065. https://doi.org/10.1111/gcb.15065

Sussarellu, R., Suquet, M., Thomas, Y., Lambert, C., Fabioux, C., Pernet, M.E.J., and Huvet, A. (2016). Oyster reproduction is affected by exposure to polystyrene microplastics. Proceedings of the National Academy of Sciences, 113(9), 2430–2435. https://doi.org/10.1073/pnas.1519019113

Taddia, Y., Russo, P., Lovo, S., and Pellegrinelli, A. (2019). Multispectral UAV monitoring of submerged seaweed in shallow water. Applied Geomatics, 12. https://doi.org/10.1007/s12518-019-00270-x

Tait, L., Bind, J., Charan-Dixon, H., Hawes, I., Pirker, J., and Schiel, D. (2019). Unmanned Aerial Vehicles (UAVs) for Monitoring Macroalgal Biodiversity: Comparison of RGB and Multispectral Imaging Sensors for Biodiversity Assessments. Remote Sensing, 11(19), 2332. https://doi.org/10.3390/rs11192332

Tamondong, A. M., Cruz, C. A., Guihawan, J., Garcia, M., Quides, R. R., Cruz, J. A., and Blanco, A. C. (2018). Remote sensing-based estimation of seagrass percent cover and LAI for above-ground carbon sequestration mapping. October 2. https://doi.org/10.1117/12.2324695

Tang, L., and Shao, G. (2015). Drone remote sensing for forestry research and 473 practices. J. For. Res. 26, 791–797. https://doi.org/10.1007/s11676-015-0088

Taylor, R.B., Morrison, M.A., and Shears, N. (2011). Establishing baselines for recovery in a marine reserve (Poor Knights Islands, New Zealand) using recollections of long–term divers. Biological Conservation 144 (12): 3038–3046.

Thomsen, M.S., Mondardini, L., Alestra, T., Gerrity, S., Tait, L., South, P.M., and Marzinelli, E.M. (2019). Local Extinction of Bull Kelp (*Durvillaea* spp.) Due to a Marine Heatwave. Frontiers in Marine Science, 6 (March), 1–10. https://doi.org/10.3389/fmars.2019.00084

Thorngren, L., Holthuis, T. D., Lindegarth, S., and Lindegarth, M. (2017). Developing methods for assessing abundance and distribution of European oysters (*Ostrea edulis*) using towed video. PLoS ONE, 12(11), 1–20. https://doi.org/10.1371/journal.pone.0187870

Topouzelis, K., Makri, D., Stoupas, N., Papakonstantinou, A., and Katsanevakis, S. (2018). Seagrass mapping in Greek territorial waters using Landsat-8 satellite images. International Journal of Applied Earth Observation and Geoinformation, 67(October 2017), 98–113. https://doi.org/10.1016/j.jag.2017.12.013

Papakonstantinoub, A., Topouzelis, K., Spondylidisa, S.C., and Soulakellisb, N. (2016). The use of Sentinel-2 imagery for seagrass mapping: Kalloni Gulf (Lesvos Island, Greece) case study. Proc. SPIE 9688, Fourth International Conference on Remote Sensing and Geoinformation of the Environment (RSCy2016), 96881F (August 12, 2016), https://doi.org/10.1117/12.2242887

Papakonstantinou, A., Batsaris, M., Spondylidis, S., & Topouzelis, K. (2021). A citizen science unmanned aerial system data acquisition protocol and deep learning techniques for the automatic detection and mapping of marine litter concentrations in the coastal zone. *Drones*, *5*(1), 1–21. https://doi.org/10.3390/drones5010006

Traganos, D., and Reinartz, P. (2018). Interannual change detection of Mediterranean seagrasses using RapidEye image time series. Frontiers in Plant Science, 9(February), 1–15. https://doi.org/10.3389/fpls.2018.00096

Traganos, D., and Reinartz, P. (2018). Mapping Mediterranean seagrasses with Sentinel-2 imagery. Marine Pollution Bulletin, 134, 197–209. https://doi.org/10.1016/j.marpolbul.2017.06.075

Traganos, D., Cerra, D., and Reinartz, P. (2017). Cubesat-derived Detection of Seagrasses Using Planet Imagery following Unmixing-based Denoising: Is Small the next Big? The International Archives of the Photogrammetry, Remote Sensing and Spatial Information Sciences, Volume

XLII-1/W1, 2017 ISPRS Hannover Workshop: HRIGI 17 – CMRT 17 – ISA 17 – EuroCOW 17, 6–9 June 2017, Hannover, Germany.

Trasvina-Moreno, C. A., Blasco, R., Marco, A., Casas, R., and Trasvina-Castro, A. (2017). Unmanned aerial vehicle-based wireless sensor network for marine-coastal environment monitoring. Sensors (Switzerland), 17(3), 1–22. https://doi.org/10.3390/s17030460

Tucker, C. (1979). Red and Photographic Infrared Linear Combinations for Monitoring Vegetation. Remote Sensing of Environment 8, 127–150.

Turner, D., Lucieer, A., and de Jong, S. M. (2015). Time series analysis of landslide dynamics using an unmanned aerial vehicle (UAV). Remote Sensing, 7(2), 1736-1757. https://doi:10.3390/rs70201736

Turner, D., Lucieer, A., Malenovsky, Z., King, D. H., and Robinson, S. A. (2014). Spatial co-registration of ultra-high resolution visible, multispectral and thermal images acquired with a micro-UAV over Antarctic moss beds. Rem. Sens. 6, 4003–4024. http://dx.doi.org/10.3390/rs6054003

Turner, S., and Schwarz, A. (2006). Management and conservation of seagrass in New Zealand: An Introduction. Science for Conservation (monograph series) vol 264. Science and Technical Publishing, Department of Conservation, Wellington, New Zealand. 90 pp.

Turner, S.J. (2007). Growth and Productivity of Intertidal *Zostera Capricorni* in New Zealand Estuaries. N. Z. J. Mar. Freshw. Res. 41, 77–90. http://doi.org/10.1080/00288330709509897

Turner, S.J., Hewitt, J.E., Wilkinson, M.R., Morrisey, D.J., Thrush, S.F., Cummings, V.J., and Funnell, G. (1999). Seagrass patches and landscapes: the influence of wind-wave dynamics and hierarchical arrangements of spatial structure on macrofaunal seagrass communities. Estuaries 22: 1016–1032.

Turner, W., Buchanan, G., Rondinini, C., Dwyer, J., Herold, M., and Koh, L.P. (2013) Satellites: make data freely accessible. Nature, 498, 37.

Hoque, M. R., Islam, K. A., Perez, D., Hill, V., Schaeffer, B., Zimmerman, R., and Li, J. (2018). Seagrass Propeller Scar Detection using Deep Convolutional Neural Network. 2018 9th IEEE Annual Ubiquitous Computing, Electronics, and Mobile Communication Conference, UEMCON 2018, 659–665. https://doi.org/10.1109/UEMCON.2018.8796636

Unsworth, R. K. F., McKenzie, L. J., Nordlund, L. M., and Cullen-Unsworth, L. C. (2018). A changing climate for seagrass conservation? Current Biology, 28(21), R1229–R1232. https://doi.org/10.1016/j.cub.2018.09.027

Uto, K., Seki, H., Saito, G., Kosugi, Y., and Komatsu, T., (2017). Coastal observation using new hyperspectral imager for UAVs. IEEE International Geoscience and Remote Sensing Symposium (IGARSS-2017), 3614-3617. https://doi.org/10.1109/IGARSS.2017.8127781

Van Houte-Howes, K.S.S., Turner, S.J., and Pilditch, C.A. (2004). Spatial differences in macroinvertebrate communities on intertidal sandflats: a comparison between seagrass habitats and unvegetated sediment in three estuaries on the Coromandel Peninsula, New Zealand. Estuaries 27: 945–957.

Vann-Sander, S., Clifton, J., and Harvey, E. (2016). Can citizen science work? Perceptions of the role and utility of citizen science in a marine policy and management context. Marine Policy, 72, 82–93. https://doi.org/10.1016/j.marpol.2016.06.026

Vayssade, J.-A., Arquet, R., and Bonneau, M. (2019). Automatic activity tracking of goats using drone camera. Comput. Electron. Agric.,162, 767–772. http://doi.org/10.1016/j.compag.2019.05.021

Veettil, B. K., Ward, R. D., Lima, M. D. A. C., Stankovic, M., Hoai, P. N., and Quang, N. X. (2020). Opportunities for seagrass research derived from remote sensing: A review of current methods. Ecological Indicators, 117(December 2019). https://doi.org/10.1016/j.ecolind.2020.106560

Ventura, D., Bonifazi, A., Gravina, M. F., Belluscio, A., and Ardizzone, G. (2018). Mapping and classification of ecologically sensitive marine habitats using unmanned aerial vehicle (UAV) imagery and Object-Based Image Analysis (OBIA). Remote Sensing, 10(9), 1–23. https://doi.org/10.3390/rs10091331

Ventura, D., Bonifazi, A., Gravina, M. F., and Ardizzone, G. D. (2017). Unmanned Aerial Systems (UASs) for Environmental Monitoring: A Review with Applications in Coastal Habitats. Aerial Robots - Aerodynamics, Control, and Applications. https://doi.org/10.5772/intechopen.69598

Ventura, D., Bruno, M., Jona Lasinio, G., Belluscio, A., and Ardizzone, G. (2016). A low-cost drone-based application for identifying and mapping of coastal fish nursery grounds. Estuarine, Coastal and Shelf Science, 171, 85–98. https://doi.org/10.1016/j.ecss.2016.01.030

Verhoeven, G. (2011). Taking computer vision aloft-archaeological three-dimensional reconstructions from aerial photographs with photoscan. Archaeol. Prospect. 18 (1), 67e73. http://refhub.elsevier.com/S0272-7714(16)30030-0/sref69

Wang, C. and Myint, S.W. (2015). A Simplified Empirical Line Method of Radiometric Calibration for Small Unmanned Aircraft Systems-Based Remote Sensing. IEEE J. Sel. Top. Appl. Earth Obs. Remote Sens. 8, 1876–1885. http://dx.doi.org/10.1109/JSTARS.2015.2422716

Warner, T. (2011). Kernel-based texture in remote sensing image classification. Geogr. Compass. 5, 781–798. http://dx.doi.org/10.1111/j.1749-8198.2011.00451.x

Watts, A. C., Perry, J. H., Smith, S. E., Burgess, M. A., Wilkinson, B. E., Szantoi, Z., Ifju, P. G., and Percival, H. F. (2010). Small, unmanned aircraft systems for low altitude aerial surveys. Journal of Wildlife Management, 74(7), 1614-1619. https://doi:10.2193/2009-425

Waycott, M., Duarte, C. M., Carruthers, T. J. B., Orth, R. J., Dennison, W. C., Olyarnik, S., and Williams, S. L. (2009). Accelerating loss of seagrasses across the globe threatens coastal ecosyste Proceedings of the National Academy of Sciences of the United States of America, 106(30), 12377–12381. https://doi.org/10.1073/pnas.0905620106

Weerman, E.J., van de Koppel, J., Eppinga, M.B., Montserrat, F., Liu, Q., and Herman, P.M.J. (2010). Spatial self-organization on intertidal mudflats through biophysical stress divergence. Am. Nat. 176, E15–E32. https://doi.org/10.1086/652991.

Wernberg, T., Bennett, S., Babcock, R.C., De Bettignies, T., Cure, K., Depczynski, M., Dufois, F., Fromont, J., Fulton, C.J., and Hovey, R.K. (2016). Climate-driven regime shift of a temperate marine ecosystem. Science 353, 169–172. http://dx.doi.org/10.1126/science.aad8745

Wicaksono, P., and Lazuardi, W. (2018). Assessment of Planet Scope images for benthic habitat and seagrass species mapping in a complex optically shallow water environment. International Journal of Remote Sensing, 39(17), 5739–5765. https://doi.org/10.1080/01431161.2018.1506951

Windle, A. E., Poulin, S. K., Johnston, D. W and Ridge, J. T. (2019). Rapid and accurate monitoring of intertidal Oyster Reef Habitat using unoccupied aircraft systems and structure from motion. Remote Sensing, 11(20). https://doi.org/10.3390/rs11202394

Wood, N. and Lavery, P. (2001). Monitoring Seagrass Ecosystem Health—The Role of Perception in Defining Health and Indicators. Ecosystem Health. 6. 134 - 148. https://doi.org/10.1046/j.1526-0992.2000.00015

Woods, C.M.C., and Schiel, D.R. (1997). Use of seagrass Zostera novazelandica (Setchell, 1933) as habitat and food by the crab *Macrophthalmus hirtipes* (Heller, 1862) (*Brachyura: Ocypodidae*) on rocky intertidal platforms in southern New Zealand. Journal of Experimental Marine Biology and Ecology 214: 49–65.

Xue, J., and Su, B. (2017). Significant remote sensing vegetation indices: A review of developments and applications. Journal of Sensors, 2017. https://doi.org/10.1155/2017/1353691

Yang, B., Hawthorne, T. L., Searson, H., and Duffy, E. (2020). High-Resolution UAV Mapping for Investigating Eelgrass Beds Along the West Coast of North America. International Geoscience and Remote Sensing Symposium (IGARSS), 6317–6320. https://doi.org/10.1109/IGARSS39084.2020.9324230

Yang, D., and Yang, C. (2009). Detection of seagrass distribution changes from 1991 to 2006 in Xincun Bay, Hainan, with satellite remote sensing. Sensors, 9(2), 830-844. https://doi.org/10.3390/s90200830

Zeng, C., Richardson, M., and King, D. J. (2017). The impacts of environmental variables on water reflectance measured using a lightweight unmanned aerial vehicle (UAV)-based spectrometer system. ISPRS Journal of Photogrammetry and Remote Sensing, 130, 217–230. https://doi.org/10.1016/j.isprsjprs.2017.06.004